FATTY ACID UPTAKE IN *ESCHERICHIA COLI:* DEVELOPMENT OF A PHOTOAFFINITY LABELING APPROACH FOR IDENTIFYING PROTEINS INVOLVED IN THE TRANSMEMBRANE MOVEMENT OF LONG CHAIN FATTY ACIDS

By

DEV MANGROO, B.Sc

A Thesis

Submitted to the School of Graduate Studies

in Partial Fulfilment of the Requirements

for the Degree

Doctor of Philosophy.

McMaster University

June 1992

FATTY ACID UPTAKE IN *ESCHERICHIA COLI*

DOCTOR OF PHILOSOPHY (1992) McMASTER UNIVERSITY

(Biochemistry) Hamilton, Ontario

TITLE: Fatty acid uptake in *Escherichia coli*: Development of a photoaffinity labeling approach for identifying proteins involved in the transmembrane movement of long chain fatty acids.

AUTHOR: Dev Mangroo, B.Sc. (McMaster University)

SUPERVISOR: Dr. Gerhard E. Gerber, Professor

NUMBER OF PAGES: xxii, 239

ABSTRACT

The photoreactive fatty acid 11-m-diazirinophenoxy-[11-^{3}H]-undecanoate was shown to be taken up specifically by the long chain fatty acid transport system expressed in *Escherichia coli* grown on oleate. This photoreactive fatty acid analogue was therefore used to identify proteins involved in fatty acid uptake in *E. coli*. The *fadL* protein, required for fatty acid permeation of the outer membrane of *E. coli* was labeled by the probe, confirmed to be exclusively in the outer membrane and to exhibit the heat modifiable behaviour typical of outer membrane proteins. The apparent pI of the incompletely denatured form of the protein having the mobility of a 33 kDa protein was 4.6 while that of the fully denatured form was consistent with the calculated value of 5.2. The denaturation was reversible depending upon the protein to detergent ratios. The photoreactive fatty acid partitions into the outer membrane, resulting in extensive photolabeling of the lipid; a high affinity fatty acid binding site is not apparent in total membranes labeled using free fatty acids due to this large capacity of the outer membrane. However, when the free fatty acid concentration was controlled by supplying it as a bovine serum albumin complex, the *fadL* protein exhibited saturable high affinity fatty acid binding, having an apparent K_d for the probe of 63 nM. The specific labeling of the *fadL* protein was increased as the pH was decreased from 8.0 to 6.5; this labeling was abolished by diethylpyrocarbonate (DEPC) pretreatment of total membranes, suggesting that binding of fatty acids to the substrate binding site of the *fadL* protein involves an electrostatic interaction, possibly with a histidine residue.

The photoreactive fatty acid is easily capable of identifying a membrane-bound fatty acid binding protein. Despite increasing the sensitivity of the method 500-fold, no evidence was found for the presence of a fatty acid binding protein in the inner membrane of *E. coli* which is consistent with the proposal that fatty acid permeation across the plasma membrane is not protein-mediated but occurs by a simple diffusive mechanism. A fatty acid binding protein was also not detected in the periplasm, the aqueous compartment that separates the inner and outer membrane of *E. coli*.

The fatty acid uptake activity in *E. coli* was reduced upon starvation whereas proline uptake was not affected. This effect was not due to de-energization of the membrane, depletion of intracellular ATP, or changes in the total amount of fatty acyl-CoA synthetase which is required for fatty acid uptake. The inhibitory effect of starvation was rapidly reversed by the addition of D-lactate, L-lactate, succinate or acetate. Fatty acid uptake was insensitive to concentrations of the uncoupler carbonyl cyanide m-chlorophenylhydrazone which abolished the $\Delta\mu_{H+}$ dependent proline uptake, suggesting that the rate-limiting step is not directly coupled to or affected by the magnitude of $\Delta\mu_{H+}$. The stimulatory effect of D-lactate on oleate uptake increased the affinity of the transport system for fatty acid and the maximal rate of uptake, the K_t values being 37.0 and 10.6 μM and the maximal rates being 0.29 and 2.30 nmole/min/mg of protein in the absence and in the presence of D-lactate, respectively. This clearly shows that the saturable, rate-limiting step is protein-mediated and is being affected by starvation and D-lactate. The *fadL*

protein is not rate-limiting nor is permeation of the periplasmic space or the inner membrane since no fatty acid binding proteins were detected with the photoreactive fatty acid probe in these compartments. The fatty acid taken up by the starved and D-lactate activated cells was used for cellular phospholipid and fatty acyl-CoA syntheses; the levels of fatty acyl-CoA were approximately 100-fold lower than the phospholipid levels which suggest that fatty acyl-CoA synthetase is involved in the rate-limiting step in the overall process. The fatty acyl-CoA and phospholipid levels were both stimulated in response to D-lactate; the fact that in such activated cells the level of fatty acyl-CoA was increased despite the higher rate of its utilization in phospholipid synthesis shows that fatty acyl-CoA synthetase is the step being regulated. This is consistent with the above interpretation that fatty acyl-CoA synthetase is rate-limiting in fatty acid uptake. The regulation of fatty acid uptake by starvation and D-lactate is therefore likely due to regulation of fatty acyl-CoA synthetase activity.

Investigation into the mechanism of regulation of fatty acyl-CoA synthetase showed that D-lactate did not affect the activity of the enzyme directly. However, fatty acyl-CoA synthetase was found to be activated by about 20-fold by Triton X-100 and by another 4-fold by the addition of bacterial membranes devoid of endogenous enzyme. It was shown that fatty acyl-CoA synthetase is co-isolated with the inner membrane in the presence of D-lactate but not in its absence; these results suggest that recruitment of the enzyme to the inner membrane by D-lactate results in its activation and consequently in the increased level of fatty acid uptake.

The involvement of fatty acyl-CoA synthetase in fatty acid uptake was studied directly using inner membrane vesicles. The vesicles were characterized functionally by assessing proline uptake. The uptake of proline in vesicles prepared from cells grown on oleate, glucose and palmitate was dependent on the state of energization of the membrane, indicating that these vesicles are functionally comparable to those prepared by others. It was determined that vesicles prepared from cells grown on oleate were destabilized by freeze-thawing which is required for trapping CoASH and ATP, while those prepared from glucose and palmitate grown cells were not. Fatty acid uptake in palmitate vesicles containing fatty acyl-CoA synthetase was dependent on exogenously trapped ATP and CoASH. These results demonstrate that fatty acyl-CoA synthetase is directly involved in fatty acid uptake in *E. coli* and suggest that the observed effects of starvation and D-lactate on oleate uptake in whole cells are related to regulation of fatty acyl-CoA synthetase. This *in vitro* system will allow for the study of the recruitment of fatty acyl-CoA synthetase to the inner membrane by D-lactate, succinate, L-lactate, acetate and their metabolites.

ACKNOWLEDGEMENTS

I would like to thank the members of my committee, Drs. R.M. Epand, R.A. Bell and R.A. Rachubinski for their helpful discussion and support. I wish to thank Dr. G.E. Gerber for his patience, support, encouragement and most importantly for his belief in my abilities.

I thank my friends, Robert Morton, Pierre Leblanc, Bernard Trigatti, Geoff Werstuck, James Cheetham, Darryl Pickering and Dan Syroid for making my stay at McMaster a memorable and enjoyable one. Special thanks are extended to my family, Frank and Pat.

I am indebted to Bonnie Murphy for her many hours spent typing the manuscript. I would also like to acknowledge Elizabeth Kim, Krishan Rajaratnam and Steve Casha for their excellent technical assistance.

Lastly, I wish to acknowledge the financial support of McMaster University.

TABLE OF CONTENTS

LIST OF FIGURES AND TABLES

FIGURES

LIST OF ABBREVIATIONS

g	acceleration of gravity
ATP	adenosine 5'-triphosphate
BSA	bovine serum albumin
CCCP	carbonyl cyanide m-chlorophenylhydrazone
cFABP	cytosolic fatty acid binding protein
$CHCl_3$	chloroform
CoASH	coenzyme A
Ci	curie
DEPC	diethylpyrocarbonate
DNase	deoxyribonuclease
DIDS	diisothiocyanostilbene-2,2'-disulfonate
DMF	dimethylformamide
K_d	dissociation constant
E	*Escherichia*
EDTA	ethylenediaminetetraacetate
fad	fatty acid degradative
g	gram
HMPA	hexamethylphosphoramide
h	hour
pI	isoelectric point
kDa	kilodalton

LPS	lipopolysaccharide
DAP	m-diazirinophenoxy
V_{max}	maximum velocity
MSH	mercaptoethanol
MeOH	methanol
μ	micro
μl	microlitre
μmole	micromole
mCi	millicurie
mmole	milligram
mg	milligram
ml	millilitre
min	minute
molar	moles/litre
MNNG	N-methyl-N'-nitro-N-nitrosoguanidine
nm	nanometer
nM	nanomolar
nmole	nanomole
$NADH^+$	nicotinamide adenine dinucleotide
NMR	nuclear magnetic resonance
pmole	picomole
PAGE	polyacrylamide gel electrophoresis

Brij	polyoxyethylene 20 cetyl ether
$\Delta\mu_{H+}$	proton electrochemical potential
K_t	rate constant of transport
$FADH_2$	reduced flavin adenine dinucleotide
R_f	retardation factor
rpm	revolution per minute
RNase	ribonuclease
SDS	sodium dodecyl sulfate
TLC	thin-layer chromatography
Tris	tris(hydroxymethyl) aminomethane
2-D	2-dimension

LIST OF PUBLICATIONS

Articles

1. Mangroo, D. and Gerber, G.E. (1988) Phospholipid synthesis: Effects of solvents and catalysts on acylation. Chem. Phys. Lipids 48: 99-108.

2. Morton, R.C., Mangroo, D. and Gerber, G.E. (1988) A novel method of complete activation by carboxyldiimidazole: application to ester synthesis. Can. J. Chem. 66: 1701-1705.

3. Mangroo, D. and Gerber, G.E. (1990) Synthesis of acyl-CoA thioesters. Biochem. & Cell Biol. 68: 308-312.

4. Nuttley, W.M., Bodnar, A.G., Mangroo, D. and Rachubinski, R.A. (1990) Isolation and characterization of membranes from oleic acid-induced peroxisomes of *Candida tropicalis*. J. Cell Sci. 95: 463-470.

5. Trigatti, B.L., Mangroo, D. and Gerber, G.E. (1991) Photoaffinity labeling and fatty acid permeation in 3T3-L1 adipocytes. J. Biol. Chem., 266, 22621-22625.

6. Mangroo, D. and Gerber, G.E. (1992) Photoaffinity labeling of fatty acid binding proteins involved in long chain fatty acid transport in *E. coli*. J. Biol. Chem., 267, 17095-17101.

Manuscripts Submitted

7. Mangroo, D. and Gerber, G.E. (1992) Fatty acid uptake in *E. coli*: Regulation by acyl-CoA synthetase activity. Submitted to Biochemistry.

8. Mangroo, D., and Gerber, G.E. (1992) Fatty acid uptake in *E. coli*: Regulation by recruitment of fatty acyl-CoA synthetase to the plasma membrane. Submitted to Biochemistry and Cell Biology.

9. Gerber, G.E., Mangroo, D., and Trigatti, B.L. (1992) Identification of high affinity membrane-bound fatty acid binding sites using photoreactive fatty acid. Submitted to Molecular and Cellular Biochemistry.

10. Mangroo, D., Steele, L., Rachubinski, R.A. and Gerber, G.E. (1992) Specific labeling of Candida Tropicalis peroxisomal proteins with photoreactive fatty acid derivatives. Submitted to Biochem. Biophys. Acta.

Abstracts

1. Nuttley, W.M., Bodnar, A.G., Mangroo, D. and Rachubinski, R.A. (1989) Isolation of membranes from peroxisomes of oleic acid-grown *Candida tropicalis* pK 233. Characterization of the polypeptide and lipid compositions. Yeast Cell Biol. pp. 204, Cold Spring Harbor, NY.

2. Mangroo, D. and Gerber, G.E. (1991) Fatty acid uptake in *E. coli*. Recruitment of acyl-CoA synthetase to the plasma membrane. FASEB J. 5, 6602.

3. Mangroo, D. and Gerber, G.E. (1991) Fatty acid uptake in *E. coli*: Identification of the rate limiting saturable step. Proc. Can. Fed. Biol. Soc. 34, 85.

4. Trigatti, B.L., Mangroo, D. and Gerber, G.E. (1991) Fatty acid uptake and photoaffinity labeling of fatty acid binding proteins in 3T3-L1 adipocytes. Proc. Can. Fed. Biol. Soc. 34, 84.

5. Gerber, G.E., Mangroo, D. and Trigatti, B.L. (1992) Identification of fatty acid binding sites using photoreactive fatty acid. FABP 2nd Int. Workshop, The Netherlands.

1.0. INTRODUCTION

1.1. Structural Organization of the Cell Envelope of *E. coli*

The cell surface of *E. coli*, a gram-negative bacterium, consists of an inner and an outer membrane separated by an aqueous compartment called the periplasmic space, and a peptidoglycan layer. The peptidoglycan layer, located in the periplasm is composed of a complex network of oligosaccharides and proteins and confers rigidity to the cell (Fig. 1) (Nikaido and Vaara, 1985).

The inner or plasma membrane is composed of 60-70% proteins, 30-40% phospholipids and approximately 1% carbohydrates (Kaback, 1971). The major class of phospholipids is phosphatidylethanolamine (65-70%) however, there are significant amounts of diphosphatidylglycerol (15%), phosphatidylglycerol (10-15%), phosphatidic acid (5-10%) and phosphatidylserine (5%) (Kaback, 1971).

The outer membrane of *E. coli* is not a typical biological membrane; the inner leaflet contains phospholipids whereas the outer leaflet is composed predominantly of lipopolysaccharides (Hancock, 1984; Nikaido and Vaara, 1985). Lipopolysaccharide (LPS) is amphipathic in nature and contains 5 or 6 fatty acids attached to the hydrophobic diglucosamine phosphate backbone (Lipid A) (Fig. 2). The hydrophilic oligosaccharide core which is attached to Lipid A, contains 2-keto-3-deoxyoctanoate and a variety of heptoses and hexoses (Fig. 3) (Hancock, 1984; Nikaido and Vaara, 1985). This complex organization of the cell envelope of *E. coli* renders the cells impermeable to both hydrophobic and hydrophilic substrates.

1.2. Transport Mechanisms in *E. coli*

Transport of metabolically important substrates across cell membranes can occur by passive or facilitated diffusion or by active transport. Passive diffusion does not involve a protein and is defined as the movement of a molecule down its electrochemical or concentration gradient without the expediture of energy. The rate of diffusion of a compound across the lipid bilayer is dependent on its hydrophobicity and is proportional to the concentration gradient across the membrane. This process lacks specificity and is not saturable. Facilitated diffusion is also not energy-dependent; however, in that process, the movement of a molecule down its electrochemical or concentration gradient is catalyzed by a permease in the membrane. This process is much faster than passive diffusion and exhibits specificity and saturability. Active transport involves the movement of a solute against an electrochemical or concentration gradient. This process is catalyzed by a permease in the membrane and requires energy. This mechanism, like facilitated diffusion, exhibits specificity and saturability (Wilson, 1978).

1.2.1 Permeation of Solutes across the Outer Membrane

The outer membrane is highly permeable to small hydrophilic molecules (600 daltons and less) due to non-specific aqueous channels called porins (Fig. 1) (Nikaido and Vaara, 1985). The diffusion rate of small negatively charged molecules however, is considerably slower than that of positively charged molecules (Nikaido and Vaara, 1985); this is thought to occur as a result of the presence of a Donnan potential (negative inside) which is generated by the presence of the highly negatively charged

membrane-derived oligosaccharides (Nikaido and Vaara, 1985). Permeation of larger hydrophilic compounds such as vitamins, nucleosides and maltose across the outer membrane are facilitated by specific proteins (Nikaido and Vaara, 1985); the maltose specific (*LamB*) and nucleoside specific (*Tsx*) outer membrane proteins were shown to have substrate binding sites (Luckey and Nikaido, 1980b; Maier *et al.*, 1988) and to form channels (Boehler-Kohler *et al.*, 1979; Nakae, 1979; Luckey and Nikaido, 1980a; Maier *et al.*, 1988)

In contrast, the outer membrane serves an impermeable barrier to hydrophobic compounds including detergents, antibiotics and long chain fatty acids (Nikaido and Vaara, 1985). This unusual property of the outer membrane was shown to be related to the highly negatively charged lipopolysaccharides bound to the extracellular face of the outer membrane (Fig. 1) (Nikaido and Vaara, 1985). However, the mechanism by which LPS affects the permeability of hydrophobic compounds across the outer membrane is unclear.

LPS is anchored to the outer membrane by non-covalent interaction with outer membrane proteins and by divalent cation cross-bridging of adjacent LPS molecules (Hancock, 1984; Nikaido and Vaara, 1985). Chelation of magnesium ions with EDTA (ethylenediaminetetraacetate) in alkaline Tris buffer results in the removal of LPS and disruption of the outer membrane. This was shown to increase the permeability of the outer membrane towards hydrophobic compounds. Furthermore, it was shown that outer membranes containing LPS with smaller hydrophilic oligosaccharide cores are permeable to hydrophobic compounds (Nikaido

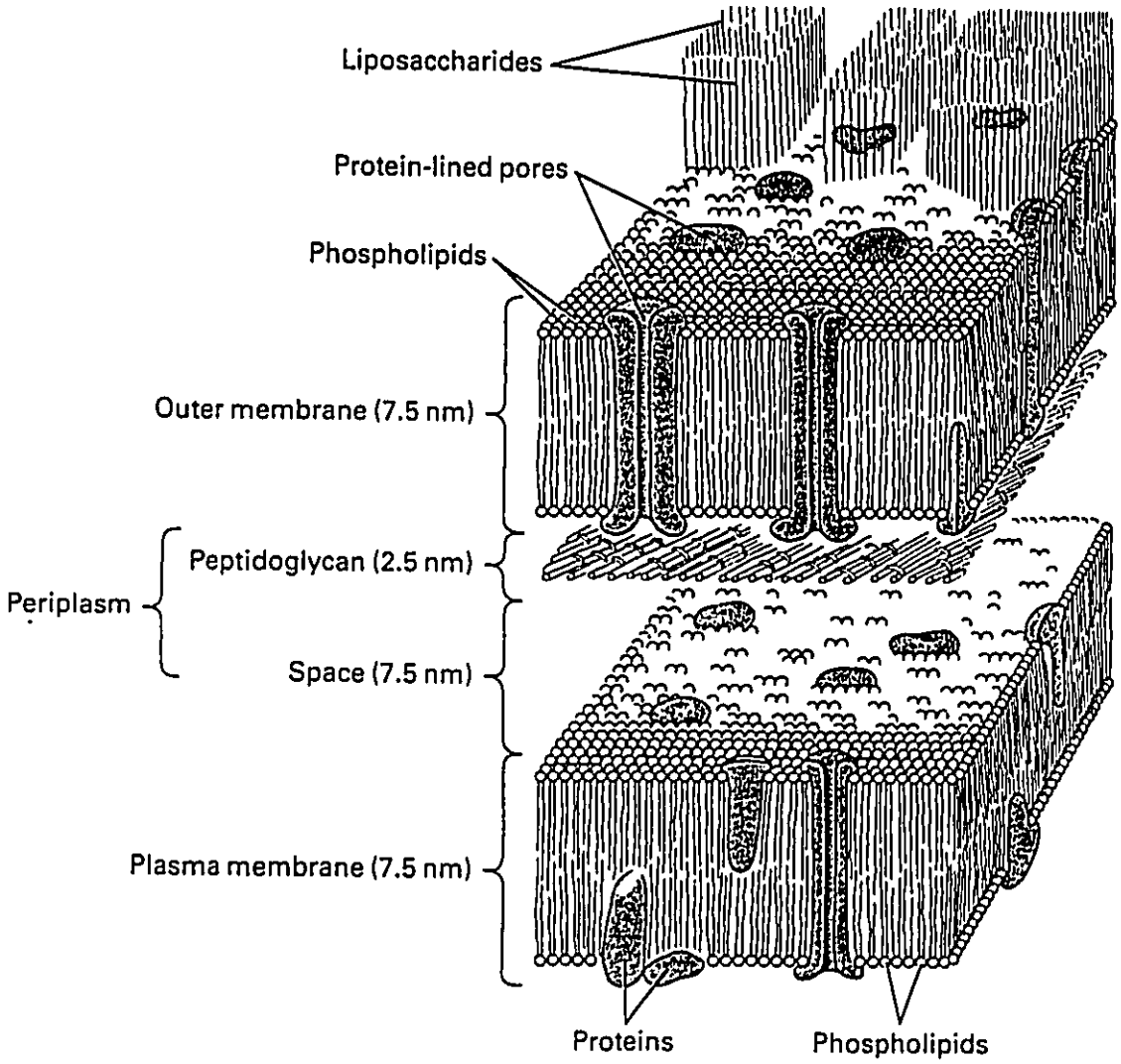

Figure 1. Structural organization of the cell envelope of *E. coli*. Taken directly from Darnell et al. (1986).

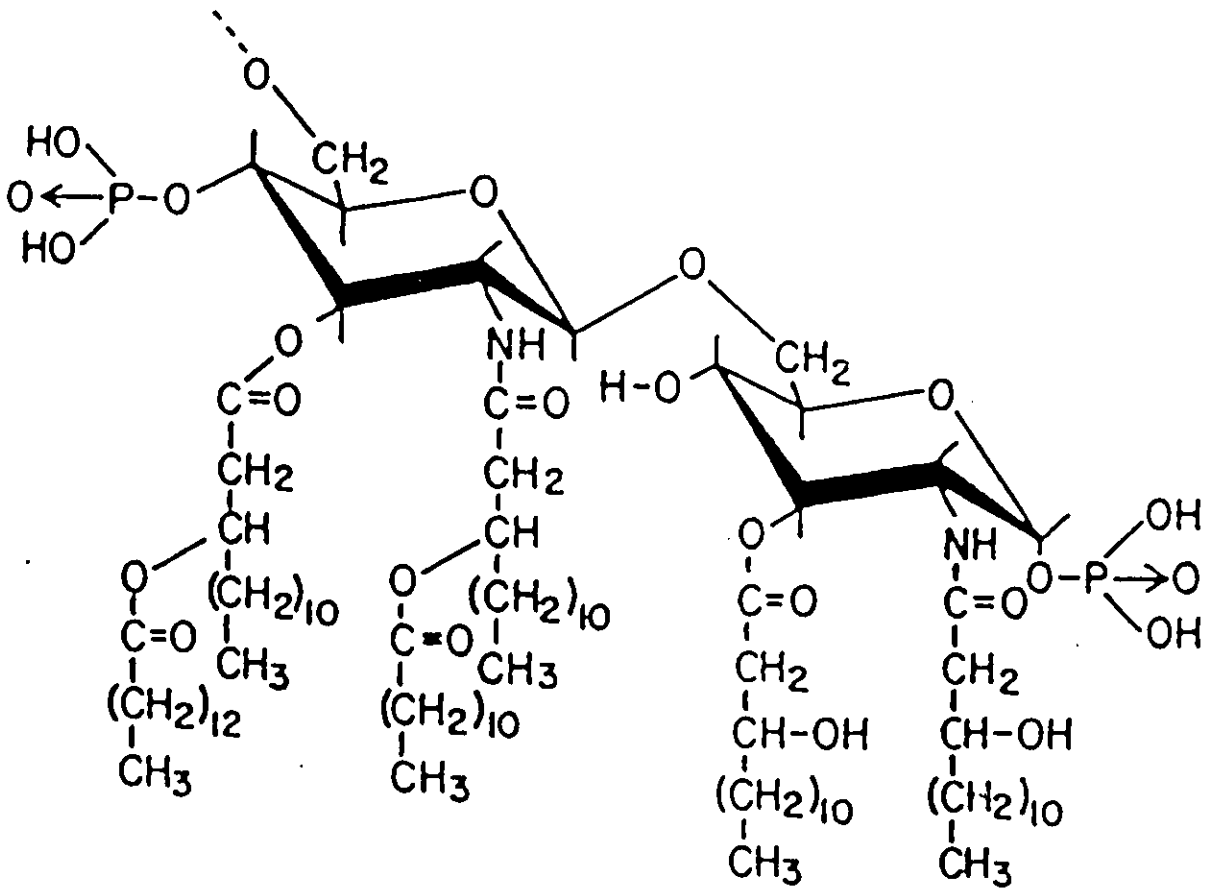

Figure 2. Structure of Lipid A. Taken directly from Nikaido and Vaara (1985).

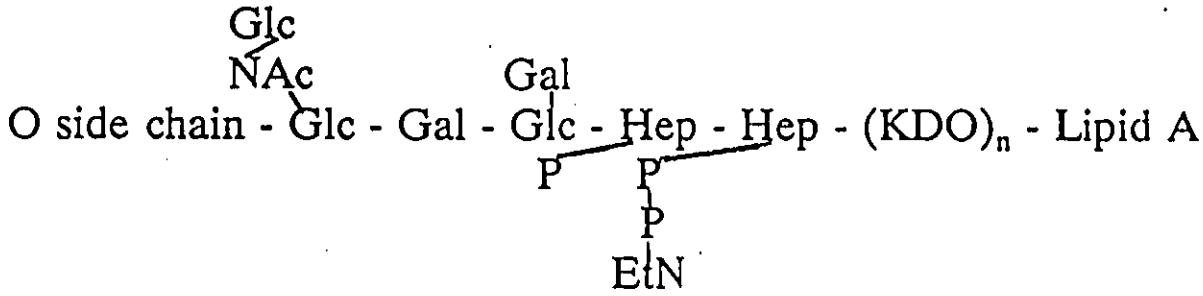

Figure 3. Structure of the hydrophilic oligosaccharide core of LPS. Modified from Nikaido and Vaara (1985).

and Vaara, 1985; Vaara *et al.*, 1990). Based on these observations it was suggested that the divalent cation bridging of LPS and the large hydrophilic surface of the cell provided by the negative charge of LPS may be responsible for the poor permeability of the outer membrane to hydrophobic compounds (Hancock, 1984; Nikaido and Vaara, 1985).

1.2.2. Permeation of solutes across the Inner Membrane

The inner membrane, unlike the outer membrane, is impermeable to almost all solutes. Permeation of metabolically important substrates across the inner membrane is facilitated by specialized active transport systems. These systems are grouped into three major classes: periplasmic binding protein system, membrane-bound system and group translocation (Wilson, 1978).

1.2.2.1 Periplasmic Binding Protein Transport Systems

Transport systems in this class are typically composed of three inner membrane-bound proteins and one periplasmic substrate binding protein (Ames, 1986). Transport is inactivated by osmotic shock due to the loss of the periplasmic binding protein (Wilson, 1978). Examples of periplasmic binding protein transport systems are those for histidine, maltose, branched-chained amino acids, oligopeptides, ribose, β-methyl galactoside and phosphate (Ames, 1986). However, the most studied are the histidine and maltose transport systems.

In general, periplasmic binding proteins have a high affinity for their substrate; they are very stable and are present in large quantities (Ames, 1986). The inner membrane-bound components are present in small quantities (Ames, 1986). The

membrane bound components of the maltose transport system, *malG* and *malF* are integral membrane proteins whereas *malK* is a peripheral membrane protein. In contrast, the membrane bound components of the histidine transport system *hisP*, *hisQ* and *hisM* are all integral membrane proteins (Ames, 1986). It was postulated that the three membrane-bound components form a complex.

The *malK* and *hisP* proteins are homologous to each other and two highly conserved regions (designated site A and B) show homology to the ATP-binding sites of several proteins, including the proton translocating ATPase, adenylate cyclase and RecA protein (Ames, 1986). Biochemical characterizations have shown that the *malK* and *hisP* proteins have at least one nucleotide binding site and that ATP is the natural substrate (Ames, 1986).

Biophysical studies have shown that the histidine (*hisJ*) and maltose (*malE*) binding periplasmic proteins undergo conformational changes upon substrate binding (Ames, 1986). Although it was never shown directly, genetic evidence suggests that this conformational change may expose a region of the binding protein which is crucial for interacting with one of the inner membrane components; genetic evidence suggests that the loaded *hisJ* protein may be interacting with the membrane-bound *hisP* protein (Ames, 1986). Based entirely on indirect evidence it was postulated that interaction of the loaded periplasmic binding protein with the membrane-bound component leads to release of the substrate from the periplamsic protein and exposure of binding site (s) on the membrane-bound component (s).

The uptake of histidine and maltose is energy-dependent. Because *hisP* and

malK are both capable of binding ATP, it was believed that uptake is dependent on ATP rather than directly on the electrochemical potential of the membrane (Ames, 1986). However, it has never been demonstrated that uptake is coupled to ATP hydrolysis. Recently, reconstitution of the maltose (Dean *et al.*, 1989; Davidson and Nikaido, 1990) and histidine (Bishop *et al.*, 1989; Prossnitz *et al.*, 1989) transport systems in inner membrane vesicles as well as in proteoliposomes have clearly shown that transport is ATP dependent.

1.2.2.2. Membrane-bound Transport Systems

The substrates transported by members of this class are not chemically modified and all of the proteins involved are firmly bound to the membrane. Transport is not inactivated by osmotic shock (Wilson, 1978; Ames, 1986). The best characterized example of this class of transport system in *E. coli* is the lactose transport system.

Transport of β-galactosides across the inner membrane is coupled to the electrochemical potential and is catalyzed by a protein (lac permease) encoded by the *lacY* gene (Kaback, 1986; Kaback, 1992). This protein, a beta-galactoside -H^+ symporter uses the electrochemical potential across the inner membrane as the driving force (Kaback, 1986; Kaback, 1992).

The *lac* permease consists of 417 amino acid residues; limited proteolysis, site-directed immunological studies, laser Raman and Fourier transform infrared spectroscopy, chemical modification, circular dichroism and studies with lac permease-alkaline phosphatase fusion proteins indicated that the protein is made up

of 12 hydrophobic alpha-helical segments (Kaback, 1992). Site-directed-mutagenesis suggested that Arg302 of segment 9 and Glu325 and His322 of segment 10 are involved in the translocation of the H^+ during lactose transport. Further, Arg302 and His322 may also be part of the substrate binding site (Kaback, 1991).

1.2.2.3. Group Translocation Transport System

Group translocation couples transport of the molecule with chemical modification. The uptake of D-glucose and certain other sugars across the inner membrane of *E. coli* is mediated by vectorial phosphorylation *via* the phosphoenolpyruvate-phosphotransferase system (PTS). This system catalyzes the transfer of phosphate from P-enolpyruvate via specific proteins to the appropriate sugar being translocated across the inner membrane by specific permeases (Dills *et al.*, 1980).

1.3. Fatty Acid Uptake and Metabolism in *E. coli*

The outer membrane of *E. coli* is impermeable to long chain fatty acids (C_{11} to C_{18}). Despite this barrier, *E. coli* can grow on these as a sole carbon source due to the co-ordinated expression of enzymes involved in both fatty acid uptake and metabolism (Overath *et al.*, 1967; Overath *et al.*, 1969; Weeks *et al.*, 1969; Klein *et al.*, 1971; Hill and Anglemaier, 1972). The genes encoding the proteins for fatty acid uptake and metabolism are located in different regions of the chromosome and make up a regulon called the *fad* regulon (Overath *et al.*, 1967; Klein *et al.*, 1971; Hill and Anglemaier, 1972; Nunn and Simons, 1978).

1.3.1. Regulation of the *fad* Regulon

The enzymes of the *fad* regulon are expressed when *E. coli* is grown on long chain fatty acids (C_{11}-C_{18}) (Overath *et al.*, 1967; Overath *et al.*, 1969; Weeks *et al.*, 1969; Klein *et al.*, 1971; Nunn *et al.*, 1979) but not by medium chain fatty acids (C_7-C_{10}) even though they can serve as substrates for metabolism (Overath *et al.*, 1967; Overath *et al.*, 1969; Weeks *et al.*, 1969). Mutants capable of growth on both long and medium chain fatty acids have been isolated; these mutants express the *fad* regulon constitutively (Overath *et al.*, 1969; Weeks *et al.*, 1969; Simons *et al.*, 1980a; Simons *et al.*, 1980b). It was postulated that they contained lesions in a gene encoding some regulatory element which was called *fadR* (Overath *et al.*, 1969).

The gene for *fadR* was mapped to 25.5 min on the chromosome (Simons *et al.*, 1980a) and has been cloned (DiRusso and Nunn, 1985) and sequenced (DiRusso, 1988). It codes for a single polypeptide having a molecular mass of 26,954 daltons calculated from the deduced protein sequence (DiRusso, 1988). A helix-turn-helix motif, typical of regulatory proteins which bind DNA is located in a 20 amino acid segment near the N-terminus (DiRusso, 1988). The *fadR* protein was shown to act as a repressor (Simons *et al.*, 1980a; Simons *et al.*, 1980b). Moreover, using the *lacZ* gene fused to the *fadABC*, *fadE* and *fadL* genes, it was clearly shown that the *fadR* protein regulates expression of the *fad* regulon at the transcriptional level (Clark, 1981; Sallus *et al.*, 1983; Nunn, 1986a). In addition to the *fad* regulon, the *fadR* protein negatively regulates the expression of the enzymes involved in acetate metabolism (*ace* operon) (Maloy *et al.*, 1980; Maloy and Nunn, 1981; Maloy and

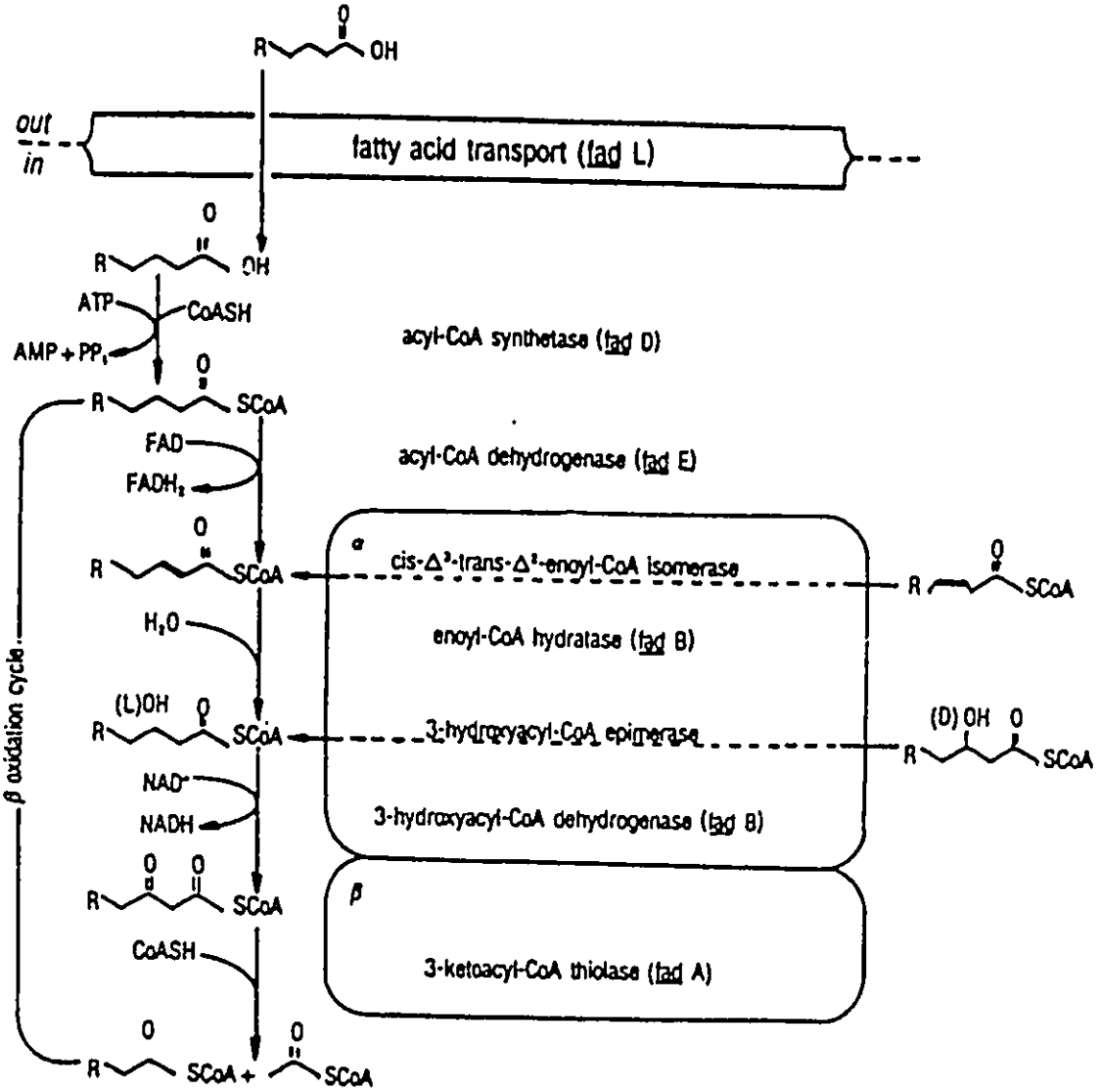

Figure 4. Fatty acid oxidation pathway. Taken directly from Nunn (1986a).

Nunn, 1982; Nunn, 1986a) and positively regulates the expression of the enzymes required for unsaturated fatty acid biosynthesis (Nunn *et al.*, 1983, Nunn, 1986a).

1.3.2. Fatty Acid Metabolism

Fatty acids are degraded by the β-oxidative pathway (Fig. 4). The first step is activation of the fatty acid to the fatty acyl-CoA derivative. This reaction is dependent on ATP and CoASH and is catalyzed by fatty acyl-CoA synthetase. This enzyme is essentially cytosolic (Kameda and Nunn, 1981) and is encoded by the *fadD* gene (Overath *et al.*, 1969). Purification and subsequent biochemical characterization of the enzyme showed that the native fatty acyl-CoA synthetase has a molecular mass of 130 kDa and a monomeric molecular mass of 47 kDa (Kameda and Nunn, 1981). The purified enzyme has been shown to have specificity for fatty acids of various chain lengths (Kameda and Nunn, 1981). The *fadD* gene was recently cloned (Black, 1991).

The fatty acyl-CoA is dehydrogenated to the corresponding α, β unsaturated fatty acyl-CoA by fatty acyl-CoA dehydrogenase. During this reaction one molecule of reduced flavin adenine dinucleotide ($FADH_2$) is produced. Although it is known that fatty acyl-CoA dehydrogenase is encoded by the *fadE* gene, very little is known about this enzyme.

The α, β unsaturated fatty acyl-CoA is hydrated to form β-hydroxy fatty acyl-CoA. The oxidation of the hydroxy fatty acyl-CoA to the 3-ketoacyl-CoA is accompanied by the reduction of one molecule of nicotinamide adenine dinucleotide ($NADH^+$). The 3-ketoacyl-CoA then undergoes thiolytic cleavage to give acetyl-CoA

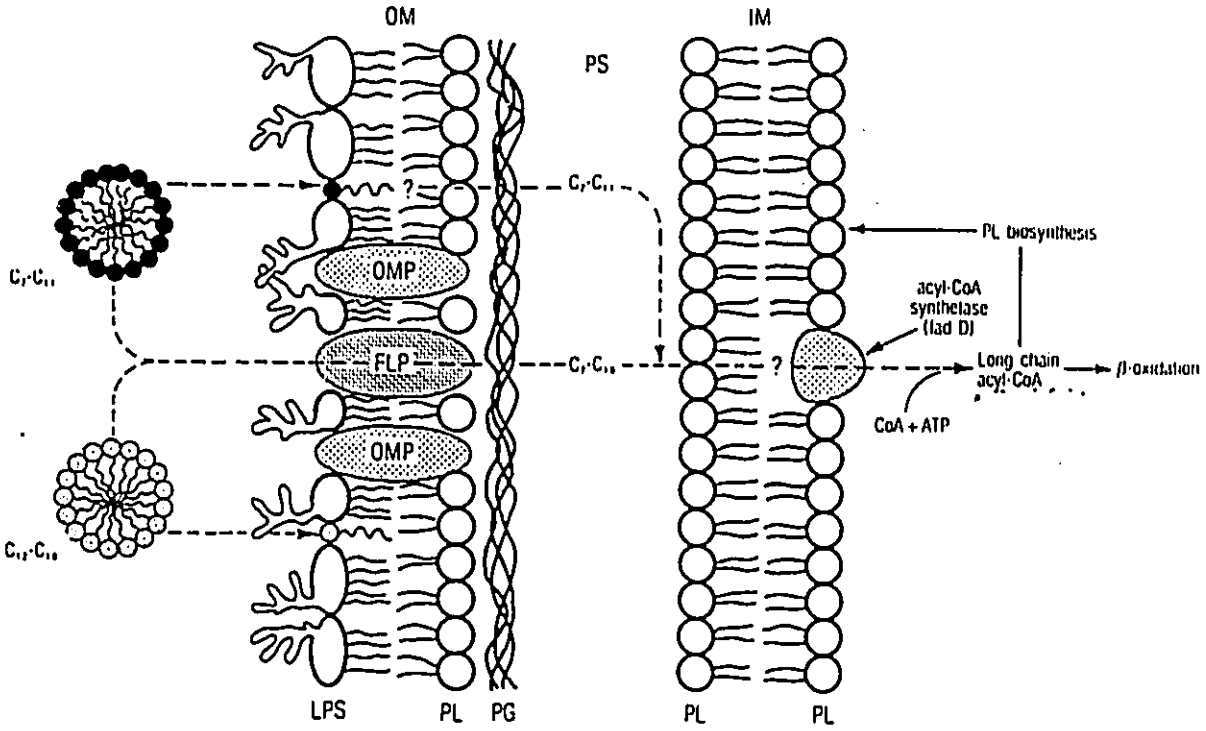

Figure 5. Model of fatty acid uptake in *E. coli*. Taken directly from Nunn (1986a).

and a two carbon shorter acyl-CoA which re-enters the cycle at the second step (Nunn, 1986).

The hydration, oxidation and thiolytic cleavage steps are catalyzed by enoyl-CoA hydratase, 3-hydroxyacyl-CoA dehydrogenase and 3-ketoacyl-CoA thiolase, respectively. These enzymes together with the isomerase and the epimerase are part of a multienzyme complex (Binstock *et al.*, 1977; O'Brien and Frerman, 1977; Pramanik *et al.*, 1979; Pawar and Schultz, 1981; Feigenbaum and Schultz, 1985). This complex was purified and found to have an $\alpha_2\beta_2$ arrangement; the α subunit has a molecular mass of 78 kDa and the β subunit has a molecular mass of 42 kDa (Binstock *et al.*, 1977; Pramanik *et al.*, 1979; Pawar and Schultz, 1981). Thiolase activity was shown to be associated with the 42 kDa β subunit whereas the other four activities are associated with the 78 kDa α subunit (Binstock *et al.*, 1977; Praminik *et al.*, 1979; Binstock and Schultz, 1981; Pawar and Schultz, 1981; Spratt *et al.*, 1984). The α and β subunits are encoded by the *fadB* and the *fadA* genes, respectively (Spratt *et al.*, 1984), which have been cloned (Spratt *et al.*, 1984) and sequenced (DiRusso, 1990).

1.3.3. Mechanism of Fatty Acid Uptake

The uptake of long chain fatty acids in *E. coli* was shown to occur by a saturable and energy-dependent process (Frerman and Bennet, 1973; Maloy *et al.*, 1981; Kameda *et al.*, 1987). Genetic analysis has shown that this process involves fatty acyl-CoA synthetase, the first enzyme of the β-oxidation pathway (Fig. 5) (Klein *et al.*, 1971). Subsequent genetic and biochemical characterizations have established

that a 43 kDa protein encoded by the *fadL* gene was also required for fatty acid uptake (Nunn and Simons, 1978; Nunn *et al.*, 1979; Ginsburg *et al.*, 1984). The *fadL* protein was purified to homogeneity and shown unambiguously to be located in the outer membrane (Fig. 5) (Black *et al.*, 1985; Black, 1988). This protein has an apparent isoelectric point (pI) of 4.6 (Ginsburg *et al.*, 1984) and exhibits a heat-modifiable behaviour on sodium dodecyl sulfate polyacrylamide gel electrophoresis (SDS-PAGE) (Black et al., 1985) which is typical of outer membrane proteins of *E. coli* (Schnaitman, 1973; Nakamura and Mizushima, 1976); the *fadL* protein has a molecular mass of 33 kDa when solubilized at 25°C in the presence of SDS whereas solubilization at 100°C (in the presence of the same amount of SDS) causes the protein to migrate more slowly, exhibiting a molecular mass of 43 kDa on SDS-PAGE (Black *et al.*, 1985).

1.3.3.1. Cloning and Sequencing of the *fadL* Protein

The gene for the *fadL* protein has been cloned (Black *et al.*, 1985) and sequenced (Black, 1991). It contains a region of hyphenated dyad symmetry at -74 (5'-TTTCTTAGATCATATTTGAAA-3') which has some homology to sequences involved in binding of cyclic AMP and catabolite gene activator protein (Black, 1991). Two other regions of hypenated dyad symmetry were found at positions +12 (5'-TCTAAGATGTACCTCAGA-3') and +44 (5'-CTCTGTTACAGCACGTAACATAG-3'), respectively; it is thought that these regions may play a role in the regulation of the *fadL* gene (Black, 1991).

The molecular mass of the *fadL* protein deduced from the DNA sequence is

48,831 daltons. The first 27 amino acid residues contain features common to the signal sequence of other outer membrane proteins; the sequence has a charged segment followed by a hydrophobic segment and a signal peptidase I recogonition site Ala-Trp-Ser (Black, 1991). Comparison of the predicted amino acid sequence of the *fadL* protein to that of other outer membrane proteins showed that the *fadL* protein is significantly homologous only to the P1 outer membrane protein of *H. influenzae* type b bacteria (Black, 1991).

1.3.3.2. Role of the *fadL* protein in Fatty Acid Permeation of the Outer Membrane

It was shown that the rate of oleate uptake in *fadL* deficient cells complemented with the cloned gene was much higher (2-3-fold) than cells expressing wild-type *fadL* protein (Black *et al.*, 1985). Binding analyses using cells that are unable to transport fatty acids due a defect in fatty acyl-CoA synthetase showed that *fadL*$^+$ cells were capable of binding 4-7 times more fatty acid than *fadL* cells (Nunn *et al.*, 1986; Black, 1990). Furthermore, antibodies against the *fadL* protein partially inhibited fatty acid binding to *fadD fadL*$^+$ cells (Black, 1991). Based on these findings it was proposed that the *fadL* protein functions as a long chain fatty acid receptor. Linker mutagenesis studies suggested that in addition to its receptor function, it may also act as a fatty acid translocase (Kumar and Black, 1991); this study also provided evidence suggesting that a region at the N-terminus of the *fadL* protein is important for long chain fatty acid binding while a region at its C-terminus is involved in translocation.

1.3.3.3. Mechanism of Fatty Acid Permeation of the Plasma Membrane of *E. coli*

Protein-mediated translocation of many solutes across the plasma membrane of *E. coli* is rate-limiting in their uptake and coupled to the electrochemical potential (Wilson, 1978; Ames, 1986; Kaback, 1986; Kaback, 1991). Fatty acid uptake has been reported to be inhibited when the membrane potential was abolished by uncouplers (Frerman and Bennet, 1973; Maloy *et al.*, 1981; Kameda *et al.*, 1987), and to increase as the magnitude of the proton gradient was increased (Kameda *et al.*, 1987); this led to the proposal that translocation of fatty acids across the plasma membrane may be rate-limiting and involve a proton-fatty acid co-transporter.

1.4. Fatty Acid Uptake in Eukaryotic Cells

Fatty acid uptake in Ehrlich Ascites tumor cells (Spector *et al.*, 1965) adipocytes (Abumrad *et al.*, 1981; Abumrad *et al.*, 1984; Schwieterman *et al.*, 1988; Sorrentino *et al.*, 1989), 3T3-L1 adipocytes (Trigatti *et al.*, 1991) hepatocyte (Stremmel *et al.*, 1985a; Stremmel and Berk, 1986b; Stremmel, 1987; Potter *et al.*, 1989; Sorrentino *et al.*, 1989), heart myocyte (Stremmel, 1988; Sorrentino *et al.*, 1989; Stremmel, 1989), alveolar type II cells (Maniscalco *et al.*, 1990), jejunum (Stremmel *et al.*, 1985), and *Candida tropicalis* (Trigatti *et al.*, 1992), occurs by a high affinity and saturable process (Stremmel *et al.*, 1986; Stremmel, 1987). Limited proteolysis (Mahadevan and Sauer, 1974; Stremmel and Berk, 1986) and α-bromo-palmitate treatment (Mahadevan and Sauer, 1971; Mahadevan and Sauer, 1974) of the plasma membrane of intact hepatocytes, and treatment of adipocytes with 4,4'-diisothiocyanostilbene-2,2'-disulfonate (DIDS) and sulfo-N-succinimidyl derivatives

of fatty acids (Abumrad *et al.*, 1984; Harmon *et al.*, 1990) resulted in substantial loss of fatty acid uptake. It was therefore proposed that permeation of fatty acids across the plasma membrane involves a protein and is the saturable, rate-limiting step in the overall process instead of fatty acid metabolism.

1.4.1. Possible Involvement of a 40 kDa Protein, a 85 kDa Protein and a 22 kDa Protein in Fatty Acid Permeation of the Plasma Membrane

A 40 kDa protein, although it is similar to the mitochrondrial glutamate-oxaloacetate transaminase (Berk *et al.*,1990), was presumed to be involved in fatty acid permeation across the membrane since antibodies against this protein, initially isolated from the plasma membrane of hepatocytes, partially inhibited fatty acid uptake in these cells (Stremmel *et al.*, 1985a; Stremmel and Theilman, 1986) and binding to isolated plasma membranes (Stremmel, *et al.*, 1986a). These antibodies were also shown to cross-react with a 40 kDa protein in the plasma membrane of adipocytes (Sorrentino, *et al.*, 1989), heart myoctyes (Sorrentino, *et al.*, 1988) and jejunal microvillous membranes of the gut (Stremmel, *et al.*, 1985b). In addition to the 40 kDa protein, a 85 kDa protein in adipocytes was heavily labeled by DIDS and sulfo-N-succinimidyl derivative of fatty acids which have been shown to result in inhibition of fatty acid uptake (Abumrad *et al.*, 1984; Harmon *et al.*, 1991). The 40 kDa protein or the 85 kDa protein was not detected with a photoreactive fatty acid analogue in the plasma membrane of 3T3-L1 adipocytes; the photoreactive probe did, however, label a 22 kDa protein which appears to be present in small amounts and to have a high affinity for fatty acid (Trigatti *et al.*, 1991).

1.4.2. Fatty Acid Permeation of the Plasma Membrane occurs by Passive Diffusion

The above studies suggest that the 22 kDa, 40 kDa and 85 kDa proteins may be involved in fatty acid uptake. However, the roles of these proteins in the process is not clear. Other studies using erythrocyte ghosts (Broring *et al.*, 1989), heart myocytes (Rose *et al.*, 1989; DeGrella and Light, 1980a, DeGrella and Light, 1980b) and perfused livers (Cooper *et al.*, 1987; Noy *et al.*, 1986) suggest that fatty acid permeation of the plasma membrane occurs by diffusion rather than by a protein-mediated event. Moreover, model membrane studies have shown that long chain fatty acids readily partition into the membrane and undergo flip-flop (Doody *et al.*, 1980; Brecher *et al.*, 1984; Pjura *et al.*, 1984; Hamilton and Cistola, 1986; Storch and Kleinfeld, 1986; Cooper *et al.*, 1989). Flip-flop is thought to be facilitated as a result of the pKa of the fatty acid being increased upon partitioning into the hydrophobic environment of the membrane (Storch and Kleinfeld, 1986). These studies also suggest that fatty acid can cross the lipid bilayer without the involvement of a plasma membrane protein and that desorption of the fatty acid from the membrane would be slow.

1.4.3. Involvement of Low Molecular Weight Cytosolic Fatty Acid Binding Protein

Desorption of fatty acid from the inner leaflet of the plasma membrane was postulated to be rate-limiting in the process of fatty acid uptake in mammalian cells. Indirect evidence suggests that this step may be facilitated by low molecular weight cytosolic fatty acid binding proteins (cFABP) (Brecher *et al.*, 1984; Peeters *et al.*, 1989a; Peeters and Veerkamp, 1989; Trotter and Storch, 1989; Paulussen *et al.*, 1990;

Waggoner and Bernlohr, 1990; Trigatti *et al.*, 1991). These proteins are found in a variety of tissues from different species including human (Ishaque *et al.*, 1982; Das *et al.*, 1988; Jones *et al.*, 1988; Lam *et al.*, 1988; Stewart and Driedzic, 1988; Peeters *et al.*, 1989b; Sa *et al.*, 1989; Schoentgen *et al.*, 1989; Kanada *et al.*, 1989; Baxa *et al.*, 1989; Armstrong *et al.*, 1990; Paulussen and Veerkamp, 1990; Veerkamp *et al.*, 1991) and comprise about 2-5% of all cytosolic proteins (Bass *et al.*, 1985a; Bass *et al.*, 1985b; Paulussen *et al.*, 1989; Veerkamp *et al.*, 1991). The cFABPs vary in size (14-16 kDa) (Veerkamp *et al.*, 1991;) and many of their genes have been cloned and sequenced (Gordon *et al.*, 1983; Lowe *et al.*, 1985; Heuckeroth, *et al.*, 1987; Sweetser *et al.*, 1987; Billich *et al.*, 1988; Tweedie and Edwards, 1989; Veerkamp *et al.*, 1991), indicating that they belong to a family of genes encoding low molecular weight cytosolic proteins involved in binding hydrophobic ligands (Neerkamp, *et al.*, 1991).

The low molecular weight cFABPs were shown to bind fatty acids using fluorescence spectroscopy (Storch *et al.*, 1989; Trotter and Storch, 1989), electron spin resonance (Fournier and Rahim, 1985; Fournier and Richard, 1988), nuclear magnetic resonance (Cistola *et al.*, 1989) and a highly radioactive photoreactive fatty acid analogue (Trigatti *et al.*, 1991). The affinity constant of these proteins for long chain fatty acids vary between 0.10 and 2.0 μM (Bass, 1985; Lowe *et al.*, 1987; Schulenberg-Schell *et al.*, 1988; Veerkamp *et al.*, 1991). In general, the stoichiometry of fatty acid bound to the various cFABPs is about one, indicating that these proteins have 1 binding site (Wilkinson and Wilton, 1987; Paulussen *et al.*, 1988; Chinander and Bernlohr, 1989). The fatty acid binding site for these proteins has not been

identified. However, x-ray crystallography of the rat intestinal cFABP showed that the fatty acid is located in the interior of the protein which appears to be hydrophobic; orientation of the carboxylate group of the fatty acid suggest that it may be interacting electrostatically with arginine-106, glutamine-115 and two water molecules (Sacchettini *et al.*, 1988; Sacchettini *et al.*, 1989; Veerkamp *et al.*, 1991).

1.5. Photoaffinity Labeling Approach for Identifying Receptors, Substrate-Binding Sites and Translocases

Chemical cross-linking derivatives and suicide inhibitors have been used to identify the active sites of enzymes, the amino acid residues involved in catalysis and for the identification of receptors. Another approach, involving photoaffinity labeling has also been used to identify receptors (Walter *et al.*, 1977; Mohler *et al.*, 1980; Pascual *et al.*, 1982; Bayley, 1983; Seidman *et al.*, 1984), to identify the subunit in a multi-subunit protein that binds the substrate or cofactor and to determine the number of binding sites (Lau, 1977; Standring and Knowles, 1980; Munson, 1981; Chen and Guillory, 1981; Knight and McEntee, 1985; Julin and Lehman, 1987; Powers-Lee and Corina, 1987; Scholz and Kwok, 1989; Lin *et al.*, 1980), and to identify proteins involved in transport (Chowdhry and Westheimer, 1979; Staros and Knowles, 1978; Kaczorowski *et al.*, 1980). The major adavantages of using the photoreactive derivatives instead of the traditional chemical cross-linking reagents is that the photoreactive groups are stable under physiological conditions and chemically unreactive prior to photoactivation; this facilitates preliminary experiments such as binding assays and biological activity determination (Bayley, 1983). The

reactive intermediates (carbenes or nitrenes) can be generated at will and are extremely reactive, capable of reacting covalently with carbon-hydrogen and carbon-carbon bonds (Bayley, 1983). Furthermore, these reactive intermediates have a short half-life and, unlike chemical cross-linking reagents, their chemical reactivity is not dependent on the presence of carboxylic, amino, thiol or hydroxyl functional groups at target sites (Bayley, 1983). This is an important property since the binding site of a receptor may be devoid of the above nucleophilic groups. Thus, unlike chemical reagents, the photolytically generated reactive intermediates are capable of reacting indiscriminately.

1.5.1. Aryl Diazirine Precursors of Carbenes

Diazo compounds and 3-H-3-aryl-diazirine have commonly been used as carbene precursors. The synthesis of the more commonly used 3-H-3-aryl-diazirine is depicted in Fig. 6. Photolysis of the diazirine group at 360 nm results in the generation of carbene. This species reacts with nucleophiles and is capable of inserting into carbon-hydrogen bonds and double bonds of unsaturated hydrocarbons (Bayley, 1983). Another product of photolytic activation of diazirines is the linear diazo isomer (Bayley, 1983; Ross *et al.*, 1982; Smith and Knowles, 1973) (Fig. 7). This species reacts only with available nucleophiles. Labeling by the linear diazo species may be misleading, especially when attempting to identify receptors or proteins involved in transport since the proteins labeled may not necessarily be the proteins of interest. The linear diazo isomer can be converted to carbene by longer photolysis time or inactivated by inclusion of thiol containing scavengers (Smith and

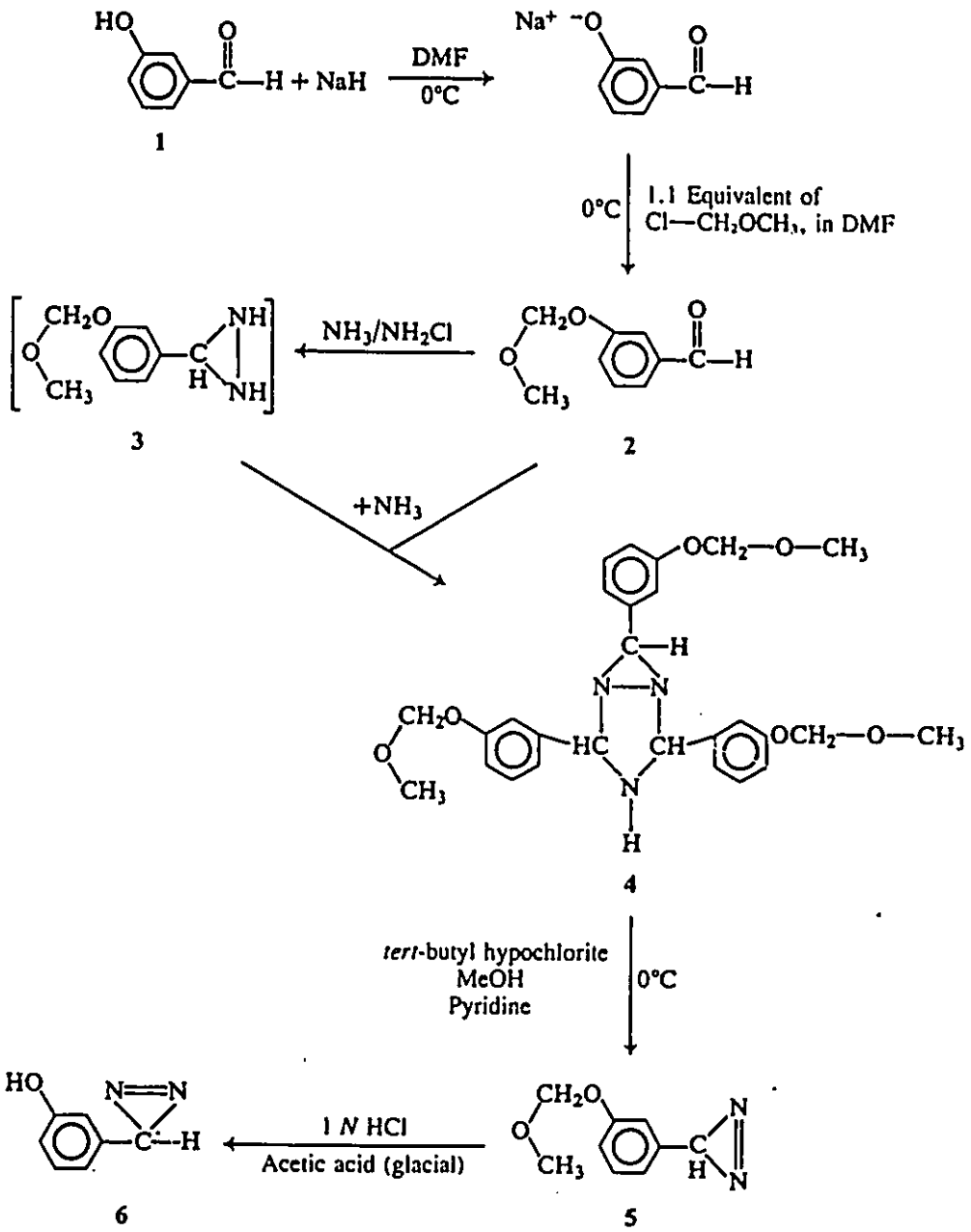

Figure 6. Scheme for the synthesis of m-diazirinophenol. Taken directly from Leblanc and Gerber (1984b).

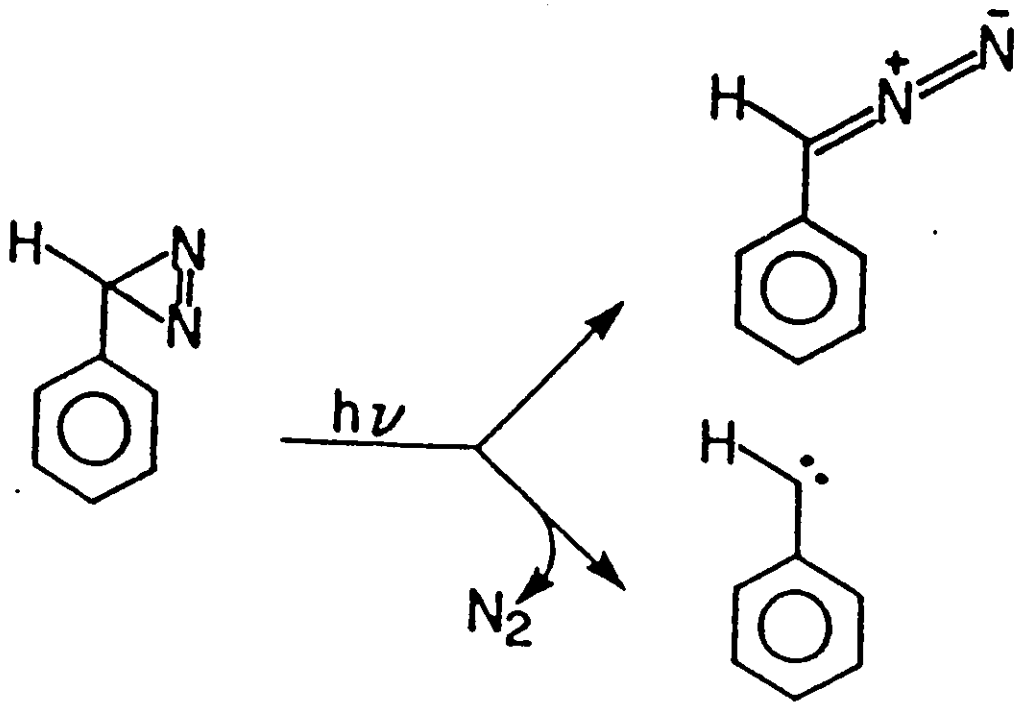

Figure 7. Products of photoactivation of the diazirine. Taken directly from Bayley (1983).

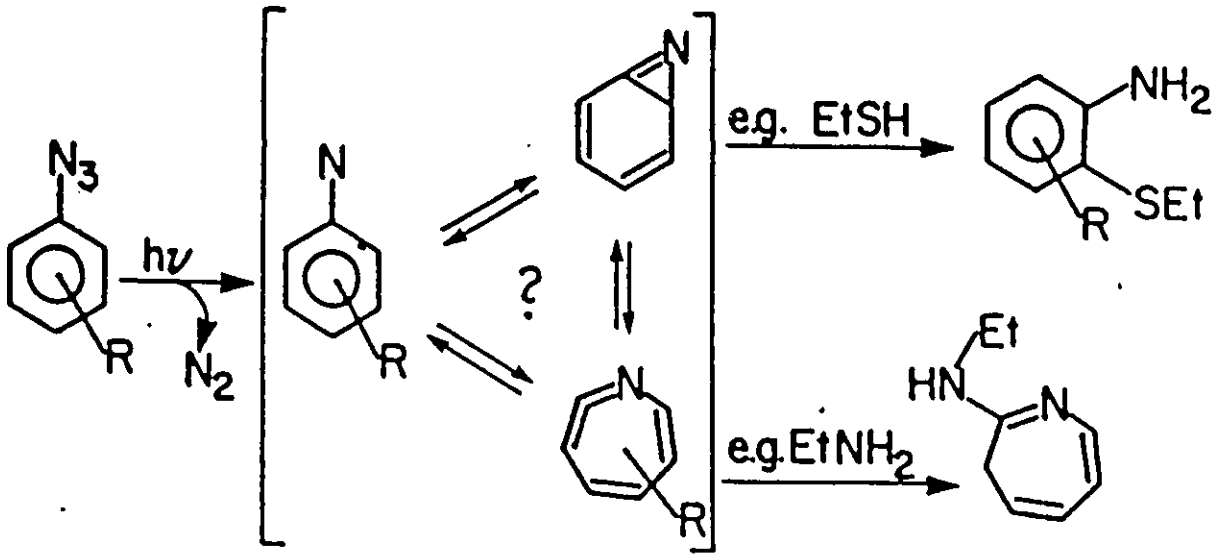

Figure 8. Intramolecular reacton of the nitrene to form electrophilic products. Taken directly from Bayley (1983).

Knowles, 1973; Smith and Knowles, 1975; Bayley, 1983). Alternatively, the 3-proton can be replaced with a CF_3 group. Although the linear diazo isomer is still generated upon photolysis, it is unreactive towards nucleophiles (Brunner *et al.*, 1980; Bayley, 1983).

1.5.2. Aryl Azide Precursors of Nitrenes

A variety of nitrene precursors have been synthesized (Bayley, 1983). However, nitro aryl azides are the most frequently used since photolysis can be performed with visible light rather than ultraviolet which can cause protein damage (Bayley, 1983). One of the disadvantages of using aryl azides is that they are reduced to amines by thiols (dithiothreitol, mercaptoethanol) that are commonly used in buffers (Staros *et al.*, 1978; Bayley, 1983).

The photolytically derived nitrenes are capable of inserting into carbon-hydrogen bonds and carbon-carbon double bonds, and of reaction with nucleophiles. However, they are much less reactive than carbenes and therefore, may be unsuitable for labeling binding sites made up of hydrophobic amino acid residues (Bayley and Knowles, 1978a; Bayley and Knowles, 1978b, Bayley, 1983). In addition, during photolysis the nitrene undergoes intramolecular rearrangements (Fig. 8). These species are very electrophilic and have a long half-life (Bayley, 1983).

1.6. Ojectives and Rationale

The mechanism of fatty acid uptake in *E. coli* is poorly understood at the biochemical level. It is known that the process is energy-dependent and involves the cytoplasmic fatty acyl-CoA synthetase and the outer membrane *fadL* protein.

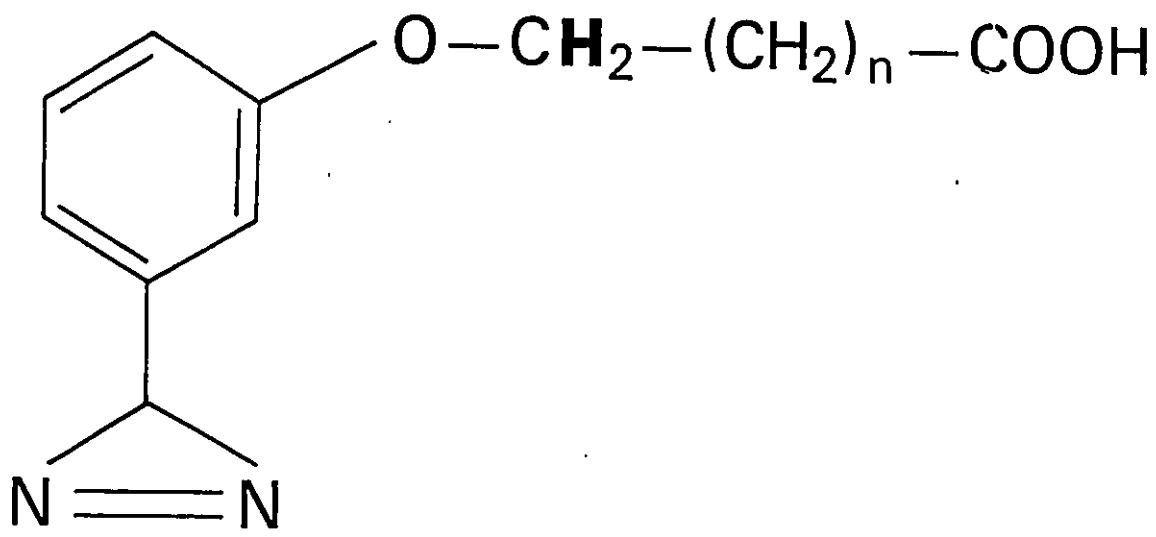

Figure 9. Structure of the diazirinophenoxy fatty acid analogues. The bold face lettering represents tritium.

However, the mechanism by which cellular energy is coupled to the overall process, the mechanism by which the *fadL* protein facilitates the movement of fatty acids across the outer membrane or the role of fatty acyl-CoA synthetase, and the mechanisms of fatty acid translocation across the inner membrane or the periplasmic space are not understood. Furthermore, it is not known whether the observed saturability of fatty acid uptake is due to specific binding to the *fadL* outer membrane protein, to the fatty acyl-CoA synthetase, to a protein in the periplasmic space or to some protein which may be required for fatty acid translocation or its desorption from the cytoplasmic face of the inner membrane.

The ultimate objective of this work is to identify the saturable, rate-limiting step in the process of fatty acid uptake. To attain this goal attempts were made to gain further insight into the mechanisms of fatty acid translocation at each individual step in the process. To accomplish this objective, a photochemical approach using the radioactive diazirinophenoxy fatty acid analogue (Fig. 9) was used to directly assess the possible involvement of proteins in fatty acid permeation of the periplasmic space, the inner membrane and finally to determine whether the *fadL* protein is capable of binding fatty acids since this has never been shown directly.

Photoreactive fatty acid analogues, used to identify the hydrophobic domains of integral membrane proteins (Bayley and Knowles, 1979; Brunner *et al.*, 1980; Brunner and Semenza, 1981; Quay *et al.*, 1981; Ross *et al.*, 1982; Takagaki *et al.*, 1983a; Takagaki *et al.*, 1983b; Brunner, 1989) have the potential for identifying membrane-bound fatty acid binding proteins which may be involved in the

transmembrane movement of fatty acids. The photoreactive fatty acid analogues have been shown to be incorporated into the phospholipids of *E. coli in vivo* (Olson *et al.*, 1979; Quay *et al.*, 1981) and to be used as long chain fatty acids by rat liver microsomal enzymes for the synthesis of fatty acyl-CoA and phospholipids as well as for phospholipid synthesis and fatty acid acylation of membrane proteins in L-cells (Leblanc and Gerber, 1983; Capone *et al.*, 1983). It is therefore expected that these photoreactive fatty acid probes would label proteins involved in the transmembrane movement of fatty acids.

E. coli cells expressing the *fad* regulon but defective in the cytoplasmic fatty acyl-CoA synthetase, are unable to take up fatty acids. It was suggested that this enzyme is essential for fatty acid uptake. However, this was never shown directly or biochemically. To study whether fatty acyl-CoA synthetase was involved, right side out inner membrane vesicles essentially devoid of cytoplasmic enzymes were used.

2.0. MATERIALS AND METHODS

2.1. Materials

The ML308 ($i^- z^- y^+$) and K12 (W3001) strains of *E. coli* were obtained from the American Type Culture Collection. The RS3338 strain (*fadR fadL*) was obtained from the *E. coli* Genetic stock Centre, Yale University, New Haven, CT. The MC1060 strain was obtained from Dr. Bialkoska-Hobranska of the Cancer Research Group, McMaster University, Hamilton, Ontario. All bacterial strains were stored in Luria-Bertani medium containing 15% glycerol (w/v) at - 20°C (Sambrook *et al.*, 1989).

The lithium salts of D-lactate and L-lactate, the sodium salts of (ATP) adenosine 5'-triphosphate and coenzyme A (CoASH), the luciferase-luciferin assay kit, thiamine, polyoxyethylene 20 cetyl ether (Brij 58), lysozyme, deoxyribonuclease (DNase) I, ribonuclease (RNase) A, succinic acid, palmitic acid, chloramphenicol, o-nitrophenyl-β-D-galactoside, bovine serum albumin (BSA) (Fraction V), N-methyl-N'-nitro-N-nitrosoguanidine (MNNG), L-proline and isoelectric point (pI) marker proteins (3.6-6.6) were purchased from Sigma Chemical Co. Teflon screw-cap vials (1.5 ml) were purchased from Pierce. HVLP (0.45 μM) filters and nitrocellulose paper were obtained from Millipore Corporation and vaccenic acid from Serdary. Prestained molecular weight markers, reagents for sodium dodecyl sulfate polyacrylamide gel electrophoresis (SDS-PAGE), 2-dimensional polyacrylamide gel electrophoresis (2-D PAGE) and silver staining were obtained from BioRad and [^{125}I]protein A and liquid scintillation fluid were purchased from Amersham.

[^{3}H]oleic acid (10 Ci/mmole), L-[^{3}H]proline (15 Ci/mmole), the tissue and gel solubilizer, Solvable, Atomlight, [^{3}H]-oleoyl-CoA and [^{3}H]$NaBH_4$ (15-60 Ci/mmole) were purchased from New England Nuclear. Oleic acid was purchased from Fisher Chemical Co. Osmium tetraoxide and triphenyl phosphite methiodide were obtained from Aldrich Chemical Co. Sodium meta periodate was purchased from J.T. Baker. X-ray films (XAR) were purchased from Eastman Kodak and preparative thin-layer chromatography (TLC) silica gel plates (PLK 5 linear K) were from Whatman. Solvents dimethylformamide (DMF), methanol, hexamethylphosphoramide (HMPA), petroleum ether, chloroform, diethyl ether) were purchased from Caledon or J.T. Baker.

2.2. Methods

2.2.1. Synthesis of 11-DAP-[11-^{3}H]-undecanoic acid

The synthesis of 11-DAP-[11-^{3}H]-undecanoic acid was performed as described with some modifications (Leblanc *et al.*, 1982).

2.2.1.1. Oxidation of Vaccenic Acid

Vaccenic acid (3.5 mmoles) was dissolved in 35 ml of 20% water in dioxane and neutralized by the addition of 1.1 equivalents of an aqueous solution of 1 N NaOH. The oxidation was initiated by the addition of 4.6 ml of a 2.5% solution of osmium tetraoxide in butanol and 3.5 g of finely ground sodium meta-periodate. The reaction was allowed to proceed in the dark at room temperature with vigorous shaking for 5 min. Another 3.5 g of finely ground sodium meta-periodate was added and the incubation continued. After 1 h, 3.5 g of finely ground sodium meta-

periodate was added and the reaction was allowed to proceed. Upon completion of the reaction, as judged by TLC analysis using petroleum ether/diethyl ether (1:4) as the developing solvent, the solvent was evaporated under reduced pressure. The resulting residue was resuspended in 35 ml of water. The pH of this solution was adjusted to 3-4 with 1 N HCl and extracted 3 X with 35 ml of petroleum ether/diethyl ether (1:1). The ether extracts were pooled and evaporated under reduced pressure. The oily residue was dissolved in 7 ml of 250 mM Na_2CO_3 and residual aldehyde was removed by extracting 3 X with 7 ml of petroleum ether. The semialdehyde was recovered by adjusting the pH of the aqueous phase to 3-4 with 1 N HCl followed by extraction with 7 ml of petroleum ether/diethyl ether (1:1) three times. The extracts were pooled and the ether was evaporated under reduced pressure. The residue was dissolved in 5 ml of 250 mM Na_2CO_3 and extracted 3 X with 5 ml of petroleum ether to remove residual osmium tetraoxide. The aqueous phase was acidified to pH 3-4 with 1N HCl and the semialdehyde was extracted into petroleum ether/diethyl ether (1:1). The ether was evaporated under reduced pressure and the semialdehyde was dissolved in absolute ethanol at a concentration of 500 mM. To purify the semialdehyde further, the ethanol was diluted to 10% with water and applied to an ODS column (bed volume of 5 ml). The column was washed with 30 ml of water to remove polar contaminants. The semialdehyde was eluted with 20 ml of diethylether. The ether was evaporated under reduced pressure and the semialdehyde was dissolved in absolute ethanol at a concentration of 500 mM. The yield of semialdehyde was 50%-60%. The semialdehyde was

characterized by ^{1}H-NMR spectroscopy (Leblanc, 1991).

2.2.1.2. Reduction of the Semialdehyde with [^{3}H]NaBH$_4$

An equivalent of the ethanolic solution of semialdehyde was titrated to pH 10 with 1 N NaOH and added to solid sodium borohydride. After the reaction was allowed to proceed for 15 min at room temperature, another equivalent of semialdehyde was added. Additions of semialdehyde was continued in 15 min intervals until no bubbling was observed upon addition of an aliquot of the reaction to 10 ml of diethylether containing 12 mM HCl. After the sixth addition of semialdehyde, the reaction was allowed to proceed for another 2 h. The pH of the reaction mixture was adjusted to pH 3-4 with 1 N HCl and the ethanol was diluted to 10% with water and the reduced product was extracted into diethyl ether. The extracts were combined and the ether was evaporated under a gentle stream of nitrogen. The residue was dissolved in a small volume of diethyl ether and applied to a preparative silica gel plate. The plate was developed with diethyl ether/petroleum ether (15:1). After autoradiography the hydroxy fatty acid was scraped from the plate and eluted with diethyl ether. The yield of the hydroxy fatty acid, based on radioactivity, was greater than 90%.

2.2.1.3. Preparation of the Methyl Ester of the Hydroxy Fatty Acid

The diazomethane was prepared by reacting 5 mmoles of MNNG with 1 equivalent of KOH (5 N) in 1 ml of cold water. The diazomethane was collected into 5 ml of cold diethyl ether that was overlaying the reaction. The diethyl ether solution containing the diazomethane was distilled into another 5 ml of cold diethyl

ether by gentle warming.

To the dried hydroxy fatty acid was added 10 equivalents of a chilled diethyl ether solution of diazomethane and the reaction was allowed to proceed for 10 min on ice. The esterification reaction was terminated by evaporation of the ether and diazomethane under a stream of nitrogen while on ice. The residue was dissolved in a small volume of diethyl ether and applied to a preparative TLC plate. The plate was developed with diethyl ether/petroleum ether (15:1). The hydroxy fatty acid ester was visualized by autoradiography and eluted with diethyl ether. The yield of the ester was 80%-90%, based on radioactivity.

2.2.1.4. Preparation of the Iodo Fatty Acid Methyl Ester

To the dried hydroxy fatty acid methyl ester was added 10 equivalents of triphenyl phosphite methiodide (1 M) in dry DMF and the reaction was allowed to proceed at room temperature in the dark. Upon completion of the reaction as determined by TLC analysis using diethyl ether/petroleum ether (4:1) as the developing solvent, the DMF was diluted to 25% with water and applied to an ODS column (5 ml). The column was washed with 30 ml of water prior to elution of the iodo fatty acid methyl ester with diethyl ether. The iodo fatty acid methyl ester was further purified by preparative TLC using diethyl ether/petroleum ether (4:1). The product was visualized by autoradiography and eluted with diethyl ether. The yield of the iodo fatty acid ester was 80%-90%, based on radioactivity.

2.2.1.5. Preparation of 11-DAP-[11-^{3}H]-undecanoate Methyl Ester

Diazirinophenol was prepared and characterized by ^{1}H-NMR spectroscopy

as described (Leblanc and Gerber, 1983). The diazirinophenol in 1 ml of HPLC grade methanol was reacted with an equivalent of sodium methoxide. After removal of the solvent under reduced pressure the phenoxide was dissolved in dry HMPA at a concentration of 100 mM; 2 equivalents of the phenoxide was added to the dried iodo fatty acid methyl ester and the reaction was allowed to proceed at room temperature in the dark under nitrogen. Upon completion of the reaction as determined by TLC analysis using petroleum ether/diethyl ether (4:1) as the developing solvent, the reaction mixture was applied directly to preparative TLC plate and developed with petroleum ether/diethyl ether (4:1). The product was visualized by autoradiography and eluted with diethyl ether.

2.2.1.6. Saponification of 11-DAP-[11-^{3}H]-undecanoate Methyl Ester

To the dried ester was added 10 equivalents of KOH (100 mM in 95% ethanol) and the reaction was allowed to proceed for 10 h at room temperature in the dark. The pH of the solution was adjusted to 3-4 and the DAP-fatty acid was extracted into diethyl ether. The ether extracts were combined and evaporated under a stream of nitrogen. The residue was dissolved in a small volume of diethyl ether and applied to a preparative TLC plate and developed with diethyl ether/petroleum ether (4:1). The DAP-fatty acid was visualized by autoradiography and eluted with diethyl ether. The yield of the photoreactive fatty acid, based on radioactivity, was 80%-90%. The specific activity of the DAP-fatty acid was determined based on the molar extinction coefficient of the diazirine at 350 nm (ϵ=310). The photoreactive fatty acid was routinely stored in diethyl ether at -20°C

in the dark.

2.2.2. Cell Growth

Aliquots of cells grown initially in Luria-Bertani media at 37°C with shaking, were diluted into M9-minimal media (42 mM Na_2HPO_4, 22 mM KH_2PO_4, 8.6 mM NaCl, 18.9 mM NH_4Cl, 1 mM $MgSO_4.7H_2O$ and 0.1 mM $CaCl_2$) supplemented with 5 μg/ml thiamine, 5 mg/ml Brij 58, 5 mM oleate or 25 mM glucose and grown at 37°C with shaking (Maloy *et al.*, 1981). After reaching a cell density of 4.8 x 10^8 cells/ml the cells were diluted into fresh complete M9-minimal media and grown at 37°C with shaking to a cell density of 4.8-6.4 x 10^8 cells/ml. RS3338 was grown as described above using 3.5 mM oleate and 30 mM acetate as the carbon source (Overath and Raufuss, 1967).

2.2.3. Uptake Assays in Whole Cells

Cells were harvested by centrifugation at 10,000 x g for 10 min at 4°C and washed twice with cold washing buffer (M9-minimal media containing 0.5% Brij 58 (w/v), pH 7.0). The cells were resuspended in washing buffer at a cell density of 2.4 x 10^9 cells/ml; an aliquot (500 μl) of cells was diluted into an equal volume of washing buffer containing 200 μg/ml chloramphenicol and incubated at 25°C with shaking (gyrorotary shaker) for 30 min (Klein *et al.*, 1971; Nunn *et al.*, 1979; Black *et al.*, 1987). D-lactate (40 μmoles) in 500 μl of incubation buffer (washing buffer containing 100 μg/ml chloramphenicol) was added and the incubation continued. After 5 min, either [^{3}H]oleate (500 μl of 300 μM; 250 mCi/mmole) or L-[^{3}H]proline (500 μl of 200 μM; 750 mCi/mmole) in incubation buffer was added and the

incubation continued at 25 °C with continuous shaking. At the specified time, a 250 μl aliquot of the incubation mixture was diluted into 5 ml cold washing buffer, vacuum filtered, and washed twice with 5 ml cold washing buffer. The filter was air dried and the retained radioactivity determined by liquid scintillation counting.

2.2.4. Proline Uptake in Inner Membrane Vesicles

Proline uptake was routinely performed as described (Kaback, 1971). An aliquot (50 μl) of vesicles in 100 mM phosphate, pH 6.6 was added to 50 μl of 20 mM magnesium sulfate (in water) and incubated at 37 °C with vigorous shaking (gyrorotary shaker). After 15 min, 50 μl of 80 mM D-lactate in 50 mM potassium phosphate, pH 6.6 was added followed by the addition of 50 μl of 20 μM [^{3}H]proline in 50 mM potassium phosphate, pH 6.6. The incubation was continued at 37 °C with shaking and at the specified time 40 μl of the reaction was diluted into 2.5 ml of 100 mM lithium chloride and filtered. The filter was washed once with 2.5 ml of 100 mM lithium chloride and the radioactivity retained was quantitated by liquid scintillation counting.

2.2.5. Determination of Cytoplasmic ATP Content

Washed cells (1.2 x 10^9) in 500 μl of washing buffer were added to an equal volume of washing buffer containing 200 μg/ml chloramphenicol and incubated with shaking at 25 °C for 30 min; 500 μl of incubation buffer with or without D-lactate (40 μmoles) was added. After a 5 min incubation at 25 °C, 500 μl of cold incubation buffer was added and cellular ATP was isolated (Joshi *et al.*, 1989) by adding 500 μl of the incubation mixture to 250 μl of ice-cold 24% perchloric acid

(v/v) and incubation on ice for 20 min. The sample was centrifuged for 5 min using a Beckman microcentrifuge at 4°C and 500 μl of the supernatant was added to 125 μl of 4 M KOH and 125 μl of 2 M $KHCO_3$. After 30 min on ice, the sample was centrifuged as described above and the supernatant was diluted 100-fold and assayed for ATP. An aliquot of the diluted cell extract (40 μl) was added to 100 μl of 135 mM glycylglycine, pH 8.0 containing 37.5 mM $MgCl_2$. After the addition of 60 μl of H_2O and 50 μl of luciferase-luciferin solution (40 mg/ml), light emission was recorded using a Thorn Emi Gencom Inc. C-10 photon counter. The ATP isolated from the same number of unstarved cells was also determined.

2.2.6. Lipid Analysis

ML308 cells were incubated with [^{3}H]oleate as described in Section 2.2.3. At the specified time, an aliquot (300 μl) of the incubation mixture was added to 900 μl of cold washing buffer and centrifuged at 15,000 rpm for 10 min at 4°C. The cell pellet was washed once with 500 μl of cold washing buffer and resuspended in 100 μl of distilled water. A solution (375 μl) of $CHCl_3$/MeOH (1:2,v/v) was added and incubated at 25°C for 30 min; to this mixture was added 125 μl of $CHCl_3$ and 125 μl of distilled water (Bligh and Dyer, 1959). Phase separation was achieved by centrifugation of the sample and the solvent from each phase was evaporated under reduced pressure. The dried residues from the organic phase and aqueous phase were dissolved in $CHCl_3$/MeOH (1:1, v/v) and MeOH/H_2O (1:1, v/v), respectively and analyzed by TLC using $CHCl_3$/MeOH/H_2O (65:25:4, v/v/v) for the former or butanol/H_2O/acetic acid (50:30:20, v/v/v) for the latter. The radioactive product

was visualized by fluorography (Randerath, 1970) and quantitated by liquid scintillation counting.

2.2.7. Measurement of Acyl-CoA Synthetase Activity

Acyl-CoA synthetase activity was assayed at 37°C as previously described (Kameda and Nunn, 1981). The incubation mixture consisted of 200 mM Tris-HCl, pH 7.5, 8 mM $MgCl_2$, 5 mM mercaptoethanol (MSH), 20 mM NaF, 0.1% Triton X-100 (w/v), 75 μM [^{3}H]oleate (1.2 Ci/mmole), 10 mM ATP and 2.5 mM CoASH. The reaction was terminated by diluting 100 μl of the incubation mixture into 500 μl of a mixture of isopropyl alcohol/heptane/1 M sulfuric acid (40:10:1, v/v/v). To this mixture was added 300 μl of heptane and 300 μl of water. After phase separation was obtained the organic phase was removed and the aqueous phase was extracted 4 times with 1 ml of diethyl ether. The total radioactivity in the aqueous phase was determined by liquid scintillation counting. Control reactions in the absence of ATP and CoASH were subtracted as blank values.

2.2.8. Measurement of β-galactosidase Activity

β-galactosidase activity was assessed at 25°C by measuring the release of o-nitrophenol at 420 nm (Malamy and Horecker, 1964). The reaction mixture consisted of 40 mM sodium phosphate, pH 7.5, 0.1% Triton X-100 (w/v) and 0.5 mM o-nitrophenyl-β-D-galactoside.

2.2.9. Isolation of Total Membranes

Total membranes were prepared by a modified procedure of Witholt et. al. (1976). Cells grown in M9-minimal media as described in Section 2.2.2 were

harvested at 10,000 x g for 10 min at 4°C and washed once with cold 10 mM Tris-HCl, pH 8.0. The washed cells were resuspended in 200 mM Tris-HCl, pH 8.0 at 2.4 x 10^9 cells/ml. After the addition of 400 µl of 100 mM potassium EDTA, pH 7.8 and 400 µl of 12 mg/ml lysozyme, the suspension was diluted with 81 ml of H_2O and incubated with stirring at 25°C for 30 min. The suspension was diluted with 19.5 ml H_2O followed by the addition of 20.5 ml of 1 mg/ml DNase 1 and 1 ml of 1 M $MgSO_4$. This mixture was incubated at 37°C with shaking for 30 min, and then centrifuged at 1200 x *g* for 15 min at 4°C. The supernatant was centrifuged at 210,000 x *g* for 90 min at 4°C and the pellet obtained was washed twice with 25 mM sodium phosphate, pH 6.5. The washed membrane, resuspended in 25 mM sodium phosphate, pH 6.5 at a protein concentration of 5-10 mg/ml, was frozen in liquid nitrogen and stored at -80°C.

2.2.10. Inner and Outer Membrane Separation

Inner and outer membrane separation was performed as described (Osborn *et al.*, 1972). ML308 grown in M9-minimal media as described in Section 2.2.2 were harvested at 12,000 x g for 5 min at 4°C and resuspended in cold 10 mM Tris-Acetate, pH 7.8, containing 750 mM sucrose at 7 x 10^9 cells/ml. After the addition of 714 µl of 2 mg/ml lysozyme, the suspension was incubated in an ice-water bath with stirring for 2 min and 30 ml of 1.5 mM sodium EDTA, pH 7.5 was added slowly over a 10 min period. The incubation was continued for an additional 30 min and the suspension was slowly transferred to 179 ml of cold stirring water. This suspension was incubated for 10 min and then centrifuged at 1200 x *g* for 15 min at

4°C. The resulting supernatant was centrifuged at 50,000 rpm for 3 hr at 4°C. The membrane pellet was resuspended in a small volume of cold 250 mM sucrose, 3.3 mM Tris-Acetate, pH 7.8, 1 mM sodium EDTA using a 23 gauge needle and diluted to 30 ml with the above buffer. After centrifugation at 50,000 rpm for 3 h at 4°C, the pellet was resuspended in 800 μl of 25% sucrose (w/v), 5 mM sodium EDTA, pH 7.5 and subjected to equilibrium density centrifugation 35,000 x *g* for 14 hr in a discontinous sucrose density gradient (Osborn *et al.*, 1972). The inner and outer membranes were pelleted by centrifugation at 50,000 rpm for 3 hr at 4°C. Inner and outer membranes, resuspended in 25 mM sodium phosphate, pH 6.5, were frozen in liquid nitrogen and stored at -80°C.

2.2.11. Preparation of Inner Membrane Vesicles in the Presence or Absence of D-lactate

ML308 grown in M9-minimal media as described in Section 2.2.2 were harvested at 10,000 x *g* for 10 min at 4°C, washed twice with cold 10 mM Tris-HCl, pH 8.0 and envelope vesicles prepared essentially as described (Konings and Kaback, 1973). The cells (3 g wet wt) were resuspended in 240 ml of digestion buffer (30 mM Tris-HCl, pH 8.0 containing 20% sucrose (w/v) and 100 μg/ml chloramphenicol) with or without 20 mM D-lactate and stirred at 25°C. The potassium salt of EDTA, pH 7.0 and lysozyme were added to final concentrations of 10 mM and 2.3 mg/ml, respectively, and the digestion was allowed to proceed at 25°C for 30 min. The spheroblasts were harvested at 10,000 x *g* for 10 min at 4°C and resuspended in 15 ml lysis buffer (10 mM potassium phosphate, pH 6.6

containing 5 mM $MgSO_4$, 10 μg/ml DNase 1 and 10 μg/ml RNase A) with or without 20 mM D-lactate and incubated at 37°C for 30 min with continuous shaking. Following centrifugation at 800 x *g* for 60 min at 4°C the resulting supernatants (crude lysate) were centrifuged at 46,000 x *g* for 60 min at 4°C. The pellets (vesicles) were resuspended in 12.5 ml of cold 100 mM potassium phosphate, pH 6.6 with or without 20 mM D-lactate and centrifuged at 46,000 x *g* for 60 min at 4°C. The washed vesicles were resuspended in a small volume of cold 50 mM potassium phosphate, pH 6.6 and frozen in liquid nitrogen in small aliquots and stored at -80°C.

2.2.12. Preparation of Inner Membrane Vesicles for Uptake Assays

2.2.12.1. Extensively Washed Vesicles

ML308 was grown as described in Section 2.2.2 in MA-minimal media (40.2 mM K_2HPO_4, 22.1 mM KH_2PO_4, 1.7 mM Na_3citrate. $3H_2O$, 0.407 mM $MgSO_4$. $7H_2O$, 7.6 mM $(NH_4)_2SO_4$) supplemented with 35 mg/ml Brij 58 and 5 mM palmitate or 25 mM glucose to 5.6 x 10^8 cells/ml (Kaback, 1971). Envelope vesicles were prepared essentially as described (Kaback, 1971). The cells were harvested by centrifugation at 10,000 x *g* for 10 min at 4°C and washed twice with cold 10 mM Tris-HCl, pH 8.0. The cells (1 g wet wt) were resuspended in 80 ml 30 mM Tris-HCl, pH 8.0 containing 20% sucrose (w/v). After the addition of potassium EDTA, pH 7.0 and lysozyme to final concentrations of 10 mM and 2.3 mg/ml, respectively, the suspension was incubated at 25°C with stirring for 40 min. The suspension was centrifuged at 16,000 x *g* for 30 min at 4°C. The pellet was transferred to a cold

motor driven Potter homogenizer containing 2 ml of cold 100 mM potassium phosphate, pH 6.6 containing 20% sucrose (w/v) and 20 mM magnesium sulfate, 10 mg/ml DNase 1 and 10 mg/ml RNase A and homogenized at 4°C. The uniformly dispersed pellet was transferred to 500 ml 50 mM potassium phosphate, pH 6.6 pre-equilibrated at 37°C and incubated at 37°C with vigorous shaking for 15 min. Potassium EDTA, pH 7.0 was added to a final concentration of 10 mM and the incubation continued at 37°C. After 15 min magnesium sulfate was added to a final concentration of 20 mM and the incubation continued for another 15 min. The lysate was centrifuged at 16,000 x *g* for 30 min at 4°C. The pellet was resuspended in 1 ml of cold 100 mM potassium phosphate, pH 6.6 containing 20% sucrose (w/v) and 10 mM magnesium sulfate by homogenization and diluted to 4 ml with the same buffer. Aliquots (2 ml) of the homogenate were layered on top of 8 ml of cold 100 mM phosphate, pH 6.6 containing 60% sucrose (w/v) and 10 mM magnesium sulfate and centrifuged at 64,000 x *g* for 90 min at 4°C. The layer of pure vesicles at the interface were removed and diluted to 12 ml with cold 100 mM potassium phosphate, pH 6.6 containing 10 mM potassium EDTA and centrifuged at 45,000 x *g* for 30 min at 4°C. The pellets were homogenized vigorously in 1 ml of cold 100 mM potassium phosphate, pH 6.6 containing 10 mM potassium EDTA and diluted to 12 ml with the same buffer and centrifuged at 45,000 x *g* for 30 min at 4°C. The pellet was washed two times more as described and resuspended in 100 mM potassium phosphate, pH 6.6 at a protein concentration of 5-10 mg/ml. The vesicles were frozen and stored in liquid nitrogen.

2.2.12.2. Less Extensively Washed Vesicles

ML308 was grown in MA-minimal media supplemented with 35 mg/ml Brij 58 and 5 mM palmitate as described in Section 2.2.2. The cells were converted to spheroblasts as described in Section 2.2.12.1 and collected by centrifugation at 10,000 x *g* for 10 min at 4°C. The spheroblasts (2 g wet wt) were resuspended in 10 ml of 10 mM potassium phosphate, pH 6.6 containing 2 mM magnesium sulfate, 10 μg/ml DNase 1 and 10 μg/ml RNase A (Konings and Kaback, 1973) and incubated at 37°C with vigorous shaking for 15 min. Magnesium sulfate, DNase 1 and RNase A were added to bring the final concentrations to 5 mM, 20 μg/ml and 20 μg/ml, respectively, and the incubation continued for another 15 min. The lysate was centrifuged at 800 x *g* for 60 min. The supernatant was carefully removed and centrifuged at 46,000 x *g* for 60 min. The pellet, resuspended in 50 mM potassium phosphate, pH 6.6 at a protein concentration of 5-10 mg/ml, was frozen and stored in liquid nitrogen.

2.2.13. Preparation of Antisera to a Synthetic Peptide of the *fadL* Protein

A peptide (acetyl-INEGPYQFESEGK-NH_2) at the C-terminus of the *fadL* protein was synthesized and linked covalently to keyhole limpet hemocyanin using m-maleimidobenzoic acid-N-hydroxysuccinimide ester (Multiple Peptide Systems, San Diego, CA). Antisera to the coupled peptide were raised in rabbits as described (Black, *et al.*, 1987) and screened by western immunoblotting as described (Burnette, 1981) except the blots were treated with 1% BSA. Bound antibodies were detected with [^{125}I]protein A followed by autoradiography (Burnette, 1981).

2.2.14. Determination of the Unbound 11-DAP-[11-^{3}H]-undecanoate Concentration in the Presence of Various BSA Concentration

2.2.14.1. Determination of the Partition Ratio of 11-DAP-[11-^{3}H]-undecanoate at Various Concentration in the Absence of BSA

The partition ratio of 11-DAP-[11-^{3}H]-undecanoate at 1 μM to 400 μM was determined as described (Spector *et al.*, 1969). The sodium salt of the probe (27 Ci/mmole) in 500 μl of 25 mM sodium phosphate, pH 6.5 was placed in 1.5 ml vials. The fatty acid solution was overlayed with 500 μl of heptane. The vials were sealed with a teflon screw-cap and incubated with gentle shaking for 16 h at 37°C. The radioactivity in each phase was determined by subjecting a small aliquot to liquid scintillation counting. The equilibrium probe concentration in each phase and the partition ratio were calculated as described (Spector *et al.*, 1969).

2.2.14.2. Determination of the Unbound Probe Concentration

To 1.5 ml vials containing 500 μl of 200 μM 11-DAP-[11-^{3}H]-undecanoate (sodium salt) and varying concentrations of BSA (2000 μM to 50 μM) in 25 mM sodium phosphate, pH 6.5 were added 500 μl heptane. The vials were sealed with teflon screw-cap and incubated with gentle shaking at 37°C for 16 h. The amount of radioactivity in each phase was determined by liquid scintillation counting and the equilibrium concentration of the probe in each phase was calculated. Using the information obtained in Section 2.2.14.1 and as described (Spector *et al.*, 1969) the unbound probe concentration at the various BSA concentrations was determined.

2.2.15. Fatty Acid-BSA Method of Labeling

[11-^{3}H]11-m-DAP-undecanoate (26 nmoles) was incubated with BSA (26 nmoles) in 125 μl of 25 mM sodium phosphate, pH 6.5 at 37°C in a polystyrene cuvette. After 60 min, 25 μl of total membranes (75 μg of protein) were added and the incubation continued for 15 min. The sample was placed in a metal cell holder located at the focal point of 1000 watt xenon/mercury lamp and photolyzed for 30 sec at 365 nm. Light at wavelengths below 310 nm was filtered by passing the light through a filter (Corning 7-51) contained in a water-filled optical glass cell (5 x 5 cm) and a filter (Corning 7-51) attached to the window of the metal cell housing (Leblanc *et al.*, 1982). The photolyzed sample was centrifuged at 435,000 x *g* for 90 min at 4°C using a Beckman TL-100 ultracentrifuge. The membrane pellet was washed twice with 200 μl of 25 mM sodium phosphate, pH 6.5 containing 0.4% BSA (w/v) pre-equilibrated at 25°C. The washed membrane was resuspended in water at a protein concentration of 0.5 mg/ml.

2.2.16. Free Fatty Acid Method of Labeling

Unless otherwise indicated, isolated membrane, 0.5 mg/ml of protein, in 25 mM sodium phosphate, pH 6.5 or 4.8 x 10^8 cells/ml in M9-minimal media, pH 6.5 were incubated with 10 μM [11-^{3}H]11-m-DAP-undecanoate at 4°C for min and photolyzed as described in Section 2.2.17.

2.2.17. Preparation of Whole Cells for SDS-PAGE

The photolyzed cells were centrifuged for 5 min at 25°C using a Beckman Microcentrifuge. The cell pellet was resuspended in 10 μl of 10 mM Tris-HCl, pH

8.0; 5 μl of a solution containing 100 μg/ml lysozyme and 1.5 mM sodium EDTA, pH 7.8, was added and the suspension incubated at 25°C for 30 min. The incubation mixture was diluted with 5 μl of a solution containing 20 mM magnesium sulfate and 600 μg/ml DNase 1 and incubated at 37°C for 30 min. After an equal volume of 125 mM Tris-HCl, pH 6.8 containing 10% SDS (w/v), 20% MSH (v/v), 20% glycerol (w/v) and 0.02% bromophenol was added, the sample was boiled for 5 min and analyzed by SDS-PAGE as described (Laemmli, 1970).

2.2.18. Sample Preparation for 2-D PAGE

An aliquot (40 μl) of membrane (20 μg of protein) was added to 10 μl of 250 mM Tris-HCl, pH 6.8 containing 2.5 mM $MgCl_2$ and 0.53% SDS (w/v) (A) or 1.2% SDS (w/v) (B) and boiled for 5 min; a solution (20 μl) containing 17.5% MSH (v/v), 7% ampholytes (3.5/10:4/6:6/8, 1:2:2) and 2.1% NP-40 (w/v) or 4.8% NP-40 was added to preparations A and B, respectively (Ames and Nikaido, 1976). Urea (18 mg) was added to 17.5 μl (5 μg of protein) of each preparation and analyzed by 2-D PAGE as described in Section 2.2.19.

2.2.19. 2-D PAGE Analysis

Isoelectric focusing was performed as described (Ames and Nikaido, 1976) using a BioRad Minifocusing Protean 2 apparatus. The samples were overlayed with buffer composed of 4.5 M ultrapure urea and 1% ampholine (3.5/10:4/6:6/8, 1:2:2) and electrophoresed at 500 volts for 10 min followed by 750 volts for 5 h. The focused gels were equilibrated for 5 min in 5 ml of 62.5 mM Tris-HCl, pH 6.8 containing 10% glycerol (w/v), 5% MSH (v/v), 5% SDS (w/v), and 0.01%

bromophenol blue and electrophoresed on 10% polyacrylamide gels using a BioRad Mini Protean 2 apparatus (O'Farrell, 1975).

2.2.20. Preparation of Periplasmic Proteins

The periplasm was isolated from oleate grown MC1060 cells by osmotic shock (Neu and Heppel, 1965). Cells were washed twice with 10 mM Tris-HCl, pH 8.0 containing 30 mM NaCl and resuspended in 30 mM Tris-HCl, pH 7.3 containing 20% sucrose at a density of 1.0×10^{10} cells/ml. A solution of potassium EDTA (250 mM), pH 7.0 was added to a final concentration of 1 mM and the mixture was incubated at 25°C with continuous shaking. After 10 min the incubation mixture was centrifuged at 10,000 x *g* for 10 min at 4°C. The cells were resuspended in cold distilled water at a density of 1.0×10^{10} cells/ ml and incubated at 4°C for 10 min. The cell suspension was centrifuged as above and the supernatant containing the periplasmic proteins was collected.

2.2.21. Partial Purification of Acyl-CoA Synthetase

2.2.21.1. Lysis of Cells

Spheroblasts of oleate grown ML308 cells (7 g wet weight) were prepared and lysed in 10 mM potassium phosphate, pH 7.5 containing 5mM $MgSO_4$, 10 μg/ml DNase 1, 10 μg/ml RNase A and 0.1% Triton X-100 as described in Section 2.2.12.2. The crude lysate was centrifuged at 46,000 x *g* for 60 min at 4°C. All subsequent steps were performed at 4°C as described (Kameda and Nunn, 1981).

2.2.21.2. DEAE-Sepharose Chromatography

The supernatant was applied to a DEAE-Sepharose column (45 ml bed

volume) pre-equilibrated with 10 mM potassium phosphate, pH 7.5. The column was eluted with 45 ml of potassium phosphate, pH 7.5 followed by a 320 ml linear gradient of 10 mM potassium phosphate, pH 7.5 to 300 mM potassium phosphate, pH 7.5. Elution was monitored at 280 nm and by acyl-CoA synthetase activity. Fractions containing acyl-CoA synthetase were combined.

2.2.21.3. Ammonium Sulfate Precipitation

The enzyme solution from Section 2.2.21.2 was brought to 60% saturation with finely ground ammonium sulfate. The precipitate was collected by centrifugation at 14,500 x g for 10 min at 4°C. The pellet was redissolved in 10 ml of 10 mM potassium phosphate, pH 7.5 containing 20% glycerol (w/v) and dialyzed against 4 l of 10 mM potassium phosphate, pH 7.5 containing 20% glycerol (w/v) for 6 hours at 4°C.

2.2.21.4. Hydroxyapatite Chromatography

The dialyzed solution was applied to a 15 ml hydroxyapatite column pre-equilibrated with 10 mM potassium phosphate, pH 7.5 containing 20% glycerol (w/v). The column was eluted with a 120 ml linear gradient from 50 mM to 300 mM potassium phosphate, pH 7.5 containing 20% glycerol (w/v). The elution was monitored at 280 nm and by acyl-CoA synthetase activity. The fractions containing acyl-CoA synthetase were combined. Small aliquots of the enzyme solution were frozen in liquid nitrogen and stored at -80°C.

2.2.22. Miscellaneous Methods

Protein was quantified as described (Lowry *et al.*, 1951) using BSA as the

standard. Silver staining of proteins was performed as specified by the supplier (BioRad). Polyacrylamide gels were processed for fluorography as described (Bonner and Laskey, 1974). Electrophoretic transfer of proteins onto nitrocellulose was performed for 14 h at 30 volts using transfer buffer composed of 25 mM Tris, 192 mM glycine, 20% methanol (v/v) and 0.05% SDS (w/v), pH 8.3. The radioactivity in protein on polyacrylamide gels was quantitated by eluting the protein from the excised gel using Solvable, as described by the supplier, followed by liquid scintillation counting in 10 ml of Atomlight. Radioactivity was determined by liquid scintillation counting in 10 ml of aqueous counting scintillant. Oleic acid was neutralized with 1.1 equivalents of KOH in 50% ethanol. 11-DAP-[11-^{3}H]-undecanoic acid in 1 ml of 95% ethancl was neutralized with 1.1 equivalents of NaOH; the solvent was removed under reduced pressure and the fatty acids were dissolved in the appropiate buffer at the desired concentration. Liquid scintillation counting was performed on a Beckman LS 7800 counter.

3.0. RESULTS AND DISCUSSION

3.1. Optimization of Photolysis Conditions

The demonstration of the involvement of a translocase in the permeation of fatty acids across the plasma membrane of cells is a formidable task. This is in part due to the lack of alternate stereoisomers or analogues of fatty acids; the use of stereoisomers has played a pivotal role in establishing the involvement of a translocase in the membrane permeation of other metabolically important substrates such as glucose. In addition, the lack of methods for the identification of membrane-bound fatty acid translocases is another reason for the slow progress in the understanding of fatty acid permeation of cell membranes.

The development of a synthesis for highly radioactive photoreactive fatty acid analogues (Leblanc *et al.*, 1982; Gupta *et al.*, 1977; Brunner and Richards, 1980) has provided a novel approach which has the potential to facilitate the direct identification of proteins having a high affinity for fatty acids in cell membranes. Optimum conditions for the labeling of such proteins were therefore assessed.

The high reactivity of the carbene generated from the diazirine by photolysis at 365 nm allows for rapid crosslinking of the photoreactive fatty acid analogue to proteins in membranes (Bayley, 1983). However, it has been reported that the efficiency of activation of the diazirine to the carbene can be affected in the presence of membranes (Bayley, 1983; Takagaki *et al.*, 1983). The time required for complete activation of the diazirine to the carbene was therefore assessed in the presence of membranes. This was monitored indirectly by the intensity of labeling

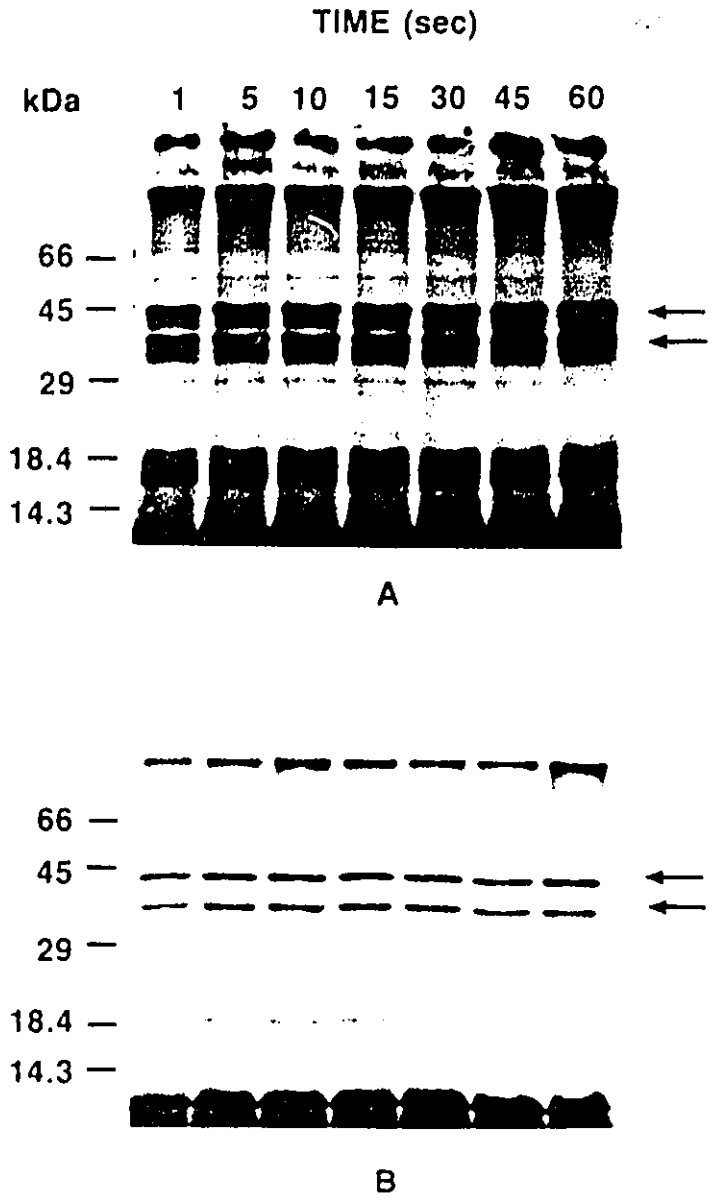

Figure 10. Time course of photolysis of 11-DAP-[11-^{3}]-undecanoate in the presence of varying amounts of membranes. Total membranes prepared from MC1060 cells grown on oleate, were incubated with 10 μM 11-DAP-[11-^{3}H]-undecanoate (3.75 Ci/mmole) at 0.1 mg/ml (A) or 0.5 mg/ml (B) of protein at 4°C for 5 min, as described in Section 2.2.16. After photolysis at 365 nm for the times indicated, a portion of the samples (10 μg of protein) was solubilized and analyzed by electrophoresis on 12% polyacrylamide gels as described in Section 2.2.17. The gels were processed for fluorography as described in Section 2.2.22.

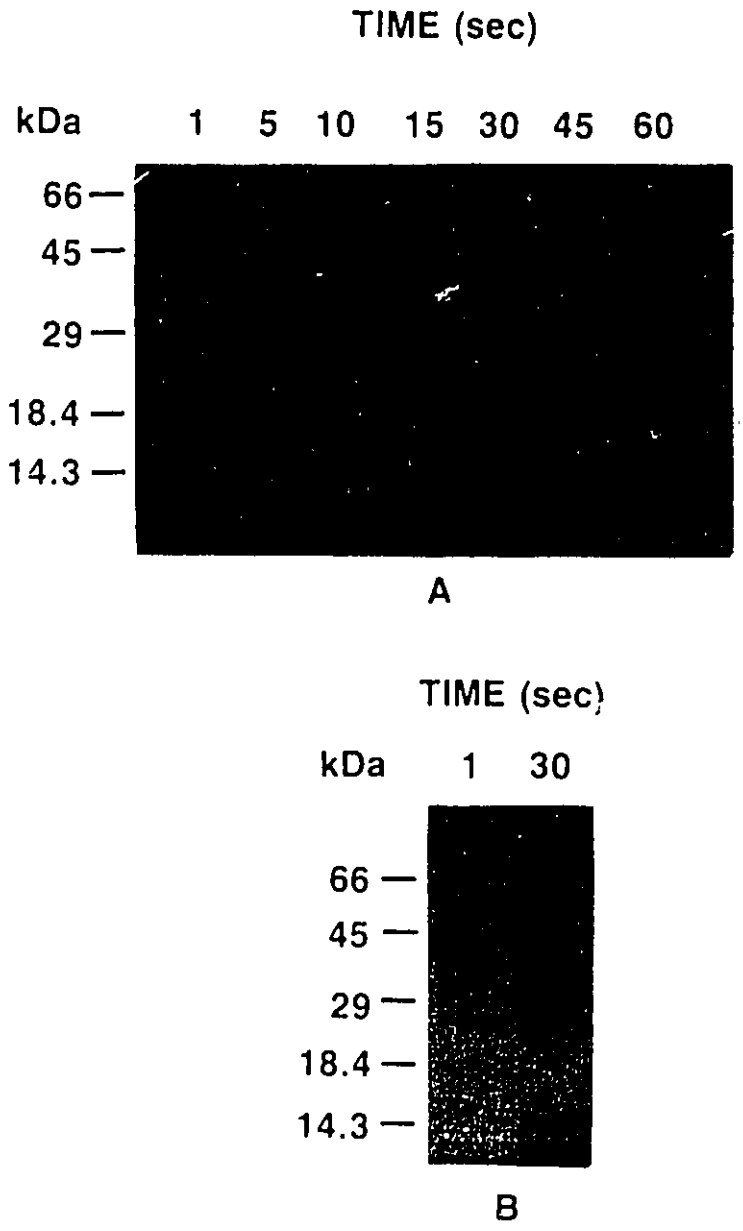

Figure 11. Effect of photolysis times at different power output on non-carbene related labeling of proteins. 11-DAP-[11-^{3}H]-undecanoate (20 μM, 3.75 Ci/mmole) in 25 mM sodium phosphate, pH 6.5 was photolyzed at 1000 (A) or 200 (B) watts for the times indicated and immediately incubated with membranes (0.5 mg/ml) at 25°C for 1 h in the dark. A portion of the samples (10 μg of protein) was solubilized and analyzed by electrophoresis on 12% polyacrylamide gels as described in Section 2.2.17. The gels were processed for fluorography as described in Section 2.2.22.

of various proteins by 11-DAP-[11-^{3}H]-undecanoate in isolated membranes (Fig. 10). In the presence of 100 μg of membrane protein/ml, the intensity of labeling of a 43 kDa protein and a 37 kDa protein was maximal after 5 sec of photolysis (Fig. 10A, arrows). Furthermore, when the photolysis was performed at a protein concentration of 500 μg/ml maximum labeling of the 43 kDa and 37 kDa proteins were also obtained within 5 sec (Fig. 10B, arrows).

Rearrangement of the diazirine to the linear diazo form was reported to occur during photolysis at 365 nm (Bayley, 1983; Smith and Knowles, 1973). The linear diazo species has a long half-life and reacts preferentially with thiol, carboxylic, hydroxyl and amino groups (Bailey, 1983; Smith and Knowles, 1973). The photoreactive group of the fatty acid analogue in the linear diazo form will react preferentially with proteins having one of the aforementioned functional group exposed. This is of particular concern since proteins labeled by the photoreactive fatty acid analogue may not necessarily have a role in the transmembrane movement of fatty acid.

To assess whether the linear diazo species was generated during photolysis at 365 nm, post-photolytic labeling of proteins by 11-DAP-[11-^{3}H]-undecanoate in isolated membrane was monitored (Fig. 11). This was accomplished by photolyzing the photoreactive fatty acid analogue followed by incubation with the membranes for 1 h in the dark. Irrespective of the length of time of photolysis no membrane proteins were labeled (Fig. 11A). However, when the intensity of the 365 nm light was reduced by decreasing the power output of the lamp from 1000 to 200 watts, several proteins were labeled post-photolytically (Fig. 11B). These results

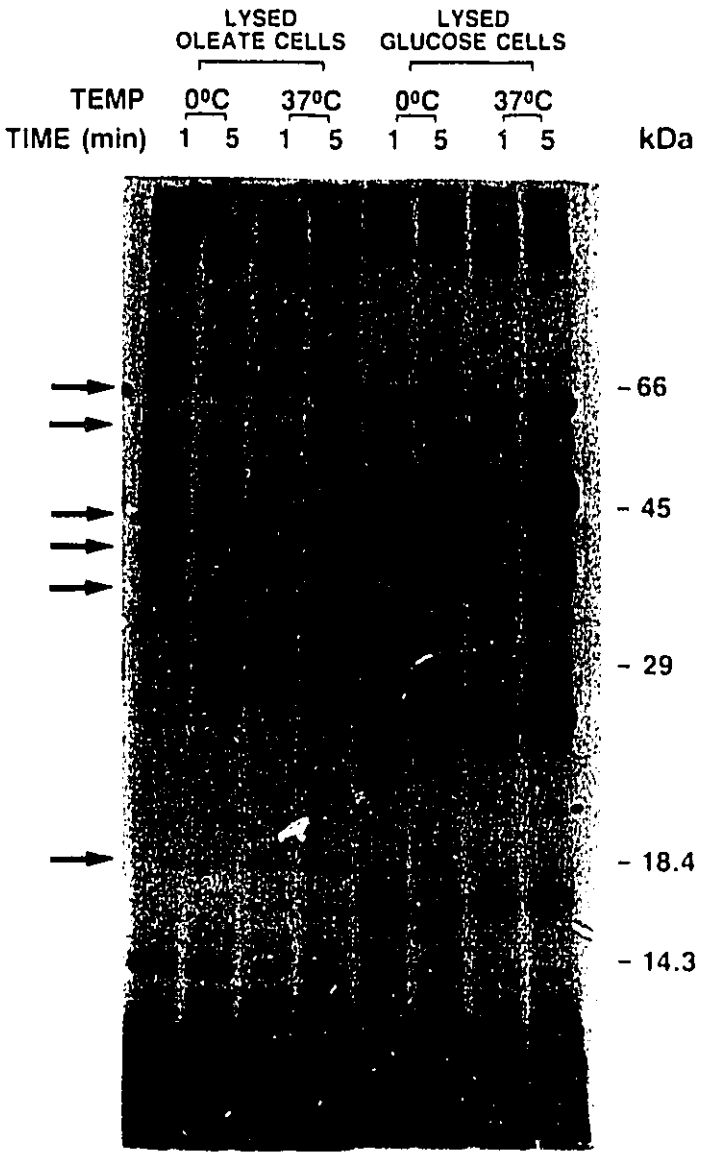

Figure 12. SDS-PAGE analysis of proteins labeled with 11-DAP-[11-^{3}H]-undecanoate in total lysates of MC1060 grown on oleate or glucose. The cells (4.7×10^9) were lysed and treated with DNase I as described in Section 2.2.9. The total cell lysate (0.1 mg/ml) was incubated with 10 μM 11-DAP-[11-^{3}H]-undecanoate and 0.08% deoxycholate in 50 Tris-HCl, pH 8.0 at 0°C or 37°C. After photolysis at the times specified, the sample (25 μg of protein) was solubilized and analyzed by electrophoresis on a 12% polyacrylamide gel as described in Section 2.2.17. The gel was processed for fluorography as described in Section 2.2.22.

show that under optimum photolysis conditions (1000 watt), very little linear diazo species is generated. The labeling of proteins by the photoreactive fatty acid probe at 1000 watt (Fig. 10) was most likely due to the carbene rather than the linear diazo species.

3.2. Labeling of Fatty Acid Binding Proteins in Total Lysate of *E. coli*

The photoreactive fatty acid analogues were shown previously to be biologically active (Leblanc and Gerber, 1984; Leblanc *et al.*, 1982; Capone *et al.*, 1983). It is therefore expected that 11-DAP-[11-^{3}H]-undecanoate would label fatty acid binding proteins in *E. coli*. Several proteins were labeled with the probe in total lysate prepared from both fatty acid and glucose grown cells (Fig. 12); the absence of labeling of the 70 kDa, 55 kDa, 43 kDa, 40 kDa, 37 kDa and 18 kDa proteins (arrows) in the lysate of glucose grown cells shows that the expression of these proteins is induced by fatty acid and repressed by glucose. The levels of labeling of proteins in the lysate of cells grown on glucose are insensitive to the temperature or time of preincubation with the photoreactive probe. The extent of labeling of the proteins in the lysate from cells grown on oleate also remained constant at 0°C as the incubation was increased from 1 to 5 min. However, at 37°C the intensities of labeling of the 43 kDa, 37 kDa, 35 kDa and 18 kDa proteins (arrows) at 1 min were much higher than those observed at 0°C. As the incubation at 37°C was increased to 5 min, in addition to an increase in the intensity of labeling of the above proteins, two other proteins having molecular masses of 70 kDa and 55 kDa (arrows) were intensely labeled. The fact that these proteins were not significantly labeled at 0°C, as well as the latency of labeling at 37°C, suggest

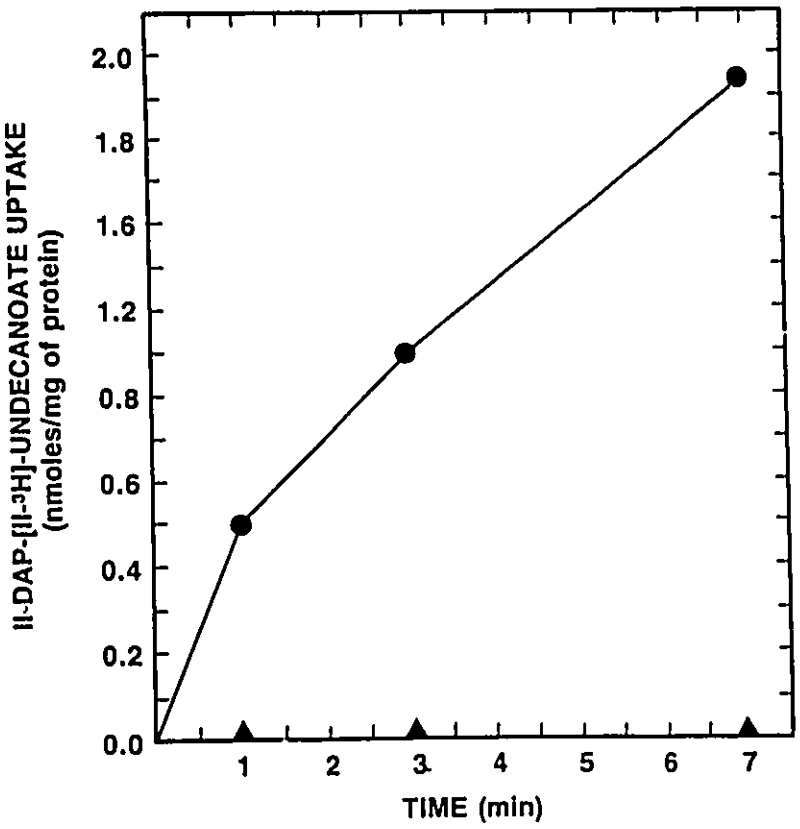

Figure 13. Uptake of 11-DAP-[11-^{3}H]-undecanoate in ML308 grown on oleate or glucose. Washed oleate (●) or glucose (▲) grown cells (1.2×10^9) in 1.0 ml of incubation buffer were incubated at 25°C for 30 min with shaking. D-lactate (40 μmoles) in 500 μl of incubation buffer was added and the incubation continued at 25°C for 5 min. 11-DAP-[11-^{3}H]-undecanoate (0.15 μmole, 3.75 Ci/mmole) in 500 μl of incubation buffer was added and the incubation continued. At the specified times, the incubation mixtures were assayed for uptake of the probe as described in Section 2.2.3.

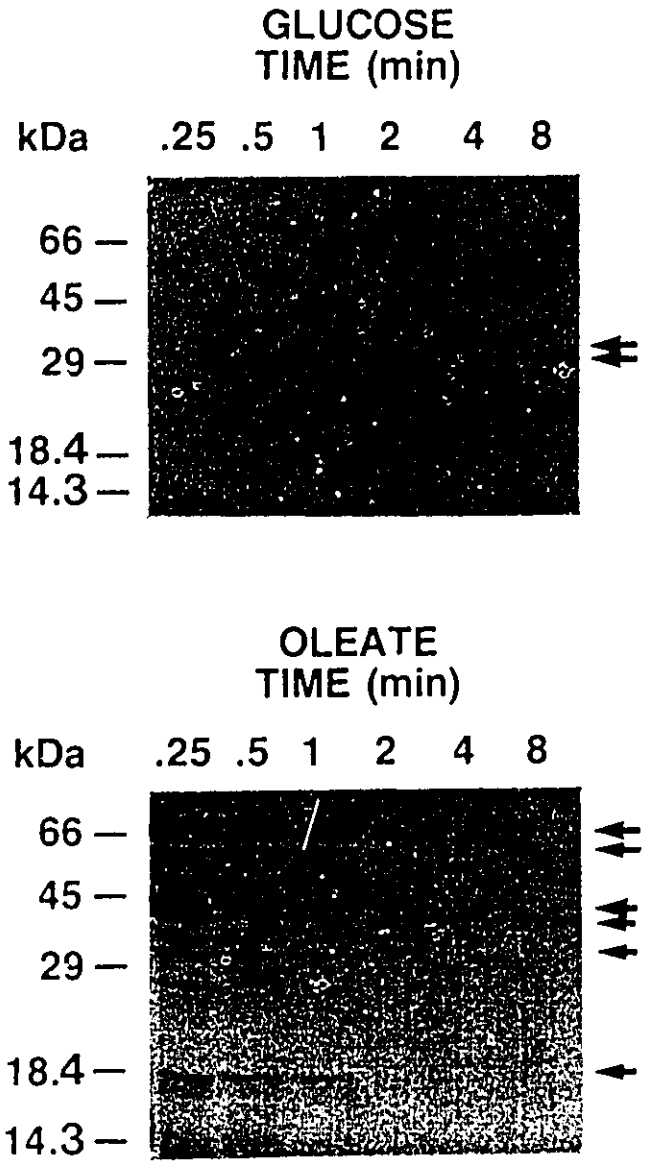

Figure 14. SDS-PAGE analysis of the time dependent labeling of proteins in glucose or oleate grown MC1060 cells. MC1060 was starved at 37°C for 15 min as described in Section 2.2.3 and incubated with 11-DAP-[11-^{3}H]-undecanoate (3.75 Ci/mmole) at 37°C as described in Section 2.2.16. At the times indicated, 150 µl of the incubation mixture was photolyzed. A portion of the labeled cells (4.3 x 10^7) was solubilized and analyzed by electrophoresis on 12% polyacrylamide gels as described in Section 2.2.17. The gels were processed for fluorography as described in Section 2.2.22.

that these proteins were labeled by the photoreactive fatty acid analogue that had undergone metabolism. This conclusion is consistent with other studies showing that 11-DAP-[11-^{3}H]-undecanoate was recognized as long chain fatty acids by a variety of mammalian (Leblanc, *et al.*, 1982; Capone, *et al.*, 1983; [illegible] and Gerber, 1984a) and *E. coli* metabolic enzymes (Greenberg, *et al.*, 1976; Olson, *et al.*, 1979).

3.3. Uptake of 11-DAP-[11-^{3}H]-undecanoate by *E. coli*

Cells grown on oleate were capable of taking up the probe while glucose grown cells were not (Fig. 13). The internalization of 11-DAP-[11-^{3}H]-undecanoate was also monitored by labeling of the proteins which were labeled in the cell lysate (Fig. 12). Incubation of cells grown on glucose with 10 μM 11-DAP-[11-^{3}H]-undecanoate at 37°C resulted in minor labeling of the 37 kDa and 35 kDa proteins (Fig. 14A, arrows). The extent of labeling of these proteins remained essentially constant as the incubation was continued for 8 min. The fact that absolutely no labeling was observed for the proteins labeled in the cell lysate (Fig. 12) indicates that these cells totally exclude the probe. Photolysis of oleate grown cells after a brief pre-incubation with 11-DAP-[11-^{3}H]-undecanoate (10 μM) resulted in significant labeling of the 70 kDa, 55 kDa, 43 kDa, 40 kDa and minor labeling of the 35 kDa and 18 kDa proteins (Fig. 14B, arrows). The extent of labeling of these proteins was dramatically reduced with increasing pre-incubation times beyond 1 min, indicating that the probe was being depleted. These results showed that the photoreactive fatty acid analogue was being taken up specifically by the transport system expressed in oleate grown cells. The lack of uptake in glucose grown cells

showed that the level of passive permeation in the absence of the transport system is very low. The observation that the photoreactive fatty acid is recognized as a long chain fatty acid by the *E. coli* transport system and metabolic enzymes showed that this probe is appropriate for labeling proteins involved in this process.

3.4. Labeling and Identification of the *fadL* Protein

The *fadL* protein was shown to be necessary for fatty acid permeation of the outer membrane of *E. coli* (Ginsburg *et al.*, 1984; Maloy *et al.*, 1981; Nunn and Simons, 1978; Black *et al.*, 1987; Black, 1990; Kumar and Black, 1991). However, the mechanism by which this protein facilitates the transmembrane movement of fatty acids is not understood. It was proposed by others (Nunn *et al.*, 1986; Black, 1990; Kumar and Black, 1991) that the *fadL* protein binds fatty acids based on the following observations: *fadD fadL*$^+$ cells bind 4-7 times more fatty acids than *fadD fadL* cells (Nunn *et al.*, 1987; Black, 1990); antibodies against the *fadL* protein partially inhibited fatty acid binding to *fadD fadL*$^+$ cells (Black, 1990); mutations in the N-terminus of the *fadL* protein resulted in reduced binding and fatty acid uptake (Kumar and Black; 1991). Although these studies showed a correlation between binding and the presence of a functional *fadL* protein, they have not demonstrated directly that this protein is responsible for the binding observed. An alternative explanation might be the binding of fatty acids to sites within the periplasm of the *fadD fadL*$^+$ cells; these sites being inaccessible to fatty acids when the *fadL* proteins's function was inhibited by antibody binding or mutation of the *fadL* gene.

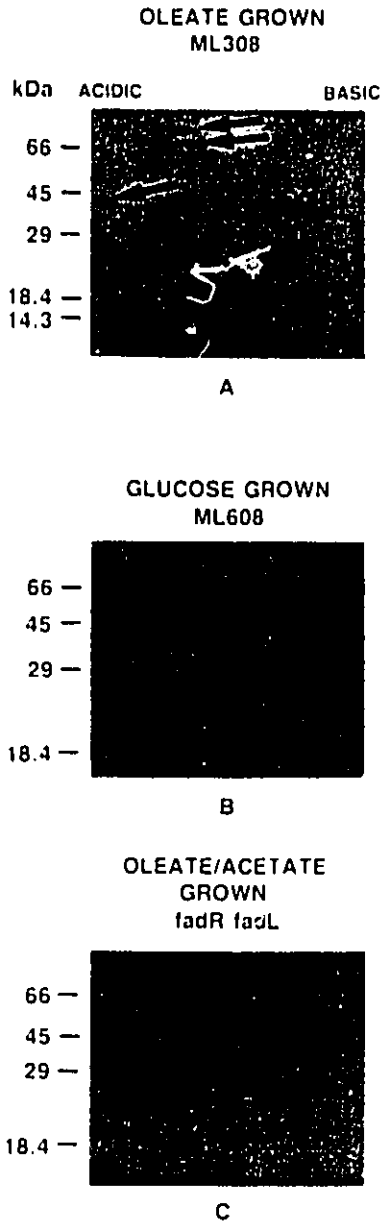

Figure 15. 2-D PAGE analysis of proteins labeled with 11-DAP-[11-^{3}H]-undecanoate in ML308 and *fadR fadL* cells. ML308 grown on oleate or glucose and *fadR fadL* cells were starved for 15 min at 37°C as described in Section 2.2.3, and then labeled with 11-DAP-[11-^{3}H]-undecanoate (3.75 Ci/mmole) at 4°C using the free fatty acid method as described in Section 2.2.16. The labeled cells were lysed as described in Section 2.2.17 and solubilized as described in Section 2.2.18 using 5 µl of 250 mM Tris-HCl, pH 6.8 containing 1% SDS (w/v) and 10 µl of a solution containing 17.5% MSH (v/v), 7% ampholytes and 4% NP-40. Urea (15 mg) was added to 14 µl of the preparation (4.8×10^7 cells) and analyzed by 2-D PAGE as described in Section 2.2.19. The gels were processed for fluorography as described in Section 2.2.22.

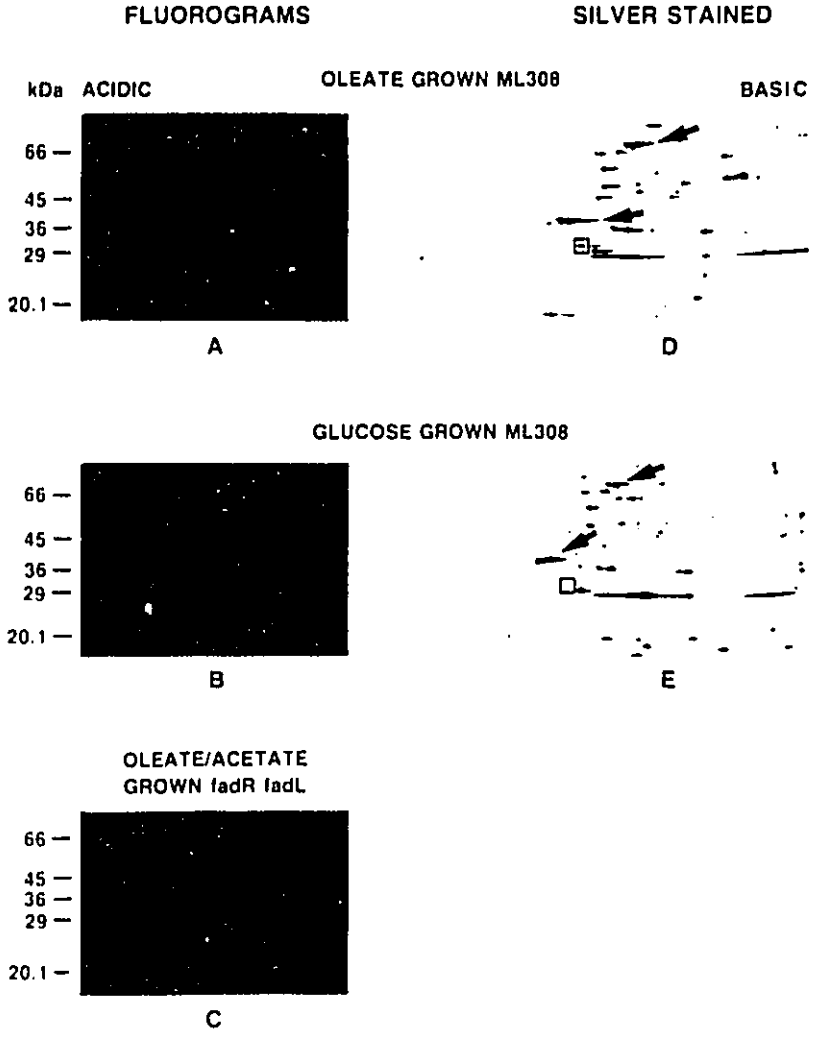

Figure 16. 2-D PAGE analysis of proteins labeled with 11-DAP-[11-^{3}H]-undecanoate in total membranes prepared from *fadR fadL* and glucose or oleate grown ML308 cells. The membranes were labeled with 11-DAP-[11-^{3}H]-undecanoate (15 Ci/mmole) at 4 °C using the free fatty acid method, as described in Section 2.2.16. The labeled membranes were solubilized at an SDS to protein ratio of 2.6 using Condition A of Section 2.2.18. 2-D PAGE analysis was performed as described in Section 2.2.19 and the gels were silver stained or processed for fluorography as decribed in Section 2.2.22.

Therefore, to determine more directly whether the *fadL* protein is capable of binding fatty acids, the photoreactive fatty acid analogue 11-DAP-[11-^{3}H]-undecanoate was used.

Labeling of oleate grown ML308 cells with a high concentration (10 μM) of the probe followed by 2-D gel electrophoresis showed light labeling of proteins having molecular masses of 75 kDa, 66 kDa and 37 kDa (arrows) while a 33 kDa protein having an apparent pI of 4.6 (box) was heavily labeled (Fig. 15A). In ML308 grown on glucose (Fig. 15B) and *fadR fadL* cells (Fig. 15C) the 75 kDa, 66 kDa and 37 kDa proteins (arrows) were also labeled; however, the 33 kDa protein (box) could not be detected. Furthermore, the 33 kDa protein was labeled by the probe in total membranes prepared from ML308 grown on oleate (Fig. 16A, box) but not from ML308 grown on glucose (Fig. 16B, box) or *fadR fadL* cells (Fig. 16C, box). The induced expression of the 33 kDa protein by growth of the cells on fatty acid, its presence in the membrane, the fact that it was not detected in the *fadL* deficient mutant and that it has pI comparable to that reported for the *fadL* protein (Ginsburg *et al.*, 1984; Black *et al.*, 1987; Black *et al.*, 1985) suggest that the labeled 33 kDa protein is the *fadL* protein.

3.5. Specificity and Saturability of Labeling of the *fadL* Protein

Labeling of the *fadL* protein by 11-DAP-[11-^{3}H]-undecanoate suggested that the protein is capable of binding fatty acids. However, in addition to the *fadL* protein being labeled by the probe, other proteins having molecular masses of 75 kDa and 37 kDa (arrows) were also labeled in total membranes prepared from

oleate grown cells (Fig. 16A, arrows) and in the intact cells (Fig. 15A, arrows). In whole cells the *fadL* protein (box) was labeled more heavily than the 75 kDa and 37 kDa proteins (arrows) (Fig. 15A). As indicated by a shorter exposure of the gel of Figure 16A, the *fadL* protein was labeled to the same extent as the 75 kDa and 37 kDa proteins in the isolated membranes. This increase in labeling of the 75 kDa and 37 kDa proteins in isolated membranes was attributed to increased accessibility of the probe as a result of the removal of the lipopolysaccharide during the preparation of the membranes. As detected by silver staining, the 75 kDa and 37 kDa proteins are major membrane proteins (Fig. 16D, arrows and Fig. 16E, arrows) whereas the *fadL* protein is less abundant (Fig. 16D, box). Qualitatively, the ratio of the intensity of labeling to the intensity of silver staining of the 75 kDa and 37 kDa proteins is low as would be expected for proteins having a low affinity for fatty acids. Therefore, labeling of these proteins may be non-specific, most likely due to the photoreactive fatty acid probe partitioning into the membrane and interacting with the hydrophobic domains of the proteins. In contrast, the ratio of the intensity of labeling to the intensity of silver staining of the *fadL* protein is high suggesting that this protein has a high affinity for fatty acids. The non-specific labeling of the major proteins suggests that some proportion of labeling of the *fadL* protein was also due to non-specific labeling under these conditions.

The detection of high affinity fatty acid binding sites requires the use of nanomolar concentrations of the fatty acid. However, at these concentrations a high

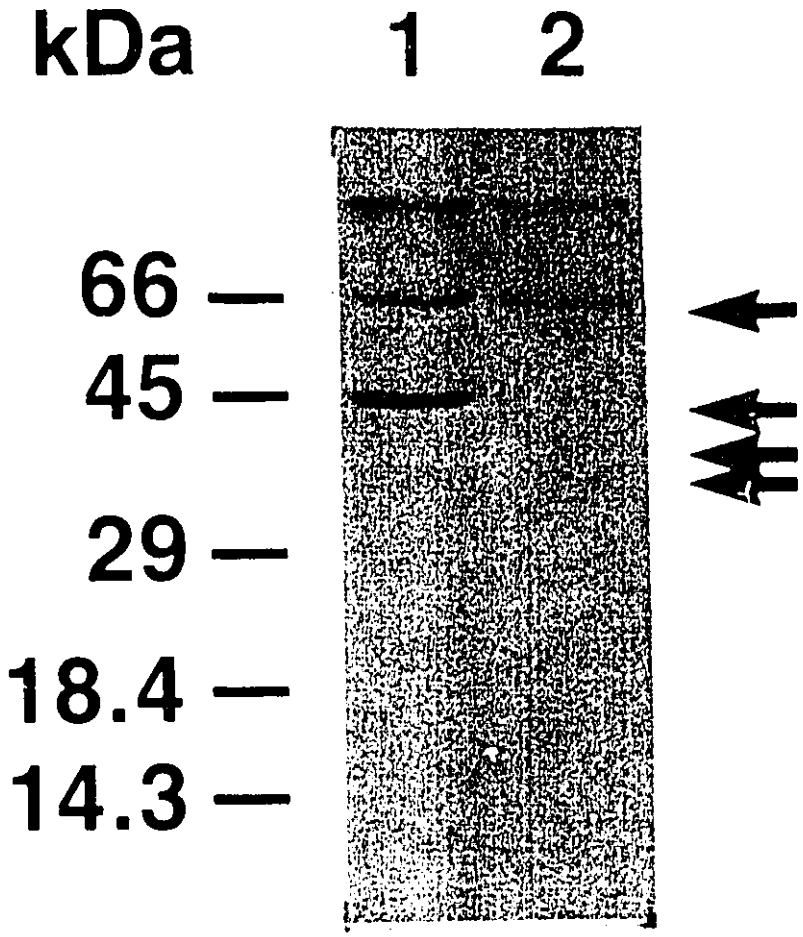

Figure 17. SDS-PAGE analysis of total membranes labeled with 11-DAP-[11-^{3}H]-undecanoate using the fatty acid-BSA method. Total membranes prepared from ML308 grown on oleate (lane 1) or glucose (lane 2) were labeled with 200 nM of 11-DAP-[11-^{3}H]-undecanoate (3.75 Ci/mmole) and washed as described in Section 2.2.15. Labeled and non-labeled membranes were solubilized and analyzed by electrophoresis on a 10% polyacrylamide gel as described in Section 2.2.17. The gel was processed for fluorography as described in Section 2.2.22.

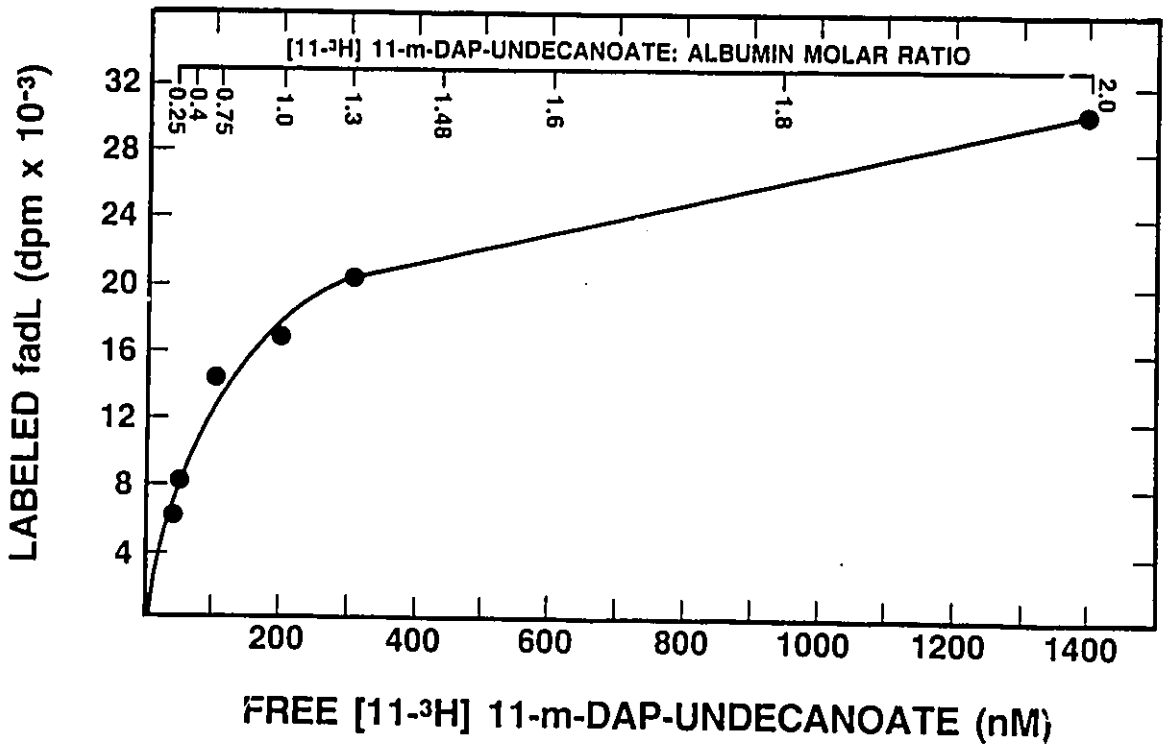

Figure 18. Labeling of the *fadL* protein with varying 11-DAP-[11-^{3}H]-undecanoate concentration using the fatty acid-BSA method. 11-DAP-[11-^{3}H]-undecanoate (103.8 nmoles, 3.75 Ci/mmole) was incubated with various amounts of BSA in 500 µl of 25 mM sodium phosphate, pH 6.5 at 37°C. After 1 h, 100 µl of total membranes (300 µg of protein) isolated from oleate grown oleate cells were added and the incubation continued for 15 min. After photolysis, 510 µl of the samples were centrifuged at 435,000 x g for 90 min at 4°C and the membrane pellets were washed twice with 600 µl of 25 mM sodium phosphate, pH 6.5 containing 0.4% BSA. The membranes were resuspended in 100 µl of water, solubilized and analyzed by electrophoresis on a 12% polyacrylamide gel as described in Section 2.2.17. The *fadL* protein was visualized by fluorography and its radioactive content was quantitated as described in Section 2.2.22.

affinity site in membranes is usually not apparent due to the fatty acid interacting with the large number of low affinity sites (membranes, surface of the glassware) available (Spector *et al.*, 1965). To saturate the low affinity sites without affecting the free fatty acid concentration, the fatty acid is routinely presented as a BSA complex which serves as a reservoir for free fatty acid.

Labeling of total membranes prepared from oleate grown cells with a low concentration of 11-DAP-[11-^{3}H]-undecanoate (200 nM) using the fatty acid-BSA method resulted in preferential labeling of the *fadL* protein (lane 1 of Fig. 17, arrow). The reduction of labeling of major proteins (37 kDa and 35 kDa, arrows; determined by coomassie staining) in total membranes isolated from oleate (lane 1) or glucose (lane 2) grown cells suggests that the *fadL* protein was labeled specifically under these conditions and confirms our conclusion that the major abundant proteins (37 kDa and 35 kDa) were labeled non-specifically by the probe when used in the low micromolar concentration range. The 66 kDa protein (arrow) present in both membranes is due to the residual BSA that is not removed during washing of the photolyzed membrane.

The fact that the *fadL* protein was labeled specifically at low concentration of 11-DAP-[11-^{3}H]-undecanoate suggests that this protein has a fatty acid binding site. In order to confirm the presence of such a site the saturability of labeling of the *fadL* protein was determined using the fatty acid-BSA method. The free probe concentration was varied by modulating the probe to BSA molar ratio. As the free probe concentration was increased from 50 nM to 1400 nM the *fadL* protein was

labeled saturably (Fig. 18). Lineweaver-Burke analysis of the data from Fig. 18, indicated that the K_d for 11-DAP-[11-^{3}H]-undecanoate was 63 nM which is approximately 4 times lower than that obtained from binding assays using *fadD fadL*$^+$ cells (Black, 1990). These results demonstrated for the first time that the *fadL* protein has a high affinity for fatty acid and that this binding is saturable. This also shows that the photoreactive fatty acid analogue can identify a membrane-bound fatty acid binding protein. The saturability of labeling of the fadL protein demonstrates that his protein has a substrate binding site. The *lamB* and *Tsx* proteins, required for permeation of maltose and nucleoside respectively, across the outer membrane of *E. coli*, have been shown to have substrate binding (Luckey and Nikaido, 1980b; Maier, *et al.*, 1988) and to function as substrate specific channels (Luckey and Nikaido, 1980a; Maier, 1988). Although the precise mechanism of the *fadL* protein in facilitating fatty acid permeation across the outer membrane is not known, it is possible that the *fadL* protein functions similarly.

3.6. Binding of Fatty Acid to the *fadL* Protein Involves an Ionic Interaction

Fatty acid uptake in *E. coli* has been reported to be maximal at pH 7.0 (Maloy *et al.*, 1981) whereas binding of fatty acids to *fadD fadL*$^+$ cells was not significantly affected over a range of pH (Black, 1990). Others have concluded that the effect of pH on fatty acid uptake was related to metabolism of fatty acid rather than *fadL* activity; further, they also concluded that binding of fatty acids to the *fadL* protein occurs by a hydrophobic interaction (Black, 1990). However, evidence

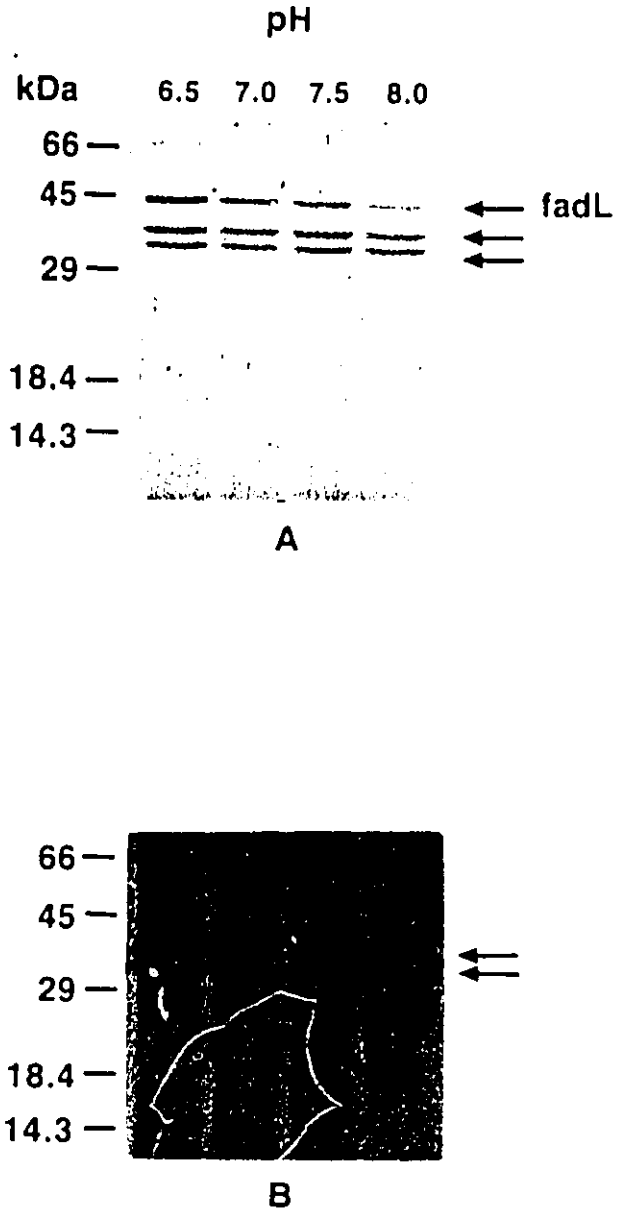

Figure 19. Labeling of total membranes with 11-DAP-[11-^{3}H]-undecanoate in sodium phosphate at various pH. Total membranes prepared from MC1060 grown on oleate (A) or glucose (B) were labeled with 11-DAP-[11-^{3}H]-undecanoate (3.75 Ci/mmole) at the indicated pH as described in Section 2.2.16. A portion of the labeled samples (10 μg of protein) was solubilized and analyzed by electrophoresis on 12% polyacrylamide gels as described in Section 2.2.17. The gels were processed for fluorography as described in Section 2.2.22.

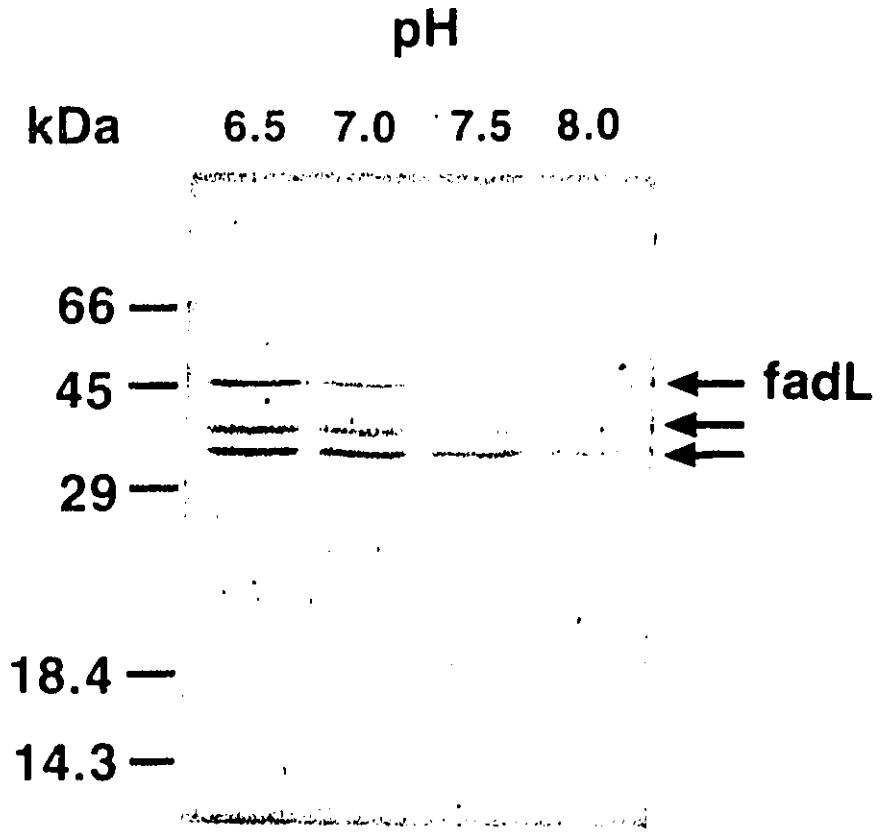

Figure 20. Labeling of total membranes with 11-DAP-[11-^{3}H]-undecanoate in imidazole-HCl at various pH. Total membranes prepared from MC1060 grown on oleate was labeled with 11-DAP-[11-^{3}H]-undecanoate at the indicated pH as described in Section 2.2.16. A portion of the labeled samples (10 µg of protein) was solubilized and analyzed by electrophoresis on a 12% polyacrylamide gel as described in Section 2.2.17. The gel was processed for fluorography as described in Section 2.2.22.

has been presented which showed that binding of fatty acids to mammalian low molecular weight cytosolic fatty acid binding proteins (Sacchettini *et al.*, 1988) and BSA (Jonas and Weber, 1990) involves an arginine residue. It is therefore possible that binding of fatty acids to the *fadL* protein involves an ionic interaction. This was determined directly by assessing the effect of varying the pH on labeling of the *fadL* protein. The free fatty acid method was used instead of the fatty acid-BSA method since the unbound probe concentration may vary as the pH was changed.

The intensity of labeling of the *fadL* protein increased as the pH was decreased from 8.0 to 6.5 (Fig. 19A, arrow). Although non-specific labeling also increased as judged by the increased labeling of the major proteins (37 kDa and 35 kDa, arrows), the ratio of the intensity of labeling of the *fadL* protein at pH 6.5 to the intensity of labeling at pH 8.0 was significantly higher than that of the 37 kDa and 35 kDa proteins. In membranes prepared from glucose grown cells, labeling of the 37 kDa and 35 kDa proteins increased only slightly as the pH was changed from 8.0 to 6.5 (Fig. 19B, arrows). This effect was reproduced in other buffers (Fig. 20) which excludes the possibility of some specific ionic effect due to the components of the buffer used. The increase in labeling of the *fadL* protein as the pH decreases is therefore not due to an increase in non-specific labeling but rather to an increase in specific labeling. This suggests that binding of fatty acids to the *fadL* protein involves an ionic interaction and is indicative of the involvement of histidine rather than lysine or arginine. These results however, do not exclude the possibility that

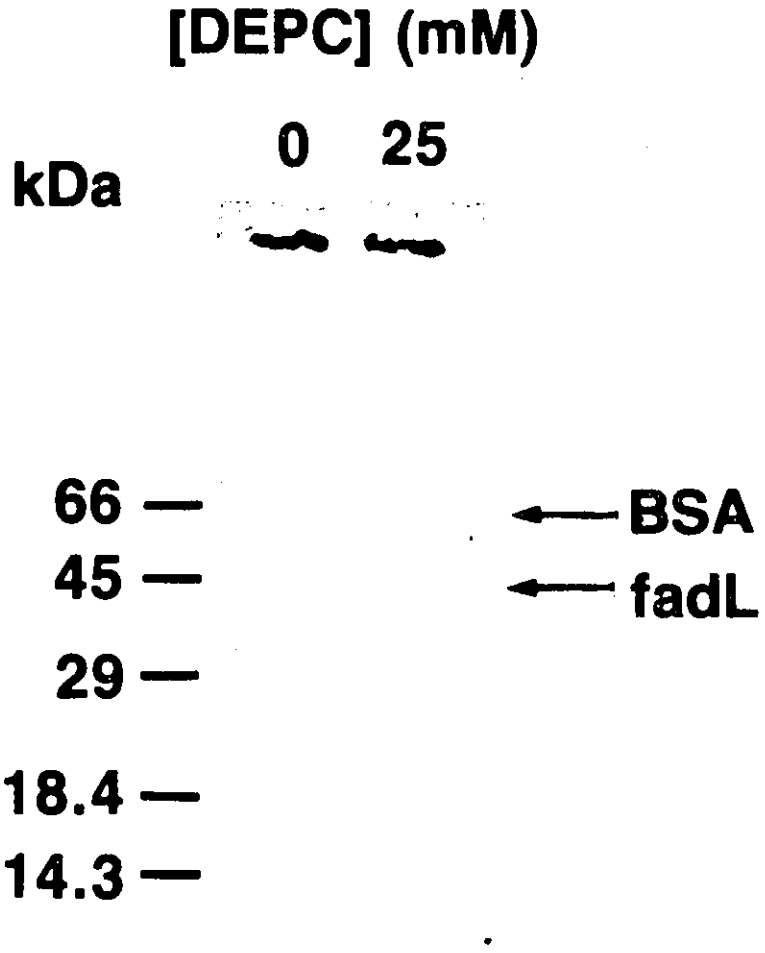

Figure 21. Effect of DEPC on labeling of the *fadL* protein. Total membranes (0.5 mg/ml) prepared from MC1060 grown on oleate were incubated without or with DEPC (25 mM in dry DMF) in 25 mM sodium phosphate, pH 6.5 for 1 h at 4°C. The membranes were pelleted by centrifugation at 125,000 x g for 60 min at 4°C and washed once with chilled 25 mM sodium phosphate, pH 6.5. The membranes were labeled 50 nM 11-DAP-[11-^{3}H]-undecanoate (3.75 Ci/mmole) and washed as described in Section 2.2.15. The labeled membranes (5 μg of protein) were solubilized and analyzed by electrophoresis on a 12% polyacrylamide gel as described in Section 2.2.17. The gel was processed for fluorography as described in Section 2.2.22.

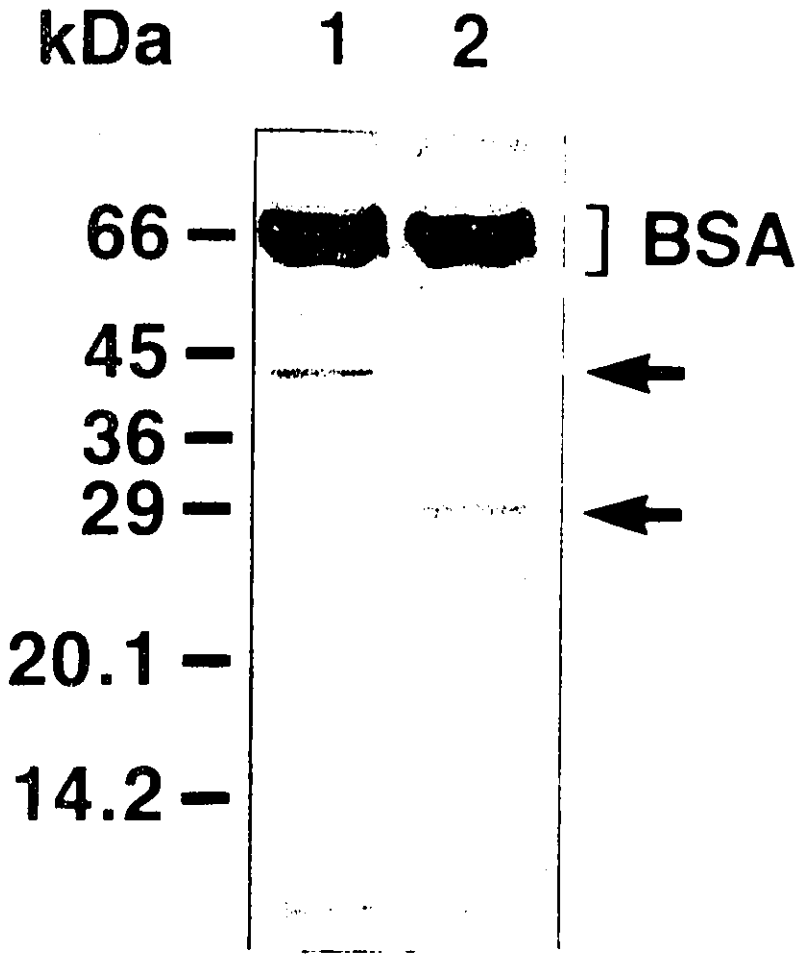

Figure 22. Heat-modifiable behaviour of the *fadL* protein. Total membranes prepared from ML308 grown on oleate were labeled with 200 nM 11-DAP-[11-^{3}H]-undecanoate (3.75 Ci/mmole) and washed as described in Section 2.2.15. An aliquot (10 µl) of the sample was added to 10 µl of 125 mM Tris-HCl, pH 6.8 containing 2 mM NaEDTA, 4.7% SDS (w/v), 20% glycerol (w/v), 20% MSH (v/v) and 0.02% bromophenol blue and solubilized at 100°C (lane 1) or 25°C (lane 2) for 5 min prior to electrophoresis on a 10% polyacrylamide gel. The gel was processed for fluorography as described in Section 2.2.22.

binding may also involve a hydrophobic interaction.

Diethylpyrocarbonate is used routinely for modifying histidine residues and has been used to show that histidine residues are involved in the catalytic activities of ribonuclease (Miles, 1977) and aminopeptidase of brain cortical synaptosomes (Chan *et al.*, 1983). The involvement of histidine in fatty acid binding was therefore studied by assessing the effect of diethylpyrocarbonate on labeling of the *fadL* protein in total membranes. At a diethylpyrocarbonate concentration of 25 mM, labeling of the *fadL* protein was completely inhibited (Fig. 21). This further suggests the involvement of histidine in fatty acid binding.

3.7. Electrophoretic Behaviour of the *fadL* Protein

The mobility of *E. coli* outer membrane proteins on SDS-PAGE is dependent on the temperature of solubilization (Nakamura and Mizushima, 1976; deGeus *et al.*, 1979). The *fadL* protein exhibits the same heat-modifiable behaviour (Black *et al.*, 1985). When the protein is solubilized at 25°C, the apparent molecular mass of the protein is 28 kDa (Fig. 22, lane 2, arrow). However, solubilization at 100°C results in the protein migrating more slowly with an apparent molecular mass of 43 kDa (Fig. 22, lane 1, arrow), which is comparable to that reported (Black *et al.*, 1985) and to the size deduced from its DNA sequence (Black, 1991). This suggests that under these solubilization conditions the protein is fully denatured while under less vigorous conditions the protein is not and consequently, migrates anomolously.

The apparent pI of the *fadL* protein was also affected by the conditions of

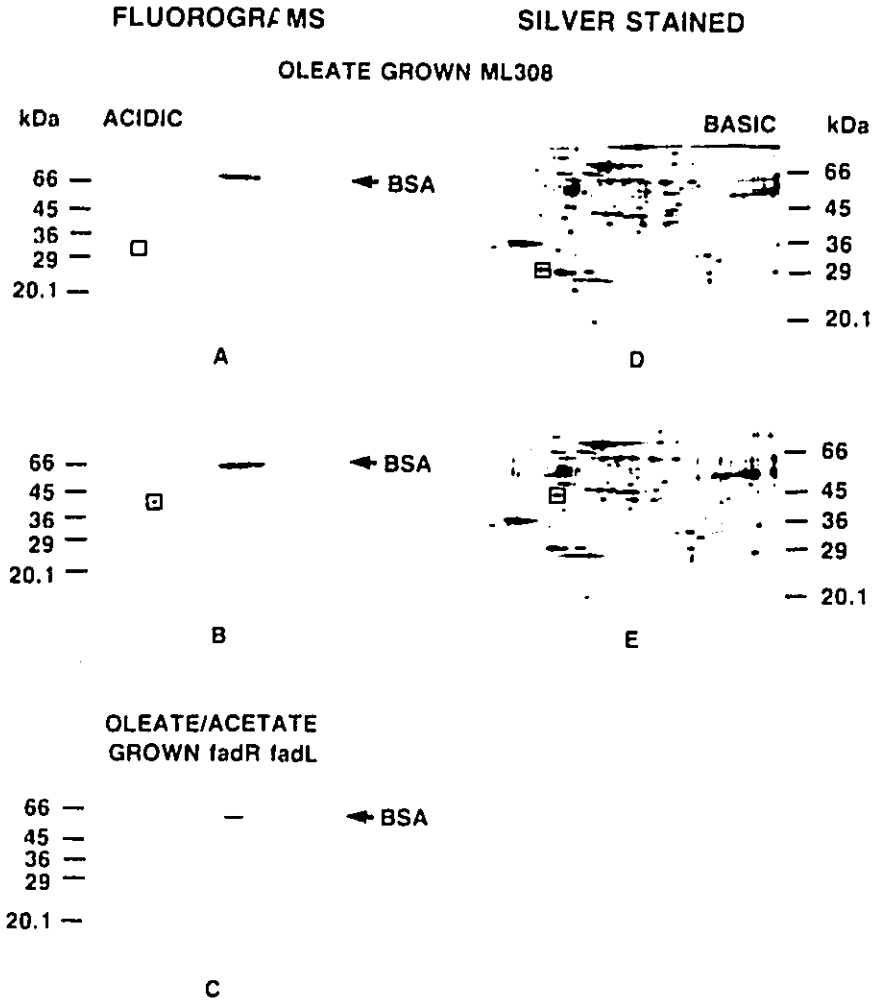

Figure 23. 2-D PAGE analysis of labeled membranes solubilized at varying SDS to protein ratio. Total membranes isolated from oleate grown ML308 and *fadR fadL* cells, were labeled with 200 nM 11-DAP-[11-^{3}H]-undecanoate (3.75 Ci/mmole) using the fatty acid-BSA method and washed as described in Section 2.2.15. The ML308 membranes were solubilized at an SDS to protein ratio of 2.6 (Panels A and D) or 6 (Panels B and E) using Conditions A and B of Section 2.2.18, respectively. The *fadR fadL* membranes were solubilized at an SDS to protein ratio of 6 (Panel C). 2-D PAGE analysis was performed as described Section 2.2.19 and the gels were silver stained or processed for fluorography as described in Section 2.2.22.

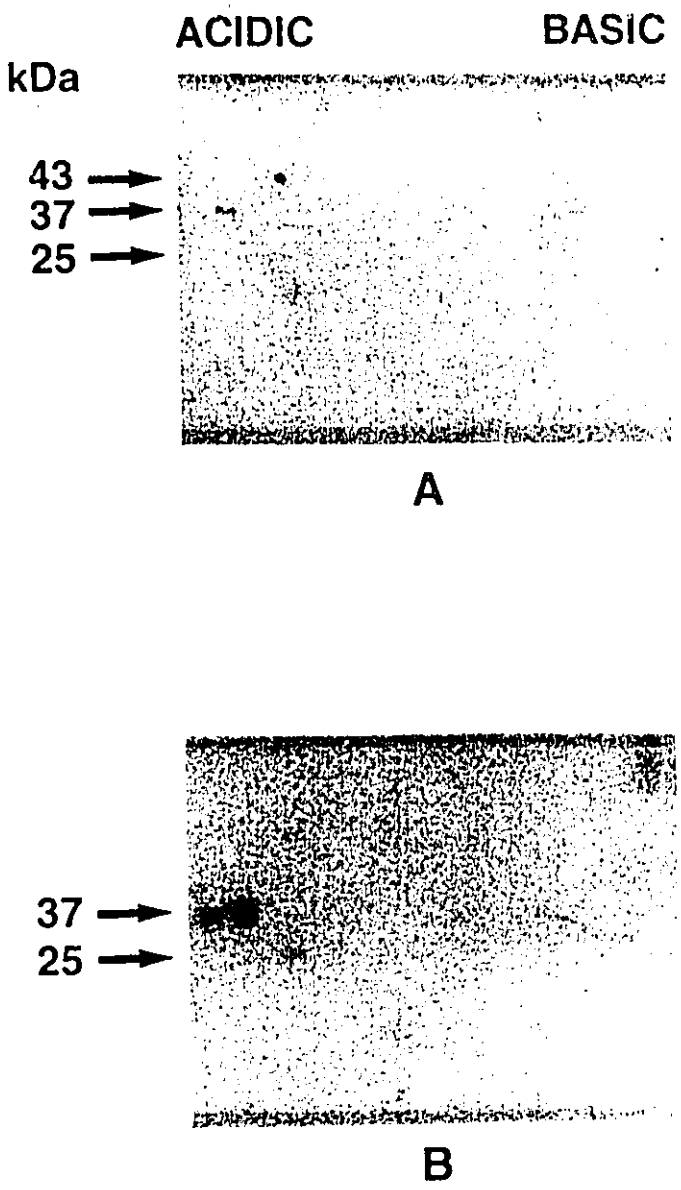

Figure 24. Western immunoblot analysis of total membranes. Total membranes prepared from ML308 grown on oleate (A) or from *fadR fadL* cells (B) were solubilized at an SDS to protein ratio of 6 using Condition B of Section 2.2.18. The proteins were separated by 2-D PAGE as described in Section 2.2.19, transferred to nitrocellulose as described in Section 2.2.22 and probed with a polyclonal antiserum to the *fadL* peptide (1:2000 dilution). The bound antibody was detected by incubation with [^{125}I]-protein A followed by exposure to a Kodak XAR film at -80°C.

solubilization. The *fadL* protein has a molecular mass of 33 kDa and an apparent pI of 4.6 despite the sample being boiled at an SDS to protein ratio of 2.6 (Fig. 23A, box). This pI is the same as that previously reported (Ginsburg *et al.*, 1984) but it is not in agreement with the calculated value of 5.2 based on its published sequence (Black, 1991). However, solubilization by boiling at an SDS to protein ratio of 6 resulted in the *fadL* protein migrating as a 43 kDa fully denatured protein with the expected pI of 5.2 (Fig. 23B, box). Silver staining also showed that the increase in the SDS to protein ratio resulted in a shift of the molecular mass of the protein from 33 kDa (Fig. 23D, box) to 43 kDa (Fig. 23E, box).

Immunoblot analysis of separated membranes with a polyclonal antiserum to a synthetic peptide at the C-terminus of the *fadL* protein showed that the 43 kDa protein having a pI of 5.2 was recognized by the antiserum in membranes prepared from ML308 grown on oleate (Fig. 24A). This result, together with the observations that a 43 kDa protein was not detected in the membranes prepared from *fadL* deficient cells by labeling (Fig. 23C) or by immunoblot analysis (Fig. 24B) further support the conclusion that the 43 kDa protein is the *fadL* protein whose pI is 5.2 when the protein is completely denatured. These results also showed that under conditions reported (Ginsburg *et al.*, 1984) the protein is behaving anomolously. The nature of this behaviour is not understood. However, it has recently been shown that the outer membrane porin protein renatures in the presence of the negatively charged LPS (Eisele and Rosenbusch, 1990); it is therefore possible that

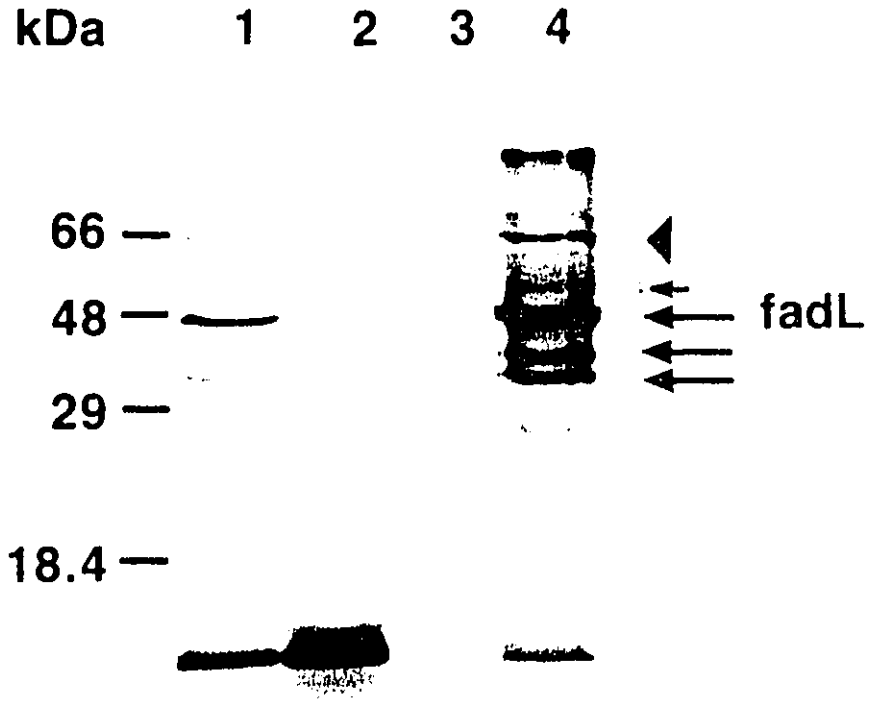

Figure 25. SDS-PAGE analysis of proteins labeled with 11-DAP-[11-^{3}H]-undecanoate in the periplasm of ML308 grown on oleate. Oleate grown cells (1.0×10^{10}) were washed and treated with 1 ml of Tris-EDTA as described in Section 2.2.20. The permeabilized cells were centrifuged and the supernatant (Tris-EDTA) was removed. The cell pellet was resuspended in 1 ml of cold water and incubated at 4°C for 10 min. The incubation mixture was centrifuged and the supernatant (osmotic shock fluid) was removed. The cell pellet (shock pellet) was resuspended in 1 ml of 30 mM Tris-HCl, pH 7.3 containing 20% sucrose. Proportionate samples of untreated cells (lane 1), Tris-EDTA supernatant (lane 2), osmotic shock fluid (lane 3) and the shock pellet (lane 4) were labeled 11-DAP-[11-^{3}H]-undecanoate (3.75 Ci/mmole) at 4°C as described in Section 2.2.16. Each sample was solubilized and analyzed by electrophoresis on a 12% polyacrylamide gel as described in Section 2.2.17. The gel was processed for fluorography as described in Section 2.2.22.

the observed behaviour is related to an association between LPS and the *fadL* protein. The fact that the pI of the protein becomes more basic when the protein is fully denatured is consistent with this interpretation.

3.8. Labeling of Periplasmic Proteins with 11-DAP-[11-^{3}H]-undecanoate

The passage of many hydrophilic molecules such as histidine and maltose (Ames, 1986) through the periplasmic space of *E. coli* is facilitated by specific periplasmic binding proteins. At present it is not known whether a similar mechanism is involved in the movement of fatty acids across the periplasmic space. To assess whether periplasmic proteins may be involved, the periplasm was isolated from Tris-EDTA permeabilized cells by osmotic shock (Neu and Heppel, 1965) and labeled with the photoreactive fatty acid probe.

In the intact cells the *fadL* protein (large arrow) was heavily labeled while proteins having molecular masses of 66 kDa (arrow head), 47 kDa (small arrow), 37 kDa (large arrow) and 35 kDa (small arrow) were lightly labeled (Fig. 25, lane 1). These proteins are outer membrane proteins (Fig. 27D) and were labeled more intensely in osmotically shocked cells (Fig. 25, lane 4). This is due to increased accessiblity of probe to the outer membrane as a result of removal of lipopolysaccharides during the Tris-EDTA treatment. In contrast, no proteins were labeled by the probe in the osmotic shock supernatant (Fig. 25, lane 3) or in the supernatant after Tris-EDTA treatment of the intact cells (Fig. 25, lane 2). The radioactive material at the bottom of the gel (lanes 1, 2 and 3) is related to labeling of LPS. The absence of a fatty acid binding protein in the periplasm strongly

suggests that fatty acid permeation of the periplasm of *E. coli* is not protein-mediated.

3.9. Mechanism of Fatty Acid translocation across the Inner Membrane of *E. coli*

Protein-mediated translocation of many solutes across the inner membrane of *E. coli* is rate-limiting in their uptake and coupled to the electrochemical potential (Kaback, 1971; Ramos and Kaback, 1977). Fatty acid uptake has been reported to be inhibited when the membrane potential was abolished by uncouplers (Kameda *et al.*, 1985; Maloy *et al.*, 1981), and to increase as the magnitude of the proton gradient was increased (Kameda *et al.*, 1987). This led others to propose that translocation of fatty acids across the inner membrane may be rate-limiting and involves a proton-fatty acid co-transporter (Kameda *et al.*, 1985). In contrast, physiochemical studies using artificial lipid bilayers have shown that long chain fatty acids by virtue of their hydrophobic nature, readily partition into the membrane and undergo flip-flop rapidly (Noy and Zakim, 1985; Cooper *et al.*, 1989; Storch and Kleinfeld, 1986; Cooper *et al.*, 1987). Flip-flop is most likely facilitated as a result of the pKa's of the fatty acid being increased upon partitioning into the hydrophobic environment of the membrane (Hamilton and Cistola, 1986). These studies argued that removal of fatty acids from the bulk solution and their subsequent transfer across the lipid bilayer by a membrane bound protein is not required (Noy and Zakim, 1985; Cooper *et al.*, 1985; Cooper *et al.*, 1987). To assess directly whether an inner membrane protein may be required for the transmembrane movement of

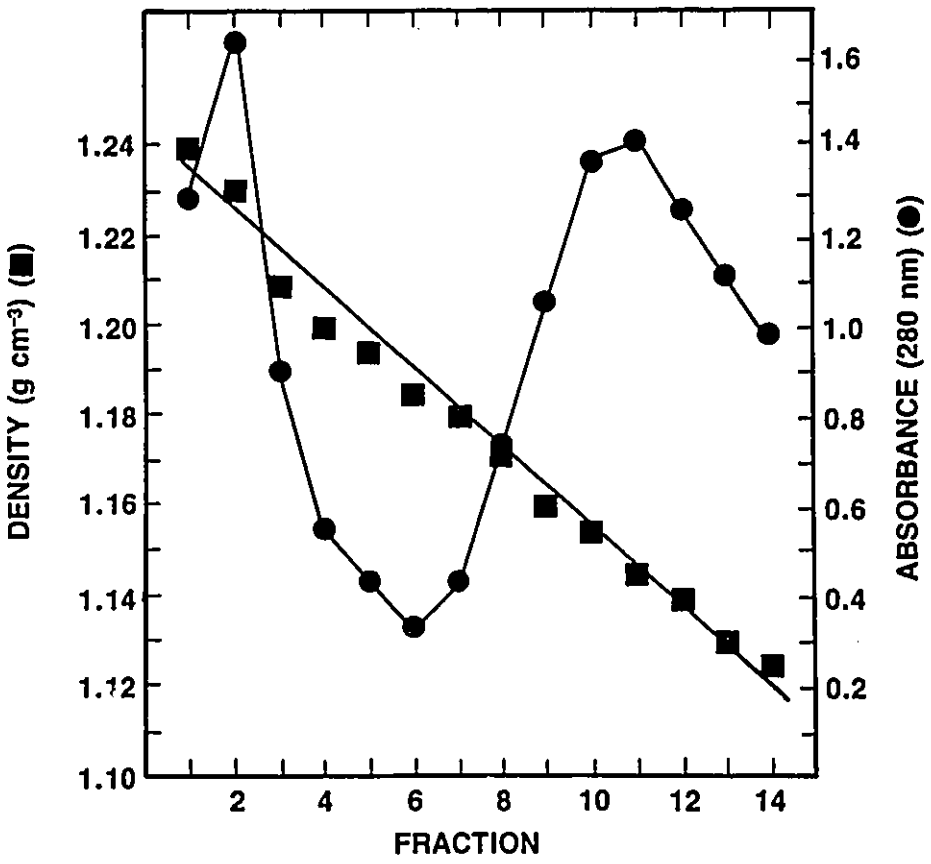

Figure 26. Separation of inner and outer membranes from ML308 grown on oleate by equilibrium density centrifugation in a discontinuous sucrose gradient. Inner and outer membranes were separated from total membranes by equilibrium density centrifugation as described in Section 2.2.10. Fractions (1 ml) were collected and analyzed for density and absorbance at 280 nm.

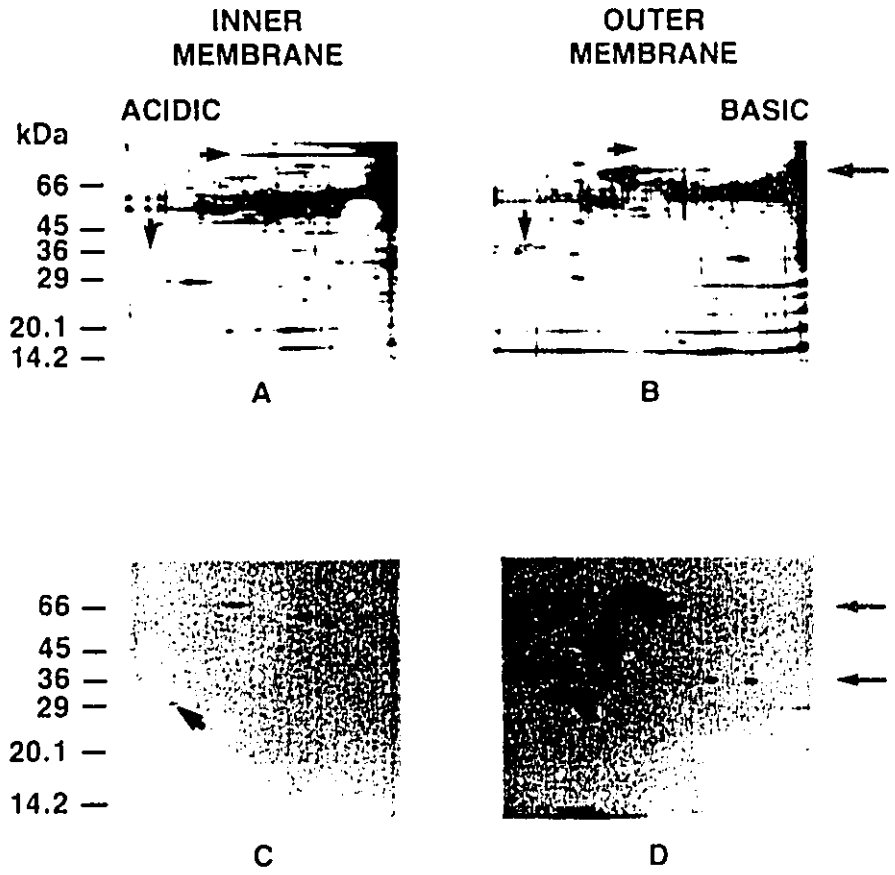

Figure 27. 2-D PAGE analysis of proteins labeled with 11-DAP-[11-^{3}H]-undecanoate in inner and outer membranes isolated from ML308 grown on oleate. Inner and outer membranes were labeled with 20 μM 11-DAP-[11-^{3}H]-undecanoate (15 Ci/mmole) at 4°C using the free fatty acid method as described in Section 2.2.16. The labeled membranes were solubilized at an SDS to protein ratio of 2.6 using condition A of Section 2.2.18. 2-D PAGE analysis was performed as described in Section 2.2.19. The gels were silver stained (Panels A and B) or processed for fluorography (Panels C and D) as described in Section 2.2.22.

fatty acids the photoreactive fatty acid probe was used to label pure inner membrane.

Inner and outer membranes were separated from total membranes prepared from ML308 grown on oleate by equilibrium density centrifugation in a discontinuous sucrose gradient (Osborn *et al.*, 1972). Fractions were collected and analyzed for density and absorbance at 280 nm. The outer membrane has an equilibrium density of 1.23 g cm^{-3} whereas the inner membrane has a density of 1.15 g cm^{-3} (Fig. 26). These values are comparable to those reported for inner and outer membrane of *E. coli* (Osborn *et al.*, 1972). The isolated inner and outer membranes were labeled separately with a high, non-limiting concentration (20 μM) of 11-DAP-[11-^{3}H]-undecanoate under equilibrium conditions and analyzed by 2-D PAGE. The method was modified in order to increase the sensitivity by at least 500-fold (the specific activity of the probe was increased to 15 Ci/mmole; the probe concentration was increased to 20 μM; the analysis of purified membranes allowed an increase in the amount of relevant protein on the gel; the exposure time was increased from 12h to 15 days). This increase of sensitivity is confirmed by the observed increase in labeling of the *fadL* protein in the outer membrane (compare Fig. 27D, inner arrows to Fig. 16A, box). Silver staining showed that several outer membrane proteins are present in the inner membrane in small quantities (Fig. 27A); these include the 75 kDa (outer arrow) and the 37 kDa proteins (inner arrow); furthermore, the outer membrane is contaminated with a small amount of the inner membrane, indicated by the presence of a major inner membrane protein having a

molecular mass greater than 100 kDa (Fig. 27B, inner arrow). These results clearly show that the separation method is efficient and that the resulting inner and outer membrane fractions are essentially pure.

In the outer membrane (Fig. 27D), several proteins including 75 kDa (outer arrow), 37 kDa (outer arrow) and the *fadL* proteins distributed between the incompletely and completely denatured forms (33 kDa and 43 kDa, inner arrows, respectively), are labeled while the only labeled proteins (75 kDa and 37 kDa) observed in the inner membrane (Fig. 27C) are those derived from the small percentage of the outer membrane contaminant. The fact that the increased sensitivity method was unable to detect any fatty acid binding proteins in purified inner membrane strongly suggests that translocation of fatty acid across the inner membrane of *E. coli* does not involve such a protein. The process is therefore likely to be one of non-protein-mediated passive diffusion of the fatty acid across the inner membranes.

3.10. Effects of Starvation and Metabolic Substrates on Fatty Acid Uptake in *E. coli*

Prior to assaying fatty acid uptake activity, the cells are routinely starved of a carbon source by others (Klein *et al.*, 1971; Nunn *et al.*, 1979; Black *et al.*, 1987; Kameda *et al.*, 1987; Black, 1990; Kumar and Black, 1991) to deplete fatty acids carried over from the growth media. This is done in order to avoid dilution of radioactive fatty acid used to monitor to fatty acid uptake. However, this starvation resulted in a substantial reduction in the rate of oleate uptake in ML308 grown on

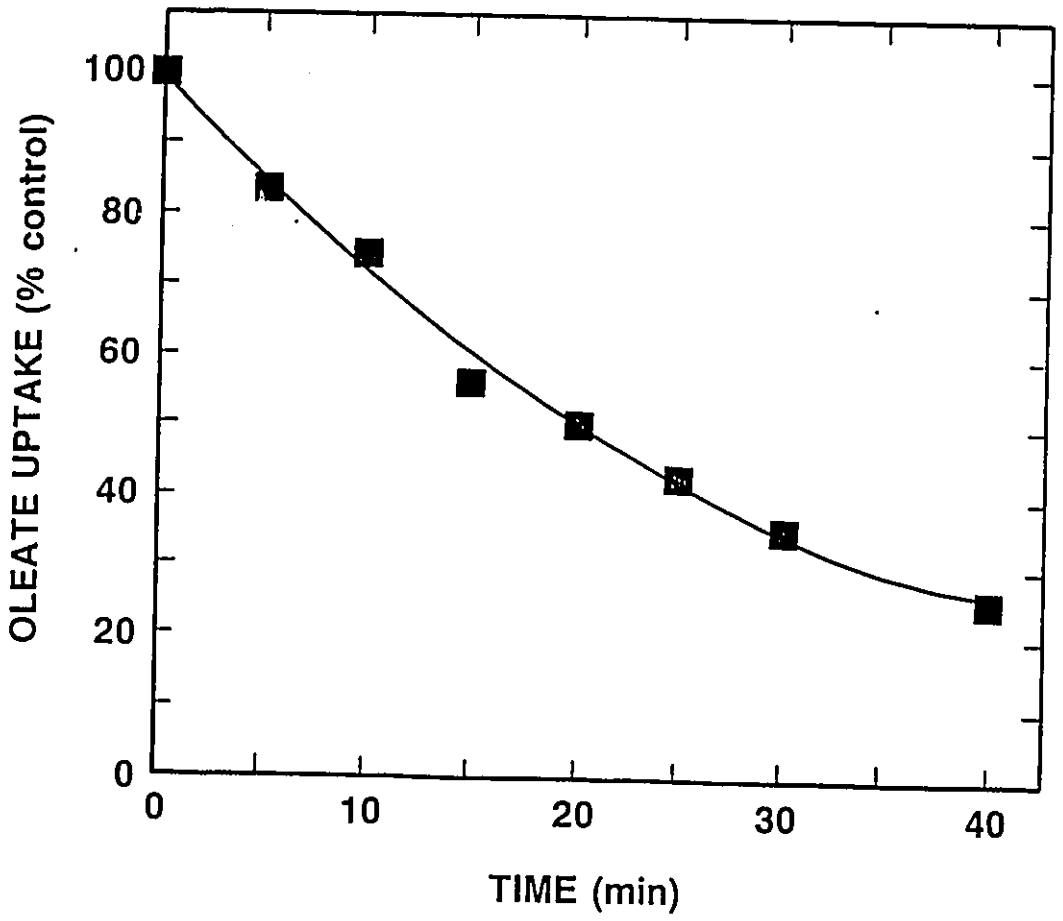

Figure 28. Effect of starvation times on the rate of oleate uptake into ML308 grown on oleate. cells (1.2×10^9) in 1.0 ml of incubation buffer were incubated with continuous shaking at 25°C for the times indicated. [^{3}H]-Oleate (0.15 μmoles) in 1.0 ml of incubation buffer was added and after 1 min, the uptake of oleate was assayed as described in Section 2.2.3. The rate of oleate uptake was expressed as a percentage of the rate observed after 1 min starvation.

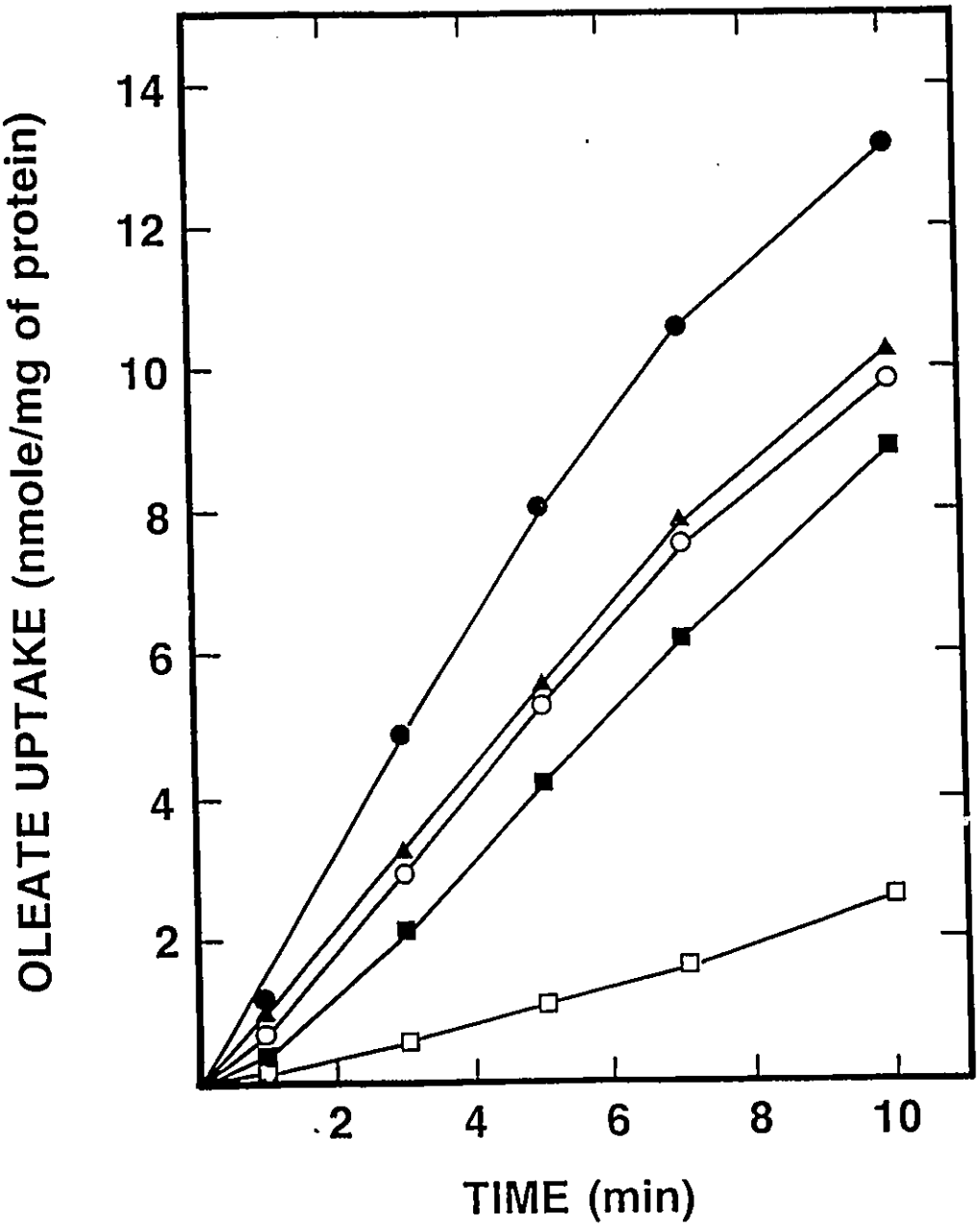

Figure 29. Effect of various metabolic substrates on oleate uptake into starved ML308 cells. Oleate grown cells (1.2×10^9) in 1.0 ml of incubation buffer were incubated at 25°C with shaking. After 30 min, 500 µl of incubation without (□) or with 40 µmoles of D-lactate (●) or acetate (▲) or L-lactate (○) or succinate (■) was added and the incubation continued at 25°C for 5 min. [^{3}H]-Oleate (0.15 µmoles) in 500 µl of incubation buffer was added and the incubation continued. At the specified times, the incubation mixtures were assayed for oleate uptake as described in Section 2.2.3.

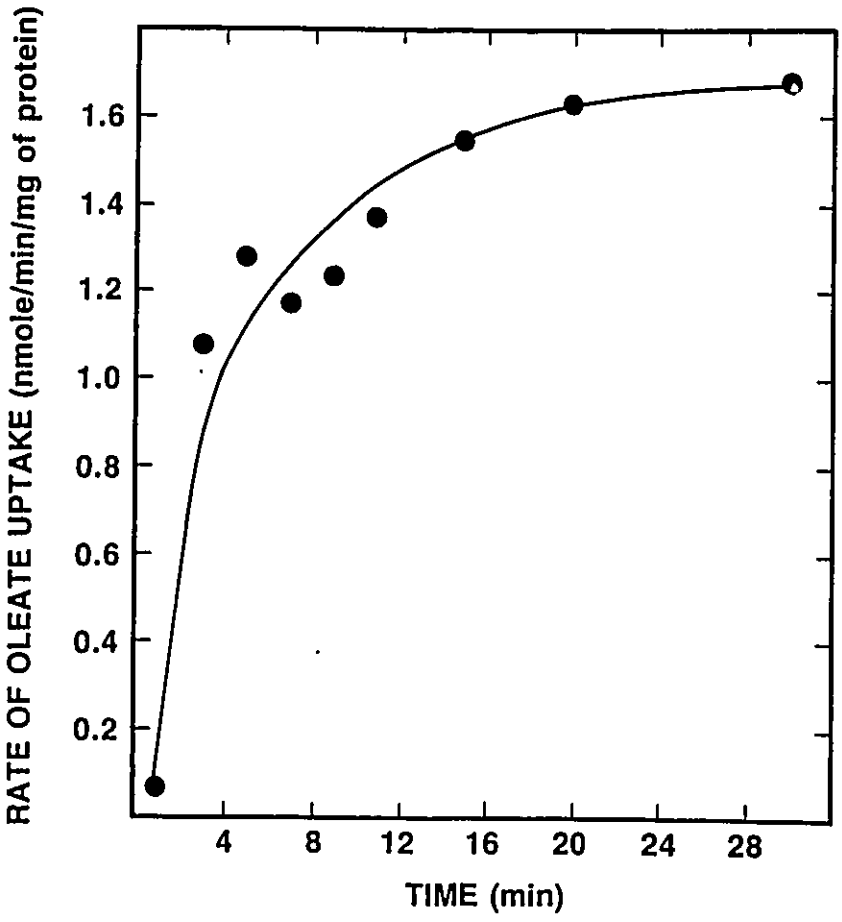

Figure 30. Time-course of D-lactate activation on the rate of oleate uptake into starved ML308 cells. Washed oleate grown cells (1.2×10^9) in 1.0 ml of incubation buffer were starved by incubation for 30 min at 25°C with continuous shaking. D-lactate (40 μmoles) in 500 μl of incubation buffer was added and the incubation continued for the times indicated. [^{3}H]-Oleate (0.15 μmoles) in 500 μl of incubation buffer was added and the incubation continued. After 1 min, the mixture was assayed for oleate uptake as described in Section 2.2.3.

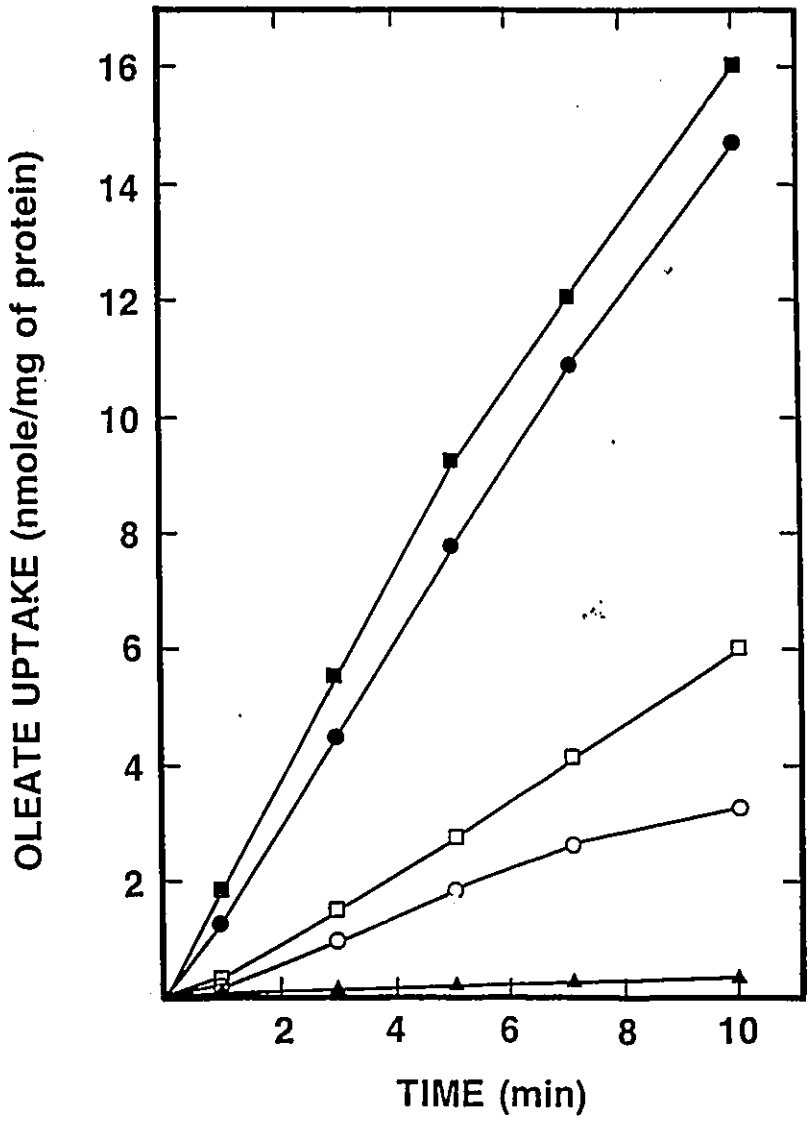

Figure 31. Effect of D-lactate on oleate uptake into starved ML308 and K-12 cells grown on oleate or glucose. Cells were grown on oleate (ML308: □,■; K-12: ○,●) or on glucose (ML308: ■), washed and suspended in incubation buffer at a density of 1.2 x 10^9 cells/ml as described in Section 2.2.3. After starvation of the cells (1.0 ml) for 30 min at 25°C, 500 µl of incubation buffer without (□,○) or with 40 µmoles of D-lactate (■,●,▲) was added. After 5 min, [^{3}H]-oleate in incubatiion buffer (500 µl of 300 µM) was added and the incubation continued at 25°C. At the times specified aliquots of the incubation mixtures were assayed for oleate uptake as described in Section 2.2.3.

oleate (Fig. 28).

The reduction in the rate of oleate uptake was attributed to partial de-energization of the cells during starvation. Therefore, the effect of various energy sources on oleate uptake in starved ML308 cells was investigated (Fig. 29). The addition of D-lactate, L-lactate, acetate or succinate resulted in a marked stimulation in the rate of oleate uptake. While D-lactate was the best, L-lactate was about 80% as effective; acetate was almost as effective as L-lactate whereas succinate was 70% as effective as D-lactate. The stimulation of oleate uptake by D-lactate was close to maximal by 15 min (Fig. 30).

The stimulatory effects of the metabolic substrates on oleate uptake further suggest that starvation might be de-energizing the cells. However, it was reported that the rate of oleate uptake in starved *fadR* cells was not affected by succinate or other energy sources (Maloy *et al.*, 1981). It is therefore possible that the effect of starvation on oleate uptake is unique to the ML308 strain. The effect of starvation on oleate uptake in the wild-type K-12 strain was determined (Fig. 31). The starved oleate grown cells exhibit similar rates of uptake, the ML308 strain being a little more active than the K-12 strain. A brief incubation of the starved cells with D-lactate stimulated oleate uptake in both ML308 and K-12 cells grown on oleate by about 3-4-fold but not in ML308 grown on glucose. The observed effects are therefore not related to the strain of *E. coli* used.

3.11. Effects of Starvation and D-lactate on the State of Energization of the Cells

Fatty acid uptake in *E. coli* was reported to be energy-dependent and coupled

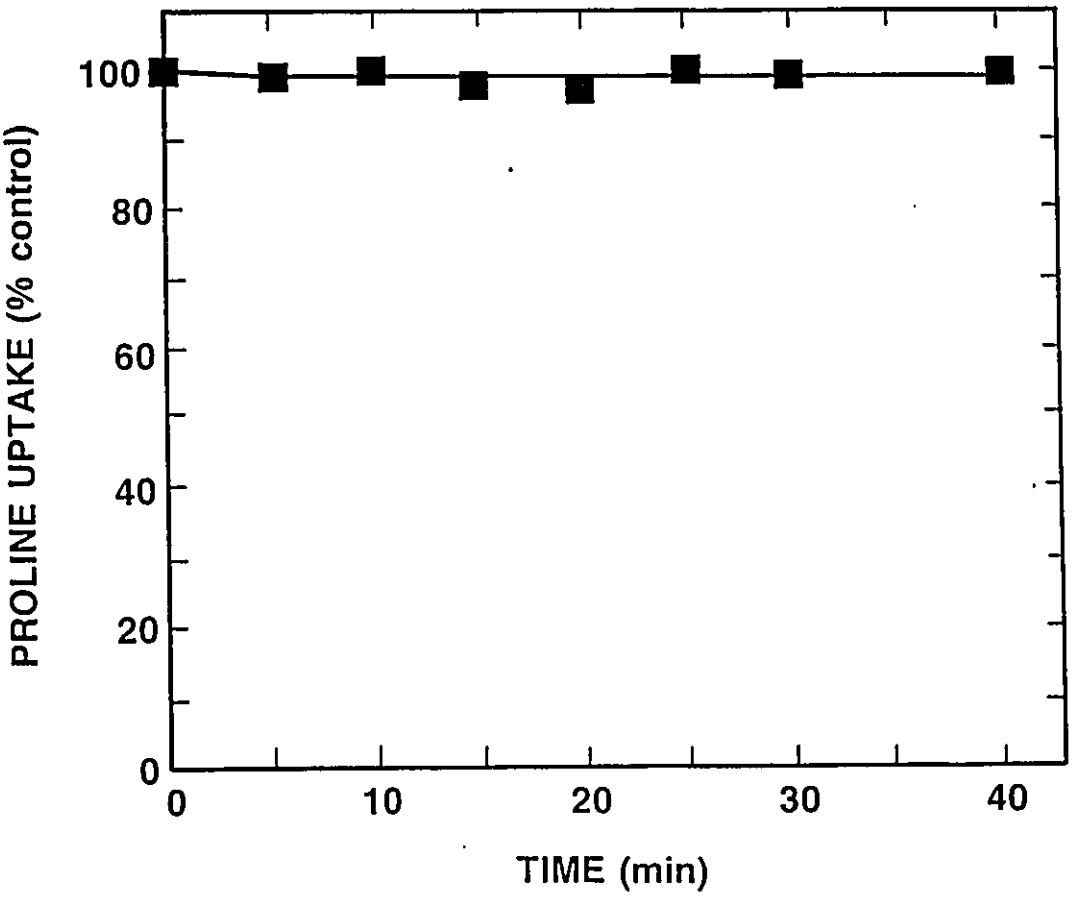

Figure 32. Effect of starvation times on the rate of proline uptake into ML308 grown on oleate. Cells (1.2×10^9) in 1.0 ml of incubation buffer were incubated with continuous shaking at 25°C for the times indicated. [^{3}H]-Proline (0.10 μmoles) in 1.0 ml of incubation buffer was added and after 1 min, proline uptake was assayed as described in Section 2.2.3. The rate of proline uptake was expressed as a percentage of the rate observed after 1 min starvation.

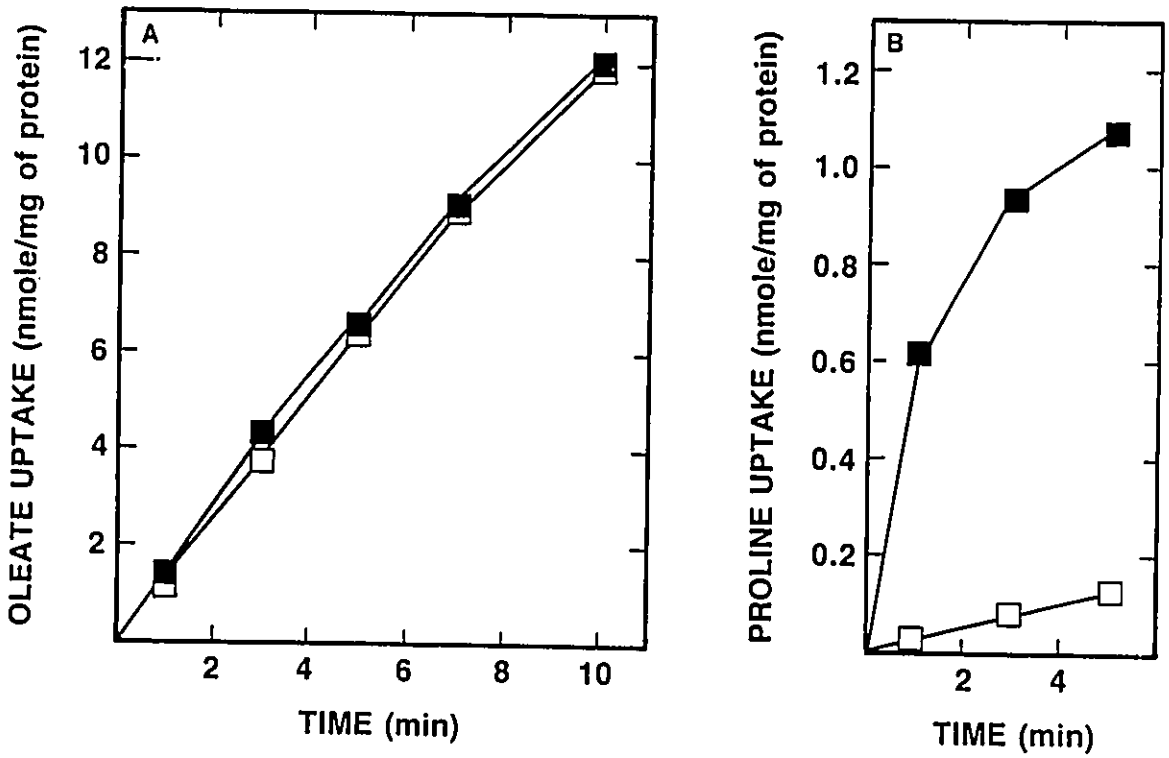

Figure 33. Effect of CCCP on oleate and proline uptake into D-lactate activated ML308 cells. Washed oleate grown ML308 cells were resuspended in 100 mM Tris-HCl, pH 8.0 containing 0.5 mM KEDTA at a density of 1.2 x 10^{10} cells/ml and incubated at 25°C. After 2, 100 µl of the permeabilized cells were added to 900 µl of incubation buffer and incubated at 25°C with shaking for 30 min. D-lactate (40 µmoles) in 250 µl of incubation buffer was added. After 5 min, 250 µl of incubation buffer without (■) or with CCCP (16 nmoles) (□) was added. After 2 min, 500 µl of [^{3}H]-oleate (0.15 µmoles) (A) or [^{3}H]-proline (0.1 µmoles) (B) in incubation buffer was added. At the specified times, the incubation mixtures were assayed for uptake as described in Section 2.2.3.11

to the electrochemical potential (Maloy *et al.*, 1981; Kameda *et al.*, 1987). The observed effect of starvation on oleate uptake may be related to de-energization of the membrane. However, proline uptake which is known to be coupled to the electrochemical potential (Kaback, 1971; Kaback, 1972), was not affected during the starvation (Fig. 32). This indicated that the magnitude of the electrochemical potential was not affected by the starvation and that the observed effects of starvation and D-lactate on oleate uptake were not related to the membrane potential.

To assess more directly whether the electrochemical potential was involved in fatty acid permeation of the inner membrane, the effect of the uncoupler CCCP on oleate uptake was determined. The amount of uncoupler required to abolish the electrochemical potential was ascertained by determining the amount required to maximally inhibit proline uptake. The use of 8 μM of CCCP which was found to inhibit proline uptake essentially completely (Fig. 33B), had no effect on oleate uptake (Fig. 33A). This clearly showed that the rate-limiting step in fatty acid uptake is not directly coupled to or affected by the magnitude of the electrochemical potential. This conclusion differs from that of others who have concluded that fatty acid uptake is coupled to the proton gradient (Kameda, 1987). This apparent discrepancy may be due to the fact that their experiment was performed with a much higher concentration of the uncoupler. The inhibitory effect they observed is may be due to the loss of acyl-CoA synthetase activity resulting from depletion of cellular ATP rather than a direct effect on the electrochemical potential.

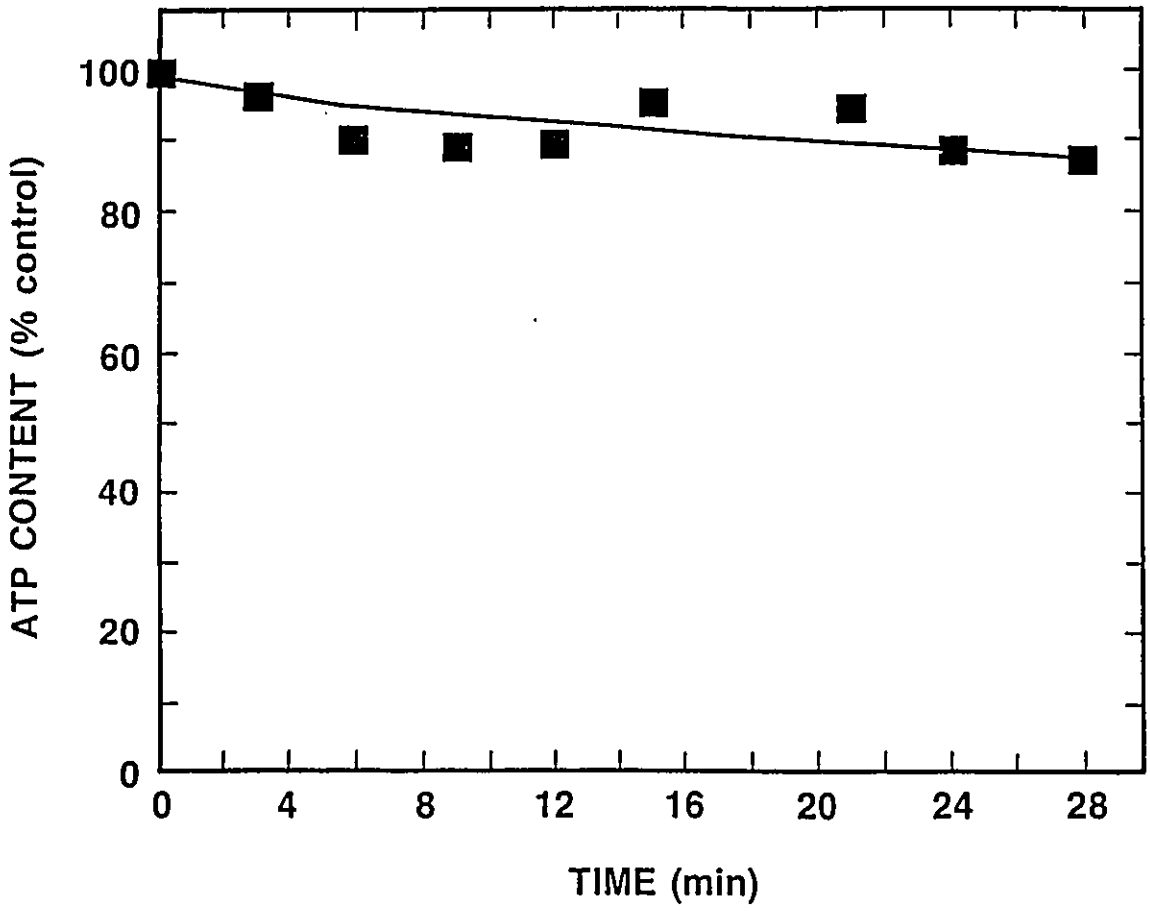

Figure 34. Determination of the cellular ATP content during starvation of oleate grown ML308 cells. Cells (1.2×10^9) in 1.0 ml of incubation buffer were incubated with continuous shaking at 25°C for the times indicated. Cold incubation buffer (1.0 ml) was added and cellular ATP was isolated and quantitated as described in Section 2.2.5.

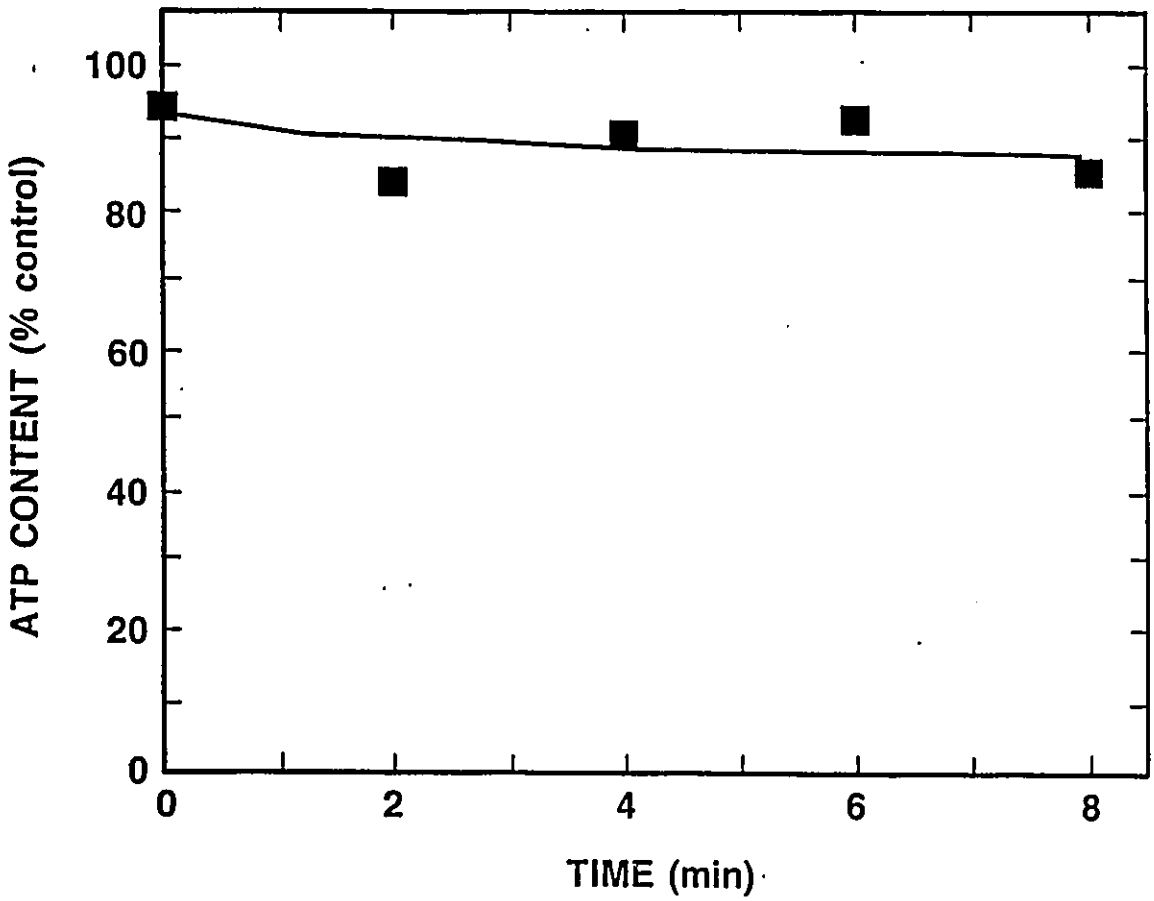

Figure 35. Determination of the cellular ATP content during incubation of the starved ML308 cells with D-lactate. Oleate grown cells (1.2×10^9) in 1.0 ml of incubation buffer were incubated with continous shaking at 25°C for 30 min. D-lactate (40 μmoles) in 500 μl of incubation buffer was added and the incubation continued for 5 min. Cold incubation buffer (500 μl) was added and cellular ATP was isolated and quantitated as described in Section 2.2.5.

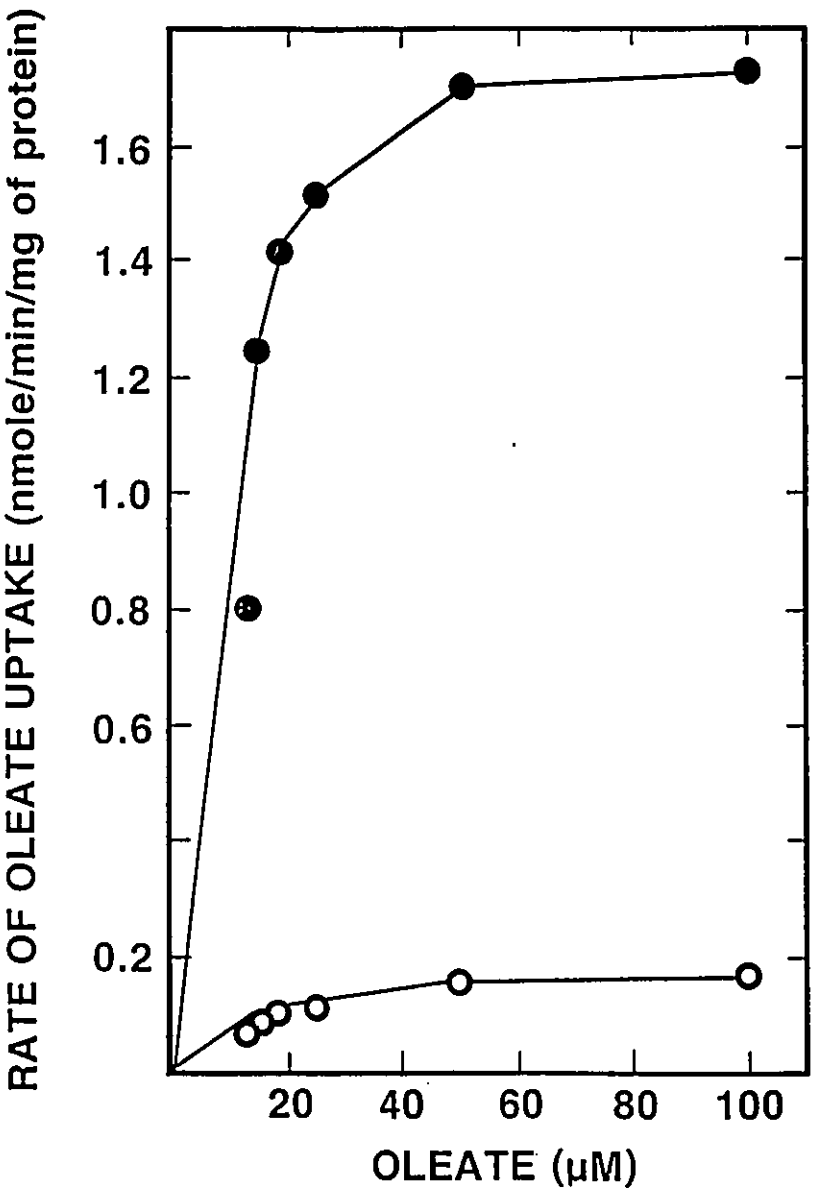

Figure 36. Effect of oleate concentration on the initial rates of oleate uptake into unactivated or D-lactate activated ML308 cells. Washed oleate grown cells (1.2×10^9) in 1.0 ml of incubation buffer were incubated with continuous shaking at 25°C for 30 min. Incubation buffer (500 μl) with (●) or without (○) D-lactate (40 μmoles) was added. After 5 min, 500 μl of the appropiate concentration of [^{3}H]-oleate in incubation buffer was added. After 1 min of incubation the mixture was assayed for oleate uptake as described in Section 2.2.3.

The above results suggest that the observed effects of starvation and D-lactate on oleate uptake are not related to changes in the electrochemical potential. Furthermore, the cytoplasmic ATP content measured using a luciferase-luciferin assay (Joshi, 1989), was not significantly affected during the starvation (Fig. 34) or during the incubation of the starved cells with D-lactate (Fig. 35). This is consistent with literature reporting that much more extensive starvation was required to deplete cellular ATP (Joshi, 1989) or to de-energize the membrane as judged by proline uptake (Berger, 1973). Therefore, the effects of starvation and D-lactate on fatty acid uptake do not appear to be related to the state of energization of the cells.

3.12. Effects of Starvation and D-lactate Activation on the Rate Constant of Transport

The affinity of the transport system for oleate as well as the maximal rate of oleate uptake was affected by starvation and D-lactate (Fig. 36). The K_t was reduced by about 3.5-fold by the addition of D-lactate, being 37.0 μM in its absence and 10.6 μM in its presence; the V_{max} was increased about 8-fold by the addition of D-lactate, being 0.29 nmole/min/mg of protein in its absence and 2.30 nmole/min/mg of protein in its presence (the K_t and V_{max} were determined by Lineweaver-Burke analysis of the data of Fig. 36). It was observed that D-lactate activation can increase the affinity by as much as 5-fold and the transport rate by as much as 10-fold. This shows that D-lactate activation resulted in a higher affinity (K_t is reduced 3.5-fold) as well as in a higher overall transport rate (V_{max} increased

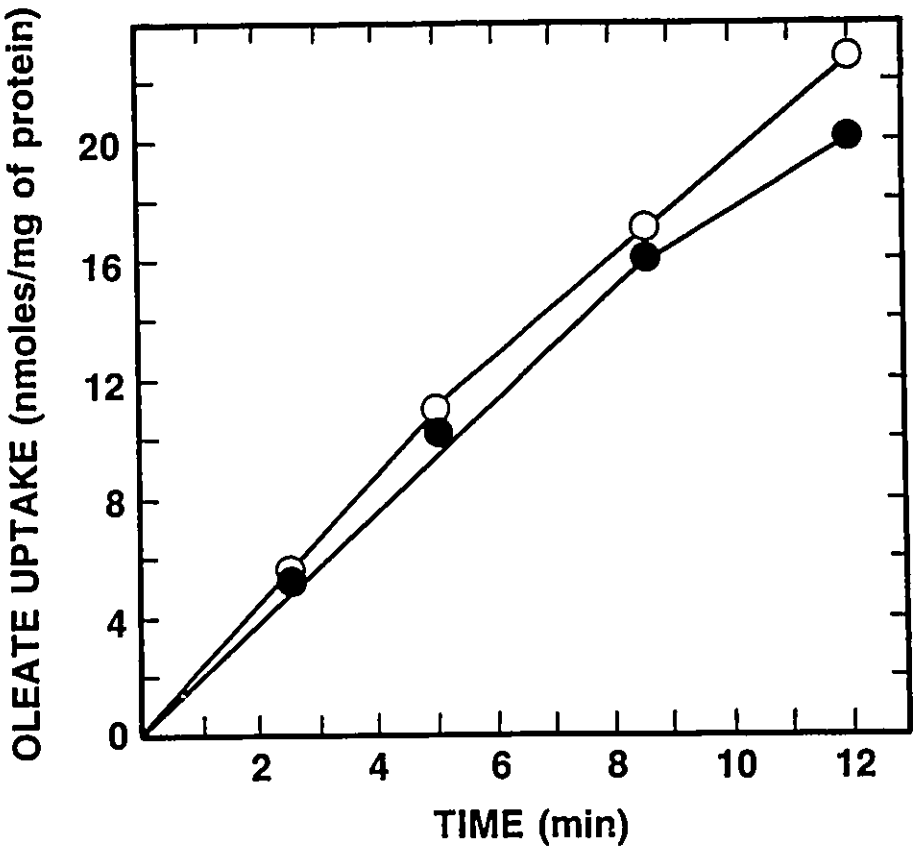

Figure 37. Effect of Tris-EDTA permeabilization of ML308 cells on fatty acid uptake. Washed oleate grown cells were resuspended in incubation buffer (●) or in 100 mM Tris-HCl, pH 8.0 containing 0.5 mM KEDTA (o) at a density of 1.2×10^{10} cells/ml and incubated at 25°C. After 2 min, 100 µl of the cells were added to 900 µl of incubation buffer and incubated at 25°C with shaking for 30 min. D-lactate (40 µmoles) in 500 µl of incubation buffer was added. After 5 min, [^{3}H]-oleate (0.15 µmoles) in 500 µl of incubation buffer was added and the incubation continued at 25°C. At the times specified an aliquot of the incubation mixture was assayed for oleate uptake as described in Section 2.2.3.

8-fold). The observation that both the affinity for the fatty acid and the V_{max} of transport were affected, suggests that the rate-limiting, saturable step in the uptake process was being regulated by starvation and D-lactate.

3.13. The Rate-Limiting, Saturable Step in the Fatty Acid Uptake Process

The saturability of fatty acid uptake (Fig. 36) clearly showed that the rate-limiting step is protein-mediated. However, the identity of the rate-limiting step is not known. Permeation of fatty acids across the outer membrane is facilitated by the *fadL* protein. Although this protein binds fatty acid saturably and with high affinity (Fig. 18) it is not involved in the rate-limiting step. This conclusion is based on the observation that Tris-EDTA disruption of the outer membrane which leads to an increase in the uptake of hydrophobic compounds (Nikaido and Vaara, 1985) did not affect fatty acid uptake (Fig. 37 and Black *et al.*, 1987). The absence of a fatty acid binding protein in the periplasmic space indicates that translocation of fatty acids across this compartment is not rate-limiting (Fig. 25). Furthermore, the observations that oleate uptake was not affected when the membrane potential was abolished (Fig. 33A) and that a fatty acid binding protein was not detected in the inner membrane using photoreactive fatty acid analogue (Fig. 27C) suggest that the transmembrane movement of fatty acids across the inner membrane is not rate-limiting.

Mutants deficient in β-oxidation enzymes were shown to be capable of fatty acid uptake, suggesting that degradation is also not rate-limiting (Maloy et al., 1981). It is therefore possible that either activation of fatty acid to the thioester by acyl-

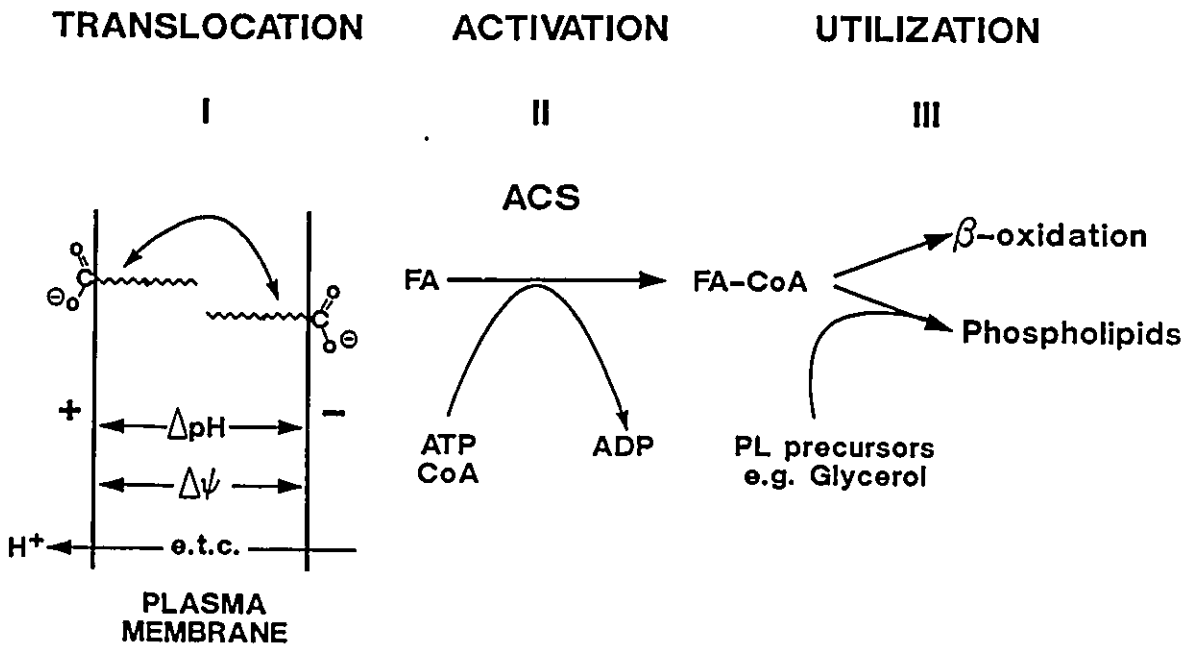

Figure 38. A schematic representation of possible rate-limiting steps in the process of fatty acid uptake. e.t.c., electron transport chain; ACS, acyl-CoA synthetase; ΔpH, proton gradient; $\Delta\psi$, electrical potential.

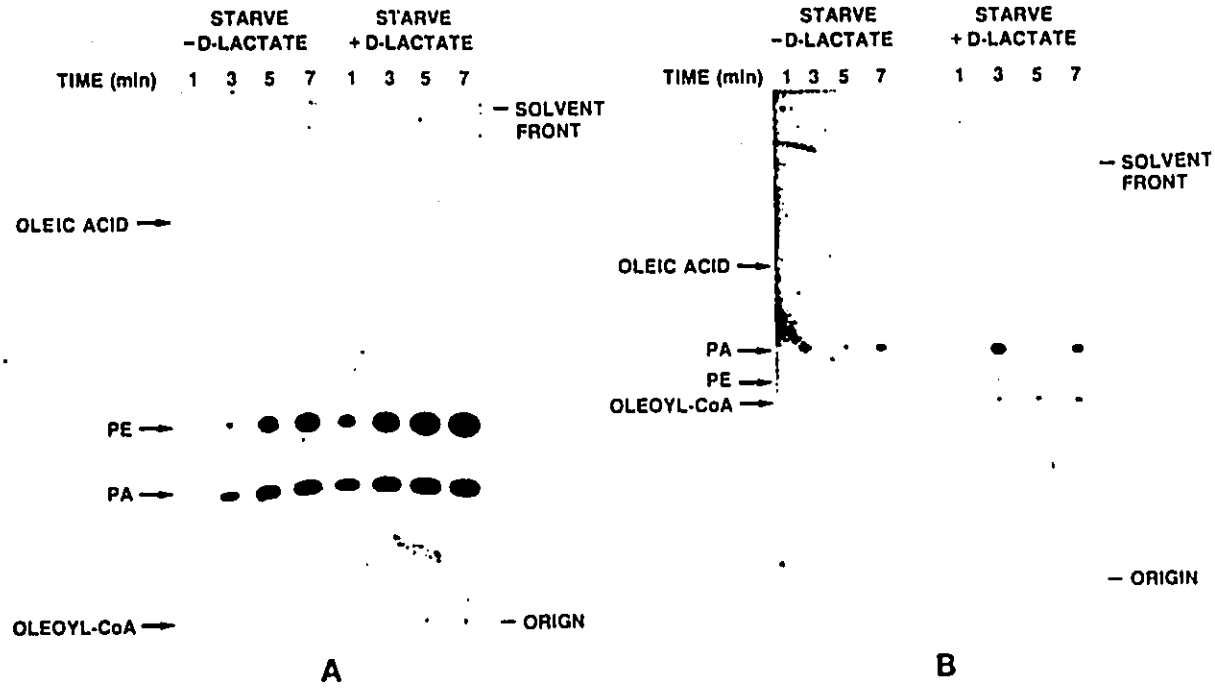

Figure 39. TLC analysis of cellular phospholipid and fatty acyl-CoA syntheses during oleate uptake.

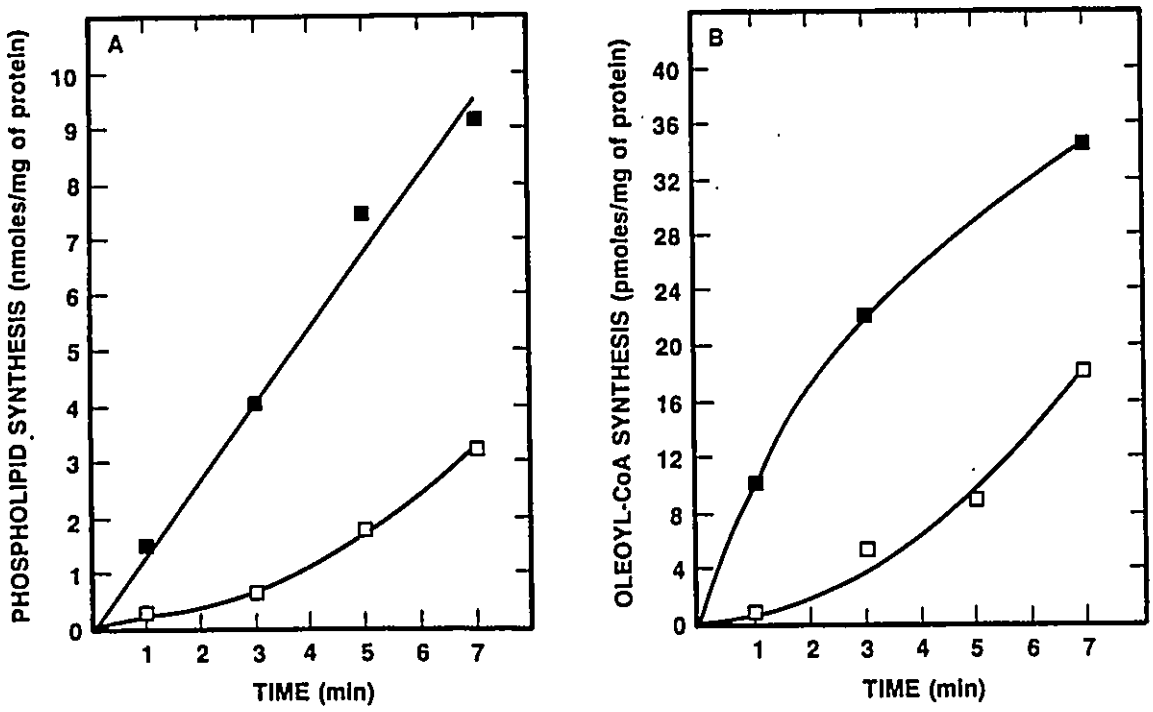

Figure 40. Effect of D-lactate on fatty acyl-CoA and phospholipid syntheses in starved ML308 cells. Washed oleate grown cells (1.2×10^9) in 1 ml of incubation buffer were incubated for 30 min at 25°C with continuous shaking. Incubation buffer (500 µl) without (□) or with (■) D-lactate (40 µmoles) was added and the incubation continued for 5 min. [^{3}H]-Oleate (0.15 µmoles; 7.4 Ci/mmole) in 500 µl of incubation buffer was added. At the specified times, the incubation mixtures were assayed for the extent of phospholipid (A) and fatty acyl-CoA (B) synthesis as described in Section 2.2.6.

CoA synthetase or utilization of fatty acyl-CoA for phospholipid synthesis is rate-limiting (Fig. 38). To assess whether activation or utilization may be rate-limiting, the use of oleate taken up by starved and starved, D-lactate activated cells for the syntheses of cellular fatty acyl-CoA and phospholipids was determined. At the times indicated during the uptake assay, the cells were subjected to a Bligh-Dyer extraction. The organic phase containing phospholipids and the aqueous phase containing acyl-CoA were analyzed by TLC (Fig. 39). In both the starved and starved, D-lactate activated cells, the internalized oleate was incorporated in phosphotidylethanolamine (PE) (R_f = 0.42) and phosphatidic acid (PA) (R_f= 0.24) (Fig. 39A). The syntheses of phospholipid (Fig. 39A) and oleoyl-CoA (R_f = 0.45) (Fig. 39B) were both much higher in D-lactate activated cells than in starved, unactivated cells. Quantitatively, D-lactate activation resulted in a 6-fold increase in the synthesis of both phospholipids (Fig. 40A) and fatty acyl-CoA (Fig. 40B). Furthermore, the levels of fatty acyl-CoA in starved and starved D-lactate activated cells were at least 100-fold lower than the phospholipid levels. This suggests that activation rather than utilization (Fig. 38) is rate-limiting in the overall process of fatty acid uptake. The increase in the level of cellular fatty acyl-CoA in response to D-lactate under conditions of increased phospholipid synthesis suggests that the observed effects of starvation and D-lactate on fatty acid uptake are related to the regulation of acyl-CoA synthetase activity: D-lactate must result in increased fatty acyl-CoA synthetase activity in order to produce higher levels of fatty acyl CoA despite higher rates of its utilization in phospholipid synthesis.

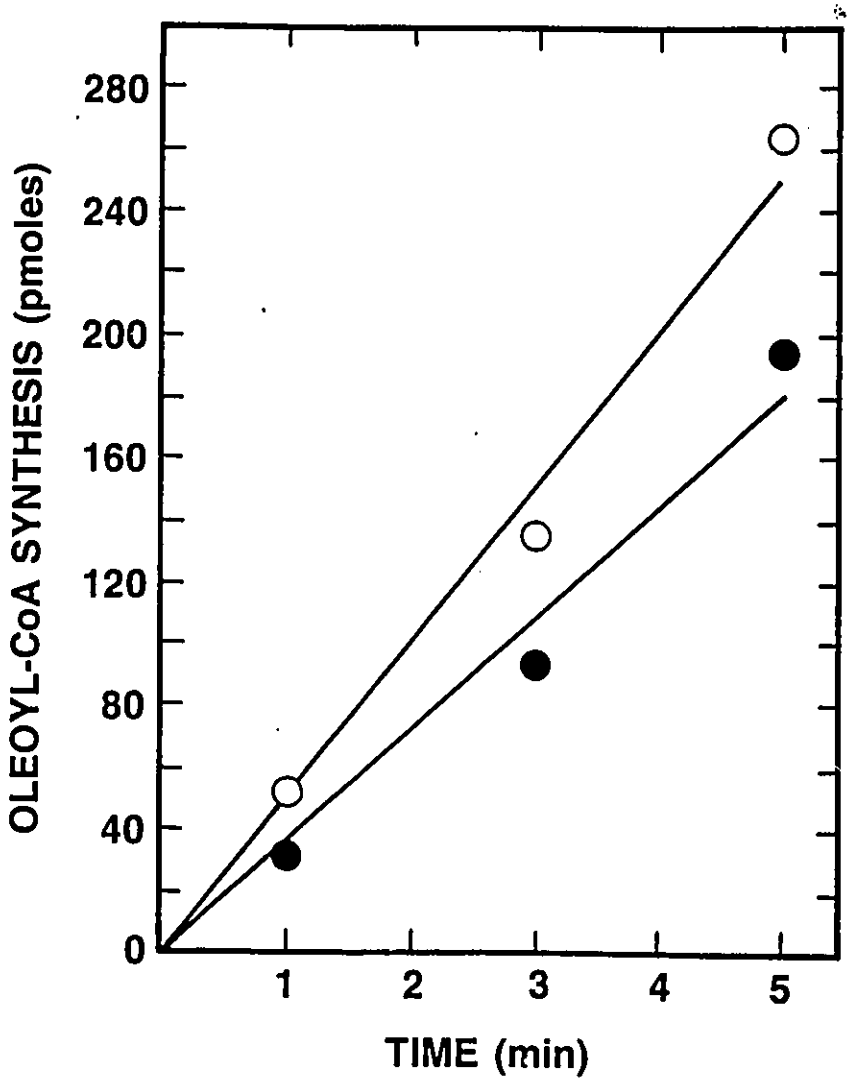

Figure 41. Determination of acyl-CoA synthetase activity in starved and D-lactate activated ML308 cells. Washed oleate grown cells (1.2×10^9) was starved and activated with D-lactate as described in Section 2.2.3. The cells were lysed as described in Section 2.2.10. Acyl-CoA synthetase activity in total lysate prepared from starved (o) or starved, D-lactate activated (●) cells, was assayed as described in Section 2.2.7.

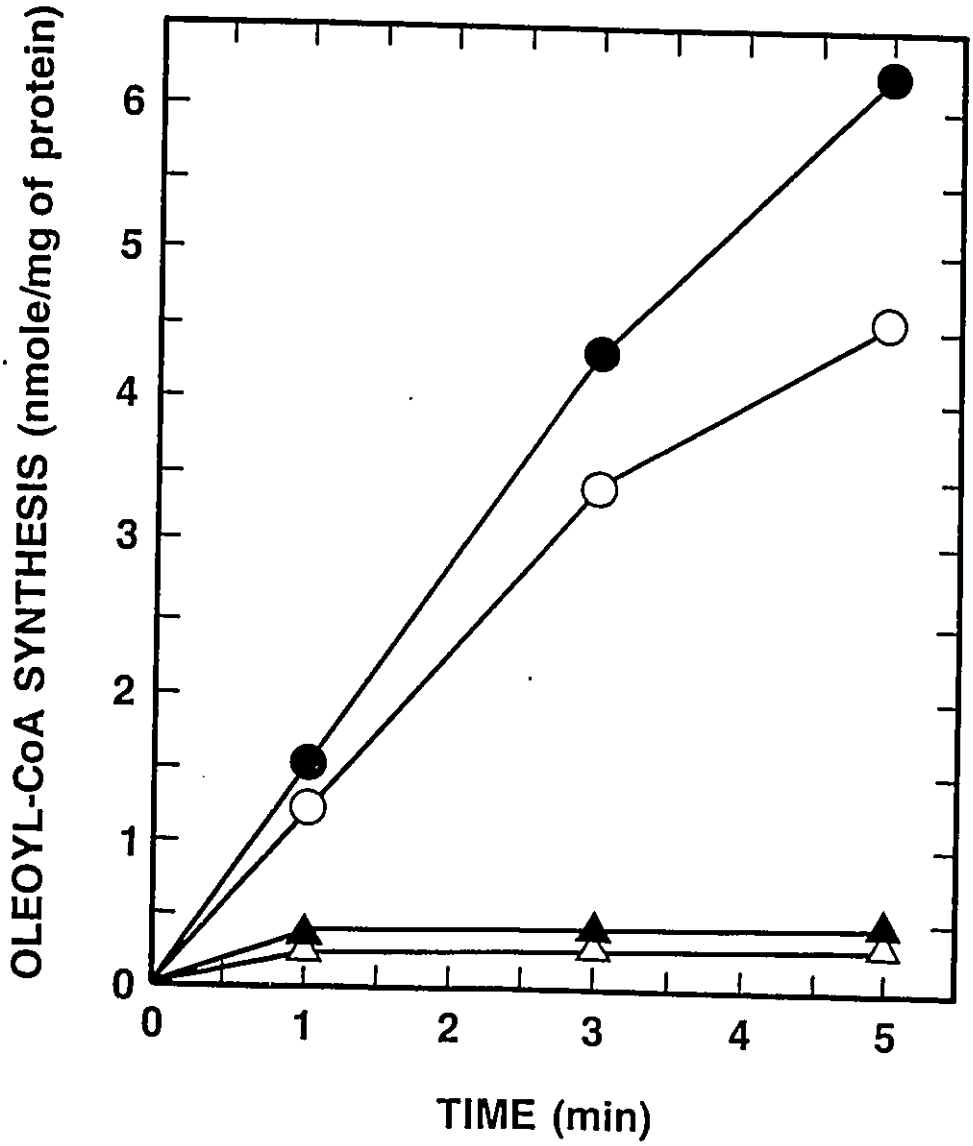

Figure 42. Effect of D-lactate on the activity of crude *E. coli* acyl-CoA synthetase. Spheroblasts of ML308 grown on oleate were prepared and lysed in the absence of D-lactate as described in Section 2.2.11. The crude lysate was centrifuged at 46,000 x g for 60 min at 4°C. The supernatant was assayed for acyl-CoA synthetase activity as described in Section 2.2.7. using 400 μM [^{3}H]-oleate (247 Ci/mole) in the presence (closed symbols) or absence (open symbols) of 20 mM D-lactate and in the presence (●,○) or absence (▲,△) of 0.1% Triton X-100.

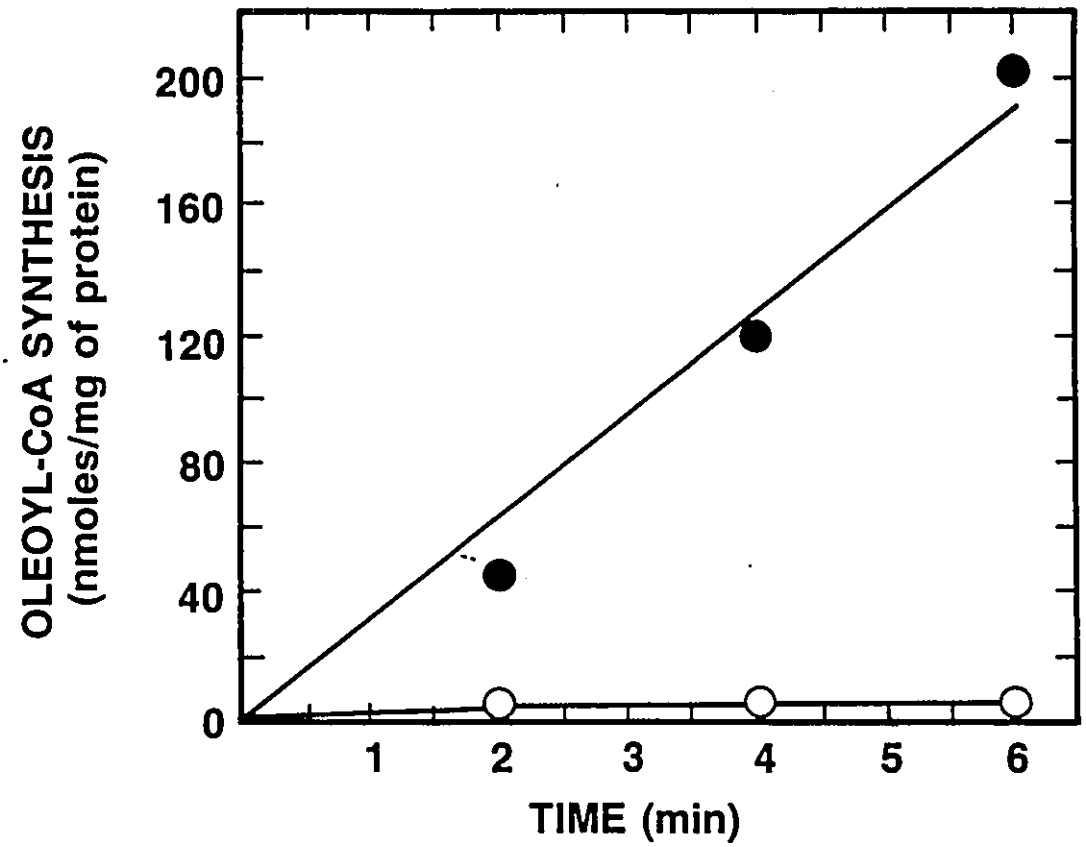

Figure 43. Effect of Triton X-100 on the activity of partially purified *E. coli* acyl-CoA synthetase. Acyl-CoA synthetase was purified as described in Section 2.2.21 and assayed in the presence (●) or absence (○) of 0.1% Triton X-100 as in Section 2.2.7 using 400 μM [^{3}H]-oleate (300 Ci/mole).

3.14. Regulation of Fatty Acyl-CoA Synthetase

The effect of D-lactate on fatty acid uptake appears to be related to an increase in acyl-CoA synthetase activity. This was not due to an increase in the amount of the enzyme during the incubation of the starved cells with D-lactate (Fig. 41). The observed changes in fatty acyl-CoA synthetase activity must therefore be due to regulation of existing enzyme by another mechanism. To assess whether acyl-CoA synthetase is directly activated by D-lactate, the activity of the enzyme in cytosol prepared from oleate grown cells was measured (Fig. 42). When the assay mixture contained Triton X-100 as described (Kameda and Nunn, 1981), the activity of acyl-CoA synthetase in the presence or absence of D-lactate was not significantly different. The activity of the enzyme was not affected by the addition of D-lactate when Triton X-100 was excluded. However, removal of Triton X-100 from the assay resulted in a 4-fold reduction in the activity of acyl-CoA synthetase. Activation by Triton X-100 (by 20-fold) was also observed with DEAE-sepharose, ammonium sulfate precipitation and hydroxyapatite purified enzyme (Fig. 43). These results clearly show that the enzyme is not directly activated by D-lactate. Instead it appears that fatty acyl-CoA synthetase becomes activated when associated with a hydrophobic surface.

Activation of fatty acyl-CoA synthetase in the presence of Triton X-100 implied that the enzyme may require lipids for full activation. In the presence of extensively washed inner membrane vesicles prepared from *E. coli* grown on oleate (essentially devoid of endogenous acyl-CoA synthetase) and Triton X-100, the

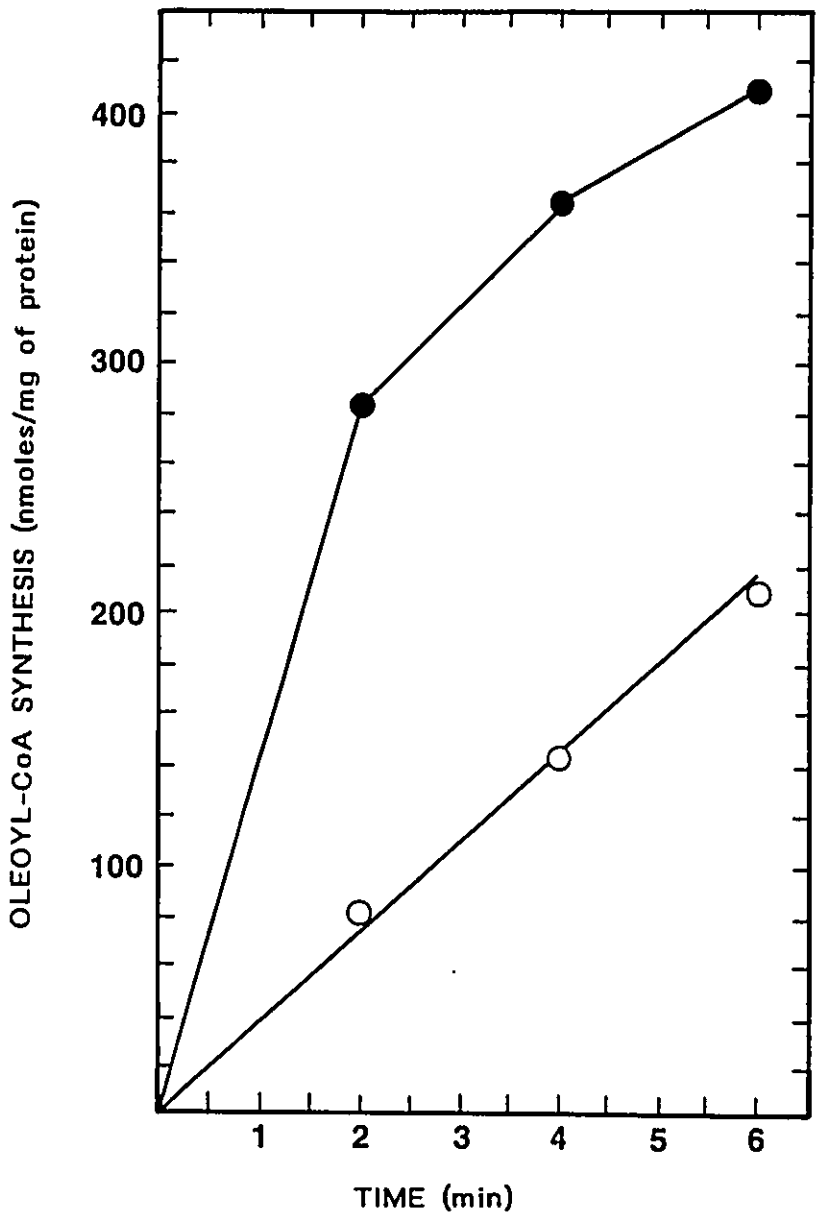

Figure 44. Effect of Triton X-100 solubilized *E. coli* membranes on the activity of partially purified *E. coli* acyl-CoA synthetase. Acyl-CoA synthetase was purified as described in Section 2.2.21 and assayed with (●) or without (o) extensively washed inner membrane vesicles as described in Section 2.2.7. The final concentration of [^{3}H]-oleate (300 Ci/mole) was 400 μM.

TABLE 1

A. + D-LACTATE

			Acyl-CoA Synthetase			β-Galactosidase		
	Total Protein (mg)	Protein Recovery (%)	Specific Activity (pmoles/min/mg)	Total Activity (pmoles/min)	% Total Activity	Specific Activity (ΔA_{420}/min/mg)	Total Activity (ΔA_{420}/min)	% Total Activity
CRUDE LYSATE	22.2	100	171	3800	100	11.6	255	100
PELLET (WASHED 1X)	3.8	17.1	1315	5000	132	1.6	6	2.3
PELLET (WASHED 3X)	3.3	14.9	679	2227	59	1.0	3.4	1.3

B. - D-LACTATE

			Acyl-CoA Synthetase			β-Galactosidase		
	Total Protein (mg)	Protein Recovery (%)	Specific Activity (pmoles/min/mg)	Total Activity (pmoles/min)	% Total Activity	Specific Activity (ΔA_{420}/min/mg)	Total Activity (ΔA_{420}/min)	% Total Activity
CRUDE LYSATE	50.0	100	222	11120	100	24.6	1231	100
PELLET (WASHED 1 X)	7.3	14.6	322	2320	20.8	5.7	44	3.6

TABLE 1

Effect of D-lactate on the membrane association of fatty acyl-CoA synthetase

A. Membranes, prepared and washed in the presence of D-lactate as described in Section 2.2.11, were washed twice by resuspension and vigorous homogenization in cold 100 mM potassium phosphate, pH 6.6 containing 20 mM D-lactate. The final membrane pellet was resuspended in 1.7 ml of cold 59 mM potassium phosphate, pH 6.6. The fractions were assayed for β-galactosidase and fatty acyl-CoA synthetase activities as described in Sections 2.2.8 and 2.2.7, respectively.

B. Membranes were prepared and washed in the absence of D-lactate as described in Section 2.2.11. The washed membrane pellet was resuspended in 2 ml of cold 50 mM potassium phosphate, pH 6.6. The fractions were assayed for β-galactosidase and fatty acyl-CoA synthetase activities as described in Sections 2.2.8 and 2.2.7, respectively.

activity of partially purified fatty acyl-CoA synthetase, based on initial rates, was 4 times higher than that obtained in the presence of just Triton X-100 (Fig. 44). However, the actual level of activation of the enzyme in the presence of membranes is most likely higher than that observed since the assay was performed under limiting conditions. These results therefore suggest that activation of fatty acyl-CoA synthetase may be lipid dependent.

The observations that fatty acyl-CoA synthetase activity was stimulated by Triton X-100 solubilized membranes and that fatty acid uptake as well as cellular acyl-CoA synthesis was stimulated in response to D-lactate, suggest that *in vivo* it is possible that D-lactate stimulates fatty acyl-CoA synthetase activity by promoting its association with the inner membrane. To test this possibility, inner membrane vesicles were prepared in the presence and absence of D-lactate. The extent to which fatty acyl-CoA synthetase was in the membrane bound fraction was determined; the removal of cytoplasm during lysis and washing was assessed using the constitutively expressed beta-galactosidase as a marker enzyme. The first wash of the membrane prepared in the presence of D-lactate removed essentially all of the cytoplasm (2% of the beta-galactosidase activity remained) while the fatty acyl-CoA synthetase activity remained associated with the membrane (Table 1A). Further washing of the pellet by vigorous homogenization as described (Kaback, 1971) resulted in 59% of the fatty acyl-CoA synthetase activity still being retained in the pellet (Table 1A). In contrast, membranes prepared in the absence of D-lactate and washed once retained 4% of the beta-galactosidase activity and only

21% of the acyl-CoA synthetase activity (Table 1B). After correction for retention of the soluble cytoplasmic fraction, the recovery of acyl-CoA synthetase in the membrane fraction was 17% in the absence of D-Lactate and 130% in the presence of D-lactate. These results show that the presence of D-lactate during lysis results in isolation of essentially all of the acyl-CoA synthetase in the membrane fraction while in the absence of D-lactate, lysis results in removal of most of the enzyme from the membrane. These results together with the ones discussed above suggest that the observed effects of starvation and D-lactate on oleate uptake may be related to regulation of acyl-CoA synthetase activity by reversible association with the inner membrane.

3.15. Biochemical Analysis of the Involvement of Acyl-CoA Synthetase in Fatty Acid Uptake

Genetic studies have shown that fatty acyl-CoA synthetase is necessary for fatty acid uptake in *E. coli* (Klein *et al.*, 1971; Overath *et al.*, 1969; Maloy *et al.*, 1981; Black *et al.*, 1987). Results obtained from this study suggest that this enzyme is rate-limiting and regulates fatty acid uptake. Moreover, regulation of fatty acid uptake by fatty acyl-CoA synthetase appears to be related to changes in its activity by reversible association with the inner membrane. However, the involvement of fatty acyl-CoA synthetase in the uptake process was never demonstrated unambiguously. To assess more directly whether fatty acyl-CoA synthetase is involved in the uptake process, fatty acid uptake in inner membrane vesicles was studied.

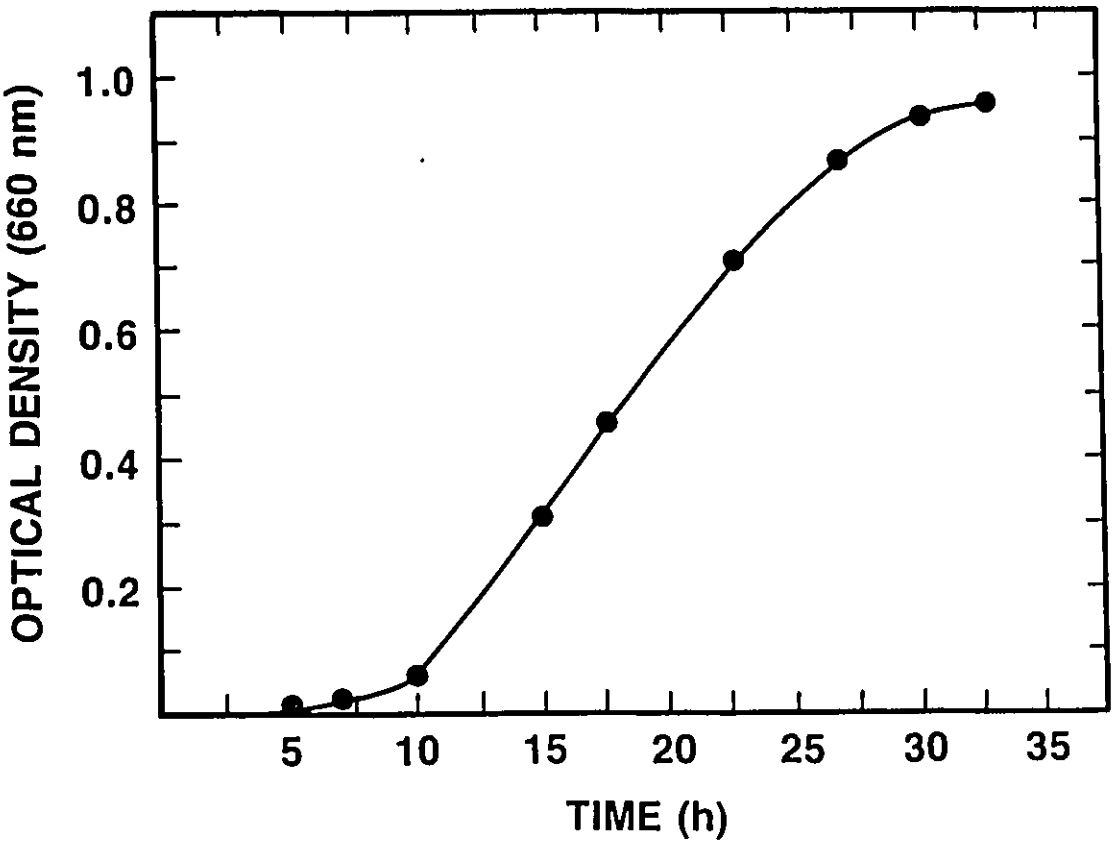

Figure 45. Time-course of growth of ML308 on oleate. ML308 grown in Luria-Bertani media was diluted 1000-fold in M9 minimal media containing 5 mM oleate and grown as described in Section 2.2.2. After reaching a density of 4.8×10^8 cells/ml the cells were diluted into fresh M9 minimal media containing 5 mM oleate and grown as described in Section 2.2.2. At the specified times an aliquot of the culture was used to determine the O.D. at 660 nm.

These vesicles are in the same orientation as the inner membrane in intact cells and have been used extensively to study the mechanism of sugar and amino acid transport across the inner membrane of *E. coli* (Kaback, 1972). However, more importantly, these vesicles are essentially devoid of cytoplasm; consequently, the role of acyl-CoA synthetase can be unambiguously assessed in the absence of other cytoplasmic enzymes. Unlike in whole cells, hydrophobic compounds are now directly accessible to the inner membrane due to the removal of the outer membrane.

The strain of *E. coli* that is commonly used to isolate inner membrane vesicles is ML308; the yield of vesicles is higher and less contaminated with outer membrane that other strains, including the wild-type K-12 strain (Kaback, 1971). The ML308 strain expresses β-galactosidase constitutively which can be used as a marker to assess the extent of removal of the cytoplasm during the preparation of the vesicles. In addition to this strain being able to grow on fatty acid (growth constant (k) = 0.11, doubling time (DT) = 2.75 h) (Fig. 45), it is as active in fatty acid uptake as the wild type K-12 strain (Fig. 31). These cells are therefore suitable for studying the involvement of acyl-CoA synthetase in fatty acid uptake using inner membrane vesicles.

3.15.1. Characterization of Vesicles Prepared from Cells Grown in Different Media

It has been shown that the membrane of inner membrane vesicles is de-energized and that it can be re-energized by D-lactate or ascorbate/PMS (Kaback, 1972). The level of energization of the membrane of vesicles prepared from ML308

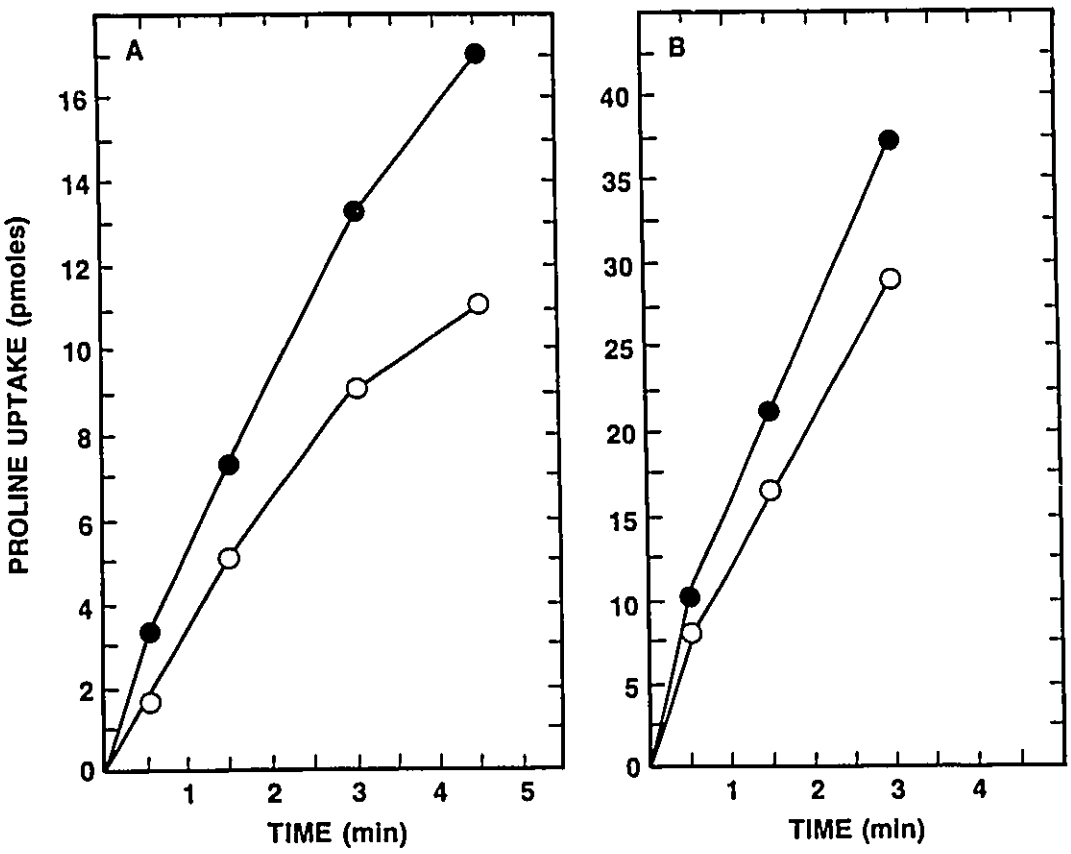

Figure 46. Effect of D-lactate on proline uptake in inner membrane vesicles prepared from ML308 grown in M9 minimal media containing oleate or glucose. ML308 was grown in M9 minimal media containing 5 mM oleate (A) or 25 mM glucose (B) as described in Section 2.2.2. Extensively washed vesicles were prepared as described in Section 2.2.12.1. Proline uptake was assayed in the absence (o) or presence (●) of 20 mM D-lactate as described in Section 2.2.4.

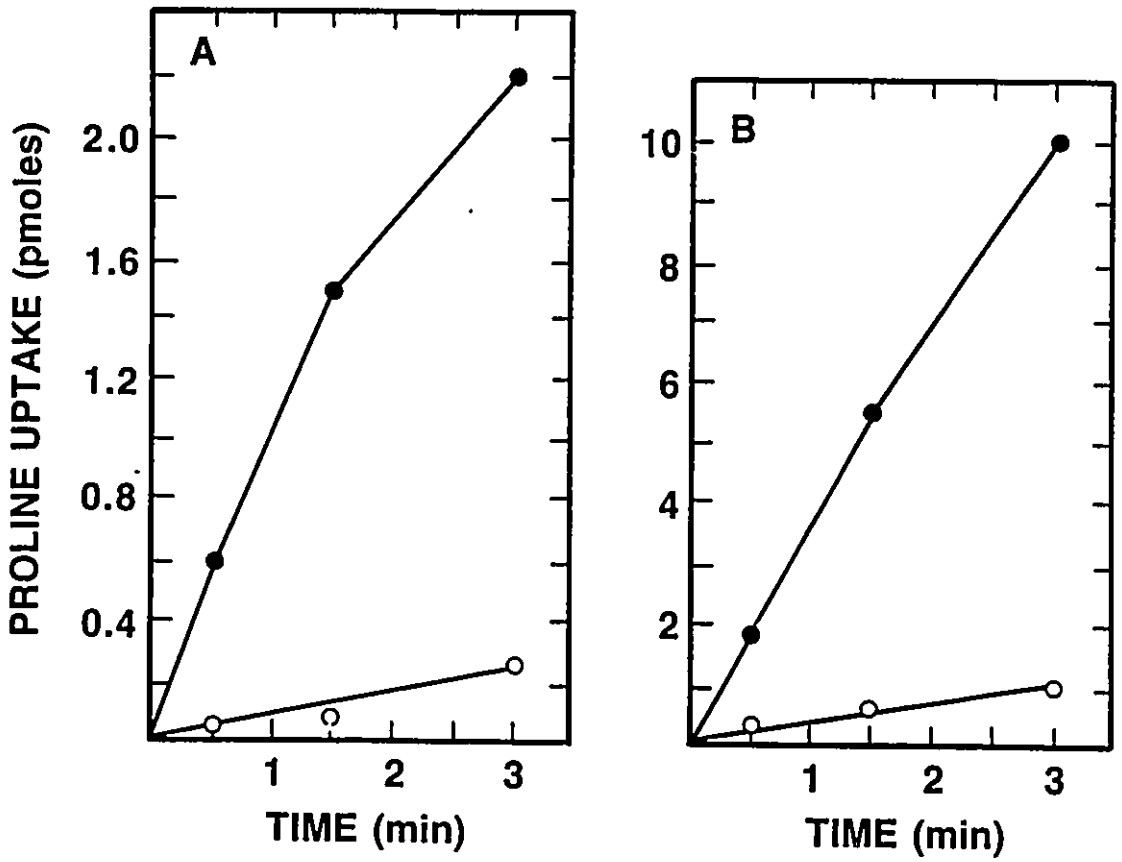

Figure 47. Effect of D-lactate on proline uptake in inner membrane vesicles prepared from ML308 grown in MA minimal media containing oleate or glucose. ML308 was grown in MA minimal media containing 5 mM oleate (A) or 25 mM glucose (B) as described in Section 2.2.12.1. Extensively washed vesicles were prepared as described in Section 2.2.4. Proline uptake was assayed in the absence (o) or presence (●) of 20 mM D-lactate as described in Section 2.2.4.

grown in M9 minimal medium containing oleate as the carbon source was determined. This was assessed indirectly by monitoring proline uptake. The rate of proline uptake in the presence of D-lactate was about 1.4-fold of that obtained in the absence of D-lactate (Fig. 46A). This shows that the membrane of these vesicles is still energized. The membrane of vesicles prepared from cells grown in M9 minimal medium containing glucose was also energized (Fig. 46B), indicating that this was not due to the substrate used for growth.

The possibility that this lack of de-energization of the membrane is related to the medium used for growth was considered. Vesicles were prepared from ML308 grown in MA minimal media containing oleate and assayed for proline uptake. In the absence of D-lactate, the rate of proline uptake was very low in comparison to that obtained in the presence of D-lactate (Fig. 47A). Similarly, the rate of proline uptake in vesicles prepared from cells grown in MA minimal media containing glucose is low (Fig. 47B). These results confirm that the lack of de-energization of the membrane prepared from cells grown in M9 minimal medium is related to the growth medium used. Therefore, the cells used to prepare vesicles were routinely grown in MA minimal media.

3.15.2. Stability of the Vesicles to Freeze-thawing

Acyl-CoA synthetase requires ATP and CoASH for activity. Both of these can be introduced into the vesicles by freeze-thawing. It was reported that the stability of inner membrane vesicles was not affected by freeze-thawing (Kaback, 1971). To ensure that vesicles prepared from cells grown on oleate are stable to

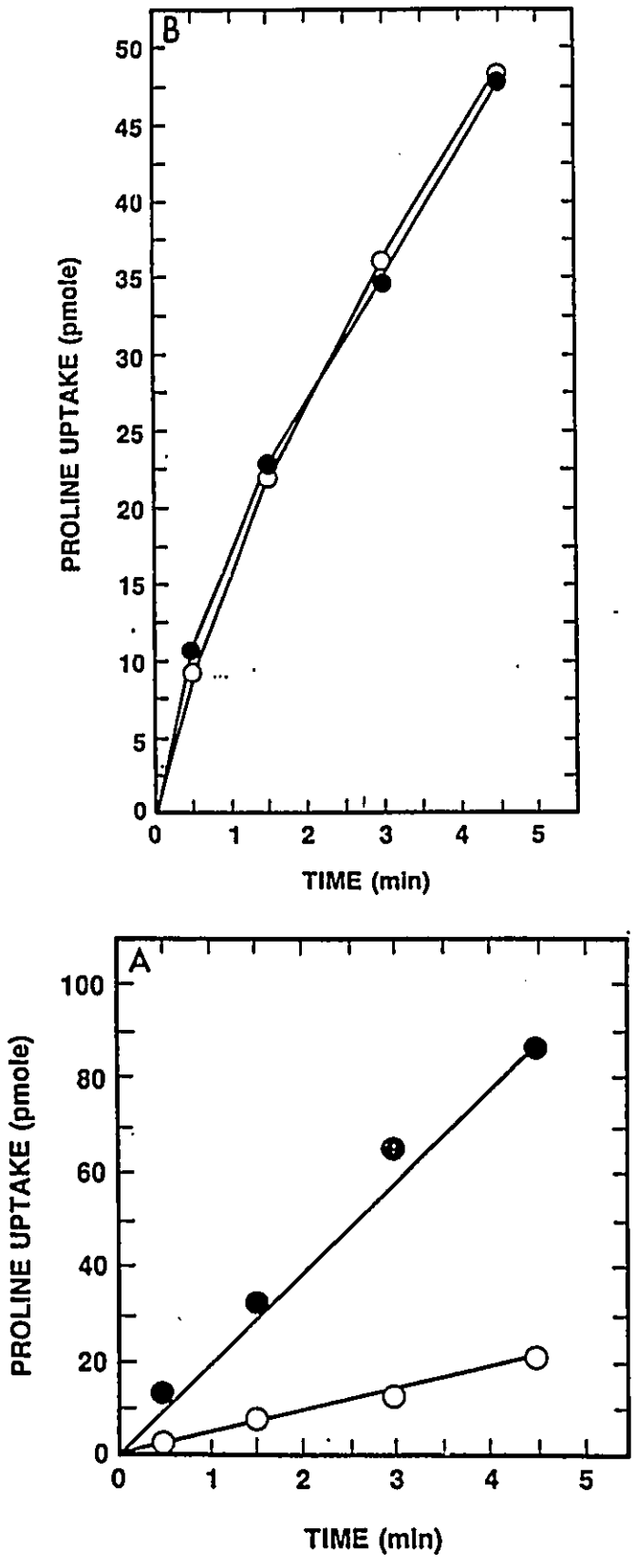

Figure 48. Effect of freeze-thawing on the stability of inner membrane vesicles prepared from ML308 grown in MA media containing oleate or glucose. Extensively washed inner membrane vesicles were prepared from ML308 grown in MA minimal media containing 5 mM oleate (A) or 25 mM glucose (B), as described in Section 2.2.12.1. Proline uptake in unfrozen (●) or freeze-thawed (o) vesicles was assayed in the presence of 20 mM D-lactate as described Section 2.2.4.

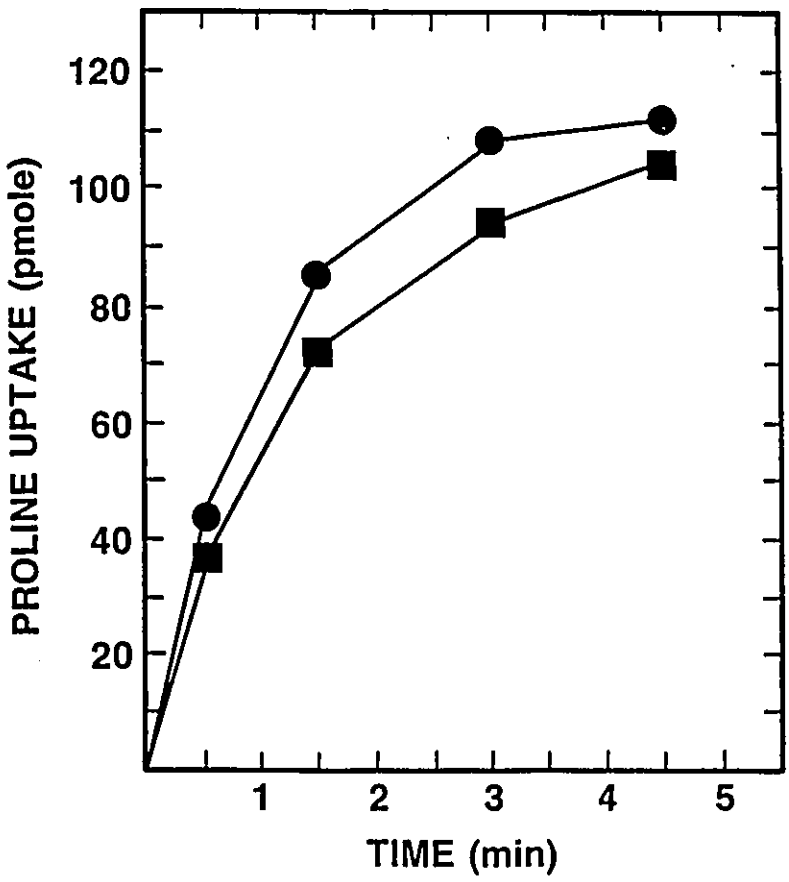

Figure 49. Effect of freeze-thawing on the stability of inner membrane vesicles prepared from ML308 grown in MA minimal media containing palmitate. Extensively washed inner membrane vesicles were prepared from ML308 grown in MA minimal media containing 3.5 mM palmitate as described in Section 2.2.12.1. Proline uptake in unfrozen (●) or freeze-thawed (■) vesicles was performed in the presence of 20 mM D-lactate as described in Section 2.2.4.

freeze-thawing, proline uptake was assessed. The rate of proline uptake in freeze-thawed vesicles was much lower than that obtained for unfrozen vesicles (Fig. 48A). However, the rate of proline in vesicles prepared from cells grown on glucose was the same before and after freeze-thawing (Fig. 48B). These results suggest that the observed instability of vesicles prepared from cells grown on oleate may be related to the substrate used for growth of the bacteria and not instability of the proteins involved in proline transport.

It is known that the membrane fluidity is affected by the fatty acid composition of the phospholipids (Nikaido, 1990). This is dependent on the substrate used as the carbon source for growth in the case of bacteria (Nikaido, 1990). Therefore, it is expected that the lipids of oleate grown cells would contain a higher percentage of oleate than cells grown on glucose. Consequently, the membrane of oleate grown cells would be expected to be more fluid than that of glucose grown cells. It is therefore possible that the increased fluidity of the membrane of vesicles prepared from cells grown on oleate affects proper resealing of the vesicles after freeze-thawing. If this is the case, then vesicles prepared from cells grown on palmitate a saturated fatty acid, should not be destabilized by freeze-thawing since the membrane should be more rigid. The rate of proline uptake in vesicles prepared from cells grown on palmitate was essentially the same before and after freeze-thawing (Fig. 49).

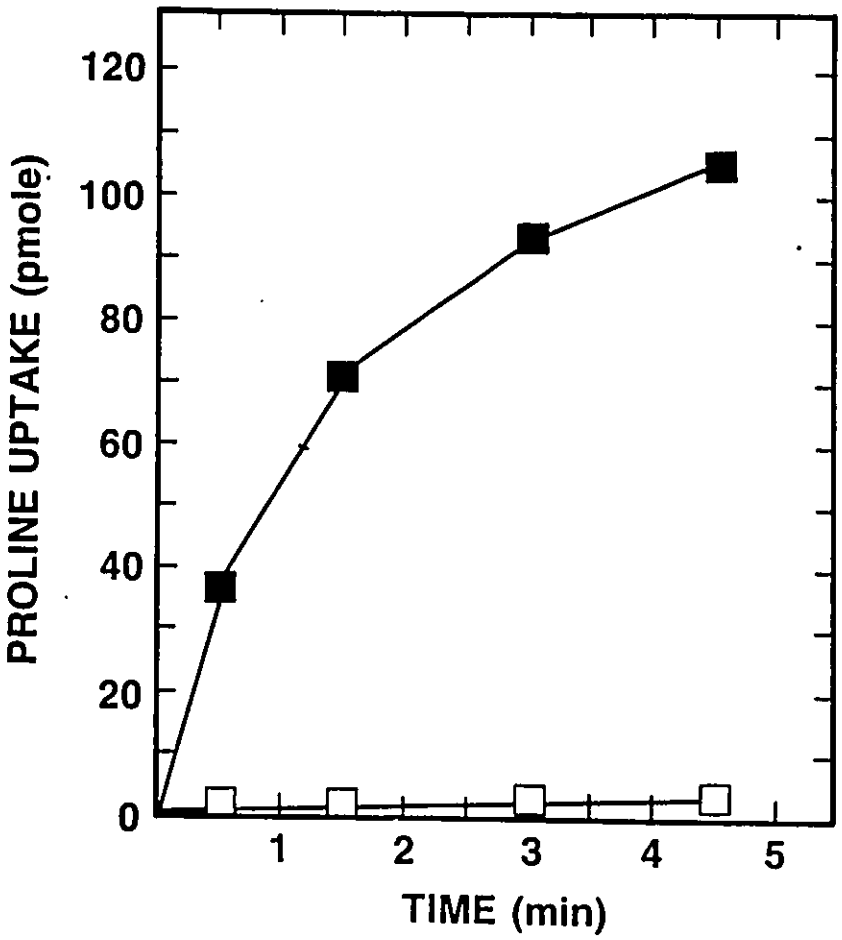

Figure 50. Effect of D-lactate in vesicles prepared from ML308 grown in MA minimal media containing palmitate. Extensively washed inner membrane vesicles were prepared from ML308 grown in MA minimal media containing 3.5 mM palmitate as described in Section 2.2.12.1. Proline uptake was assayed in the absence (□) or presence (■) of 20 mM D-lactate as described in Section 2.2.4.

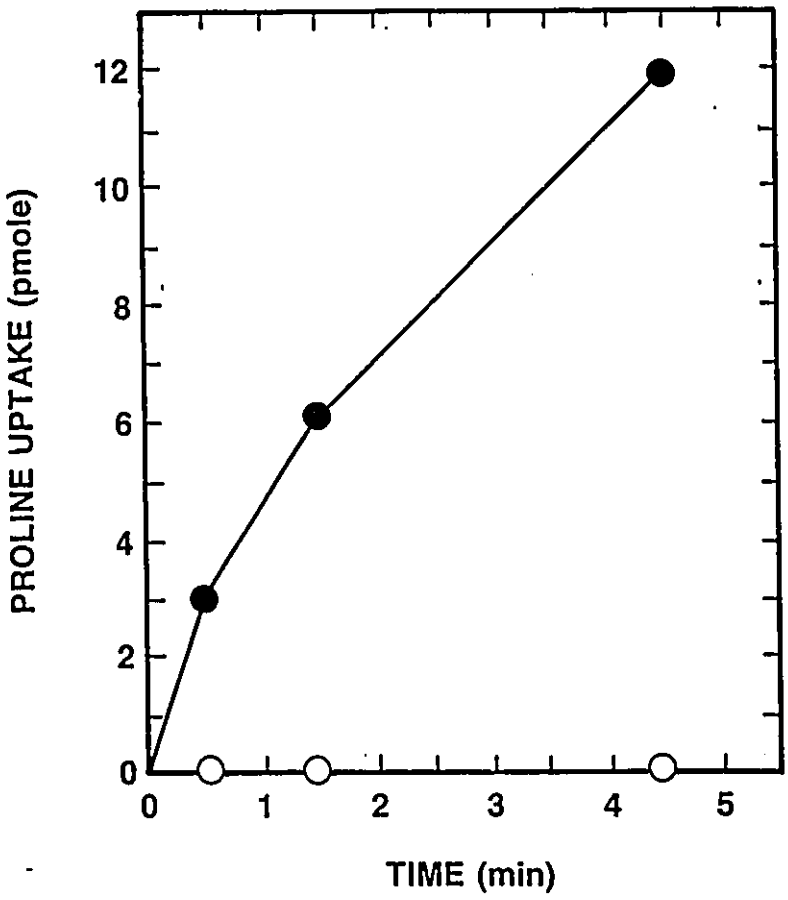

Figure 51. Effect of CCCP on proline uptake in inner membrane vesicles prepared from ML308 grown in MA minimal media containing palmitate. Extensively washed inner membrane vesicles were prepared from ML308 grown in MA minimal media containing 3.5 mM palmitate as described in Section 2.2.12.1. Prior to assaying proline uptake, inner membrane vesicles were pre-incubated without (●) or with (o) 5 μM CCCP for 2 min in the presence of 20 mM D-lactate as described in Section 2.2.4.

3.15.3. Energy Dependence of Proline Uptake in Vesicles Prepared from Cells Grown on Palmitate

The uptake of proline in inner membrane vesicles was shown to be entirely dependent on energization of the membrane (Fig. 47A and B) and as reported (Kaback, 1972). Proline uptake in vesicles prepared from cells grown on palmitate is also dependent on energization of the membrane (Fig. 50). The rate of energy driven proline uptake is approximately 2 nmoles/min/mg of protein which is the same as that reported. This shows that these vesicles are as active as those reported (Kaback, 1972). The low rate of proline uptake in the absence of an exogenous energy source implies that the vesicles are essentially devoid of endogenous substrate and/or metabolic enzymes capable of re-energizing the membrane. The fact that the vesicles are capable of energy dependent vectorial translocation shows that they are resealed in the right orientation since it was reported (Hare *et al.*, 1974) that inverted vesicles are unable to transport proline. The uncoupler CCCP de-energizes the membrane by abolishing the electrochemical potential. This leads to inhibition of proline uptake. The sensitivity of proline uptake to CCCP in vesicles prepared from cells grown on palmitate was assessed. In the presence of CCCP the rate of proline uptake was very low in comparison to that obtained in the absence of CCCP (Fig. 51). This further shows that these vesicles exhibit many of the characteristics reported for vesicles prepared by others.

3.15.4. Fatty Acid Uptake in Vesicles Containing Acyl-CoA Synthetase

The activity of acyl-CoA synthetase is dependent on CoASH and ATP.

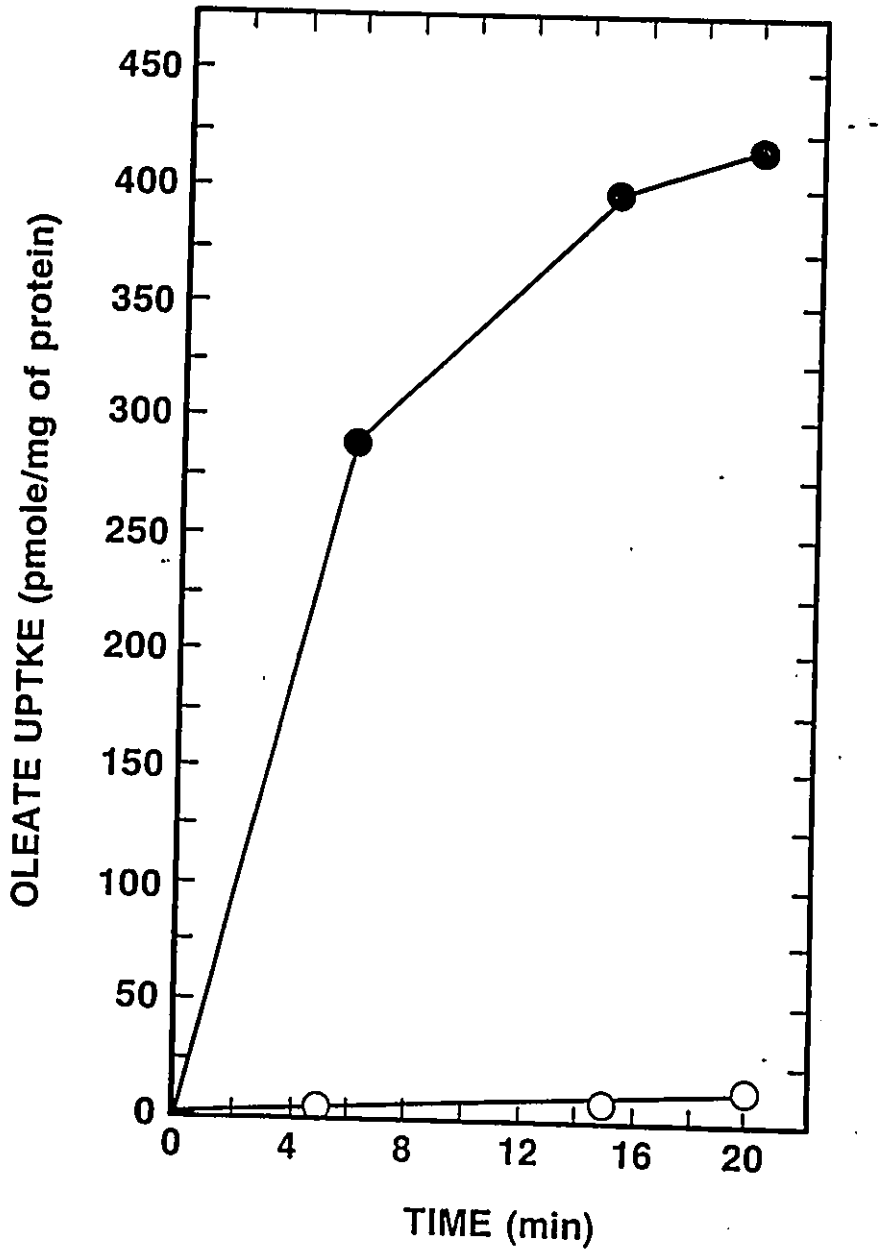

Figure 52. Effect exogenous CoASH and ATP on oleate uptake in inner membrane vesicles prepared from ML308 grown on palmitate. Inner membrane vesicles (1.1 mg of protein/ml) were frozen in liquid nitrogen in 25 mM potassium phosphate, pH 6.6 without (o) or with (●) 25 mM ATP, 3.1 mM CoASH and 10 mM magnesium sulfate. The vesicles were thawed at 37°C. An aliquot of the vesicles (150 µl) was incubated at 37°C for 15 min. The uptake assay was initiated by the addition of 150 µl of [^{3}H]-oleate (1320 Ci/mole) complexed to BSA (346 µM oleate/346 µM BSA) in 25 mM potassium phosphate, pH 6.6. At the specified times, 50 µl of the incubation mixture was added to 2.5 ml of 100 mM Tris-HCl, pH 8.0 and filtered. The filter was washed once with 2.5 ml of 100 mM Tris-HCl, pH 8.0. The filter was air dried and the retained radioactivity determined by liquid scintillation counting.

Therefore, if this enzyme is involved in fatty acid uptake, the rate of uptake in vesicles containing the enzyme should be dependent on CoASH and ATP. Exogenous CoASH and ATP was introduced into vesicles prepared from cells grown on palmitate by freeze-thawing. The vesicles contained approximately 50% of the total enzyme. The fatty acid was presented as a BSA complex instead of a detergent micelle in order to minimize lysis of the vesicles. The free fatty acid concentration under these conditions was 125 nM. In the absence of exogenous CoASH and ATP the rate of oleate uptake was low while a stimulation of oleate uptake was observed in vesicles containing CoASH and ATP (Fig. 53). This shows that acyl-CoA synthetase is involved in fatty acid uptake. The fact that no fatty acid binding proteins were found in the inner membrane together with observation that fatty acid uptake was not coupled to the electrochemical potential suggest that acyl-CoA synthetase is necessary and sufficient for fatty acid permeation of the inner membrane of *E. coli*. The results further suggest that the observed effects of starvation and D-lactate on oleate uptake in whole cells are related to regulation acyl-CoA synthetase activity.

At present the role of acyl-CoA synthetase in the fatty acid uptake process in *E. coli* is not clear. It was shown that fatty acids readily partition into the lipid bilayer. However, the rate of fatty acid removal from the membrane is very slow. This is related to the large amount of energy required to disrupt the hydrophobic interaction between the fatty acid and the membrane lipids. In cells, excessive accumulation of fatty acids in the plasma membrane would result in lysis of the

cells. In mammalian cells, low molecular weight cytosolic fatty acid binding proteins have been implicated in the desorption of fatty acids from the bilayer (Paulussen and Veerkamp, 1990; Peeters *et al., 1989*). It is possible that acyl-CoA synthetase may also be involved in a similar function in the uptake of fatty acids across the inner membrane. Consistent with the proposed role of fatty acyl-CoA synthetase is the finding that under conditions where fatty acid uptake was stimulated, acyl-CoA synthetase was found to be entirely associated with the membrane.

3.16. Overview

The mechanism of fatty acid uptake in *E. coli* was poorly understood at the biochemical level. It was known that the process is energy-dependent and involves acyl-CoA synthetase and the *fadL* protein which is required for translocation of fatty acids across the outer membrane. However, the mechanism by which cellular energy was coupled to the overall process or the mechanism of fatty acid permeation of the inner membrane or across the periplasmic space, or the role of acyl-CoA synthetase were not understood. Furthermore, it was also not known whether one of the above proteins or a protein which may be required for fatty acid translocation across the inner membrane or the periplasm, is involved in the saturable, rate-limiting step.

To identify the saturable, rate-limiting step in the overall process of fatty acid uptake, attempts were made initially to gain further insight into the mechanism of fatty translocation at the various steps. To accomplish this objective, a photochemical approach involving radioactive photoreactive fatty acid analogue was

used to directly assess the possible involvement of proteins.

The photoreactive fatty acid probe was shown functionally to be recognized by mammalian and *E. coli* (Greenberg, *et al.*, 1976; Olson, *et al.*, 1979; Leblanc *et al.*, 1982; Capone *et al.*, 1983; Leblanc and Gerber, 1984) enzymes involved in fatty acid metabolism. Uptake analysis using a filter assay (Fig. 13) showed that 11-DAP-[11-^{3}H]-undecanoate was taken up specifically by the transport system expressed in *E. coli* grown on oleate. Furthermore, the probe was capable of labeling proteins having an affinity for fatty acids in total *E. coli* cell lysate (Fig. 12) and during the uptake of the probe in cells grown on oleate (Fig. 14). Thus, the photoreactive fatty acid probe is a suitable tool for identifying fatty acid binding proteins involved in fatty acid uptake.

The mechanism by which the *fadL* protein facilitates the transmembrane movement of fatty acids across the outer membrane is not understood. Binding analysis using *fadL* mutants led to the proposal that this protein binds fatty acid (Nunn *et al.*, 1986; Kumar and Black, 1991; Black, 1990). However, no direct evidence has been reported which supports this conclusion. A 33 kDa protein having an apparent pI of 4.6 was labeled with the photoreactive fatty acid analogue 11-DAP-[11-^{3}H]-undecanoate in intact *E. coli*. The labeled 33 kDa protein was shown to be the *fadL* protein by its induced expression (compare Fig. 15A, box and Fig. 15B, box), presence in isolated membranes (Fig. 16A, box and Fig. 23B, box), the lack of detection in intact *fadL* deficient cells (Fig. 15C) and isolated membranes (Fig. 16C and Fig. 23C), heat-modifiable behaviour (Fig. 22),

localization to the outer membrane (Fig. 27D) and recognition by an antiserum to a peptide of the *fadL* protein (Fig. 24A).

The fact that the *fadL* protein was labeled specifically and preferentially over abundant membrane proteins at low concentration of the probe (nanomolar) (Fig. 17, lane 1) indicated that the protein has a fatty acid binding site. The presence of such a site was confirmed by the observed saturability of labeling of the *fadL* protein (Fig. 18). Therefore, through the use of photoreactive fatty acid analogs it was demonstrated that not only is the *fadL* protein capable of binding fatty acids, but it does so saturably and with high affinity.

The intensity of labeling of the *fadL* protein by 11-DAP-[11-^{3}H]-undecanoate was found to increase as the pH was decreased from 8.0 to 6.5 (Fig. 19A and Fig. 20). The increase in labeling of the *fadL* protein was significantly higher than that observed for the labeling of major membrane proteins. This increase in labeling is therefore not due to increased non-specific labeling, instead this was attributed to an increase in specific labeling.

The increase in the *fadL* protein's affinity for the probe as the pH was decreased from 8.0 to 6.5 must be due to protonation of an ionizable group or groups on the protein. On the basis of the pH profile of labeling and the involvement of an basic amino acid residue (arginine) in fatty acid binding to mammalian low molecular weight cytosolic fatty acid binding protein and BSA, the most likely candidate is a histidine residue. However, one cannot exclude the possibility that protonation of a carboxylic acid group on the protein leads to an

increase in it's affinity for fatty acid. In support of the involvement of a histidine residue is the finding that pre-treatment of isolated membranes with DEPC, a reagent relatively specific for histidine at pH 6.5, resulted in inhibition of labeling of the *fadL* protein (Fig. 21).

The mechanism by which fatty acid in the periplasmic space is delivered to the inner membrane is not clear. By analogy to other transport mechanisms (eg. histidine, maltose, phosphate) in *E. coli* (Ames, 1986), it is possible that fatty acid permeation of the periplasmic space is also protein-mediated. However, the fact that no fatty acid binding proteins were detected with the photoreactive fatty acid probe in the periplasm isolated from cells grown on oleate (Fig. 25, lane 3) strongly suggests that this step is not protein-mediated.

The transmembrane movement of fatty acids across the inner membrane was proposed to be coupled to the electrochemical potential and involve a permease (Kameda, 1987); this is based on the observations that fatty acid uptake in whole cells was inhibited when the membrane potential was abolished by uncouplers. Using the photoaffinity labeling method no evidence was found for the presence of a fatty acid binding protein in the inner membrane (Fig. 27C) which is consistent with the proposal that fatty acid permeation across the plasma membrane of cells is not protein-mediated, but occurs by a simple diffusive mechanism. Furthermore, it was determined that fatty acid uptake was not directly coupled to or affected by the magnitude of the electrochemical potential (Fig. 33A).

Acyl-CoA synthetase has been shown genetically to be necessary for fatty acid

uptake in *E. coli* (Klein *et al.*, 1971; Overath *et al.*, 1969; Black *et al.*, 1977). However, the involvement of this enzyme in the process was never demonstrated biochemically or unambiguously. The development of a method for preparing right-side out inner membrane vesicles has led to much of our current understanding of bacterial transport mechanisms (Kaback, 1971). Therefore, inner membrane vesicles were used to assess biochemically whether acyl-CoA synthetase is involved in fatty acid uptake. The inner membrane vesicles used in this study are stable upon storage and to freeze-thawing (Fig. 49); they are essentially devoid of endogenous energy sources (Fig. 47) and were highly impermeable (Fig. 50).

Vesicles containing acyl-CoA synthetase and exogenously introduced CoASH and ATP are able to take up fatty acid while vesicles containing just the enzyme could not (Fig. 52). The CoASH and ATP dependency of fatty acid uptake in acyl-CoA synthetase containing vesicles demonstrated directly for the first time that this enzyme is necessary for fatty acid uptake in *E. coli*. Furthermore, the observations that fatty acid translocation of the inner membrane is not coupled to the electrochemical potential or involves a protein further suggest that acyl-CoA synthetase is also sufficient for uptake across the inner membrane.

The saturability of fatty acid uptake in *E. coli* (Fig. 36) clearly showed that the rate-limiting step is protein-mediated. This step cannot be translocation of fatty acids across the periplasmic space or the transmembrane movement across the inner membrane since no fatty acid binding proteins were detected in either compartment (Fig. 25, lane 3 and Fig. 27C). Although the *fadL* outer membrane protein binds

fatty acid saturably, it is not involved in the rate-limiting step (Fig. 18). This conclusion is based on the observations that Tris-EDTA disruption of the outer membrane, which leads to increase in the uptake of hydrophobic compounds (Nikaido, 1985), did not affect fatty acid uptake (Fig. 37; Black, et al., 1987). Mutants unable to metabolize fatty acid by β-oxidation were capable of fatty acid uptake (Maloy *et al.*, 1981), suggesting that degradation of fatty acid is not rate-limiting. The involvement of acyl-CoA synthetase at the rate-limiting step in the overall process was suggested by the finding that the level of cellular fatty acyl-CoA was significantly lower than the level of phospholipids during the uptake of exogenous fatty acid (Fig. 40).

Biochemical processes in cells are highly regulated. This can occur at the level of gene expression or more directly by modulation of the activity of one or more enzymes involved in the process. Fatty acid uptake in *E. coli* is regulated by gene expression since this process is induced by growth on fatty acid. This study clearly shows that the fatty acid uptake process itself is subjected to control. The rate of fatty acid uptake was found to be inhibited by starvation (Fig. 28 and Fig. 31). The fact that the rate of oleate uptake was reactivated by D-lactate (Fig. 30 and Fig. 31) and by other energy sources (Fig. 29) suggested that during starvation the cells may have been de-energized. However, the inhibitory effect of starvation on oleate uptake did not appear to be related to de-energization of the membrane since proline uptake, which is known to be coupled to the electrochemical potential was not affected (Fig. 32) and since oleate uptake unlike proline uptake (Fig. 33B),

was virtually unaffected when the electrochemical potential was collapsed by CCCP (Fig. 33A). It was also determined that the cytoplasmic ATP content was not affected during the starvation (Fig. 34) or during the incubation with D-lactate (Fig. 35). It was therefore concluded that the effects of starvation and D-lactate on oleate uptake are not related to the state of energization of the cells.

The observation that D-lactate activation increased the V_{max} of oleate uptake by about 8-fold and reduced the K_t by 3.5-fold (Fig. 36) indicated that the rate-limiting step is being regulated by starvation and D-lactate. Evidence obtained in this study suggest that acyl-CoA synthetase may be involved in the rate-limiting step. Consequently, the utilization of oleate taken up by starved and starved, D-lactate activated cells for the synthesis of fatty acyl-CoA was determined. The results show that D-lactate activation stimulated the rate of cellular oleoyl-CoA synthesis by about 6-fold (Fig. 40B) thus, suggesting that the effects of starvation and D-lactate on oleate uptake are related to regulation of acyl-CoA synthetase activity.

The change in acyl-CoA synthetase activities in starved and starved, D-lactate activated cells are not related to changes in the amount acyl-CoA synthetase during the starvation and reactivation (Fig. 41) or to a direct interaction between D-lactate and the enzyme (Fig. 42). It was determined using a crude preparation that acyl-CoA synthetase activity is activated in the presence of Triton X-100 (Fig. 42). The fact that activation by Triton X-100 was also observed for acyl-CoA synthetase partially purified by DEAE-Sepharose chromatography, ammonium sulfate precipitation and hydroxyapatite chromatography (Fig. 43), suggests that the enzyme

becomes activated when associated with a hydrophobic surface. In addition, activation of fatty acyl-CoA synthetase also appears to be dependent on lipid (Fig. 44).

In vitro, a number of enzymes in *E. coli* (pyruvate oxidase and phosphatidylserine synthetase (Russell, *et al.*, 1977a; Russell, *et al.*, 1977b; Blake, *et al.*, 1978; Recny, *et al.*, 1985; Hamilton, *et al.*, 1986; Louie, *et al.*, 1986) and in mammalian cells (protein kinase C, phospholipase A_2) (Nishizuka, 1984; Parker, et al., 1986; Gennis, 1989) whose activities are regulated by reversible membrane association *in vivo*, are activated in the presence of membranes or detergents. The fact that acyl-CoA synthetase was stimulated by Triton X-100 suggests that *in vivo* D-lactate may activate the enzyme by promoting its association with the membrane. Preparation of inner membrane vesicles clearly showed that D-lactate promoted an association of acyl-CoA synthetase with the membrane (compare Table 1A with Table 1B). This finding strongly suggests that the effects of starvation and D-lactate on oleate uptake is due to regulation of acyl-CoA synthetase activity by reversible association with the inner membrane.

3.17. Conclusions

It was demonstrated that a photoreactive fatty acid analogue is capable of identifying a membrane-bound fatty acid binding protein and this probe was used to demonstrate directly that the *fadL* outer membrane protein of *E. coli* binds fatty acid saturably and with high affinity. Evidence obtained suggests that binding of fatty acids to the *fadL* protein may involve one or more histidine residue. Using the

photoaffinity labeling method, no evidence for a fatty acid binding protein in the periplasmic space or in the inner membrane was found. Translocation of fatty acid across the inner membrane is not rate-limiting in the overall process or directly coupled to the electrochemical potential. The observed energy-dependence of fatty acid uptake is due to the requirement of ATP.

Acyl-CoA synthetase was shown to be necessary and sufficient for fatty acid permeation of the inner membrane using inner membrane vesicles. Evidence obtained suggests that acyl-CoA synthetase is involved in the rate-limiting step and in the regulation of fatty acid uptake. Regulation of fatty acid uptake by acyl-CoA synthetase appears to be related to changes in its activity by reversible association with the inner membrane.

3.18. Future Investigations

3.18.1. Identification of the Fatty Acid Binding Site of the *FadL* Protein of *E. coli*

The saturability of labeling of the *fadL* protein shows that the protein has a fatty acid binding site. However, the location of this site is not known. The identification and characterization of the fatty acid binding site of the *fadL* protein should be pursued. This can be accomplished by determining the site of attachment of the photoreactive fatty acid to the protein using protein chemistry. Conservative mutagenesis of the region surrounding the site of attachment of the probe followed by photoaffinity labeling should determine the importance of that region in fatty acid binding to the *fadL* protein.

3.18.2. Identification of Amino Acid Residues Essential for Fatty Acid Binding to the *fadL* Protein

The pH profile of specific labeling of the *fadL* protein with the probe indicated that binding of fatty acid to the protein involves an electrostatic interaction. Based on this pH profile, inhibition of labeling by DEPC suggested that binding of fatty acid to the *fadL* protein involves a histidine residue. The protein contains 5 histidine residues. Each of these can be changed individually by site-directed mutagenesis. The effect of each change on the affinity of the *fadL* protein for the photoreactive fatty acid will establish the importance of that histidine residue in the binding of fatty acid to the protein.

3.18.3. *In Vivo* Analysis of Recruitment of Fatty Acyl-CoA Synthetase to the Inner Membrane of *E. coli*

The results obtained in this study strongly suggest that fatty acyl-CoA synthetase is rate-limiting in fatty acid uptake and regulates this process. This regulation of fatty acid uptake by fatty acyl-CoA synthetase appears to be related to changes in its activity by reversible association with the inner membrane. Regulation of fatty acyl-CoA synthetase activity by recruitment was based on the finding that under conditions where both fatty acid uptake cellular fatty acyl-CoA synthesis was stimulated, the enzyme was associated with the inner membrane. Furthermore, the activity of the enzyme was stimulated in the presence of detergent solubilized *E. coli* membranes. Recruitment as the mechanism of regulation of fatty acyl-CoA synthetase activity *in vivo* remains to be established. A method for this type of analysis however, is not currently available.

An approach which has the potential for facilitating *in vivo* analysis of recruitment is photolabeling with photoreactive fatty acid incorporated into the membrane lipids of the cells. To detect cross-linking of the photoreactive lipid to the recruited enzyme, ^{32}P-phosphate is incorporated into the phosphate group of the lipids. Preliminary experiments showed that *E. coli* can grow on 11-DAP-undecanoate supplemented with a low concentration of acetate and that the specific activity of the phosphate incorporated into the membrane lipids is high. However, recruitment of fatty acyl-CoA synthetase to the membrane was not observed. This was due to a severe background problem during autoradiography of the gel. At that

time, an antibody against the enzyme was not available. In the future, fatty acyl-CoA should be immunoprecipitated and then analyzed by SDS-PAGE.

3.18.4. Identification of the Physiological Recruiting Agent

Fatty acid uptake as well as cellular fatty acyl-CoA synthesis in starved *E. coli* was stimulated by D-lactate, L-lactate, succinate and acetate. However, D-lactate did not directly activate fatty acyl-CoA synthetase *in vitro*. It is therefore reasonable to assume that a metabolite common to the above compounds, recruits the enzyme to the inner membrane. The end product of metabolism of D-lactate, L-lactate, succinate and acetate is acetyl-CoA which is also the end product of fatty acid metabolism.

Two approaches can be used to assess whether acetyl-CoA or other metabolites is the physiological effector. The first is stimulation of pure fatty acyl-CoA synthetase activity by acetyl-CoA in the presence of inverted inner membrane vesicles to provide the enzyme with the physiologically relevant face of the membrane. The second approach which can be used to assess recruitment of fatty acyl-CoA synthetase is to determine whether more of the enzyme is associated with the membrane in the presence of acetyl-CoA. This can be done by pelleting of the membrane followed by Western immunoblot analysis.

3.18.5. Lipid Requirement of Activation of Fatty Acyl-CoA Synthetase

Fatty acyl-CoA synthetase was activated by Triton X-100 solubilized *E. coli* membranes isolated from cells grown on oleate. This stimulatory effect was also observed for Triton X-100 solubilized membranes prepared from the cells grown on

glucose. These results indicated that the enzyme may require lipids for activation. To examine the lipid requirement of activation of fatty acyl-CoA synthetase, lipids isolated from *E. coli* should be used. Studies should also be focussed on the lipid specificity of activation.

4.0 REFERENCES

Abumrad, N.A., Perkins, R.C., Park, J.H. and Park, C.R. (1981) Mechanism of long chain fatty acid permeation in the isolated adipocyte. Journal of Biological Chemistry, 256: 9183-9191.

Abumrad, N.A., Park, J.H. and Park, C.R. (1984) Permeation of long-chain fatty acid into adipocytes. Journal of Biological Chemistry, 259: 8945-8953.

Ames, G.F-L. and Nikaido, K. (1976) Two-Dimensional Gel Electrophoresis of Membrane Proteins. Biochemistry, 15: 616-623.

Ames, G.F-L. (1986). Bacterial Periplasmic transport Systems: Structure, Mechanism, and Evolution. Annual Review of Biochemistry, 55: 397-425.

Armstrong, M.K., Bernlohr, D.A., Storch, J. and Clarke, S.D. (1990) The Purification and Characterization of a Fatty Acid Binding Protein Specific to Pig (*Sus domesticus*). Biochemical Journal, 267: 373-378.

Bass, N.M. (1985) Function and Regulation of Hepatic and Intestinal Fatty Acid Binding Proteins. Chemistry and Physics of Lipids, 38: 95-114.

Bass, N.M., Manning, J.A., Ockner, R.K., Gordon, J.I., Seetharam, S. and Alpers, D.H. (1985a) Regulation of the Biosynthesis of Two Distinct Fatty Acid-binding Proteins in Rat Liver and Intestine. Influences of Sex Difference and of Clofibrate. Journal of Biological Chemistry, 260: 1432-1436.

Bass, N.M., Manning, J.A. and Ockner, R.K. (1985b) Turnover and Short-term Regulation of Fatty Acid Binding Protein in Liver. Journal of Biological Chemistry, 260: 9603-9607.

Bayley, H. and Knowles, J.R. (1978a) Photogenerated Reagents for Membrane Labeling. I. Phenylnitrene Formed with the Lipid Bilayer. Biochemistry, 17: 2414-2419.

Bayley, H. and Knowles, J.R. (1978b) Photogenerated reagents for membrane labeling. II. Phenylcarbene and Adamanytlidene Formed within the lipid bilayer. Biochemistry, 17: 2420-2423.

Bayley, H. (1983) Photogenerated Reagents in Biochemistry and Molecular Biology. In Laboratory Techniques in Biochemistry and Molecular Biology (Work, T.S., and Burdon, R.H., eds) pp. 1-188, Elsevier, New York.

Baxa, C.A., Sha, R.S., Buelt, M.K., Smith, A.J., Matarese, V., Chinander, L.L.,

Boundsy, K.L. and Bernlohr, D.A. (1989) Biochemistry, 28: 8683-8690.

Berger, E.A. (1973) Different Mechanisms of Energy Coupling for the Transport of Proline and Glutamine in *Escherichia coli*. Proceedings of the National Academy of Science USA, 70: 1514-1518.

Berk, P.D., Wada, H., Horio, Y., Potter, B.J., Sorrentino, D., Zhou, S.-L., Isola, L.M., Stump, D., Kiang, C.-L. and Thung, S. (1990) Plasma membrane fatty acid-binding protein and mitochrodrial glutamic-oxaloacetic transaminase of rat liver are related. Proceedings of the National Academy of Science USA, 87: 3484-3488.

Binstock, J.F., Pramanik, A. and Schultz, H. (1977) Isolation of a multienzyme complex of fatty acid oxidation from *Escherichia coli*. Proceedings of the National Academy of Science USA, 74: 492-495.

Binstock, J.F. and Schultz, H. (1981) Fatty acid oxidation complex from *Escherichia coli*. Methods in Enzymology, 71: 403-411.

Bishop, L., Agbayani, Jr., R., Ambudkar, S.V., Maloney, P.C. and Ames, G.F-L. (1989) Reconstitution of a bacterial periplasmic permease in proteoliposomes and demonstration of ATP hydrolysis concomitant with transport. Proceedings of the National Academy of Science USA, 86: 6953-6957.

Billich, S., Wissel, T., Kratzin, H., Hahn, U., Hagendorff, B., Lezius, A.G. and Spener, F. (1988) Cloning of a Full-Length Complementary DNA for Fatty Acid-Binding Protein from Bovine Heart. European Journal of Biochemistry, 175: 549-556.

Black, P.N., Kianian, S.F., DiRusso, C.C. and Nunn, W.D. (1985) Long-Chain Fatty Acid Transport in *Escherichai coli:* Cloning, Mapping, and Expression of the *fadL* Gene. Journal of Biological Chemistry, 260: 1780-1789.

Black, P.N., Said, B., Ghosn, C.R., Beach, J.V. and Nunn, W.D. (1987) Purification and Characterization of an Outer Membrane-Bound Protein Involved in Long-Chain Fatty Acid Transport in *Escherichia coli*. Journal of Biological Chemistry, 262: 1412-1419.

Black, P.N. (1988) The *fadL* Gene Product of *Escherichia coli* is an Outer Membrane Protein Required for Uptake of Long-Chain Fatty Acids and Involved in Sensitivity to Bacteriophage T2. Journal of Bacteriology, 170: 2850-2854.

Black, P.N. (1990) Characterization of *fadL*-Specific Fatty Acid Binding in *Escherichia coli*. Biochimica et Biophysica Acta, 1046: 97-105.

Black, P.N. (1991) Primary Sequence of the *Escherichia coli fadL* Gene Encoding an Outer Membrane Protein Required for Long-chain Fatty Acid Transport. Journal of Bacteriology, 173: 435-442.

Blake, R.,II, Hager, L.P., and Gennis, R.B. (1978) Activation of Pyruvate Oxidase by Monomeric and Micellar Amphiphiles. Journal of Biological Chemistry, 253: 1963-1971.

Bligh, E.G. and Dyer, W.J. (1959) A Rapid Method of Total Lipid Extraction and Purification. Canadian Journal of Biochemistry and Physiology, 37: 911-917.

Boehler-Kohler, B.A., Boos, W., Deiterle, R. and Benz, R. (1979) Receptor for bacteriophage lambda of *Escherichia coli* forms larger pores in black lipid membranes than the matrix protein (porin). Journal of Bacteriology, 138: 33-39.

Bonner, W.M. and Laskey, R.A. (1974) Qunatitative Film Detection of ^{3}H and ^{14}C in Polyacrylamide Gels by Fluorography. European Journal of Biochemistry, 46: 83-88.

Brecher, P., Saouaf, R., Surarman, J.M., Eisenberg, D. and LaRossa, K. (1984) Fatty Acid Transfer between Multilammelar Liposomes and Fatty Acid-binding Proteins. Journal of Biological Chemistry, 259: 13395-13401.

Broring, K., Haest, C.W.M. and Deuticke, B. (1989) Translocation of oleic acid across the erythrocyte membrane: Evidence for a fast process. Biochimica et Biophysica Acta, 986: 321-331.

Brunner, J., Senn, H. and Richards, F.M. (1980) 3-Trifluoromethyl-3-phenyldiazirine: A New Carbene Generating Group for Photolabeling Reagents. Journal of Biological Chemistry, 255: 3313-3318.

Brunner, J. and Semenza, G. (1981) Selective Labeling of the Hydrophobic Core of Membranes with 3-(Trifluoromethyl)-3-(m-[^{125}I]iodophenyl)diazirine, a Carbene-Generating Reagent. Biochemistry, 20: 7174-7182.

Brunner, J. (1989) Photochemical Labeling of Apolar Phase of Membranes. Methods in Enzymology, 172: 628-687.

Capone, J., Leblanc, P., Gerber, G.E. and Ghosh, H.P. (1983) Localization of Membrane Proteins by the Use of a Photoreactive Fatty Acid Incorporated in vivo into Vesicular Stomatitis Virus. Journal of Biological Chemistry, 258: 1395-1398.

Chan, W.W.-C., Demmer, W. and Brand, K. (1983) Some properties of aminopeptidase associated with rat brain cortical synaptosomes. Canadian Journal

of Biochemistry and Cell Biology, 61: 1185-1190.

Chen, S. and Guillory, R.J. (1981) Studies on the Interaction of Arylazido-B-alanyl NAD^+ with the Mitochrondrial NADH Dehydrogenase. Journal of Biological Chemistry, 256: 8318-8323.

Chinander, L.L. and Bernlohr, D.A. (1989) Cloning of Murine Adipocyte Lipid Binding Protein in *Escherichia coli*. Its Purification, Ligand Binding Properties, and Phosphorylation by the Adipocyte Insulin Receptor. Journal of Biological Chemistry, 264: 19564-19572.

Chowdhry, V. and Westheimer, F.H. (1979) Photoaffinity Labeling of Biological Membranes. Annual Review of Biochemistry, 48: 293-325.

Cistola, D.P., Sacchettini, J.C., Banaszak, L.J., Walsh, M.T. and Gordon, J.I. (1989) Fatty Acid Interactions with Rat Intestinal and Liver Fatty Acid-Binding Proteins Expressed in *Escherichia coli*. A Comparative ^{13}C NMR Study. Journal of Biological Chemistry, 264: 2700-2710.

Clark, D. (1981) Regulation of Fatty Acid Degradation in *Escherichia coli*: Analysis by Operon Fusion. Journal of Bacteriology, 148: 521-526.

Cooper, R., Noy, N. and Zakim, D. (1987) A Physical-Chemical Model for Cellular Uptake of Fatty Acids: Prediction of Intracellular Pool Sizes. Biochemistry, 26: 5890-5896.

Cooper, R.B., Noy, N. and Zakim, D. (1989) Mechanism for binding of fatty acids to hepatocyte plasma membranes. Journal of Lipid Research, 30: 1719-1726.

Das, T., Sa, G. and Mukherjea, M. (1988) Purification and Characterization of Fatty Acid-Binding Protein from Human Placenta. Lipids, 23: 528-533.

Davidson, A.L. and Nikaido, H. (1990) Overproduction, Solubilization, and Reconstitution of the Maltose Transport System from *Escherichia coli*. Journal of Biological Chemistry, 265: 4254-4260.

Dean, D.A., Davidson, A.L. and Nikaido, H. (1989) Maltose transport in membrane vesicles of *Escherichia coli* is linked to ATP hydrolysis. Proceedings of the National Academy of Science USA, 86: 9134-9138.

DeGrella, R.F. and Light, R.J. (1980) Uptake and Metabolism of Fatty Acids by Dispersed Adult Rat Heart Myocytes. I. Kinetics of Homologous Fatty Acids. Journal of Biological Chemistry, 255: 9731-9738.

DeGrella, R.F. and Light, R.J. (1980) Uptake and Metabolism of Fatty Acids by Dispersed Adult Rat Heart Myocytes. II. Inhibition by Albumin and Fatty Acid Homologues and the Effect of Temperature and Metabolic Reagents. Journal of Biological Chemis. y, 255: 9739-9745.

Dills, S.S., Apperson, A., Schmidt, M.R. and Saier Jr., M.H. (1980) Carbohydrate Transport in Bacteria. Microbiological Review, 44: 385-418.

DiRusso, C. and Nunn, W.D. (1985) Cloning and Characterization of a Gene (*fadR*) Involved in Regulation of Fatty Acid Metabolism in *Escherichia coli*. Journal of Bacteriology, 161: 583-588.

DiRusso, C. (1988) Nucleotide sequence of the *fadR* gene, a multifunctional regulator of fatty acid metabolism in *Escherichia coli*. Nucleic Acids Research, 16: 7995-8009.

DiRusso, C.C. (1990) Primary sequence of the *Escherichia coli fadAB* operon, encoding the fatty acid-oxidizing multi-enzyme complex, indicates a high degree of homology to eucaryotic enzymes. Journal of Bacteriology, 172: 6459-6468.

Doody, M.C., Pownall, H.J., Kao, Y.J., Smith, L.C. (1980) Mechanism and Kinetics of Transfer of a Fluorescent Fatty Acid between Single-Walled Phosphatidylcholine Vesicles. Biochemistry, 19: 108-116.

Eisele, J-L. and Rosenbusch, J.P. (1990) In Vitro Folding and Oligomerization of a Membrane Protein: Transition of Bacterial Porin from Random Coil to Native Conformation. Journal of Biological Chemistry, 265: 10217-10220.

Feigenbaum, J. and Schultz, H. (1985) Thiolases of *Escherichia coli*: purification and chain length specificities. Journal of Bacteriology, 122: 407-411.

Fournier, N.C. and Rahim, M.H. (1983) Self-aggregation, a New Property of Cardiac Fatty Acid-binding Protein. Predictable Influence on Energy Production in the Heart. Journal of Biological Chemistry, 258: 2929-2933.

Fournier, N.C. and Richard, M.A. (1988) Fatty Acid-binding Protein, a Potential Regulator of Energy Production in the Heart. Investigation of Mechanisms by Electron Spin Resonance. Journal of Biological Chemistry, 263: 14471-14479.

Frerman, F.E. and Bennet, W. (1973) Studies on the Uptake of Fatty Acids by Escherichia coli. Archives of Biochemistry and Biophysic, 159: 434-443.

Gennis, R.B. (1989) Biomembranes: Molecular Structure and Function. Springly, Verlag, New York.

Ginsburg, C.L., Black, P.N. and Nunn, W.D. (1984) Transport of Long Chain Fatty Acids in *Escherichia coli*: Identification of a Membrane Protein Associated with the *fadL* Gene. Journal of Biological Chemistry, 259: 8437-8443.

Gordon, J.I., Alpers, D.H., Ockner, R.K. and Strauss, A.W. (1985) The Nucleotide Sequence of Rat Liver Fatty Acid Binding Protein mRNA. Journal of Biological Chemistry, 258: 3356-3363.

Greenberg, G.R., Chakrabarti, P. and Khorana, H.G. (1976) Incorporation of Fatty Acids Containing Photosensitive Groups into Phospholipids of *Escherichia coli*. Proceedings of the National Academy of Science USA, 73: 86-90.

Hamilton, J.A. and Cistola, D.P. (1986) Transfer of oleic acid between albumin and phospholipid vesicles. Proceedings of the National Academy of Sciience USA, 83: 82-86.

Hamilton, S.E., Recny, M.A., and Hager, L.P. (1986) Identification of the High Affinity Lipid Binding Site in *Escherichia coli* Pyruvate Oxidase. Biochemistry, 25: 8178-8183.

Hancock, R.E.W. (1984) Alterations in Outer Membrane Permeability. Annual Review of Microbiology, 38: 237-264.

Harmon, C.M., Luce, P., Beth, A.H. and Abumrad, N.A. (1991) Labeling of Adipicyte Membranes by Sulfo-N-Succinimidyl Derivatives of Long-Chain Fatty Acids: Inhibition of Fatty Acid Transport. Journal of Membrane Biology, 121: 261-268.

Heuckeroth, R.O., Birkenmeier, E.H., Llevin, M.S. and Gordon, J.I. (1987) Analysis of the Tissue-specific Expression, Developmental Regulation, and Linkage Relationships of a Rodent Gene Encoding Heart Fatty Acid Binding Protein. Journal of Biological Chemistry, 262: 9709-9717.

Hill, F.F. and Anglelmaier, D. (1972) Specific Enrichment of Mutants of Escherichia coli with an Altered Acyl-CoA Synthetase by Tritium Suicide. Molecular and General Genetics, 117: 143-152.

Ishaque, A., Hofmann, T. and Eylar, E.H. (1982) The Complete Amino Acid Sequence of the Rabbit P2 Protein. Journal of Biological Chemistry, 257: 592-595.

Jonas, A. and Weber, G. (1971) Presence of Arginine Residues at the Strong, Hydrophobic Anion Binding Sites of Bovine Serum Albumin. Biochemistry, 10: 1335-1339.

Joshi, A.K., Ahmed, S. and Ames, G.F-L. (1989) Energy Coupling in Bacterial Periplasmic Transport Systems: Studies in Intact *Escherichia coli* Cells. Journal of Biological Chemistry, 264: 2126-2133.

Julin, D.A. and Lehman, I.R. (1987) Photoaffinity Labeling of the recBCD Enzyme of *Escherichia coli* with 8-Azidoadensosine 5'-Triphosphate. Journal of Biological Chemistry, 262: 9044-9051.

Kaback, H.R. (1991). In and Out and Up and Down with the Lactose Permease of escherichia coli. International Reviews of Cytology,.

Kaback, H.R. (1971) Bacterial Membranes. Methods in Enzymology, 22: 99-120

Kaback, H.R. (1986). Active Transport in *Escherichia coli*: Passage to Permease. Annual Review of Biophysics and Biophysical Chemistry, 15: 279-319.

Kaczorowski, G.J., LeBlance, G. and Kaback, H.R. (1980) Specific labeling of the *lac* carrier protein in membrane vesicles of *Escherichia coli* by a photoaffinity reagent. Proceedings of the National Academy of Science USA, 77: 6319-6323.

Kameda, K. and Nunn, W.D. (1981). Purification and Characterization of Acyl Coenzyme A Synthetase from *Escherichia coli*. Journal of Biological Chemistry, 256: 5702-5707.

Kameda, K., Suzuki, L.K. and Imai, Y. (1987) Transport of Fatty Acid is Obligatory Coupled with H^+ Entry in Spheroplasts of *Escherichia coli* K12. Biochemistry International, 14: 227-234.

Kanda, T., Iseki, S., Hitomi, M., Kimura, H., Odani, S., Kondo, H., Matsubara, Y., Muto, T. and Ono, T. (1989) Purification and Characterization of a Fatty Acid-Binding Protein from the Gastric Mucosa of Rats. Possible Identity with Heart Fatty Acid-Binding Protein and its Parietal Cell Location. European Journal of Biochemistry, 185: 27-33.

Klein, K., Steinberg, R., Fiethen, B. and Overath, P. (1971) Fatty Acid Degradation in *Escherichia coli*: An Inducible System for the Uptake of Fatty Acids and further Characterization of *old* Mutants. European Journal of Biochemistry, 19: 442-450.

Knight, K.L. and McEntee, K. (1985) Covalent Modification of the recA Protein from *Escherichia coli* with the Photoaffinity Label 8-Azidoadenosine 5'-Triphosphate. Journal of Biological Chemistry, 260: 867-872.

Konings, W.N. and Kaback, R.H. (1973) Anaerobic Transport in *Escherichia coli* Membrane Vesicles. Proceedings of the National Academy of Science USA, 70:

3376-3381.

Kumar, G.B. and Black, P.N. (1991) Linker Mutagenesis of a Bacterial Fatty Acid Transport Protein: Identification of Domains with Functional Importance. Journal of Biological Chemistry, 266: 1348-1353.

Laemmli, U.K. (1970) Cleavage of Structural Proteins during the Assembly of the Head of Bacteriophage T4. Nature, 227: 680-685.

Lam, K.T., Borkan, S., Claffey, K.P., Schwartz, J.H., Chobanian, A.V. and Brecher, P. (1988) Properties and Differential Regulation of Two Fatty Acid Binding Proteins in the Rat Kidney. Journal of Biological Chemistry, 263: 15762-15768.

Lau, E.P., Haley, B.E. and Barden, R.E. (1977) Photoaffinity Labeling of Acyl-Coenzyme A:Glycine N-Acyl transferase with p-Azidobenzoyl-Coenzyme A. Biochemistry, 12: 2581-2585.

Leblanc, P., Capone, J. and Gerber, G.E. (1982) Synthesis and Biosynthetic Utilization of Radioactive Photoreactive Fatty Acids. Journal of Biological Chemistry, 257: 14586-14589.

Leblanc, P. and Gerber, G.E. (1984a) Biosynthetic Utilization of Photoreactive Fatty Acids by Rat Liver Microsomes. Canadian Jounal of Biochemistry and Cell Biology, 62: 375-378.

Leblanc, P. and Gerber, G.E. (1984b) An Improved Synthesis of m-diazirinophenol. Canadian Journal of Chemistry, 62: 1767-1771.

Leblanc, P. (1991). Radioactive Photoreactive Fatty Acid Analogues: Synthesis, Biological Utilization and Tools for the Study of Fatty Acid Transport. Ph.D. Thesis.

Lin, F.C., Brown, Jr., R.M., Drake, Jr., R.R. and Haley, B.E. (1990) Identification of the Uridine 5'-Diphosphoglucose (UDP-Glc) Binding Subunit of Cellulose Synthetase in *Acetobacter xylinum* Using the Photoaffinity Probe 5-Azido-UDP-Glc. Journal of Biological Chemistry, 265: 4782-4784.

Louie, K., Chen, Y.-C., and Dowhan, W. (1986) Substrate-induced membrane association of phosphatidylserine synthetase from *Escherichia coli.* Journal of Bacteriology, 165: 805-812.

Lowe, J.B., Boguski, M.S., Sweetser, D.A., Elshourbagy, N.A., Taylor, J.M. and Gordon, J.I. (1985) Human Liver Fatty Acid Binding Protein. Isolation of a Full Length cDNA and Comparative Sequence Analysis of Orthologous and Paralogous

Proteins. Journal of Biological Chemistry, 260: 3413-3417.

Lowe, J.B., Sacchettini, J.C., Laposata, M., McQuillan, J.J. and Gordon, J.I. (1987) Expression of Rat Intestinal Fatty Acid-binding Protein in *Escherichia coli*. Purification and Comparison of Ligand Binding Characteristics with that of *Escherichia coli*-Derived Rat Liver Fatty Acid-Binding Protein. Journal of Biological Chemistry, 262: 5931-5937.

Lowry, O.H., Rosebrough, N.J., Farr, A.L. and Randal, R.J. (1951) Protein Measurement with the Folin Phenol Reagent. Journal of Biological Chemistry, 193: 265-275.

Luckey, M. and Nikaido, H. (1980a) Specificity of diffusion channels produced by lambda phage receptor protein of *Escherichia coli*. Proceeding of the National Academy of Science USA, 77: 167-171.

Luckey, M. and Nikaido, H. (1980b) Diffusion of solutes through channels produced by phage lambda receptor protein of *Escherichia coli*: inhibition by higher oligosaccharided of maltose series. Biochemical and Biophysical Research Communication, 93: 166-171.

Mahadevan, S. and Sauer, F. (1971) Effect of α-Bromo-palmitate on the Oxidation of Palmitic Acid by Rat Liver Cells. Journal of Biological Chemistry, 246: 5862-5867.

Mahadevan, S. and Sauer, F. (1974) Effect of Trypsin, Phospholipases, and Membrane-Impermeable Reagents on the Uptake of Palmitic Acid by Isolated Rat Liver Cells. Archives of Biochemistry and Biophysics, 164: 185-193.

Maier, C., Bremer, E., Schmid, A. and Benz, R. (1988) Pore-forming Activity of the *Tsx* Protein from the Outer Membrane of *Escherichia coli*. Journal of Biological Chemistry, 263: 2493-2499.

Malamy, M.H. and Horecker, B.L. (1964) Release of Alkaline Pphosphatase from Cells of *Escherichia coli* upon Lysozyme Spheroplast Formation. Biochemistry, 3: 1889-1893.

Maloy, S.R., Bohlander, M. and Nunn, W.D. (1980) Elevated levels of glyoxylate shunt enzymes in *Escherichia coli* strains constitutive for fatty acid degradation. Journal of Bacteriology, 143: 720-725.

Maloy, S.R. and Nunn, W.D. (1981) Role of gene *fadR* in *Escherichia coli* acetate metabolism. Journal of Bacteriology, 148: 83-90.

Maloy, S.R., Ginsburg, C.L., Simons, R.W. and Nunn, W.D. (1981) Transport of Long and Medium Chain Fatty Acids by *Escherichia coli* K12. Journal of Biological Chemistry, 256: 3735-3742.

Maloy, S.R. and Nunn, W.D. (1982) Genetic regulation of the glyoxylate shunt in *Escherichia coli* K-12. Journal of Bacteriology, 149: 173-180.

Maniscalco, W.M., Stremmel, W. and Heeney-Campbell, M. (1990) Uptake of palmitic acid by rabbit alveolar type II cells. American Journal of Physiology, 259: 206-212.

Miles, E.W. (1977) Modification of Histidyl Residues in Proteins by Diethylpyrocarbonate. Methods in Enzymology, 47: 431-443.

Mohler, H., Battersby, M.K. and Richards, J.G. (1980) Benzodiazepine receptor protein identified and visualized in brain tissue by a photoaffinity label. Proceedings of the National Academy of Science USA, 77: 1666-1670.

Munson, K.B. (1981) Light-dependent Inactivation of (Na^+ + K^+)-ATPase with a New Photoaffinity Reagent, Chromium Arylazido-B-alanyl ATP. Journal of Biological Chemistry, 256: 3223-3230.

Nakae, T. (1979) A porin activity of purified lambda receptor proteins from *Escherichia coli* in reconstituted membrane vesicles. Biochemical and Biophysical Research Communication, 88: 774-781.

Nakamura, K. and Mizushima, S. (1976) Effects of Heating in Dodecyl Sulfate Solution on the Conformation and Electrophoretic Mobility of Isolated Major Outer Membrane Proteins from *Escherichia coli* K12. Journal of Biochemistry, 80: 1411-1422.

Neu, H.L., and Heppel, L.A. (1965) The release of Enzymes from *Escherichia coli* by Osomotic Shock and during the Formation of Spheroplasts. Journal of Biological Chemistry, 240: 3685-3692.

Nikaido, N. and Vaara, M. (1985) Molecular Basis of Bacterial Outer Membrane Permeability. Microbiological Reviews, 49: 1-32.

Nikaido, H. (1990) Permeability of the Lipid Domains of Bacterial Membranes. Membrane Transport and Information Storage, p., 165-190, Alan R. Liss, Inc.

Noy, N. and Zakim, D. (1985) Fatty Acids Bound to Unilamellar Lipid Vesicles as Substrates for Microsomal Acyl-CoA Ligase. Biochemistry, 24: 3521-3525.

Noy, N., Donnelly, T.M. and Zakim, D. (1986) Physical-Chemical Model for the Entry of Water-Insoluble Compounds into Cells. Studies of Fatty Acid Uptake by the Liver. Biochemistry, 25: 2013-2021.

Nunn, W.D. and Simons, R.W. (1978) Transport of long-chain fatty acids by *Escherichia coli*: Mapping and characterization of mutants in the *fadL* gene. Proceedings of the National Academy of Science USA, 75: 3377-3381.

Nunn, W.D., Simons, R.W., Egan, P.A. and Maloy, S.R. (1979) Kinetics of the Utilization of Medium and Long Chain Fatty Acids by a Mutant of *Escherichia coli* Defective in the *fadL* Gene. Journal of Biological Chemistry, 254: 9130-9134.

Nunn, W.D., Griffin, P.K., Clark, D. and Cronan Jr., J.E. (1983) Role for the *fadR* gene in unsaturated fatty acid biosynthesis in *Escherichia coli*. Journal of Bacteriology, 154: 554-560.

Nunn, W.D. (1986a) A Molecular View of Fatty Acid Catabolism in *Escherichia coli*. Microbiological Review, 50: 179-192.

Nunn, W.D., Colburn, R.W. and Black, P.N. (1986b) Transport of Long-Chain Fatty Acids in *Escherichia coli*: Evidence for Role of *fadL* Gene Product as Long-Chain Fatty Acid Receptor. Journal of Biological Chemistry, 261: 167-171.

O'Brien, W. and Frerman, F. (1977) Evidence for a complex of three beta-oxidation enzymes in *Escherichia coli*: induction and localization. Journal of Bacteriology, 132: 532-540.

O'Farrell, P.H. (1975) High Resolution Two-Dimensional Electrophoresis of Proteins. Journal of Biological Chemistry, 250: 4007-4021.

Olson, W., Schaechter, M. and Khorana, H.G. (1979) Incorporation of Synthetic Fatty Acid Analogs into Phospholipids of *Escherichia coli*. Journal of Bacteriology, 137: 1443-1446.

Osborn, M.J., Gander, J.E., Parisi, E. and Carson, J. (1972) Mechanism of Assembly of the Outer Membrane of *Salmonella typhimurium*: Isolation and Characterization of Cytoplasmic and Outer Membrane. Journal of Biological Chemistry, 247: 3962-3972.

Overath, P., Raufuss, E., Stoffel, W. and Ecker, W. (1967) The Induction of the Enzymes of Fatty Acid Degradation in *Escherichia coli*. Biochemical and Biophysical Research Communication, 29: 28-33.

Overath, P., Pauli, G. and Schairer, H.U. (1969) Fatty Acid Degradation in

Escherichia coli: An Inducible Acyl-CoA Synthetase, the Mapping of *old* Mutants, and the Isolation of Regulatory Mutants. European Journal of Biochemistry, 7: 559-574.

Pada, E., Patel, L. and Kaback, H.R. (1979). Effect of Diethylpyrocarbonate on lactose/proton symport in *Escherichia coli* membrane vesicles. Proceedings of the National Academy of Science USA, 76: 6221-6225.

Parker, P.J., Cousseuo, L., Totty, N., Rhee, L., Young, S., Chen, E., Stabel, S., Waterfield, M.D., and Ulrich, A. (1986) The Complete Primary Structure of Protein Kinase C in the Major Phorbol Ester Receptor. Science, 233: 853-859.

Pascual, A., Casanova, J. and Samuels, H.H. (1982) Photoaffinity Labeling of Thyroid Hormone Nuclear Receptors in Intact Cells. Journal of Biological Chemistry, 257: 9640-9647.

Paulussen, R.J.A., Van der Logt., C.P.E. and Veerkamp, J.H. (1988) Characterization and Binding Properties of Fatty Acid-Binding Proteins from Human, Pig and Rat Heart. Archives of Biochemistry and Biophysics, 264: 533-545.

Paulussen, R.J.A., Geelen, M.J.H., Beynen, A.C. and Veerkamp, J.H. (1989) Immunochemical Quantitation of Fatty Acid-Binding Proteins. I. Tissue and Intracellular Distribution, Postnatal Development and Influence of Physiological Conditions on Rat Heart and Liver FABP. Biochimica et Biophysica Acta, 1001: 201-209.

Paulussen, R.J.A. and Veerkamp, J.H. (1990) in Subcellular Biochemistry (Hilderson, H.J., ed) Vol 16, pp. 175-226, Plenum, New York.

Pawar, S. and Schultz, H. (1981) The structure of the multi-enzyme complex of fatty acid oxidation from *Escherichia coli*. Journal of Biological Chemistry, 256: 3894-3899.

Peeters, R.A. and Veerkamp, J.H. (1989) Does Fatty Acid-Binding Protein play a Role in Fatty Acid Transport. Molecular and Cellular Biochemistry, 88: 45-49.

Peeters, R.A., Veerkamp, J.H. and Demel, R.A. (1989a) Are Fatty Acid-Binding Proteins involved in Fatty Acid Transfer. Biochimica et Biophysica Acta, 1002: 8-13.

Peeters, R.A., Groen, M.A. and Veerkamp, J.H. (1989b) The Fatty Acid-Binding Protein from Human Skeletal Muscle. Archives of Biochemistry and Biophysics, 274: 556-563.

Pjura, W.J., Kleinfeld, A.M. and Karnovsky, M.J. (1984) Partition of Fatty Acids and Fluorescent Fatty Acids into Membranes. Biochemistry, 23: 2039-2043.

Potter, B.J., Sorrentino, D. and Berk, P.D. (1989) Mechanisms of Cellular Uptake of Free Fatty Acid. Annual Review of Nutrition, 9: 271-285.

Potter, B.J., Stump, D., Schwieterman, W., Sorrentino, D., Jacobs, L.N., Kiang, C.-L., Rand, J.H. and Berk, P.D. (1987) Isolation and Partial Characterization of Plasma Membrane Fatty Acid Binding Proteins from Myocardium and Adipose Tissue and their Relationship to Analogous Proteins in Liver and Gut. Biochemical and Biophysical Research Communication, 148: 1370-1376.

Powers-Lee, S.G. and Corina, K. (1987) Photoaffinity Labeling of Rat Liver Carbamoyl Phosphate Synthetase I by 8-Azido-ATP. Journal of Biological Chemistry, 262: 9052-9056.

Pramanik, A., Pawar, S., Antonian, E. and Schultz, H. (1979) Five different enzymatic activities are associated with the multi-enzyme complex of fatty acid oxidation from *Escherichia coli*. Journal of Bacteriology, 137: 469-473.

Prossnitz, E., Gee, A. and Ames, G.F-L. (1989) Reconstitution of the Histidine Periplasmic Transport System in Membrane Vesicles: Energy Coupling and Interactiion between the Binding Protein and the Membrane Complex. Journal of Biological Chemistry, 264: 5006-5014.

Quay, S.C., Radhakrishnan, R. and Khorana, H.G. (1981) Incorporation of Photosensitive Fatty Acids into Phospholipids of *Escherichia coli* and Irradiation-Dependent Cross-linking of Phospholipids to Membrane Proteins. Journal of Biological Chemistry, 256: 4444-4449.

Randerath, K. (1970) An Evaluation of Film Detection Methods for Weak beta-emitters, Particulary Tritium. Analytical Biochemistry, 34: 188-205.

Recny, M.A., Grabau, C., Cronan, Jr., J.E., and Hager, L.P. (1985) Characterization of the α-peptide Released upon Protease Activation of Pyruvate Oxidase. Journal of Biological Chemistry, 260: 14287-14291.

Rose, H., Hennecke, T. and Kammermeier, H. (1989) Is Fatty Acid uptake in Cardiomyocytes determined by Physiochemical Fatty acid Partitioning between Albumin and Membranes. Molecular and Cellular Biochemistry, 88: 31-36.

Ross, A.H., Radhakrishnan, R., Robson, R.J. and Khorana, H.G. (1982) The Transmembrane Domain of Glycophorin A as Studied by Cross-linking Using

Photoactivatable Phospholipids. Journal of Biological Chemistry, 257: 4152-4161.

Russell, P., Hager, L.P., and Gennis, R.B. (1977a) Characterization of the Proteolytic Activation of Pyruvate Oxidase. Control by Specific Ligands and by Flavin Oxidation-Reduction State. Journal of Biological Chemistry, 252: 7877-7882.

Russell, P., Shrock, H.L., and Gennis, R.B. (1977b) Lipid Activation and Protease Activaton of Pyruvate Oxidase. Evidence Suggesting a Common Site of Interaction of the Protein. Journal of Biological Chemistry, 252: 7883-7887.

Sa, G., Das, T. and Mukherjea, M. (1989) Purification and Characterization of Fatty Acid-Binding Proteins from Human Fetal Lung. Experimental Lung Research, 15: 619-634.

Sacchettini, J.C., Gordon, J.I. and Banaszak, L.J. (1988) The Structure of Crystalline Escherichia coli-derived Rat Intestinal Fatty Acid-binding Protein at 2.5-A° Resolution. Journal of Biological Chemistry, 263: 5815-5819.

Sacchettini, J.C., Gordon, J.I. and Banaszak, L.J. (1989) Crystal Structure of Rat Intestinal Fatty Acid-Binding Protein. Refinement and Analysis of *Escherichia coli*-derived Protein with Bound Palmitate. Journal of Molecular Biology, 208: 327-339.

Sallus, L., Haselbeck, R.J. and Nunn, W.D. (1983) Regulation of Fatty Acid Transport in *Escherichia coli*: Analysis by Operon Fusion. Journal of Bacteriology, 155: 1450-1454.

Schnaitman, C.A. (1973) Outer Membrane Proteins of *Escherichia coli*: I. Effect of Preparative Conditions on the Migration of Proteins in Polyacrylamide Gels. Archives of Biochemistry and Biophysics 157: 541-552.

Scholtz, G. and Kwok, F. (1989) Brain Pyridoxal Kinase: Photoaffinity Labeling of the Substrate-binding Site. Journal of Biological Chemistry, 264: 4318-4321.

Schoentgen, F., Pignede, G., Bonanno, L.M. and Jolles, P. (1989) Fatty Acid Binding Protein from Bovine Brain. Amino Acid Sequence and some Properties. European Journal of Biochemistry, 185: 35-40.

Schulengerg-Schell, H.,Schafer, P., Keuper, H.J., Stanislawski, B., Hoffman, E., Ruterjans, H. and Spener, F. (1988) Interaction of Fatty Acids with Neutral Fatty Acid-Binding Protein from Bovine Liver. European Journal of Biochemistry, 170: 565-574.

Schwieterman, W., Sorrentino, D., Potter, B.J., Rand, J., Kiang, C.-L., Stump, D. and Berk, P.D. (1988) Uptake of Oleate by Isolated Rat Adipocytes is Mediated by a 40

kDa Plasma Membrane Fatty Acid Binding Protein closely related to that in Liver and Gut. Proceedings of the National Academy of Science USA, 85: 359-363.

Seidman, C.E., Hess, H-J., Homcy, C.J. and Graham R.M. (1984) Photoaffinity Labeling of the Alpha1-Adrenergic Receptor Using a ^{125}I-Labeled Aryl Azide Analogue of Prazosin. Biochemistry, 23: 3765-3770.

Simons, R.W., Egan, P.A., Chute, H.T. and Nunn, W.D. (1980a) Regulation of fatty acid degradation in *Escherichia coli*: isolation and characterization of strains bearing insertion and temperature-sensitive mutations in gene *fadR*. Journal of Bacteriology, 142: 621-632.

Simons, R.W., Huges, K.T. and Nunn, W.D. (1980b) Regulation of fatty acid degradation in *Escherichia coli*: dominance studies with strains merodiploid in gene *fadR*. Journal of Bacteriology, 143: 726-730.

Smith, R.A.G. and Knowles, J.R. (1973) Aryl diazirines: Potential Reagents for Photolabeling of Biological Receptor Sites. Journal of the American Chemical Society, 95: 5072-5073.

Smith, R.A.G. and Knowles, J.R. (1975) The Preparation and Photolysis of 3-Aryl-3H-diazirines. Journal of the Chemical Society Perkin Transaction, 2: 686-694.

Sorrentino, D., Stump, D., Potter, B.J., Robinson, R.B., White, R., Kiang, C.-L. and Berk, P.D. (1988) Oleate uptake by cardiac mycocytes is carrier mediated and involves a 40 kDa plasma membrane fatty acid binding protein similiar to that in liver, adipose tissue, and gut. Journal of Clinical Investigation, 82: 928-935.

Sorrentino, D., Robinson, R.B., Kiang, C-L. and Berk, P.D. (1989) At Physiologic Albumin/Oleate Concentrations Oleate Uptake by Isolated Hepatocytes, Cardiac Myocytes, and Adipocytes is a Saturable Function of the Unbound Oleate Concentration: Uptake Kinetics are Consistent with the Conventional Theory. Journal of Clinical Investigation, 84: 1325-1333.

Spector, A.A., Steinberg, D. and Tanaka, A. (1965) Uptake of Free Fatty Acid by Ehrlich Ascites Tumor Cells. Journal of Biological Chemistry, 240: 1032-1041.

Spector, A.A., John, K. and Fletcher, J.E. (1969) Binding of long-chain fatty acids to bovine serum albumin. Journal of Lipid Research, 10: 56-66.

Spector, A.A., Fletcher, J.E. and Ashbrook, J.D. (1971) Analysis of Long-Chain Free Fatty Acid Binding to Bovine Serum Albumin by Determination of Stepwise Equilibrium Constants. Biochemistry, 10: 3229-3232.

Spratt, S.K., Black, P.N., Ragozzino, M.M. and Nunn, W.D. (1984) Cloning, mapping, and expression of genes involved in the fatty acid degradative mult-enzyme complex of *Escherichia coli*. Journal of Bacteriology, 158: 535-542.

Standring, D.N. and Knowles, J.R. (1980) Photoaffinity Labeling of Lactate Dehydrogenase by the Carbene Derived from the 3-Dazirino Analogue of Nicotinamide Adenine Dinucleotide. Biochemistry, 19: 2811-2816.

Staros, J.V. and Knowles, J.R. (1978) Photoaffinity Inhibition of Dipeptide Transport in *Escherichia coli*. Biochemistry, 17: 3321-3325.

Staros, J.V., Bayley, H., Standring, D.N. and Knowles, J.R. (1978) Reduction of Aryl Azides by Thiols: Implications for the Use of Photoaffinity Reagents. Biochemical and Biophysical Research Communications, 80: 568-572.

Stewart, J.M. and Driedzic, W.R. (1988) Canadian Journal of Zoology, 66: 2671-2675.

Storch, J. and Kleinfeld, A.M. (1986) Transfer of Long-Chain Fluorescent Free Fatty Acids between Unilamellar Vesicles. Biochemistry, 25: 1717-1726.

Storch, J., Bass, N.M. and Kleinfeld, A.M. (1989) Studies of the Fatty Acid-binding Site of Rat Liver Fatty Acid-binding Protein Using Fluorescent Fatty Acids. Journal of Biological Chemistry, 264: 8708-8713.

Stremmel, W., Strohmeyer, G., Borchard, F., Kochwa, S. and Berk, P.D. (1985a) Isolation and partial characterization of a fatty acid binding protein from rat liver plasma membranes. Proceedings of the National Academy of Science USA, 82: 4-8.

Stremmel, W., Lotz, G., Strohmeyer, G. and Berk, P.D. (1985b) Identification, Isolation, and Partial Characterization of a Fatty Acid Binding Protein from Rat Jejunal Microvillous Membranes. Journal of Clinical Investigation, 75: 1068-1076.

Stremmel, W., Strohmeyer, G. and Berk, P.D. (1986a) Hepatocellular uptake of oleate is energy dependent, sodium-linked, and inhibited by an antibody to a hepatocyte plasma membrane fatty acid binding protein. Proceedings of the National Academy of Science USA, 83: 3584-3588.

Stremmel, W. and Berk, P.D. (1986b) Hepatocellular influx of [^{14}C]oleate reflects membrane transport rather than intracellular metabolism or binding. Proceedings of the National Academy of Science USA, 83: 3086-3090.

Stremmel, W. and Theilmann, L. (1986) Selective inhibition of long-chain fatty acid uptake in short-term cultured rat hepatocytes by an antibody to the rat liver plasma

membrane fatty acid-binding protein. Biochimica et Biophysica Acta, 877: 191-197.

Stremmel, W. (1987) Translocation of Fatty Acids across the Basolateral Rat Liver Plasma Membrane is Driven by an Active Potential-sensitive Sodium-dependent Transport System. Journal of Biological Chemistry, 262: 6284-6289.

Stremmel, W. (1988) Fatty Acid Uptake by Isolated Rat Heart Myocytes Represents a Carrier-mediate Transport Process. Journal of Clinical Investigation, 81: 844-852.

Stremmel, W. (1989) Transmembrane transport of fatty acids in the heart. Molecular and Cellular Biochemistry, 88: 23-29.

Sweetser, D.A., Birkenmeier, E.H., Klisak, I.J., Zollman, S., Sparkes, R.S., Mohandas, T., Lusis, A.J. and Gordon, J.I. (1987) The Human and Rodent Intestinal Fatty Acid-Binding Protein Genes. A Comparative Analysis of their Structure, Expression, and Linkage. Journal of Biological Chemistry, 262: 16060-16071.

Takagaki, Y., Radhakrishnan, R., Gupta, C.M. and Khorana, H.G. (1983a) The Membrane-embedded Segment of Cytochrome b_5 as Studied by Cross-linking with Photoactivatable Phospholipids. I. The Transferable Form. Journal of Biological Chemistry, 258: 9128-9135.

Takagaki, Y., Radhakrishnan, R., Wirtz, K.W.A. and Khorana, H.G. (1983b) The Membrane-embedded Segment of cytochrome b_5 as Studied by Cross-linking with Photoactivatable Phospholipids. II. The Nontransferable Form. Journal of Biological Chemistry, 258: 9136-9142.

Trigatti, B.L., Mangroo, D. and Gerber, G.E. (1991) Photoaffinity Labeling and Fatty Acid Permeation in 3T3-L1. Journal of Biological Chemistry, 266: 22621-22625.

Trigatti, B.L., Baker, A.D., Rajaratnam, K., Rachubinski, R.A. and Gerber, G.E. (1992) Fatty Acid Uptake in *Candida tropicalis*: Induction of a Saturable Process. Biochemistry and Cell Biology, 70: 76-80.

Trotter, P.J. and Storch, J. (1989) 3-[p-(6-Phenyl)-1,3,5-hexatrienyl]phenylpropionic acid (PA-DHP): Characterization as a Fluorescent Membrane Probe and Binding to Fatty Acid Binding Proteins. Biochimica et Biophysica Acta, 982:131-139.

Tsuchiya, T. (1976) Oxidative Phosphorylation in Right-side-out Membrane Vesicles from *Escherichia coli*. Journal of Biological Chemistry, 251: 5315-5320.

Tweedie, S. and Edwards, Y. (1979) cDNA sequence from Mouse Heart Fatty Acid-Binding Protein, H-FABP. Nucleic Acid Research, 17: 4374.

Vaara, M., Plachy, W.Z. and Nikaido, H. (1990) Partitioning of Hydrophobic Probes into Lipopolysaccharide Bilayers. Biochimica et Biophysica Acta, 1024: 152-158.

Veerkamp, J.H., Peeters, R.A. and Maatman, R.G.H.J. (1991) Structural and Functional Features of Different Types of Cytoplasmic Fatty Acid-Binding Proteins. Biochimica et Biophysica Acta, 1081: 1-24.

Waggoner, D.W. and Bernlohr, D.A. (1990) *In situ* ling of the Adipocyte Lipid Binding Protein with 3-[^{125}I]Iodo-4-azido-N-hexadecy. cylamide: Evidence for a Role of Fatty Acid Binding Proteins in Lipid Uptake. Journal of Biological Chemistry, 265: 11417-11420.

Walter, U., Uno, I., Liu, A.Y.-C. and Greengard, P. (1977) Identification, Characterization and Quantitative Measurement of Cyclic AMP Receptor Proteins in Cytosol of Various Tissues using a Photoaffinity Ligand. Journal of Biological Chemistry, 252: 6494-6500.

Weeks, G., Shapiro, M., Burns, R.O. and Wakil, S.J. (1969) Control of Fatty Acid Metabolism. I. Induction of the Enzymes of Fatty Acid Oxidation in *Escherichia coli*. Journal of Bacteriology, 97: 827-836.

Wilkinson, T.C.I. and Wilton, D.C. (1987) Studies on Fatty Acid-Binding Proteins. The Binding Properties of Rat Liver FABP. Biochemical Journal, 247: 485-488.

Wilson, D.B. (1978) Cellular Transport Mechanism. Annual Review of Biochemistry, 47: 933-965.

Witholt, B., Boekhout, M., Brock, M., Kingma, J., Heerikhuizen, H.V. and Leiji, L.D. (1976) An Efficient and Reproducible Procedure for the Formation of Spheroblasts from Variously Grown *Escherichia coli*. Analytical Biochemistry, 74: 160-170.

APPENDICES

The synthetic work described in Appendices A and B was conducted before transferring into the Ph.D. program. The work should not be considered as being part of the main thesis since it does not have any direct relevance to the study of fatty acid uptake in *E. coli*. However, the synthetic schemes developed for micro-scale synthesis of phospholipid and fatty acyl-CoA can be used to synthesize photoreactive phospholipid and fatty acyl-CoA derivatives which could be used to identify enzymes involved in fatty acid and lipid metabolism.

Appendix A: An Improved Synthesis of Phospholipids

The peptide dinitrophenylpropylthreoninamide (DNP-Pro-Thr-NH_2) was used as a model system to develop better acylation conditions for the synthesis of phospholipids using catalyst-activated anhydride. The acylation rate was found to be inversely related to the polarity of the solvent, chloroform alone resulting in much better rates of reaction than did pyridine, dimethylformamide or mixtures of these solvents. Anhydride activated by 4-pyrrolidinopyridine (PPY) was twice as reactive as that activated with 4-dimethylaminopyridine (DMAP). It was shown that the phosphate group of phosphatidylcholine (PC) interferes with the acylation by a process which could be reversed by means of the addition of a 200-fold excess of PPY. This reversal is not due to base catalysis by the PPY; the results suggest that a mixed anhydride may be formed with the phosphate and that this can be reversed by high catalyst concentrations to produce the reactive acylating agent. The acylation rates for lysophosphatidylcholine (lyso PC) using optimum conditions were

found to be approximately 50 times faster that the best rates reported in the literature, the reaction being complete within 5 min even using only a slight excess of anhydride. Acyl group migration was assessed during these reactions and no increase in migration of the acyl groups could be detected due to these reaction conditions. The procedure described provide significant improvements over previous methods described for large scale, as well as highly radioactive micro-scale phospholipid synthesis.

Appendix B: Synthesis of Acyl-CoA Thioesters

An improved synthesis of fatty acyl-coenzyme A has been developed which permits the synthesis of highly radioactive fatty acyl-coenzyme A. Conditions were developed to solubilize the coenzyme A under anhydrous solvent for the acylation. The complete activation of fatty acid to the imidazolide is described and the acylation of the coenzyme A under anhydrous conditions was shown to result in the conversion of the fatty acid to the fatty acyl-coenzyme A derivative. The synthetic product was shown by its chemical and biochemical reactivity to be the pure thioester of coenzyme A. The purification of the fatty acyl-coenzyme A by reverse-phase chromatography is described. The yield of pure fatty acyl-coenzyme A was essentially quantitative.

APPENDIX A: AN IMPROVED SYNTHESIS OF PHOSPHOLIPIDS

TABLE OF CONTENTS

LIST OF ABBREVIATIONS

1,2-diacyl-glycero-3-phosphorylcholine	PC
glycero-3-phosphorylcholine	GPC
1-acyl-glycero-3-phosphorylcholine	LysoPC
4-dimethylaminopyridine	DMAP
4-pyrrolidinopyridine	PPY
dicyclohexylcarbodiimide	DCC
N,N-carbonyldiimidazole	CDI
N,N-dimethylformamide	DMF
pyridine	PYR
chloroform	$CHCl_3$
DNP-prolylthreoninamide	DNP-Pro-ThrNH_2
DNP-prolylserinamide	DNP-Pro-SerNH_2
High Pressure Liquid Chromatography	HPLC
tetrabutylammonium chloride	TBA-Cl

LIST OF FIGURES

INTRODUCTION

According to the model proposed by Singer and Nicolson (1, a biological membrane is composed of two major components: lipids, the most abundant being phospholipids, and proteins which are classified into two classes, integral proteins which traverse the entire span of the lipid bilayer and extrinsic proteins which are only partially embedded into the membrane. It is well established that these proteins are involved in a variety of membrane functions such as energy transduction, communication and transport of metabolically important substrates (2. Currently, most studies are directed at understanding the mechanism of action of these proteins in the aforementioned functions by using a functional approach. However, others are attempting to gain an insight into the function of the protein by determining the topology of the protein in its native form. More specifically, the topology of the transmembrane segments of these proteins are of significant interest since they are important in such functions as transport of metabolic substrates and ions, and transmembrane signalling.

A variety of experimental approaches, including in situ proteolysis, molecular genetic approaches, immunological methods, vectorial labeling using impermeable reagents and hydrophhobic labeling, are used to identify the transmembrane domain. The former three approaches allow for identification of that portion of the protein exposed at the membrane surface. In contrast, hydrophobic labeling approach allow

for identification of the transmembrane segment (3). This approach relies on the use of penetrating chemical agents which are capable of reacting with specific residues of the protein exposed to the lipid core of the membrane. However, the major disadvantage of this approach is that it relies on chemistry, which utilizes groups such as amino, sulfhydryl, phenolic or aliphatic hydroxyl and carboxylic acid groups. Therefore, these chemical reagents are only capable of reacting with amino acid residues whose side chains possess of the necessary functional groups. The other disadvantage of this approach is the chemical agents are added from the outside which diffuse into the membrane and react with groups on the protein, non-specifically with respect to site location; the location of the chemical agent is undefined (4).

Another method of hydrophobic labeling recently introduced is the use of photoreactive fatty acids attached to phospholipids (5,6,7,8). The use of this method would serve to enhance site specific labeling since the location of the photoreactive group within the membrane can be manipulated (4). That is the location of the photoreactive group within the membrane can be varied by varying the length of the fatty acul moeity of the phospholipids. urthermore, thes· ·hotor·active groups do not require the presence of specific functional groups since the reactive species is a carbene generated photolytically. Therefore, in comparison to other chemical approaches it is expected that the structural resolution obtained with the photoreactive probes would be greatly enhanced.

The chemistry that is required for the synthesis of photoreactive phospholipid

probes is analogous to those required for the synthesis of phospholipids. Of the approaches available for the synthesis of phospholipids, most involve acylation of a preformed phospholipid backbone such as glycero-3-phosphorylcholine or 1-acyl-3-phosphorylcholine (Fig. 1). The reactive derivatives of fatty acid that are used are fatty acid anhydride (10,11), fatty acid imidazolide (12,13,14), fatty acid chloride (15), fatty acid-trifluoroacetic anhydride (16) and 2-thiopyridyl fatty acid ester (17). The major drawback shared by all of these phospholipid synthetic approaches is that the secondary hydroxyl group of 1-acyl-glycero-3-phosphorylcholine is very unreactive. This usually leads to long reaction times and poor yield. To increase the yield, the activated fatty acid derivatives are usually used in large excess (10,15,16,17). Furthermore, vigorous conditions such as high temperature (13,15) and strong bases (12,14) have been attempted. Under these conditions it is possible that side reactions, such as isomerization and degradation of starting materials may be enhanced. To minimize the use of harsh conditions, catalysts such as 4-dimethylaminopyridine (DMAP) (18,19) and 4-pyrrolidinopyridine (PPY) (20,21) have been introduced. Using one equivalent of 4-dimethylaminopyridine with 1.5 equivalents of fatty acid anhydride to acylate 1-acyl-glycero-3-phosphorylcholine, Gupta and Khorana (18) were able to obtain 90% yield in 24 h. In the absence of 4-dimethylaminopyridine a yield of 10% was obtained in 20 days.

For photoreactive phospholipid synthesis the use of excessive amounts of the fatty acid derivatives and low yields are not desired since the syntheses of the

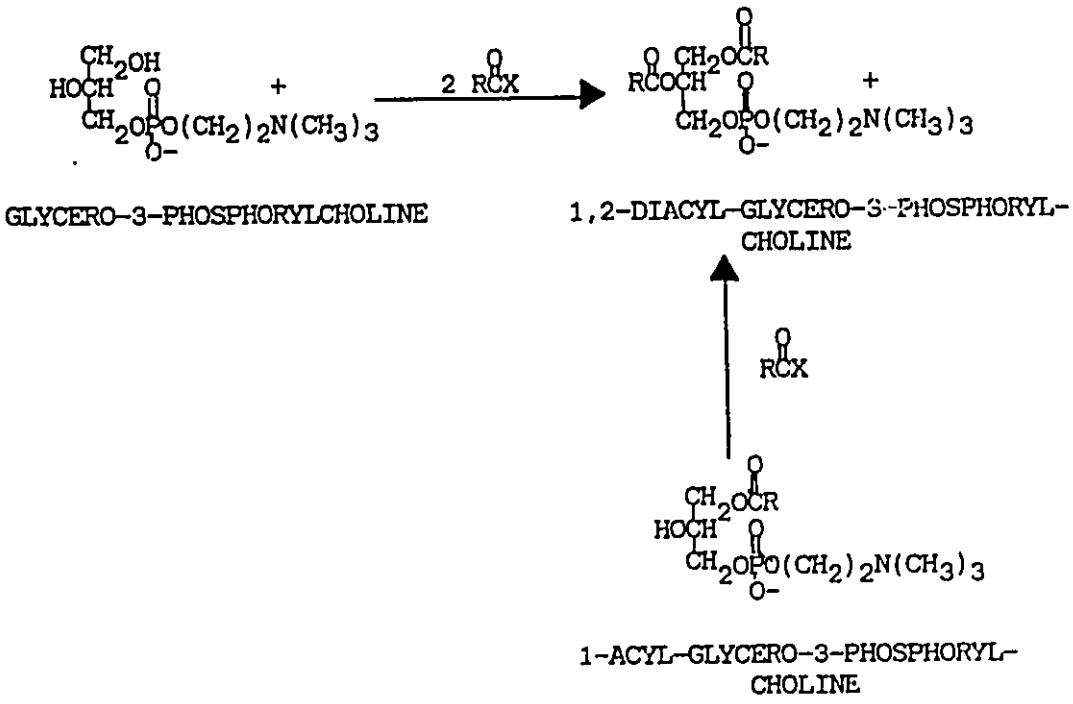

Figure 1. Phospholipid Synthetic Schemes

photoreactive fatty acid analogs are laborious. In addition, the photoreactive fatty acids are not available in large amounts and are highly radioactive. High temperature must also be avoided since the photoreactive groups are thermolabile. Long reaction time is also not desired since it has been demonstrated (22) that 1-acyl-glycero-3-phosphorylcholine undergoes isomerization under prolonged exposure to acylation conditions. This process is catalyzed by acid or base and is proposed to occur through acyl or phosphoryl migration (Fig. 2) (22). Therefore, the ideal synthetic scheme required for the synthesis of radioactive photoreactive phospholipids should result in a high yield, avoid the use of harsh conditions, allow the use of near equimolar amounts of the activated fatty acid and glycero-3-phosphorylcholine or 1-acyl-glycero-3-phosphorylcholine, and a short reaction time.

Preliminary experiments using the anhydride approach developed by Gupta and Khorana (18) to prepare radioactive photoreactive phospholipids on a nanomile scale resulted in poor yield and the reaction time extended beyond 24 h. Attempts to increase the yield by increasing the ratio of 1-acyl-glycero-3-phosphorylcholine to anhydride also resulted in poor yields and the reaction proceeded at a much slower rate. With the imidazolide approach (14) a very low yield of the radioactive photoreactive phospholipids was also obtained. These preliminary experiments indicated that these approaches were not, in general, adaptable to a small scale preparation of phospholipids. Therefore, it was evident that a new synthetic scheme had to be developed, one which would allow the preparation of small amounts of radioactive photoreactive phospholipids very efficiently. In order to accomplish this,

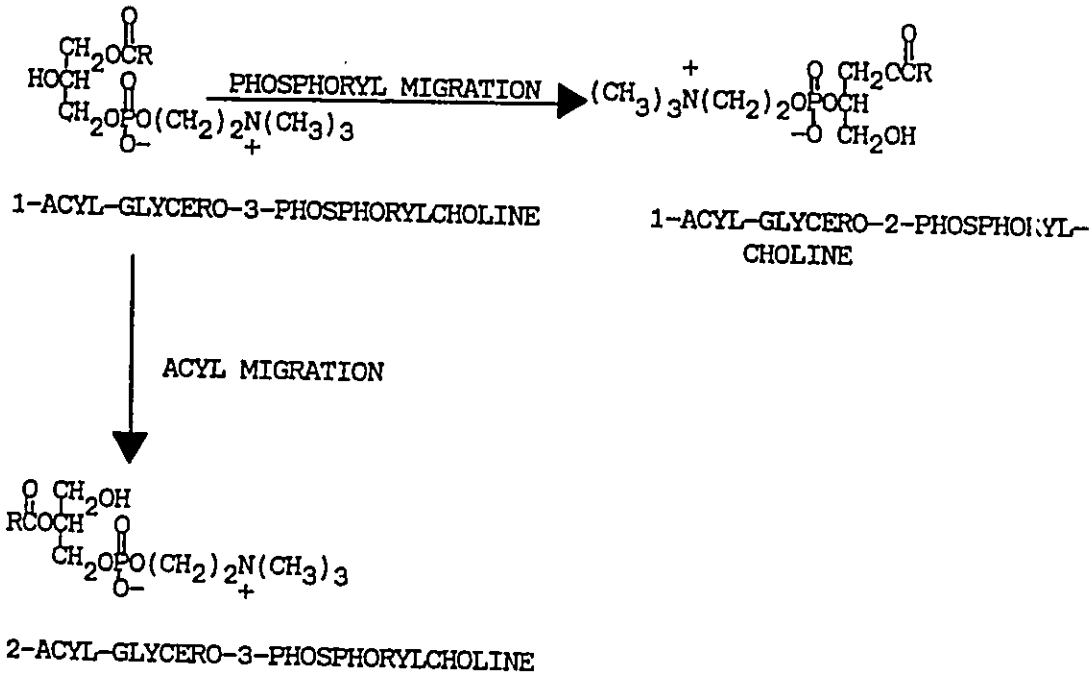

Figure 2. Isomerization Process

a critical and systematic evaluation of the different parameters involved in phospholipid synthesis was required. To perform this systematic analysis quantitatively we have taken advantage of the following properties of the peptide, DNP-Pro-Thr-NH_2:

a. The dinitrophenyl group provides a very convenient chromophore which can be monitored on the HPLC at 365 nm.

b. As illustrated below, the position of the hydroxyl group of the model peptide, DNP-Pro-Thr-NH_2 is analogous to that of 1-acyl-glycero-3-phosphorylcholine.

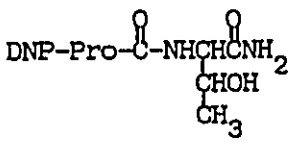

DNP-Pro-Thr-NH_2

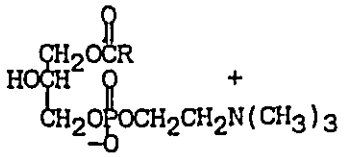

1-acyl-glycero-3-phosphorylcholine

It has been reported (18) that acylation at the phosphate occurs during the preparation of 1,2-diacyl-glycero-3-phosphorylcholine. For this reason, DNP-Pro-Thr-NH_2 was also used instead of 1-acyl-glycero-3-phosphorylcholine. Since the model peptide does not contain other reactive groups, conditions that affect acylation of the hydroxyl group can be analyzed without interference.

MATERIALS AND METHODS

Palmitic acid, 4-dimethylaminopyridine, N,N-carbonyldiimidazole, 4-pyrrolidinopyridine, 1,2-dipalmitoyl-glycero-3-phosphorylcholine and dicyclohexylcarbodiimide were purchased from Sigma. [^{3}H]palmitic acid was obtained from New England Nuclear and 1-palmitoyl-glycero-3-phosphorylcholine from Serdary.

Dry benzene was obtained by distillation over calcium hydride followed by storage over 4A° molecular sieves under nitrogen. Reagent grade dimethylformamide was rendered anhydrous by azeotroping with dry benzene under reduced pressure and stored with 4A° molecular sieves under nitrogen. Dry chloroform prepared by distillation over phosphorous pentoxide was stored under nitrogen at -20°C in the dark. Anhydrous pyridine was stored over 4A° molecular sieves and under nitrogen in the dark after it was prepared by distillation over barium oxide. During each distillation anhydrous conditions were maintained by allowing a continuous flow of nitrogen throughout the distillation apparatus.

4-dimethylaminopyridine and 4-pyrrolidinopyridine were further purified by recrystallization according to the procedures of Gupta *et al.*, (18) and Manson *et al.*, (21), respectively. The resulting pure materials were made anhydrous by repeated evaporation of dry benzene under reduced pressure.

Palmitic acid, 1-palmitoyl-glycero-3-phosphorylcholine and 1,2-dipalmitoyl-glycero-3-phosphorylcholine were freed of residual water as described above.

Preparation of fatty acid imidazolide and annydride

A. Fatty acid imidazolide:

The fatty acid imidazolide was routinely prepared by transferring 20 μmoles of the fatty acid (1 M in dry DMF) to a flamed pyrex tube containing 1.5 equivalents of CDI (0.2 M) in 15% DMF/85% benzene. After the vessel was flushed with nitrogen the reaction was allowed to proceed for 1 h at room temperature. Upon completion of the reaction the content was then diluted with dry benzene to 40 mM and transferred to another flamed pyrex tube containing 4 equivalents of dry Sephadex LH-20 (capacity 1.15 x 10^{-6} moles of hydroxyl group/mg). The tube was flushed with nitrogen and the contents shaken for 1 h at room temperature, then centrifuged to obtain the imidazolide free of Sephadex LH-20.

B.. Fatty acid anhydride:

Preparation of fatty acid anhydride was accomplished by reacting .5 equivalents of DCCD (.2 M in dry CCl_4) with fatty acid (.4 M in dry CCl_4) for 5 h at room temperature and under a nitrogen atmosphere (23). After removal of the dicyclohexylurea precipitate, the solvent was evaporated under reduced pressure and the dried residue dissolved by adding the required volume of dry benzene to afford an anhydride concentration of 40 mM.

Preparation of 1,2-diacyl-glycero-3-phosphorylcholine from glycero-3-phosphorylcholine:

To a siliconized pyrex screw cap tube (13 x 100 mm) containing an anhydrous residue of glycero-3-phosphorylcholine (as the $CdCl_2$ complex) (54 μmoles) was added

185 μmoles of palmitic acid anhydride (600 μCi). After 40 equivalents of PPY was added and the total volume adjusted to 1074.2 μl with dry chloroform, the reaction vessel was flushed with nitrogen and the reaction allowed to proceed at room temperature. After 12 h an equal volume of aqueous methanol (10% H_2O in MeOH) was added and the solvent removed under reduced pressure. The dried residue was dissolved by adding 500 μl $CHCl_3$/MeOH (1:1) and applied to a preparative TLC plate. The plate was developed with $CHCl_3$/MeOH/H_2O (65:25:4) and the products were visualized by autoradiography. The product, 1,2-diacyl-glycero-3-phosphorylcholine, was eluted with $CHCl_3$/MeOH/H_2O (1:2:0.8) and further purified by gel filtration on Sephadex LH-20. Sephadex LH-20 chromatography was performed on a 1.0 x 76 cm column with $CHCl_3$/MeOH (1:1) as the eluant. Yield of 1,2-diacyl-glycero-3-phosphorylcholine exceeded 90%.

Calculation of rate constant:

The rate constants were calculated according to the pseudo-first-order equation outlined below:

$$K = \frac{K_{app}}{[ANHYDRIDE]_{ave}} \qquad -t\,K_{app} = \ln \frac{[At]}{[Ao]}$$

[At] = [peptide] at time t

[Ao] = initial [peptide]

Synthesis of Model Peptides:

A. DNP-Proline Synthesis

During the synthesis and subsequent storage of DNP-Proline, as with the other DNP-peptides, care was taken to protect these compounds from prolonged exposure to light. L-proline (150 μmole) was dissolved in ethanol/water (3:1, 2 ml) in the

presence of 2 equivalents of triethylamine; the dinitrophenylation reaction was initiated by the addition of 2,3-dinitrofluorobenzene (DNFB) (1.3 equivalents). After 3 h at room temperature the reaction was diluted with 2 volumes of aqueous 10 mM sodium phosphate (dibasic), pH 7. Following removal of the ethanol under reduced pressure, the excess FDNB was selectively extracted into diethyl ether. Subsequent acidification of the aqueous phase to pH 1-2 by titration with 6 N HCl, permitted the extraction of DNP-proline into ethyl acetate. The extracts were washed with water and then evaporated under reduced pressure. Residual water was removed by drying the DNP-proline several times from a mixture of anhydrous benzene and DMF. DNP-proline was stored as a 0.25 M solution in anhydrous DMF over a molecular sieve (4A°) and under nitrogen.

B. DNP-Peptide Synthesis:

(a) DNP-prolylserinamide and DNP-prolylthreoninamide: DNP-proline was activated by the addition of 1.1 equivalents of CDI in dry THF as a 60 mM solution and incubated at room temperature for 1 h under nitrogen. To the reactive imidazolide derivative, 3 equivalents of the hydrochloride salt of serinamide or threoninamide was added as a freshly prepared 1.45 M aqueous solution in the presence of 1 equivalent of tetrabutylammonium hydroxide.

After a 12 h period, each peptide reaction was diluted with a 0.5 volume of water and the desired DNP-peptide extracted into ethyl acetate. Isolation and purification of the peptide products were accomplished by preparative HPLC on a reversed phase μBondapak C_{18} column which was equilibrated and run isocratically with 1% acetic

acid in aqueous methanol. The elution conditions that were used for DNP-prolylserinamide were 10% methanol while those for DNP-prolylthreoninamide were 15% methanol. The DNP-peptides were dried several times from dry benzene. DNP-prolylthreoninamide was stored as a 1 mM solution in anhydrous chloroform under a nitrogen atmosphere.

RESULTS AND DISCUSSION

A. Analysis of Parameters involved with the Imidazolide Approach

Of the approaches available for the synthesis of phospholipids, the ones using fatty acid imidazolide are particularly attractive. The reactivity of the imidazolides are considered to be comparable to the acid chloride (24). Unlike the acid chloride, the imidazolide derivative is a mild acylating agent. Preparation of phospholipids with fatty acid chloride usually result in a mixture of chloro-deoxy-glycerophosphorylcholines as the major side products (25). With the anhydride approach one equivalent of the fatty acyl substituent in the anhydride is not used since the leaving group is the fatty acyl carboxylate. Therefore, in comparison to these approaches, the imidazolide approach would appear to be the most suitable for the synthesis of radioactive photoreactive phospholipids.

A.1.0 Analysis of Parameters Required for Fatty Acid Imidazolide Preparation

A.1.1 Conditions for Complete Activation of Carboxylic Acid Groups

Other work in our laboratory has utilized the imidazolide derivative of diprotected trimesic acid ($(Me_3\ SiCH_2)_2$TMA) to derivatize hydrophobic proteins. It was established by spectral analysis at 310 nm that complete activation of the carboxyl group of diprotected trimesic acid can only be achieved if a slight excess of carbonyldiimidazole (CDI) is used. However, acylation of the model peptide, DNP-prolylserinamide (DNP-Pro-SerNH_2), with activated reagent prepared in this manner resulted in an incomplete reaction due to the formation of another product as observed from HPLC analysis of the reaction: this product was identified as an

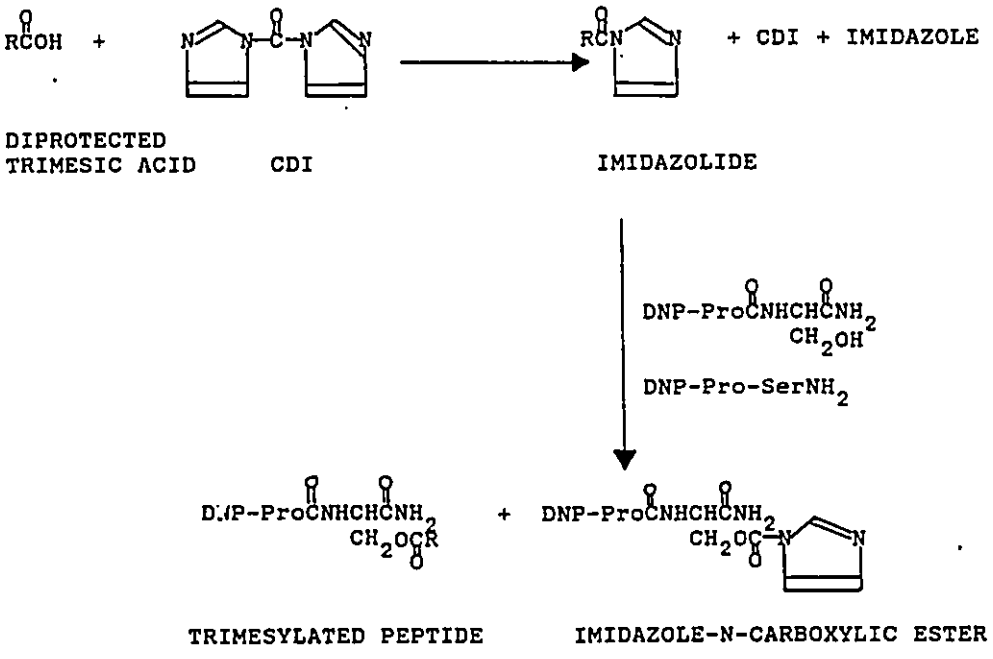

Figure 3. Acylation in the Presence of Excess CDI.

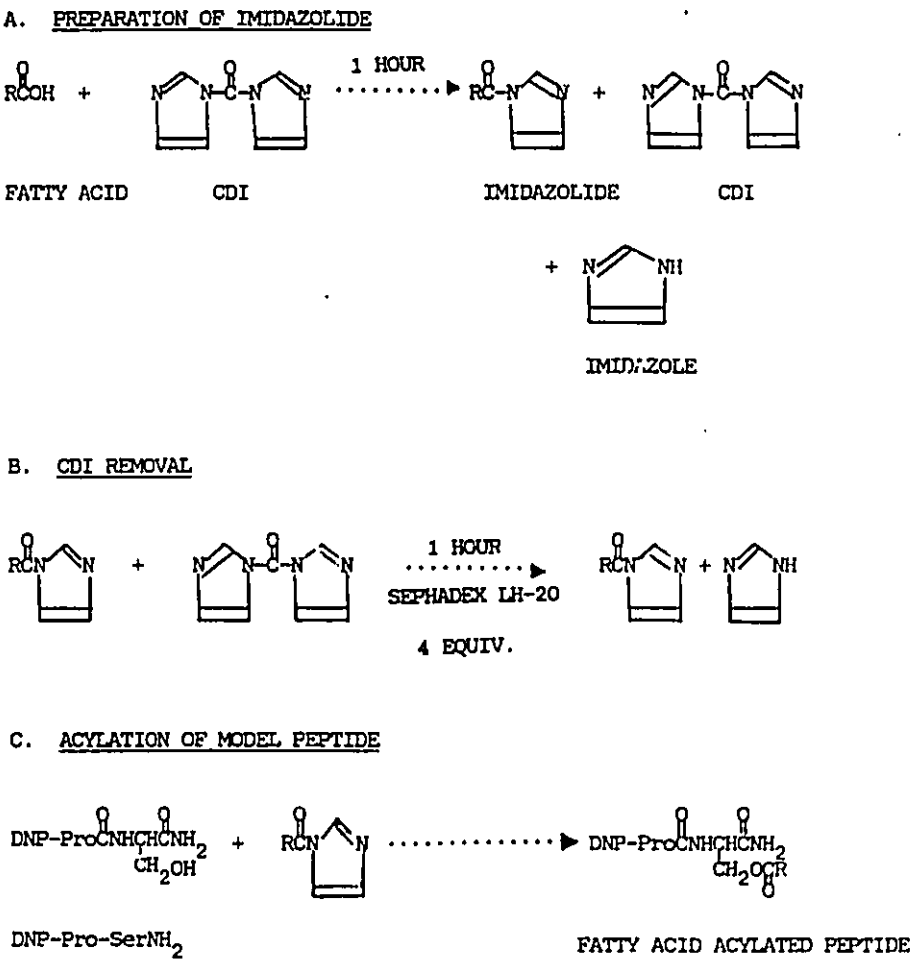

Figure 4. Scheme used for the Analysis of Parameters Involved with the Imidazolide Approach

imidazole-N-carboxylic ester of the DNP-peptide (Fig. 3). To circumvent this side reaction, it was necessary to remove the unreacted CDI prior to acylation of the DNP-peptide. Therefore, upon completion of the activation reaction removal of the unreacted CDI was accomplished by incubating the reaction mixture with dry Sephadex LH-20 in benzene for 1 h. Under these conditions it was determined that CDI reacted preferentially with the Sephadex LH-20. Accordingly, this system was adopted for the activation of fatty acids.

A.1.2 Evaluation of the Efficiency of Activation in Different Solvents:

The scheme used for the analysis of the different parameters involved with the imidazolide approach is outlined in Fig. 4. These analyses were performed with DNP-Pro-SerNH_2 instead of DNP-prolylthreoninamide (DNP-Pro-ThrNH_2) since the primary hydroxyl group of the DNP-Pro-SerNH_2 peptide is approximately 10 X more reactive than the secondary hydroxyl group of the DNP-Pro-ThrNH_2.

Although activation of the diprotected trimesic acid with CDI was routinely performed in dimethylformamide (DMF), it was necessary to determine whether this solvent was also suitable for the activation of fatty acid. Since an appropriate system to analyze the activation of fatty acid directly was not available, the time course of acylation of DNP-Pro-SerNH_2 was relied on as an indirect assay.

As illustrated in Figure 5, the efficiency of activation in two other solvents, 10% DMF in tetrahydrofuran (THF) and 25% DMF in benzene was compared to that in DMF. From the initial rates of acylation of DNP-Pro-SerNH_2 with imidazolide prepared in these three solvents indicated that activation of the fatty acid

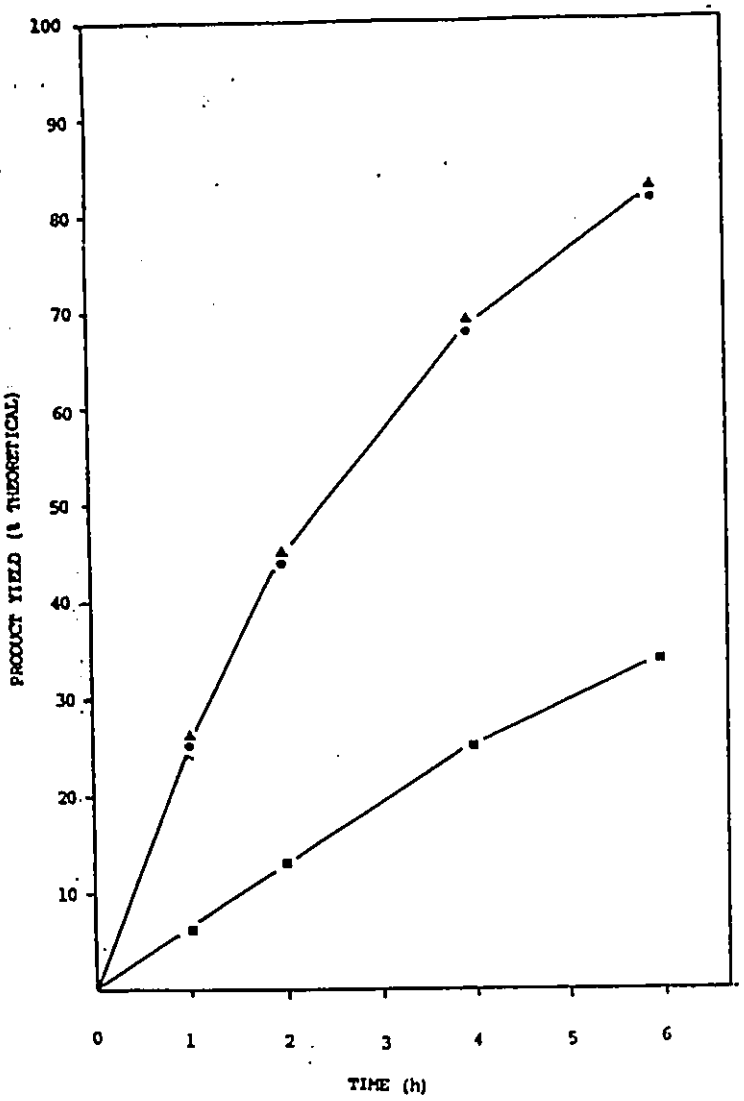

Figure 5. Time-course of acylation of DNP-Pro-SerNH$_2$ with palmitic acid imidazolide prepared in different solvent systems. The fatty acid imidazolide was prepared in DMF (□), 10% DMF in THF (▲), and 25% DMF in benzene (●) by reacting the fatty acid with 1.5 equivalents of CDI for 30 mins. After the reaction mixtures were incubated with dry Sephadex LH-20 for 1 hr, aliquots were transferred to reaction vessels and the solvent was removed under reduced pressure. To the dried residue (5 μmoles), 5 equivalents of anhydrous triethylamine (2 M in $CHCl_3$/DMF, 4:1) was added followed by 10.5 μl of $CHCl_3$/DMF (4:1). The reaction was initiated by adding 2 μl of the peptide (25 mM in DMF). The progress of each reaction was determined by HPLC. At the indicated time, an aliquot (3 μl) of each reaction was diluted in 47 μl aqueous DMF from which 30 μl was applied onto an ODS column pre-equilibrated with 30% methanol in 10 mM sodium acetate, pH 4.4. The column was eluted with a linear gradient and the eluates were detected by monitoring at 365 nm.

occurred more efficiently in 10% DMF in THF and in 25% DMF in benzene. Since these two mixed solvents are less polar than DMF suggested that the polarity of DMF promoted another side reaction during the activation reaction. This side reaction was thought to be the synthesis of fatty acid anhydride.

To determine whether anhydride formation occurs during the preparation of the imidazolide derivative in DMF diprotected trimesic acid was used. The phenyl group of this reagent provides a chromophore which can be used to monitor the reagent at 280 nm directly on the HPLC. Therefore, after the diprotected trimesic acid imidazolide was prepared in DMF or in 25% DMF in benzene the resulting imidazolides were incubated with trimethylsilylethanol (TMSE) for 2 h. Once the esterification reaction was completed, an aliquot of each incubation was diluted in aqueous DMF and analyzed by HPLC. If the reagent was fully converted to the imidazolide derivative then the only product which should result from the TMSE incubation is the triprotected trimesic acid. However, if the activation reaction resulted in a mixture of imidazolide and anhydride, two products should be observed, one corresponding to the triprotected trimesic acid and the other the diprotecteed acid. Analysis of the activation reaction performed in DMF or in 25% DMF in benzene by this approach conclusively showed that anhydride synthesis was in fact favoured in DMF but not in 25% DMF in benzene.

A.1.3 Analysis of the Time Required for Optimal Activation

Aliphatic acids are in general less reactive than aromatic acids. Consequently, the time required for complete activation of the fatty acid would be greater than the

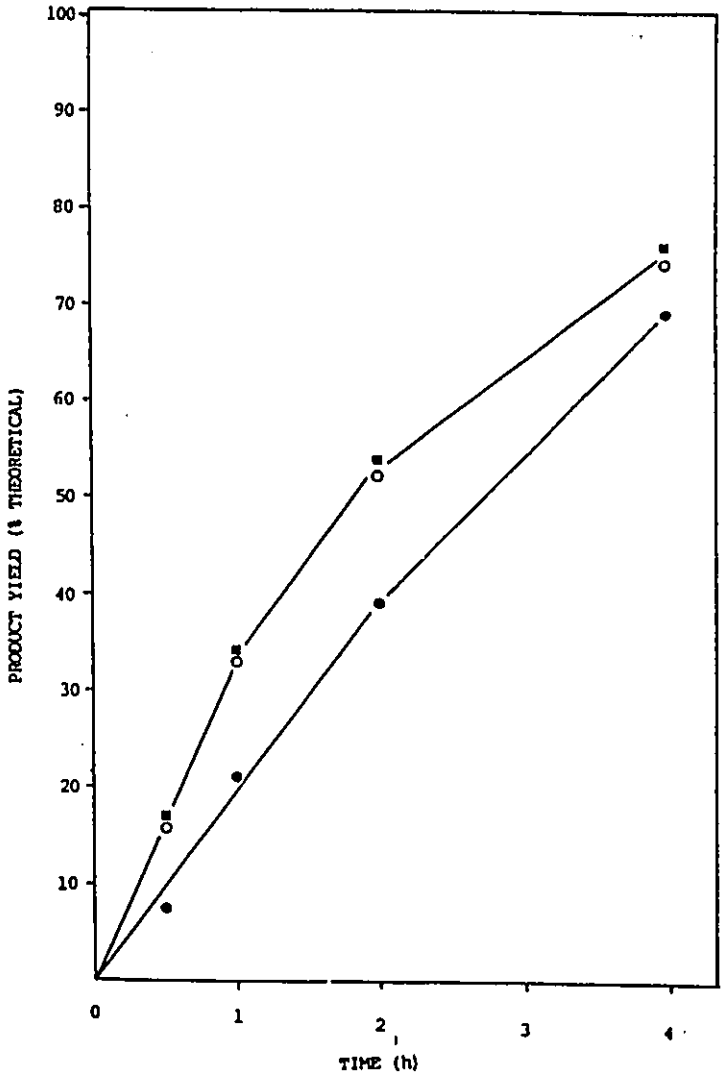

Figure 6. Time-course of acylation of DNP-Pro-SerNH$_2$. A time-course of the preparation of palmitic acid imidazolide. At 30 min (●), 60 min (○) and 120 min (□) during the preparation of palmitic acid imidazolide in 25% DMF/75% benzene an aliquot of the activation reaction mixture (20 μmoles of fatty acid) was diluted to 40 mM with dry benzene and incubated with dry Sephadex LH-20. After 1 hr 25% of the fatty acid content was transferred to a reaction vessel and the solvent was evaporated under reduced pressure. To the dried residue, 5 equivalents of triethylamine (2 M in $CHCl_3$/DMF, 4:1) was added followed by 10.5 μl of dry $CHCl_3$/DMF (4:1). The reaction was started by adding 2 μl of 25 mM DNP-Pro-SerNH$_2$. At the indicated time 3 μl of the reaction was diluted in aqueous DMF and analyzed by HPLC.

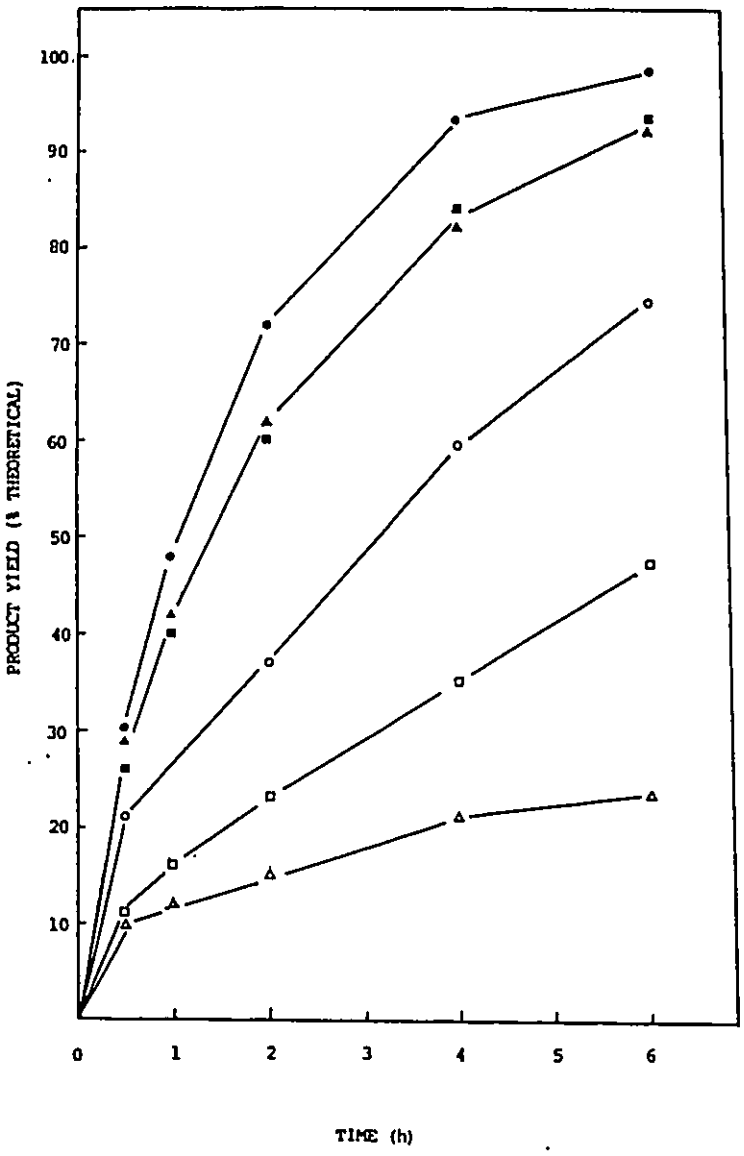

Figure 7. Effect of Solvent on the Rate of Acylation of DNP-Pro-SerNH_2. Standard acylation conditions described in the legend of Figure 1 were used to determine the kinetics of acylation in $CHCl_3$/DMF (4:1) (●), $CHCl_3$/PYR (4:1), and $CHCl_3$/DMSO (4:1) (▲). In DMF (○), PYR (□), and DMSO (Δ) the acylation reactions were performed as described except that the final concentrations of the peptide and the imidazolide were 4 mM and 100 mM, respectively. The progress of each reaction was analyzed by HPLC.

30 minutes routinely used to fully activate the COOH group of diprotected trimesic acid. To determine the optimal time required for complete activation of the fatty acid in 25% DMF in benzene, the initial rate of acylation of DNP-Pro-SerNH_2 was used. The rationale is that as more of the fatty acid imidazolide derivative is formed the rate of acylation of the DNP-peptide should also increase.

The time courses of acylation of DNP-Pro-SerNH_2 with imidazolide obtained at different times during the activation of the fatty acid are shown in Figure 6. Comparison of the rates obtained with imidazolide at 30, 60 and 120 mins during the imidazolide preparation indicated that optimal activation of the fatty acid was achieved if the activation reaction was allowed to proceed for at least 1 h.

A.2.0 Evaluation of Acylation Parameters

A.2.1 Influence of Solvents on the Rate of Acylation

It is understood that one of the factors which can also influence the rate of an acylation reaction is the solvent (26). Therefore, a number of mixed solvent systems capable of partially solubilizing 1-acyl-glycero-3-phosphorylcholine under anhydrous conditions were analyzed for their ability to promote acylation. Shown in Figure 7 are the results obtained for the acylation of DNP-Pro-SerNH_2 in these solvents. The rates of acylation of DNP-Pro-SerNH_2 obtained in the solvent systems containing 80% chloroform ($CHCl_3$) were much higher than those obtained in the neat solvents. Furthermore, since the initial rates obtained in the mixed solvent systems ($CHCl_3$/X (4:1)) were approximately the same suggested that the solvent property of chloroform was responsible for the difference in the rates observed.

This enhancement due to chloroform was initially attributed to the presence of HCl which may have formed upon storage of chloroform. Therefore, the HCl present in the chloroform would react with the fatty acid imidazolide to give the fatty acid chloride. This explanation appeared to be possible since Staab *et al.*, (27) had reported the synthesis of acid chloride derivatives by passing anhydrous HCl gas into a vessel containing imidazolide in a nonpolar solvent such as THF. However, the pH of an aqueous wash of 5 ml of chloroform in storage for a month negated the presence of HCl. Furthermore, during the acylation reaction 1 M triethylamine was present. Therefore, it would be expected that the HCl would react preferentially with the triethylamine base.

An alternative and more plausible explanation for the increased reactivity of the imidazolide in the mixed solvents is that the chloroform was capable of hydrogen bonding with the carbonyl oxygen of the fatty acid imidazolide. This could only be possible if the chloroform was also polarized. Polarization of chloroform may occur since it contains three electronegative chlorine atoms. The net result is that the carbonyl carbon of the activated fatty acid would become very electrophilic.

A.2.2 A Comparison of the Reactivity of Fatty Acid Imidazolide and Anhydride

The primary consideration which led to the analysis of the imidazolide approach was the reactivity of these derivatives. As already mentioned, Staab *et al.*, (24) suggested that the reactivity of the imidazolide derivatives are comparable to their corresponding acid chloride and anhydride counterparts. However, from the rates observed (Fig. 8) when the acylation of DNP-Pro-SerNH_2 was performed with

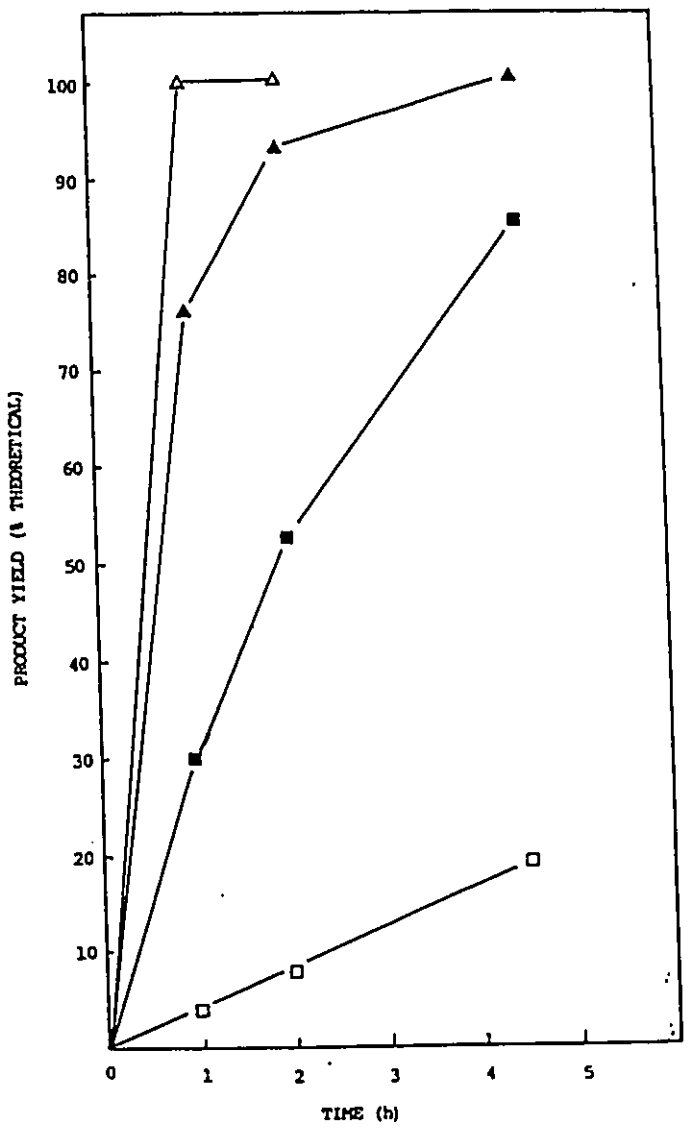

Figure 8. Time course of Acylation of DNP-Pro-SerNH_2 with Palmitic Acid Imidazolide squares) and Anhydride (triangles). Aliquots of anhydride and imidazolide were transferred to reaction vessels and the solvent was removed under reduced pressure. To the dried anhydride (5 μmoles) or imidazolide (5 μmoles), 5 equivalents of triethylamine (closed symbols) or 0.125 equivalents of anhydrous DMAP (0.5 M in dry DMF) (open symbols) were added, followed by 21.7 μl of $CHCl_3$/DMF (4:1). The reactions were started by adding 2 μl of the peptide and the progress of each reaction was monitored by HPLC.

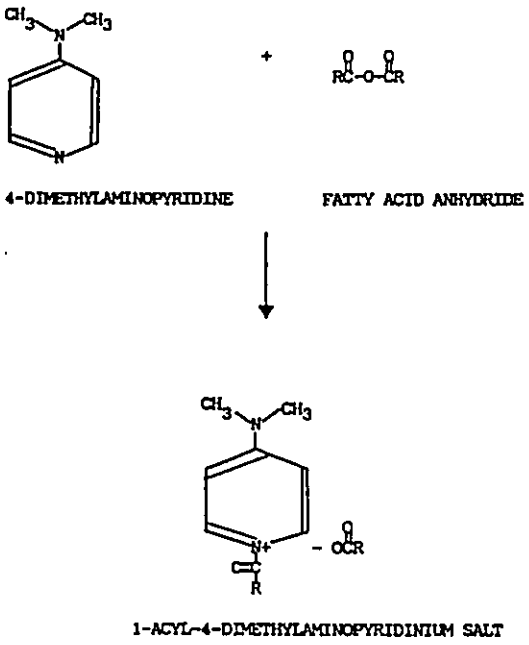

Figure 9. Preparation of 1-acyl-4-dimethylaminopyridinum Reactive Intermediate

the anhydride under standard conditions, indicated that the fatty acid anhydride was approximately 2 X more reactive than the corresponding imidazolide. This suggested that although the fatty acid is activated when converted to the imidazolide derivative, it is much more stable than the anhydride.

As a further test of the stability of the fatty acid imidazolide, the acylation reaction was performed in the presence of a nucleophilic catalyst 4-dimethylaminopyridine which is known to increase the reactivity of the anhydride (18,28) in the absence of other bases (Fig. 8). The increased reactivity of the anhydride due to 4-dimethylaminopyridine was attributed to the conversion of the anhydride to a very reactive intermediate (Fig. 9) (28). Therefore, if the imidazolide was stabilized further activation would not occur in the presence of 4-dimethylaminopyridine and consequently no increase in the acylation rate is expected. As illustrated in Figure 8, in the presence of a catalytic amount of 4-dimethylaminopyridine (0.125 equivalents) no rate enhancement was observed with the imidazolide whereas with the anhydride the action was essentially completed within 1 h. This further supported the notion that the imidazolide must be stable and therefore, less reactive than the anhydride.

An alternative explanation for the lower rate of acylation observed with the imidazolide is that under the current conditions used to remove unreacted CDI, removal of the activated fatty acid by the Sephadex LH-20 also occurred. This possibility was excluded since no loss of radioactive palmitic acid imidazolide was observed after the 1 h incubation with Sephadex LH-20.

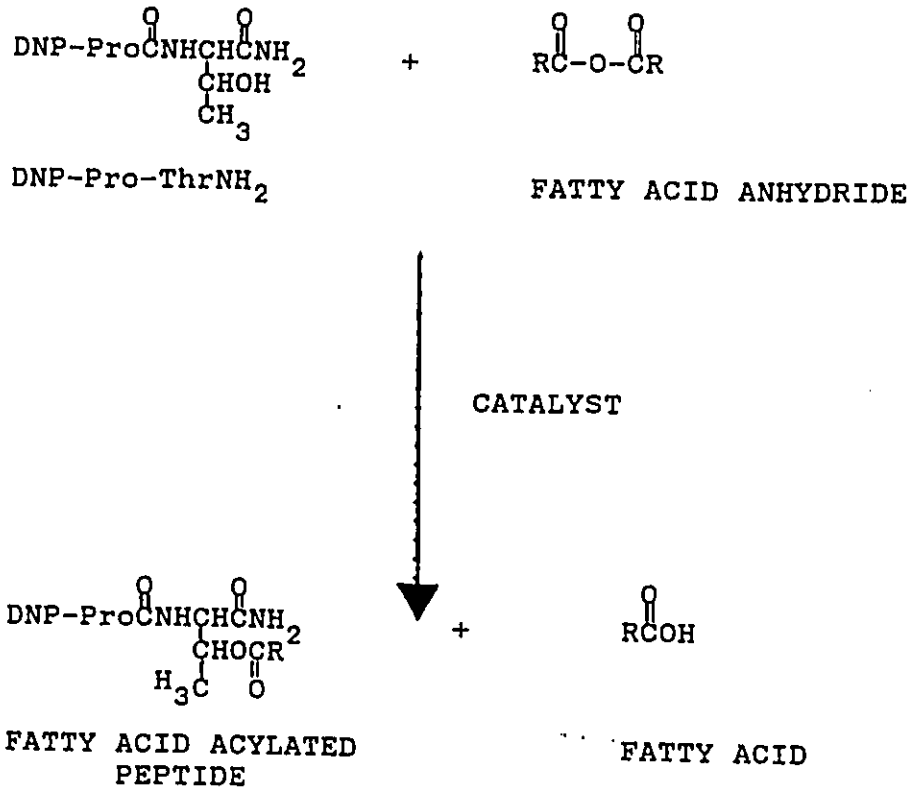

Figure 10. Scheme used to Analyzed Parameters Involved with the Anhydride Approach

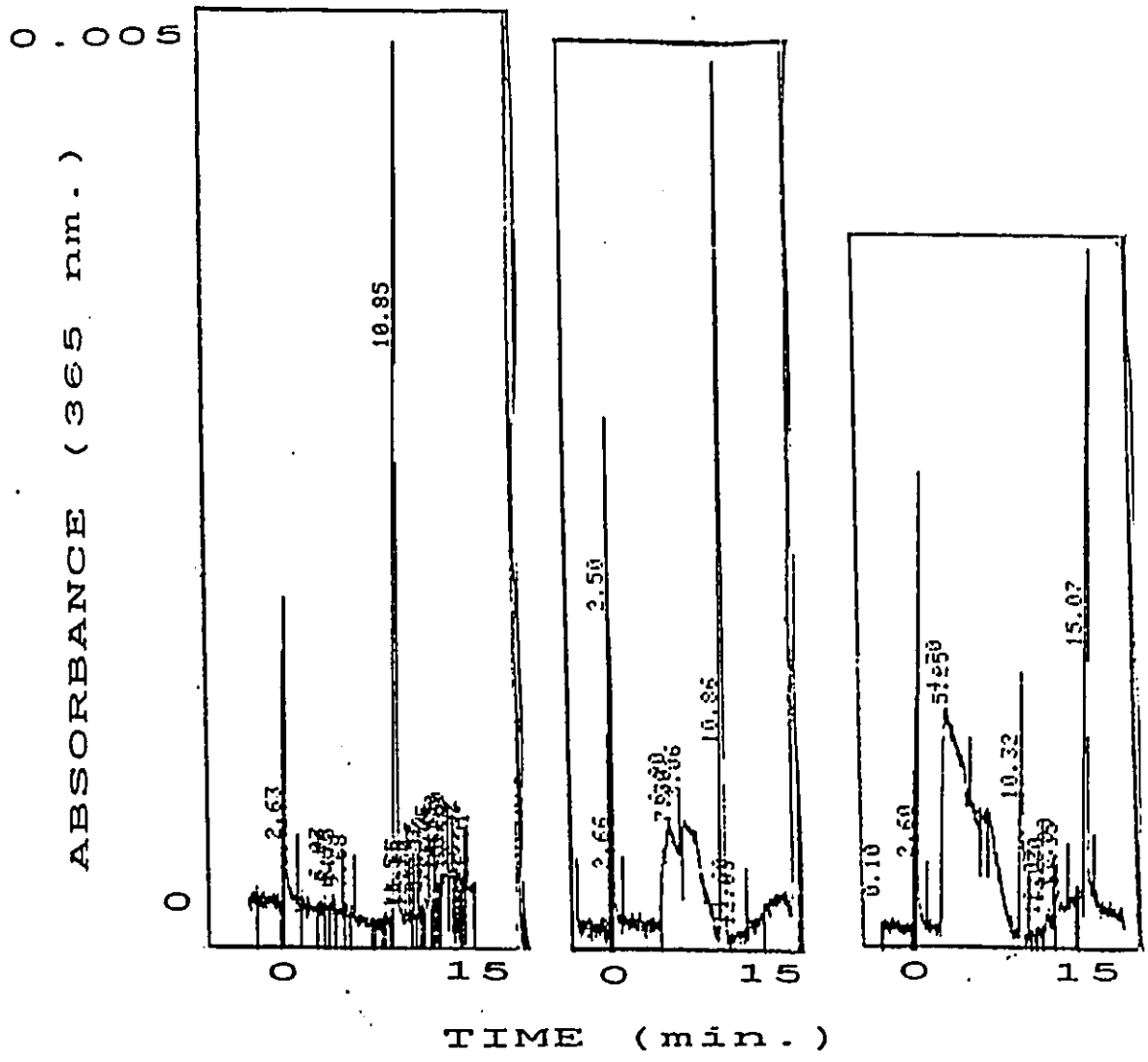

Figure 11. Reverse-phase HPLC Chromatograms of A. DNP-Pro-ThrNH$_2$, B. DNP-Pro-ThrNH$_2$ in the presence DMAP and C. Analysis of an acylation reaction between DNP-Pro-ThrNH$_2$ and DMAP activated palmitic acid anhydride.

B. Analysis of Parameters Involved with the Anhydride Approach

As a result of the increased reactivity of the anhydride over the imidazolide, especially in the presence of the catalyst 4-dimethylaminopyridine led to the work which is described.

As already shown by Gupta *et al.*, (18) and others (19,28,29), in the presence of 4-dimethylaminopyridine the reactivity of the fatty acid anhydride was greatly enhanced. By using H-NMR spectroscopy, Hofle *et al.*, (28) have shown that this was due to the conversion of the anhydride to a very reactive intermediate, 1-acyl-4-dimethylaminopyridinium salt (Figure 9). Since preliminary experiments using the approach developed by Gupta *et al.*, (18) to prepare highly radioactive photoreactive phospholipids resulted in poor yields, conditions that affect the reactivity of the 1-acyl-4-dimethylaminopridinium salt was investigated. The approach used to analyze the different conditions is outlined in Figure 10. According to this scheme, under a particular test condition, the model peptide, DNP-Pro-ThrNH_2 is acylated with the fatty acid anhydride. To determine the time course of acylation of the DNP-peptide, an aliquot of the reaction is removed at different time intervals and analyzed by HPLC. The rationale for using this approach is that if the reactivity of the 1-acyl-4-dimethylaminopyridinium salt is affected then this should be reflected in the rate of acylation of DNP-Pro-ThrNH_2.

Shown in Figure 11 are typical HPLC chromatograms of A. DNP-Pro-ThrNH_2, B. DNP-Pro-ThrNH_2 with 4-dimethylaminopyridine and C. analysis of an acylation reaction between DNP-Pro-ThrNH_2 and fatty acid anhydride activated with 4-

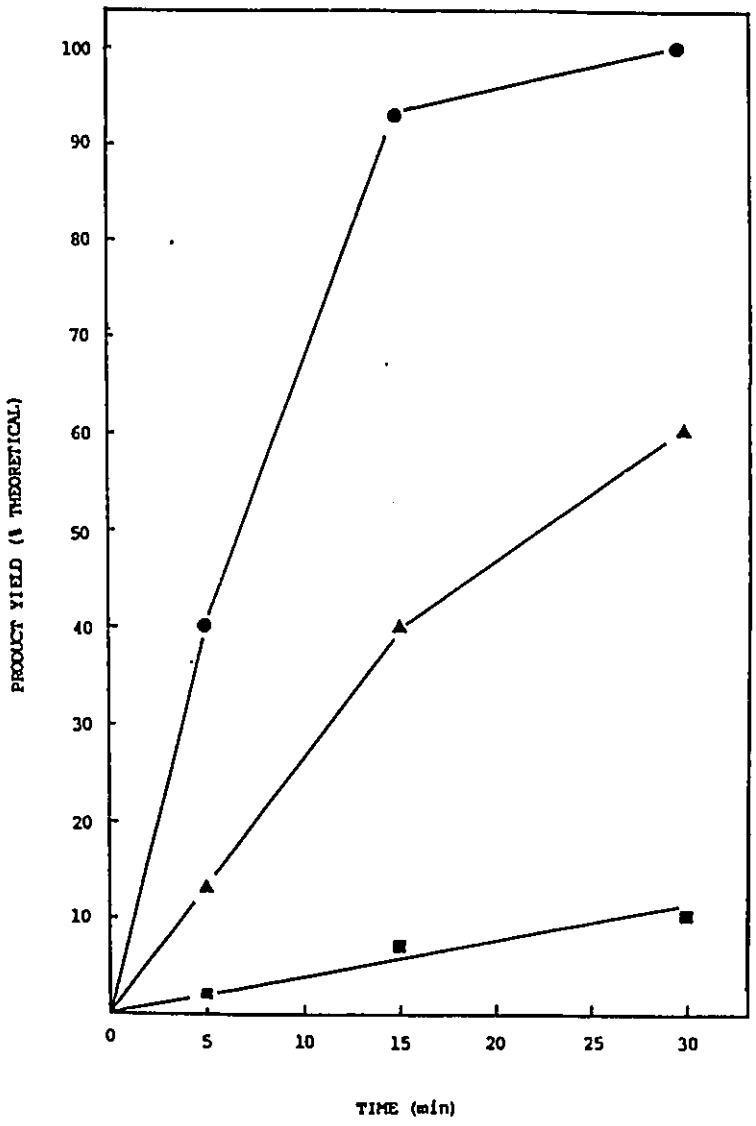

Figure 12. Solvent effects on the rate of acylation of DNP-Pro-ThrNH_2. Palmitic acid anhydride was prepared as described under Materials and Methods. Aliquots of the anhydride solution were transferred to reaction vessels and the solvent was removed under reduced pressure. To the dried fatty acid anhydride (1.25 umoles) 20 ul of Pyr (■), $CHCl_3$/Pyr (4:1) (▲), or $CHCl_3$ (●) was added; followed by 0.02 equivalents of DMAP (10 mM solution in appropriate solvent). The reaction was initiated by adding 2 ul of the peptide (623 uM in appropriate solvent). At the indicated times, 5 ul aliquots were diluted in aqueous DMF (10% H_20 in DMF) and analyzed by HPLC.

dimethylaminopyridine. The peaks eluting at 10.32 and 15.07 min in chromatogram C corresponds to DNP-Pro-ThrNH_2 and the fatty acid acylated DNP-Pro-ThrNH_2, respectively.

Since the catalyst-activated anhydride is very reactive, small amounts of the DNP-peptide (μM) are routinely used. At millimolar level of the DNP-peptide the reaction is completed almost instantaneously. Therefore, by using micromolar amounts of the peptide, meaningful information concerning the reactivity of the catalyst-activated anhydride can be obtained from the kinetics of acylation of the model peptide.

B.1.0 Analysis of Conditions that Affect the Reactivity of the Catalyst-Activated Anhydride

B.1.1 Analysis of the Effect of Solvent Polarity

Using the approach described above the effect of solvent on the reactivity of the 1-acyl-4-dimethylaminopyridinium salt was assessed. Shown in Figure 12 are the rates of acylation of DNP-Pro-ThrNH_2 obtained in chloroform, chloroform/pyridine (4:1) and pyridine. These solvents are the ones most often used for phospholipid synthesis. In chloroform the reaction was essentially completed within 30 min, whereas in chloroform/pyridine (4:1) and pyridine the reaction was only 60% and 10% completed, respectively. If the initial rate of the reactions were arranged according to the polarity of the solvents, it is apparent that the rate is optimal in the less polar chloroform than in the polar pyridine. This therefore suggested that the reactivity of the 1-acyl-4-dimethylaminopyridinium salt is enhanced in chloroform.

The enhanced reactivity of the 1-acyl-4-dimethylaminopyridinium salt in non-polar solvents was also reported by Hofle *et al.,* (28) and Jampel *et al.,* (29).

B.1.2 A Comparison of the Reactivity of 4-dimethylaminopyridine and 4-pyrrolidinopyridine-activated Anhydride

Another catalyst which was also known to enhance the reactivity of fatty acid anhydride is 4-pyrrolidinopyridine (20,21). It has been reported (28) that the 4-pyrrolidinopyridine-activated anhydride was at least 2 times more reactive than the 4-dimethylaminopyridine-activated anhydride. Furthermore, the mechanisam by which 4-pyrrolidinopyridine activates the anhydride is analogous to that of 4-dimethylaminopyridine (28,29). Shown in Figure 13 is a comparison of the kinetics of acylation of DNP-Pro-ThrNH_2 with fatty acid anhydride activated with 4-dimethylaminopyridine or 4-pyrrolidinopyridine in chloroform. In the absence of either catalysts no acylation of the DNP-peptide was observed within 6 min. However, when the fatty acid anhydride was activated with 4-dimethylaminopyridine or 4-pyrrolidinopyridine, the rate of acylation of DNP-Pro-ThrNH_2 was significantly enhanced. Calculation of the initial rate constants revealed that the catalyst-activated anhydrides were approximately 1000 times more reactive than just the anhydride. Although the 4-dimethylaminopyridinium-activated anhydride was considerably more reactive than the anhydride, it was approximately 2 times less reactive than the 4-pyrrolidinopyridine-activated anhydride. These results therefore confirmed that the 4-pyrrolidinopyridine-activated anhydride is much more reactive than the 4-dimethylaminopyridine-activated anhydride.

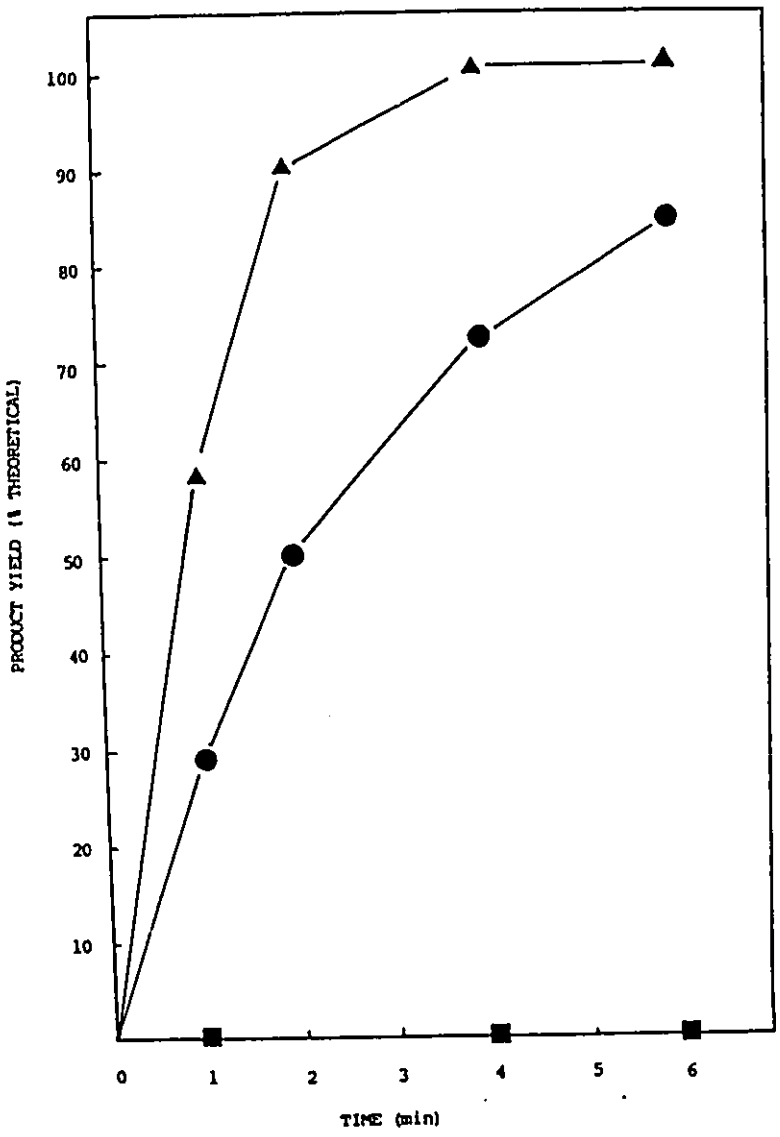

Figure 13. Effect of Catalysts on the Rate of Acylation of DNP-Pro-ThrNH_2. Palmitic acid anhydride was prepared as described under Materials and Methods. Dry chloroform (188 µl) was added to reaction vessels containing dried palmitic acid anhydride. After the anhydrides were dissolved, 10 µl of dry $CHCl_3$ (■), 0.1 M PPY (▾), or 0.1 M DMAP (●) was added. Each reaction was initiated by adding 2 µl of DNP-Pro-ThrNH_2 (623 µM in dry $CHCl_3$). At the indicated times, an aliquot of each reaction was diluted in aqueous DMF and analyzed by HPLC.

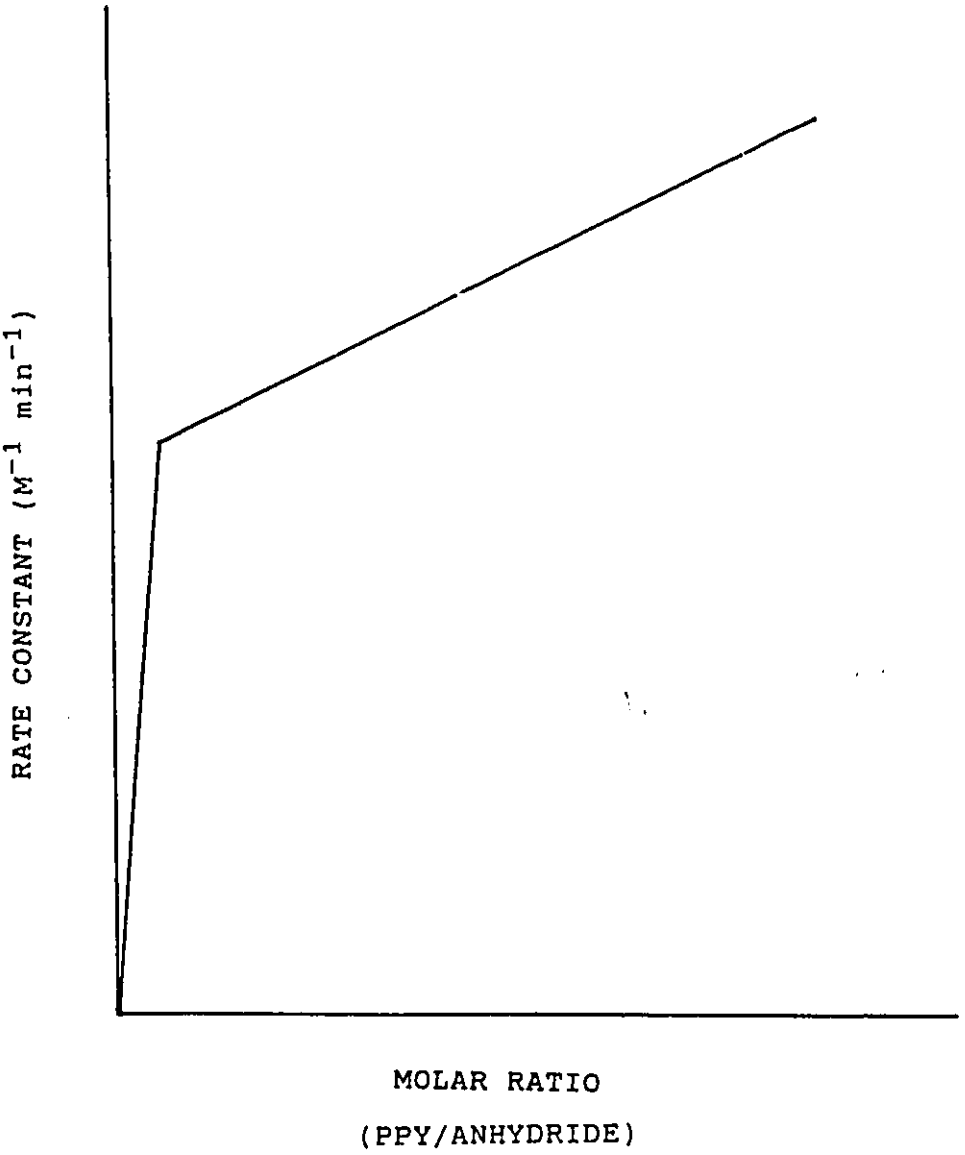

Figure 14. Theoretical Plot of the Effect of Varying the Concentration of PPY on the Rate of Acylation of DNP-Pro-ThrNH_2.

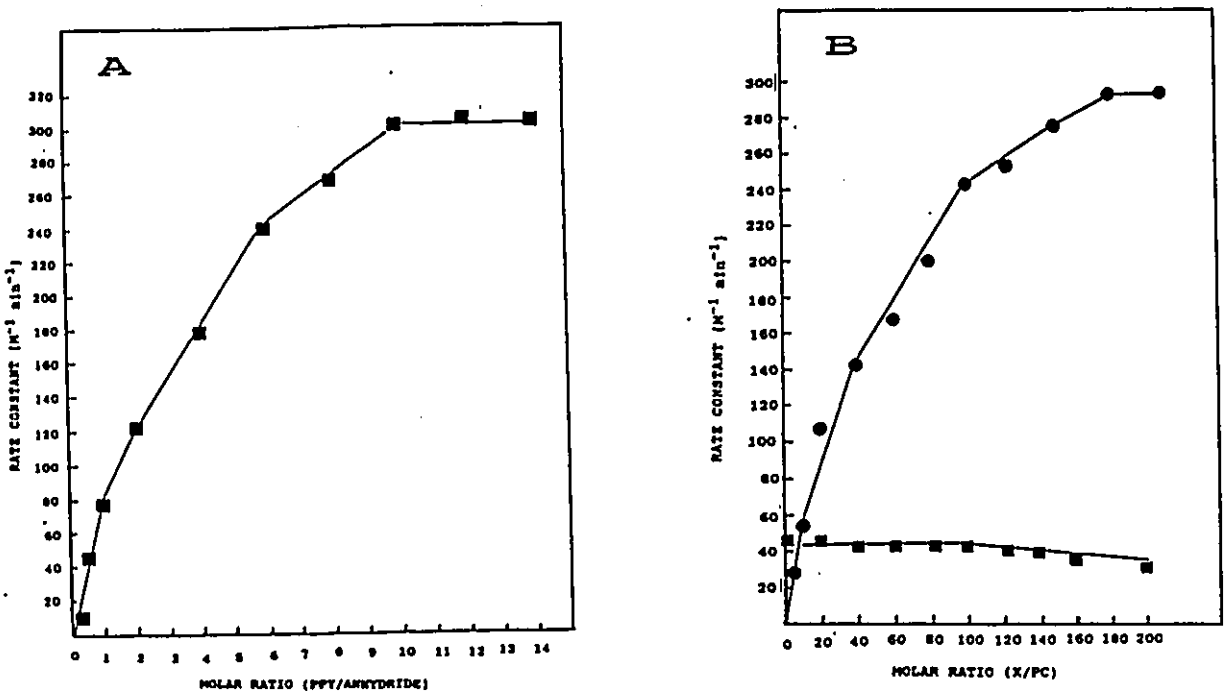

Figure 15A. Effect of Varying the Concentration of PPY on the Rate of Acylation of DNP-Pro-ThrNH$_2$. Acylation of DNP-Pro-ThrNH$_2$ in the presence of increasing amounts of PPY (0.2 M) in $CHCl_3$ was accomplished by reacting 0.63 nmoles of the DNP-peptide with 1 μmole of palmitic acid anhydride in a total volume of 100 μl. The progress of each reaction was analyzed by HPLC at 0.5, 1.0 and 1.5 min. The rate constant at each PPY to anhydride ratio was calculated from the extent of the reaction which was based on the HPLC chromatograms, as described in Materials and Methods.

Figure 15B. Effect of Increasing Amounts of Base on the Rate of Acylation of DNP-Pro-ThrNH$_2$ with Palmitic Acid Anhydride in the Presence of 1,2-diacyl-glycero-3-phosphorylcholine. To reaction vessels containing 1.0 μmole of palmitic acid anhydride dissolved in dry $CHCl_3$, varying amounts of a 2 M solution of PPY in $CHCl_3$ was added (●). To another set of reaction vessels containing 1.0 μmole of anhydride and 10 equivalents of PPY in $CHCl_3$, varying amounts of triethylamine (2 M in $CHCl_3$) was added (□). After the content of each vessel was thoroughly mixed, the total volume was adjusted to 99 μl with 50 mM PC (1.0 μmole). At 0.5, 1.0 and 1.5 min after the addition of 1 μl of 930 μM DNP-Pro-ThrNH$_3$, 25 μl aliquots of the reaction was diluted in 10% water in DMF and analyzed by HPLC. Rate constants were calculated as outlined under Materials and Methods.

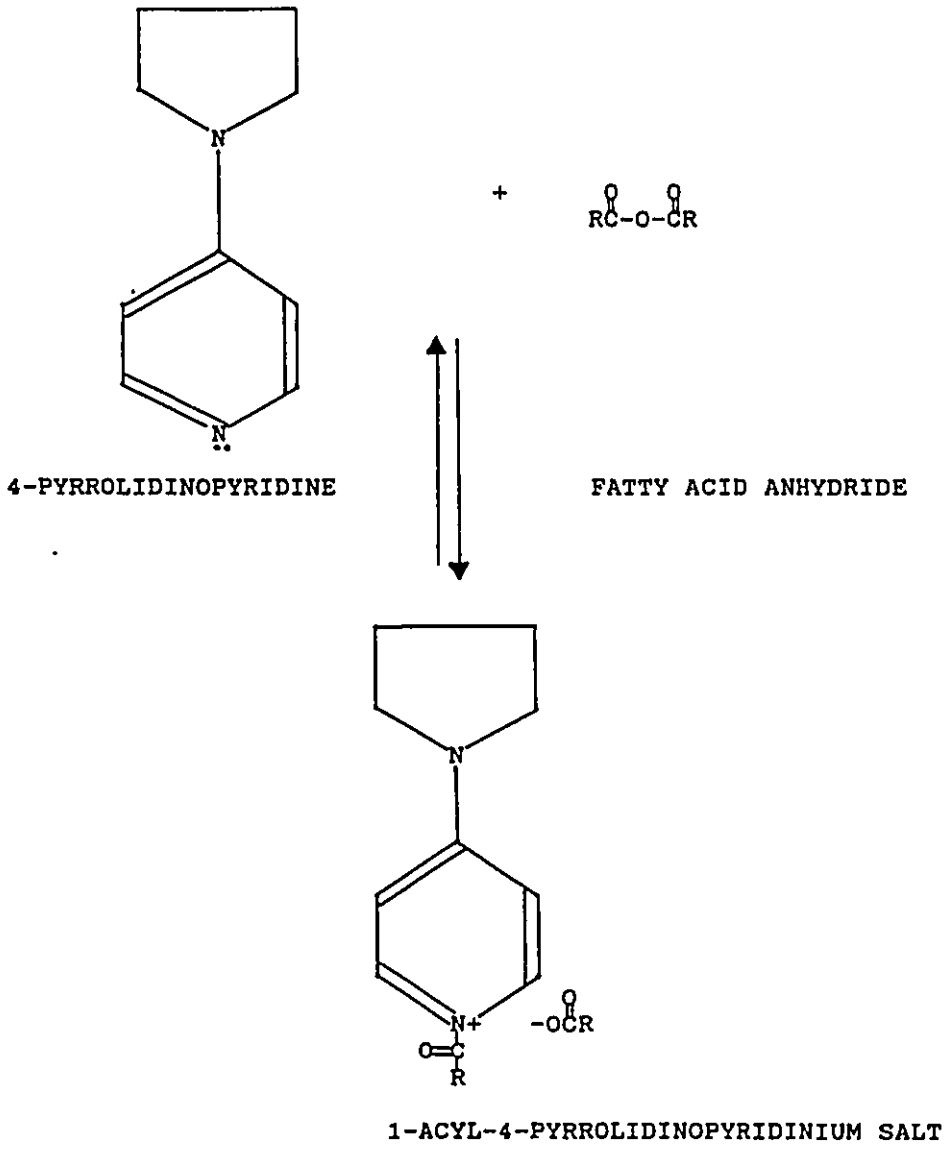

Figure 16. Preparation of 1-acyl-4-pyrrolidinopyridinium Reactive Intermediate

B.1.3 Determination of the Optimal Amount of 4-pyrrolidinopyridine Required for Maximal Rate of Acylation

The pKa's of 4-pyrrolidinopyridine and 4-dimethylaminopyridine are 9.90 and 9,70, respectively. Consequently, it was of interest to determine if the rate enhancement observed in the presence of these catalysts was also due to general base catalysis. The approach used involved varying the amounts of the catalyst use and observing the effect on the rate of acylation of DNP-Pro-ThrNH_2. The rationale is that if a base catalysis mechanism was also involved, then a plot of the rate or rate constants versus the ratio of catalyst to anhydride should result in a biphasic curve (Figure 14). The lower curve would correspond to the activating effect and the upper curve the base effect. The isolation of the base effect is of particular importance since base catalysis was suggested to be responsible for the isomerization of 1-acyl-glycero-3-phosphorylcholine under acylation conditions (22).

As shown in Figure 15A, a straight line was obtained instead of a biphasic curve. This suggested that the sole mechanism responsible for the catalytic effect of 4-pyrrolidinopyridine was its ability to convert the fatty acid anhydride to the 1-acyl-4-pyrrolidinopyridinium salt. Since the rate of acylation of DNP-Pro-ThrNH_2 increased gradually as the ratio of 4-pyrrolidinopyridine to anhydride is increased suggested that the reaction between 4-pyrrolidinopyridine and the anhydride to give the reactive 1-acyl-4-pyrrolidinopyridinium salt occurred by way of an equilibrium dependent process (Figure 16). That is, the formation of the reactive intermediate does not occur simply through a one to one interaction. Therefore, the increase in the rate

indicated that the position of the equilibrium must be pushed further in favour of the preparation of the 1-acyl-4-pyrrolidinopyridinium salt as the ratio of 4-pyrrolidinopyridine to anhydride is increased. The levelling of the rate at a ratio of 10 must signify that the anhydride was completely converted to the 1-acyl-4-pyrrolidinopyridinium salt. However, more importantly these results emphasize the direct dependency of the acylation rate on the position of the equilibrium between the anhydride and the reactive intermediate. Similar findings were reported by Jampel *et al.*, (29) and Hofle *et al.*, (28).

B.2.0 Influence of the Phosphate Group of 1,2-Diacyl-Glycero-3-Phosphorylcholine on the Rate of Acylation

An additional variable which could conceivably affect the acylation of 1-acyl-glycero-3-phosphorylcholine (lysoPC) is its phosphate group. In comparison to the secondary hydroxyl group, the phosphate would be expected to be much more reactive. Furthermore, the reactivity of the secondary hydroxyl group of lysoPC would also be affected by steric hindrance imposed by the fatty acyl chain at the first position. Therefore, under acylation conditions one would expect acylation of the phosphate group to occur much more readily than at the secondary hydroxyl group. The net effect of this interaction would be that the yield of the desired product (1,2-diacyl-glycero-3-phosphorylcholine, PC) would be reduced. For this reason it was necessary to determine if the phosphate group does interfere with the acylation at the hydroxyl group.

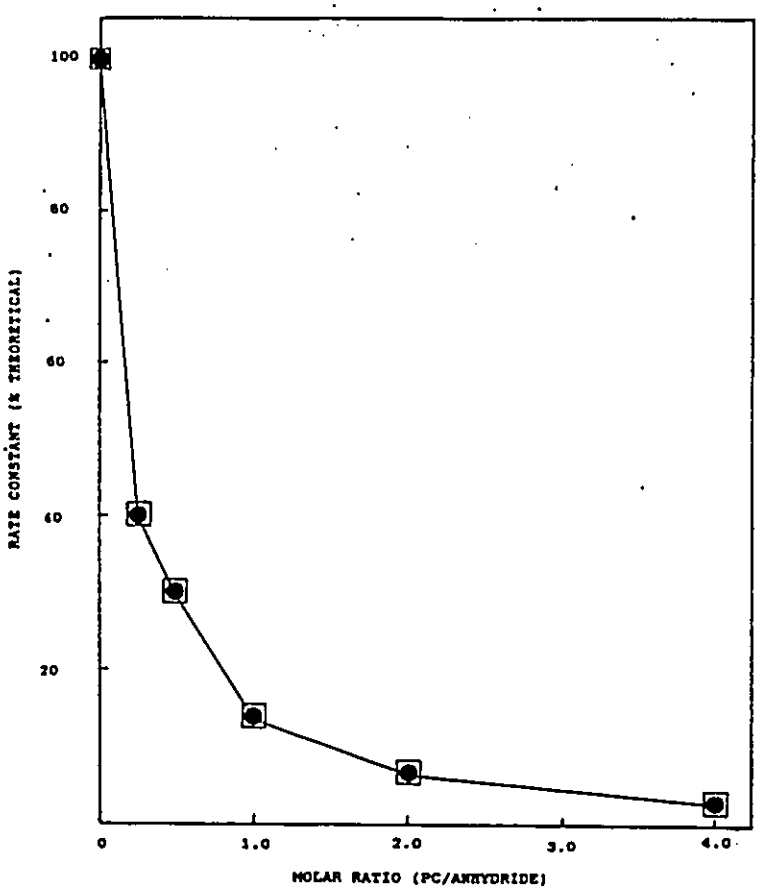

Figure 17. Effect of the Phosphate Group of 1,2-diacyl-glycero-3-phosphorylcholine on the Rate of Acylation of DNP-Pro-ThrNH_2 under Optimal Conditions. To reaction vessels containing 1.0 μmole of palmitic acid anhydride in dry $CHCl_3$, 10 equivalents of PPY was added. After the content was thoroughly mixed, the total volume was adjusted to 99 μl with 0.2 M PC that had been previously incubated with (●) or without (□) 4A° molecular sieve for 5 h. At 0.5, 1.5 and 2.5 min after the addition of 1 μl 630 μM DNP-Pro-ThrNH_2, 25 μl aliquots were diluted in aqueous DMF and analyzed by HPLC. Rate constants were calculated as described under Materials and Methods and expressed as a percentage of the rate constant obtained in a control reaction without PC.

The approach used involved performing the acylation of DNP-Pro-ThrNH_2 with completely catalyst-activated anhydride in the presence of varying amounts of PC. The reason for using PC instead of lysoPC is two-fold. Firstly, the effect of the phosphate on the kinetics of acylation of the DNP-peptide could be analyzed without an additional site competing for the reagent. Secondly, steric hindrance which would be encountered in the real system (acylation of lysoPC) would be simulated under these conditions since a very small amount of the peptide is used.

The rationale is that if the anhydride interacts with the phosphate group of PC, then the effective concentration of the activated anhydride would be reduced and as such should result in a decrease in the rate of acylation of the DNP-peptide.

As illustrated in Figure 17 (closed circle), as the ratio of PC to anhydride was increased, the rate of acylation of DNP-Pro-ThrNH_2 decreased. This suggested that the phosphate group does interfere with the acylation of the hydroxyl group by interacting with the anhydride.

Alternatively, the same observation as the above would result if water was present. In the presence of water the rate could be reduced by either hydrolysis of the activated anhydride or by an increase in the overall polarity of the solvent. Since each reaction contained the same amount of fatty acid anhydride and 4-pyrrolidinopyridine, the most likely source of water would be from hydration of the phosphorylcholine group of PC. Therefore, upon increasing the amount of PC used, the water content would also be increased. To test the possibility of water being present it was necessary to further dry the PC after it was rendered anhydrous by

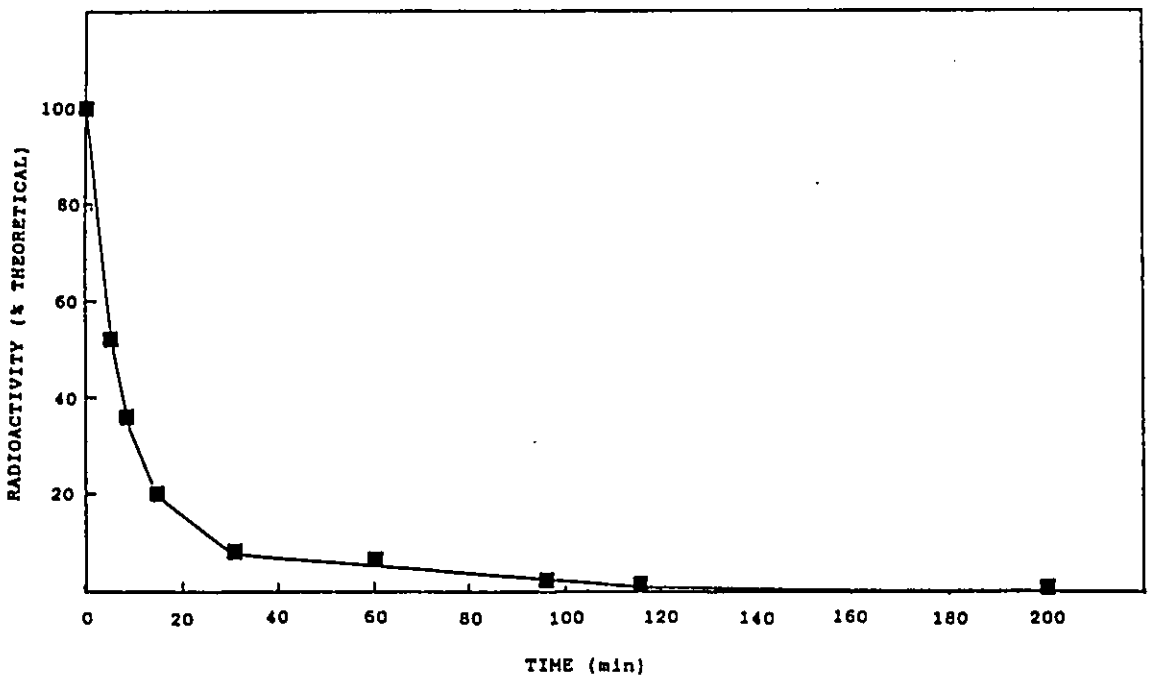

Figure 18. Time course of Water Removal by 4A• Molecular sieve. To determine the efficiency of 4Å molecular sieves in removing water in the presence of PC, 55 μmoles of anhydrous PC in 1.079 ml of dry chloroform was incubated with 10 μl of tritiated water (specific activity of 7.1 μCi/μl) under nitrogen. At the indicated times after the addition of 10 individual molecular sieve beads, the sample was centrifuged for 5 min and 2 μl of the supernatant was removed under a nitrogen atmosphere and added to Amersham aqueous scintillant. Counting was performed in a Beckman scintillation counter.

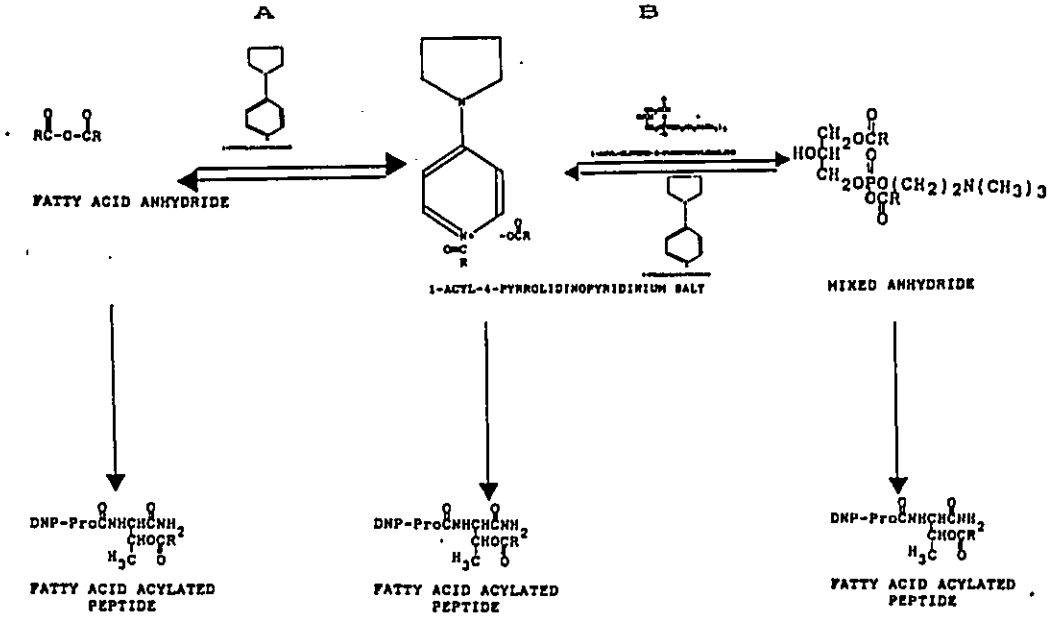

Figure 19. Schematic Representation of the Equilibria Involved with Phospholipid Synthesis via the Anhydride Approach.

azeotroping under reduced pressure.

Molecular sieves 4A° are used routinely to maintain dry conditions of anhydrous solvents. The efficiency of these molecular sieves to remove water in the presence of PC was determined by adding 550 μmoles of tritiated water to 55 μmoles of dried PC in anhydrous chloroform before the molecular sieves were added. The kinetic of removal of water by the molecular sieves showed that after a 30 min incubation 90% of the water was absorbed by the beads (Figure 18). The remaining 10% which corresponds to one molecule of water per PC molecule required an additional 2 h and 20 min before complete removal of water was attained.

Therefore, after 55 μmoles of PC was rendered anhydrous and dissolved in anhydrous chloroform, molecular sieves were added and the incubation was allowed to proceed for 5 h at room temperature. Under these conditions, residual water associated with PC should be completely removed by the molecular sieves, as indicated by the above results. After this incubation, the experiment described in the legend of Figure 17 was repeated. The results obtained, (Figure 17, open square), were identical to that obtained with PC which was not pre-incubated with molecular sieves. This further verifies that the effect observed in the presence of the phosphate could only result from an interaction between the phosphate and the anhydride.

B.3.0 Reversal of the Interaction between the Anhydride and the Phosphate Group of 1,2-Diacyl-Glycero-3-Phosphorylcholine

As suggested above, the interaction which may occur between the phosphate and the reagent is direct acylation of the phosphate (Figure 19, pathway B). The

product which would result from this interaction is a mixed anhydride. Consequently, it should be possible to convert this mixed anhydride back to the reactive intermediate by increasing the amount of 4-pyrrolidinopyridine used. Conversion of the mixed anhydride to the desired 1-acyl-4-pyrrolidinopyridinium salt is ensured since the leaving group in this mixed anhydride would be the phosphate. In general, the leaving group of a mixed anhydride is usually determined by the acidity of each acyl group (30).

To verify this suggestion, acylation of DNP-Pro-thr-NH_2 was performed with equimolar amounts of anhydride and PC in the presence of varying amounts of PPY. The rationale is that if the interaction between the phosphate and the anhydride can be reversed by using more 4-pyrrolidinopyridine then the effective concentration of the catalyst-activated anhydride should increase, and this should be reflected in the rate of acylation of DNP-Pro-ThrNH_2. As shown in Figure 15B (closed circle), as the ratio of the catalyst to PC was increased, the rates of acylation of the DNP-peptide also increased. At a molar ratio of 180, maximal rate of acylation of the DNP-peptide, DNP-Pro-ThrNH_2, was achieved. This therefore suggested that the interaction between the phosphate and the anhydride was reversible and as proposed, must represent an acylated phosphate (Figure 19, pathway B). These results are also consistent with the notion that formation of the mixed anhydride is the preferred reaction under acylation conditions (10 mM anhydride, 10 mM PC and .1 M PPY) since a large amount of the catalyst was required to regain the original rate observed in the absence of PC.

B.4.0 Evaluation of other Variables which could account for the Observed Effect of the Phosphate under Acylation conditions

B.4.1 General Base Catalysis

An alternative explanation for the decrease in the rate of acylation of the model peptide is that the presence of PC has caused the solvent ($CHCl_3$) to become more polar and as indicated by our solvent analysis results (Figure 12), this decrease could be explained by a lowering of the reactivity of the catalyst-activated anhydride intermediate. Hence, the increase in the acylation rate observed as the PPY to PC ratio increases (Figure 15B, closed circle) would not be due to the reversal of the mixed anhydride to the 1-acyl-4-pyrrolidinopyridinium salt as proposed initially (Figure 19, pathway B). It is therefore possible that this increase in the rate of acylation of the model peptide is due to general base catalysis. To test this possibility, acylation of DNP-Pro-ThrNH_2 was performed with equimolar amounts of PC and completely catalyst-activated anhydride, and varying amounts of triethylamine (pKa, 11.0).

As shown in Figure 15B (closed square), essentially no change in the rate constant was observed as the ratio of triethylamine to PC was increaed to 200. These results exclude base catalysis as the mechanism responsible for the observed increase in the acylation rate as the ratio of PPY to PC is increased. In addition, these results further support the existence of an equilibrium between the catalyst-activated anhydride and the mixed anhydride.

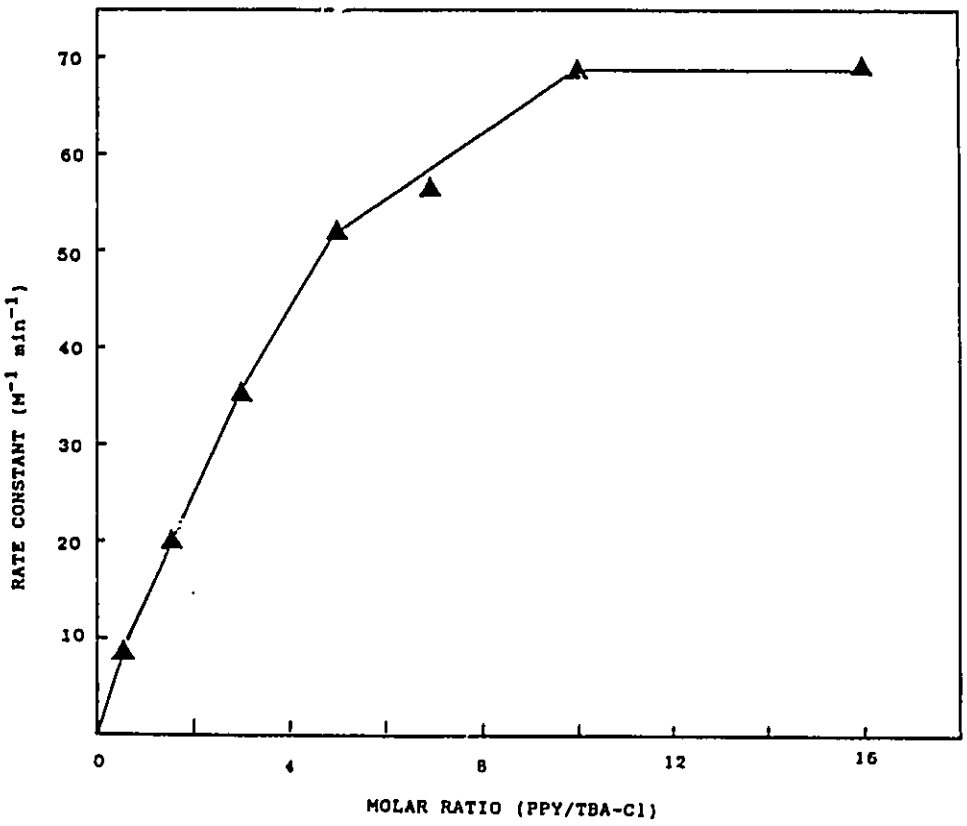

Figure 20. Effect of Increasing Amounts of PPY on the Rate of Acylation of DNP-Pro-ThrNH_2 with Palmitic Acid Anhydride in the Presence of Tetrabutylammonium Chloride. To reaction vessels containing 1.0 μmole of palmitic acid anhydride and 1 equivalent of tetrabutylammonium chloride (0.1 M in $CHCl_3$), varying amounts of PPY (0.25 M) was added. After the content of each reaction was thoroughly mixed, the total volume was adjusted to 99 μl with $CHCl_3$. At 0.5, 1.0 and 2.0 min after the addition of 1 μl 630 μl DNP-Pro-ThrNH_2, 25 μl aliquots were diluted in aqueous DMF and analyzed by HPLC. Rate constants were calculated as outlined under Matrials and Methods.

B.4.2 Ionic Effect

While there have been no reports on the effect of anhydrous organic salts on the reactivity of the catalyst-activated anhydride intermediate, Fersht *et al.,* (31), using a stop-flow kinetic approach and aqueous buffers as the solvent, have shown that in the presence of a concentrated solution of salt the reactivity of the intermediate is significantly reduced whereas the rate of formation of the reactive intermediate is increased. The increased rate of formation of the reactive intermediate was attributed to greater stabilization of the transition state developed from the interaction between the anhydride and the catalyst. Although the effect of salt on the equilibrium between the starting materials (anhydride and catalyst) was not studied, their results implied that in the presence of salt the aforementioned equilibrium remained unaffected. It was therefore of interest to determine how the equilibrium between the anhydride and PPY, and the 1-acyl-4-pyrrolidinopyridinium salt is affected when an organic salt other than PC is used, under anhydrous conditions.

For this analysis a similar approach to that described in the legend of Figure 15A was used. In essence, acylation of the DNP-peptide was performed with equimolar amounts of anhydride and the tetrabutylammonium chloride (TBA-Cl) salt in the presence of varying amounts of PPY.

As illustrated in Figure 20, maximal rate is obtained at a PPY to TBA-Cl ratio of 10. Since in the absence of any salt maximal rate was also observed at a PPY to anhydride ratio of 10 suggested that the equilibrium between the starting materials and the 1-acyl-4-pyrrolidinopyridinium salt is not affected by the presence of TBA-Cl.

However, the rate of acylation of DNP-Pro-ThrNH_2 obtained in the presence of TBA-Cl was approximately 23% of that obtained in the absence of salt. Although this result supports the findings of Fersht *et al.*, (31), more importantly it suggests that an ionic effect is not associated with the presence of PC. Therefore, the complete reversal of the inhibitory effect of PC on the rate of acylation when a large excess of PPY is used must represent the complete conversion of the mixed anhydride back to the reactive 1-acyl-4-pyrrolidinopyridinium salt (Figure 19, pathway B).

B.5.0 Acylation of 1-Acyl-Glycero-3-Phosphorylcholine

As a test of the validity of the acylation conditions derived from the model peptide work, analytical samples of 1-acyl-glycero-3-phosphorylcholine were acylated with palmitic acid anhydride and a trace amount of tritiated palmitic acid anhydride activated with different amounts of 4-pyrrolidinopyridine. The progress of each reaction as monitored by TLC and the radioactive products were visualized by fluorography. A typical TLC analysis of the kinetics of acylation of lysoPC is shown in Figure 21. As illustrated, an intense radioactive spot corresponding to PC was observed within 1 min. Quantitation of the PC product for each reaction was obtained by assaying the radioactivity in the spot and then normalizing this to the total radioactivity applied. The kinetics of acylation under conditions described above (Figure 22) indicated that as the PPY to lysoPC ratio was increased, the time required to obtain 100% yield of PC decreased. Under optimal acylation conditions derived from the model peptide system, a maximum rate of acylation of lysoPC was also observed; a 100% yield of PC was obtained in 5 min.

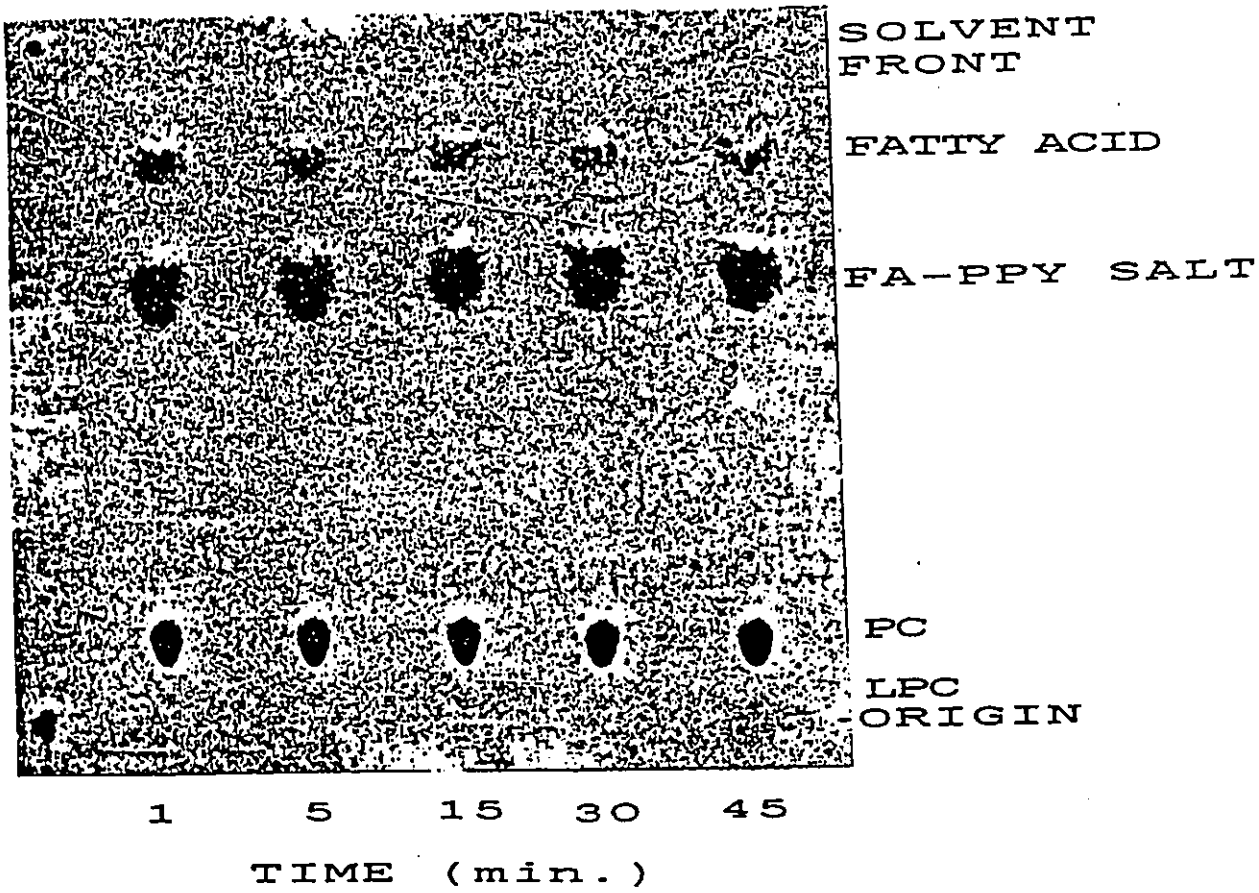

Figure 21. A Typical TLC Analysis of the Kinetic of Acylation of 1-acyl-glycero-3-Phosphorylcholine with Palmitic Acid Anhydride. After the TLC plate containing quenched aliquots of the reaction at different time intervals was developed with $CHCl_3$/MeOH/H_2O (65:25:4), the plate was dipped in 7% (w/v) solution of 2,5-diphenyl-oxeozol (PPO) in diethyl ether to enhance visualization of the radioactive products after exposure at -70°C.

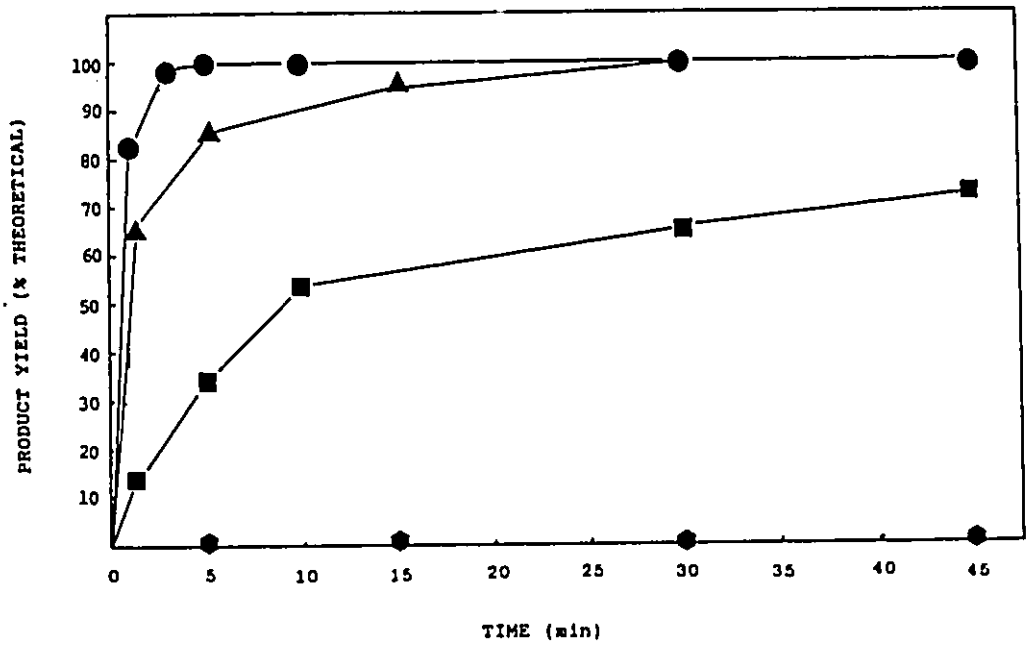

Figure 22. Time course of Acylation of 1-palmitoyl-glycero-3-phosphorylcholine. The reactions were set up by adding O ( ), 2 (□), 20 (▲) or 40 (●) equivalents of PPY (4 M in $CHCl_3$) with respect to lysoPC, to siliconized 100 µl reaction vessels containing 1.8 µmoles of palmitic acid anhydride and 4.32 µCi of [^{3}H]palmitic acid anhydride with a specific activity of 30 Ci/mmole. After the content was mixed and the total volume adjusted to 12.5 µl with dry chloroform, the reactions were initiated by adding 12.5 µl of lysoPC-TFA salt (100 mM in $CHCl_3$). At the indicated times, an aliquot of each reaction was quenched in aqueous methanol and applied to TLC plates. The plates were then developed with $CHCl_3$/MeOH/H_2O (65:25:4) and the products were visualized by fluorography. The spots corresponding to fatty acid and PC were removed and assayed for their radioactivity content. The PC was quantitated by normalizing the radioactivity associated with its spot to the total radioactivity applied.

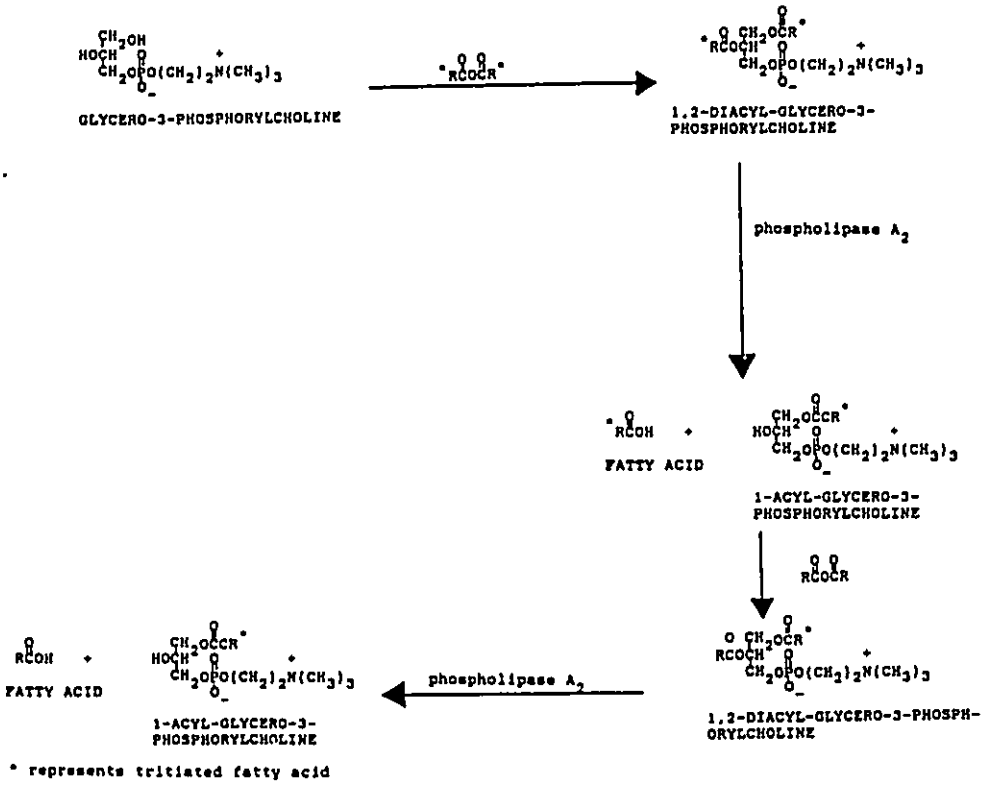

Figure 23. Strategy for the analysis of isomerization

B.6.0 Analysis of Isomerization

Another important factor which must be considered during the preparation of heterochain phospholipids is isomerization of the lysoPC starting material. As mentioned previously, this process is catalyzed by acid or base and has been demonstrated to occur under conditions where the rate of acylation is very slow (22). The strategy used to determine whether isomerization is favoured under our optimalacylation conditions is shown in Figure 23. According to this scheme, 1,2-di-[^{3}H]-acyl-glycero-3-phosphorylcholine prepared from glycero-3-phosphorylcholine (GPC) is digested with phospholipase A_2. Phospholipase A_2 specifically hydrolyzes the fatty acyl moiety bonded to the second position of phospholipids. The resulting 1-[^{3}H]-acyl-glycero-3-phosphorylcholine is acylated under optimal conditions (40 equivalents of PPY) with non-radioactive palmitic acid anhydride. The product, 1-[^{3}H],2-diacyl-glycero-3-phosphorylcholine, is subjected to a second phospholipase A_2 digestion in order to determine the extent to which acyl migration, the most prevalent form of isomerization, has occurred under acylation conditions. One should also keep in mind that isomerization could also occur during the first phispholipase A_2 digestion and subsequent purification of the resulting lysoPC. If acyl migration is induced under our acylation conditions or prior to acylation then the radiolabelled fatty acid to position 1 of 1-acyl-glycero-3-phosphorylcholine will be transferred to position 2. Therefore, TLC analysis of the phospholipase A_2 digestion of the synthetic phospholipid should indicate the liberation of radiolabelled fatty acid. On the other hand, if no migration has occurred, then a single radioactive spot

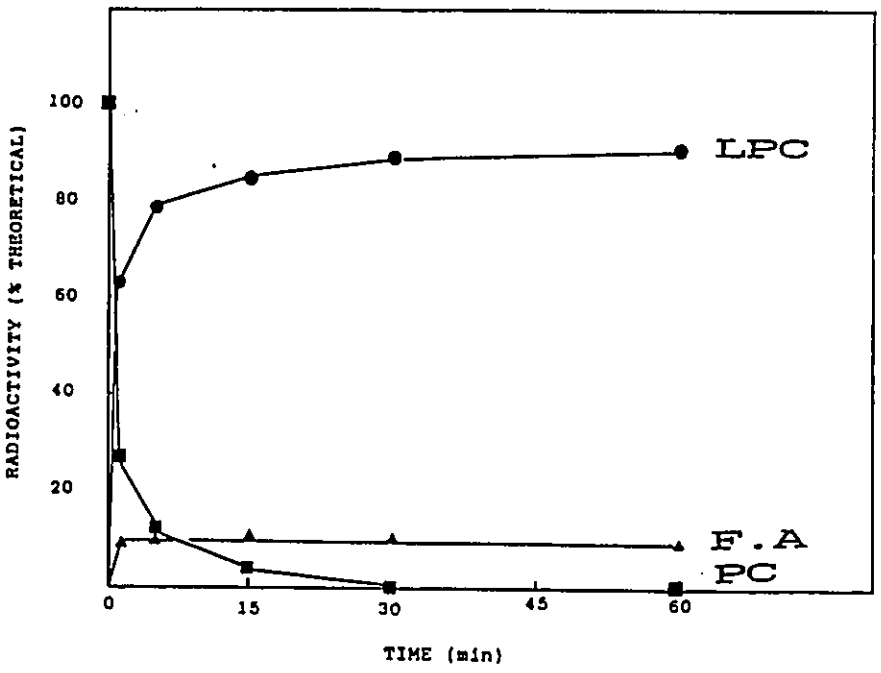

Figure 24. Time Course of Phospholipase A_2 Digestion of 1,2-diacyl-glycero-3-phosphorylcholine Prepared under Optimal Acylation Conditions. Diacyl-glycero-3-phosphorylchoine (5.5 μmoles) and 1,2-[^{3}H]diacyl-glycero-3-phosphorylcholine (8.43 μCi, 2 μmoles) prepared from glycero-3-phosphorylcholine were suspended in 98 μl 10 mM HEPES, pH 7.5 and sonicated at room temperature for 15 min. To this mixture 2 μl 1 M $CaCl_2$ and 100 μl 1.02 mg/ml phospholipase A_2 were added. After 5 min the products were extracted with 960 μl $CHCl_3$/MeOH/H_2O (1:1:0.4) and subjected to gel filtration on Sephadex LH-20 as described in Materials and Methods. The 1-[^{3}H]acyl-glycero-3-phosphorylcholine obtained by the above procedure was acylated with palmitic acid anhydride under optimal conditions (Figure 22). The resulting 1-[^{3}H],2-diacyl-glycero-3-phosphorylcholine was treated with phospholipase A_2 as described above. At the indicated times, aliquots were applied directly to a TLC plate which was then developed with $CHCl_3$/MeOH/H_2O (65:25:4). The products were visualized by fluorography and the spots corresponding to fatty acid, 1,2-diacyl-glycero-3-phosphorylcholine and 1-acyl-glycero-3-phosphorylcholine were removed and assayed for their radioactivity content.

corresponding to 1-acyl-glycero-3-phosphorylcholine will be observed. By assaying the radioactivity of the products resulting from the digestion, this should permit us to determine quantitatively the extent to which the isomerization process is favoured under our system.

Shown in Figure 24 is the time-course of phospholipase A_2 digestion of phospholipid obtained by the strategy described above. As illustrated, complete digestion of the synthetic phospholipid was obtained within one h. Comparison of the radioactivity content of the lysoPC and fatty acid products at 1 h indicated 10% migration.

Although acyl migration was observed, we do not believe this to be due to our acylation conditions for the following reasons. Firstly, Dennis and coworkers (22) have recently showed that 1-acyl-glycero-3-phosphorylcholine exposed to alkaline pHs (e.g. conditions under which the phospholipase A_2 digestion is performed) resulted in an equilibrium mixture containing 90% of the 1-acyl and 10% of the 2-acyl isomer. Secondly, from results obtained by the above authors the rate or rate constant of acyl migration in chloroform was determined to be 2.9×10^{-3} M^{-1} min^{-1}. Thus, indicating that in chlorofirm the acyl migration reaction is not favoured. Furthermore, in comparison to the experimentally determined rate constant of acylation (37.6 M^{-1} min^{-1}) of lysoPC under optimal conditions, the rate of acyl migration is approximately 1.3×10^4 times slower. However, it could be argued that under our optimal acylation conditions (2 M PPY, 75 mM anhydride, 50 mM lysoPC) the rate of acyl migration is significantly increased due to catalysis by PPY. Therefore, if the acylation reaction

was performed with a comparatively small amount of PPY, one would expect a decrease in the rate of acyl migration and thus a lower extent of migration. Acylation of 1-[^{3}H]-acyl-glycero-3-phosphorylcholine in the presence of 2 equivalents of PPY (0.1 M) also resulted in 10% migration. This result, in conjunction with the above observations, further supports our conclusion that under our acylation conditions no appreciable amount of acyl migration is induced.

Summary

Using the model peptides to systematically evaluate parameters involved with phospholipid synthesis we were able to show the following:

a. The fatty acid anhydride is approximately 2 times more reactive than the fatty acid imidazolide.

b. The reactivity of the catalyst-activated anhydride intermediate is solvent dependent. Of the solvents tested, chloroform optimally enhanced the reactivity of the catalyst-activated anhydride.

c. Preparation of the intermediate, 1-acyl-4-pyrrolidinopyridinium salt, occurs by way of an equilibrium dependent reaction.

d. The phosphate group of 1,2-diacyl-glycero-3-phosphorylcholine interacts with fatty acid anhydride under acylation conditions. This interaction causes a reduction in the rate of acylation of the secondary hydroxyl group of DNP-Pro-ThrNH_2.

e. This interaction between the phosphate and the anhydride can be completely reversed if sufficient catalyst only is used.

f. Acylation of 1-acyl-glycero-3-phosphorylcholine under optimal acylation conditions derived from the model peptide system results in a 100% yield of PC within 5 min.

g. Acyl migration does not occur to any appreciable extent under our optimal acylation conditions.

It should also be mentioned that the results obtained with the 4-pyrrolidinopyridine catalyst parallel the results obtained with 4-dimethylaminopyridine.

REFERENCES

1. Singer, S.J. and Nicolson, G.L. (1972) Science 175:720-731.

2. Stryer, L. (1981) Biochemistry, pp. 205-229, W.H. Freeman and Co., San Francisco.

3. Peters, K. and Richardson, F.M. (1977) Ann. Rev. Biochem. 46:523-551.

4. Khorana, H.G. (1980) Bioorganic Chem. 9:363-405.

5. Ross, A.L., Radhakrishnan, R., Robson, R.J. and Khorana, H.G. (1982) J. Biol. Chem. 257:4152-4161.

6. Jurgen, K., Brunner, J. and Jorgensen, B.B. (1984) Biochemistry 23:5610-5616.

7. Takagaki, Y., Radhakrishnan, R., Gupta, C.M. and Khorana, H.G. (1983) J. Biol. Chem. 258:9128-9135.

8. Takagaki, Y., Radhakrishnan, R., Wirtz, K.W. and Khorana, H.G. (1983) J. Biol. Chem. 258:9136-9142.

9. Bette-Bobillo, P., Bienvenue, A., Broquet, C. and Manrin, L. (1985) Chem. Phys. Lipids 37:215-226.

10. Robles, C. and Van Den Berg, D. (19069) Biochim. Biophys. Acta 187:520-526.

11. Gordon, D.T. and Jensen, R.G. (1972) Lipids 7:261-262.

12. Warner, T.G. and Benson, A.A. (1977) J. Lipid Res. 18:548-552.

13. Boss, W.F., Kelley, C.J. and Landsberger, F.R. (1975) Anal. Biochem. 64:289-292.

14. Hermetter, A. and Paltauf, F. (1981) Chem. Phys. Lipids 28:111-115.

15. Baer, E. and Buchnea, D. (1959) Can. J. Biochem. Physio. 37:953-959.

16. Pugh, E.L. and Kates, M. (1975) J. Lipid Res. 16:392-394.

17. Nicholas, A.W., Khouri, L.G., Ellington, J.C. and Porter, N.A. (1983) Lipids 18:434-438.

18. Gupta, C.M., Radhakrishnan, R. and Khorana, H.G. (1977) Proc. Natl. Acad. Sci. 74:4315-4319.

19. Perly, B., Duforc, E.J. and Jarrell, H.C. (1983) J. Labelled Compounds and Radiopharmaceuticals 21:1-13.

20. Patel, K.M., Morrisett, J.D. and Sparrow, J.T. (1977) J. Lipid Res. 20:674-677.

21. Manson, J.T., Broccoli, A.V. and Huang, C.H. (1981) Anal. Biochem. 113:96-101.

22. Pluckthun, A. and Dennis, A.E. (1982) Biochemistry 21:1743-1750.

23. Selinger, Z. and Lapidot, Y. (1966) J. Lipid Res. 7:174-175.

24. Staab, H.A. (1962) Angew. Chem. 1:351-366.

25. Aneja, R. and Chadha, J.S. (1971) Biochim. Biophys. Acta 239:84-91.

26. Dack, M.R.J. (1974) Chem. Britain 19:347-351.

27. Staab, H.A. and Datta, A.P. (1963) Angew. Chem. 75:1203.

28. Hofle, G., Steglich, W. and Vorbruggen, H. (1978) Angew. Chem. 17:569-583.

29. Guibe-Jampel, E., LeCorre, G. and Wakselman, M. (1979) Tet. Let. 13:1157-1160.

30. Tedder, J.M. (1955) Chem. Rev. 55:787-827.

31. Fersht, A.R. and Jencks, W.P. (1970) J. Am. Chem. Soc. 92:5432.

APPENDIX B: SYNTHESIS OF ACYL-CoA THIOESTERS

TABLE OF CONTENTS

LIST OF ABBREVIATIONS

CoASH	Coenzyme A
DMF	dimethylformamide
HPLC	high pressure liquid chromatography
CDI	N',N'-carboxyldiimimdazole
TLC	thin-layer chromatography

LIST OF FIGURES

INTRODUCTION

A variety of chemical approaches have been described for the synthesis of fatty acyl coenzyme A. These involve acylating coenzyme A as the lithium or sodium salt with commonly available fatty acid acylating reagents such as anhydride (Simon and Shemin 1953; Stadtman, 1957; Pullman 1973), mixed anhydride of ethyl hydrogen carbonate (Goldman and Vagelos 1961), acid chloride (Seubert 1960; Bishop and Hajra 1980; Hajra and Bishop 1986), N-hydroxysuccinimide ester (Lapidot et al. 1967; Chauban and Dakshinamurti 1980), and more recently, with the imidazolide (Kawaguchi et al. 1981). Due to the low solubility of coenzyme A salts in organic solvents, the acylation reactions have been routinely performed in aqueous solvents at pH 7-9 (Stadtman, 1957; Seubert 1960; Chauban and Dakshinamurti 1980; Kawaguchi et al. 1981) or high temperature (Bishop and Hajra 1980; Hajra and Bishop 1986). However, under these conditions poor solubility of the reagents or various competing reactions often result in low yields even though an excess of the acylating reagent or coenzyme A is used.

These approaches are not suitable for micro-scale syntheses involving scarce and valuable fatty acid analogues such as highly radioactive photoreactive fatty acids. This report describes a method for solubilization of coenzyme A in anhydrous organic solvents and for its acylation by fatty acylimidazolides in dilute solutions under mild conditions; this procedure results in essentially quantitative recovery of the fatty acid as the fatty acyl CoA. The purification of the fatty acyl

coenzyme A by HPLC and gel filtration methods is described.

MATERIALS AND METHODS

Palmitic acid and N',N'-carbonyldimidazole (CDI) were purchased from Sigma Chemical Co. Coenzyme A (CoASH) as the free acid was obtained from Boehringer and [^{3}H]palmitic acid (30 Ci/mmole) from New England Nuclear. 1-palmitoyl-glycero-3-phosphorylcholine was purchased from Serdary and triethylamine from Pierce.

Dry dimethylformamide (DMF), prepared by the addition of 0.1 volume of dry benzene and evaporation of 0.2 volumes under reduced pressure, was stored over 4Å molecular sieves under nitrogen. All other anhydrous solvents were prepared by distillation under nitrogen. Benzene was refluxed for 4 hours prior to distillation from calcium hydride, followed by storage over 4Å molecular sieves under nitrogen. Reagent grade chloroform ($CHCl_3$) was extracted with distilled water, distilled from phosphorous pentoxide and stored under nitrogen at -20°C in the dark. Pyridine was refluxed with barium oxide for 2 h prior to distillation. Triethylamine was distilled from ninhydrin and stored over 4Å molecular sieves under N_2 at 4°C in the dark. Palmitic acid was freed of residual water by repeated addition of dry benzene and evaporation under reduced pressure.

Solubilization of Coenzyme A

The free acid form of CoASH was suspended in dry $CHCl_3$ at a concentration of 115 mM (based on dry weight). Following the addition of 4 equivalents of anhydrous triethylamine (2 M in dry $CHCl_3$), the CoASH was

diluted to 80 mM with dry DMF, and the content was vigorously mixed. The final concentration of CoASH was determined based on the molar extinction coefficient (ϵ = 16,400) of CoASH at 260 nm (Seubert, 1960).

Preparative Synthesis of Fatty Acyl Coenzyme A

a) Preparation of fatty acyl imidazolide:

The imidazolide was prepared as described (Morton et al. 1988). The fatty acid (1 M in dry DMF) was transferred to a flamed pyrex screw cap tube containing 1.5 equivalents of CDI (2 M) in 15% DMF in benzene and the reaction was allowed to proceed for 1 h at room temperature under N_2. The imidazolide was diluted with dry benzene to 40 mM and transferred to another flamed pyrex screw cap tube containing 4 equivalents of dried Sephadex LH-20 (capacity, 1.15 x 10^{-5} mole/mg) per mole of excess CDI. The tube was flushed with N_2 and the content was rotated for 1 h at room temperature. The reaction mixture was centrifuged for 5 min and the supernatant containing pure imidazolide was recovered.

b) Acylation of Coenzyme A:

The tetra-triethylammonium salt of CoASH was routinely acylated at a final concentration of 50 mM with 1.5 equivalents of the imidazolide in $CHCl_3$ containing 20% DMF.

Small Scale Synthesis of Fatty Acyl Coenzyme A

a) The fatty acid (40 mM in dry benzene) was transferred to 2 equivalents of CDI (160 mM in dry $CHCl_3$ containing 20% benzene). The reaction was allowed

to proceed fo 4 h at room temperature under nitrogen.

b) Acylation of Coenzyme A:

Fatty acyl imidazolide prepared as described above was used to acylate 2 equivalents of the tetra-triethylammonium salt of CoASH in $CHCl_3$/DMF (4:1). The final concentration of imidazolide and CoASH were 10 mM and 20 mM, respectively.

HPLC Analysis of Acylation Reaction

The extent of acylation of CoASH was routinely analyzed by HPLC, using a Millipore-Waters system equipped with two M-450 pumps, a 720 system controller, a M-730 data module, a WISP 710B automatic injector and a 440 absorbance detector. At specific times an aliquot of the reaction was diluted into 100 mM sodium acetate, pH 4.4/methanol (1:1, v/v) and applied onto a 4.6 x 15 cm reverse-phase C_{18} Altex ion-pairing column (5 μM) pre-equilibrated with 50 mM sodium acetate, pH 4.4 at 40°C. The column was eluted at 1 ml/min as shown in Fig. 4 and the eluate monitored at 254 mm.

Purification of the Fatty acyl Coenzyme A

Fatty acyl coenzyme A was purified by HPLC on a reverse-phase C_{18} Altex ion-pairing column equilibrated with 50 mM sodium acetate, pH 4.4. The column was eluted at 1 ml/min with a linear methanol gradient for 12 min.

Purification by gel permeation chromatography was achieved by applying the mixture directly onto a Sephadex LH-20 column (1 x 76 cm) pre-equilibrated and developed with $CHCl_3$/MeOH/H_20 (1:1:0.2, v/v/v).

Characterization of Synthetic Fatty acyl Coenzyme A

a.) Biochemical:

Microsomes were obtained according to the procedure of Suzue and Marcel (1972). The microsomal fraction, suspended in a 0.25 M sucrose solution containing dithiothreitol (1 mg/ml), was aliquoted and stored at -20°C under nitrogen. Protein content was determined according to the method of Lowry et al. (1951).

Synthesis of 1,2-dipalmitoylphosphatidylcholine by rat liver microsomes using the palmitoyl coenzyme A prepared as described above, and 1-palmitoyllysophosphatidylcholine was performed as described (Leblanc and Gerber, 1984).

b.) Chemical:

Purified fatty acyl coenzyme A (20 nmoles, 1 μCi) was reacted with 9 μmoles of ethanolamine in 20 μl dry pyridine at room temperature. At various times an aliquot (2 μl) was spotted directly on a TLC plate. The plate was developed with $CHCl_3$/MeOH (9:1, v/v) containing 1% (v/v) acetic acid. The radioactivity was visualized by fluorography. The products were scraped from the plate and the radioactive content was assessed by liquid scintillation counting.

RESULTS AND DISCUSSION

Chemical synthesis of fatty acyl coenzyme A thioesters reported so far have been routinely performed in a mixture of water and tetrahydrofuran at high pH and temperature primarily to solubilize CoASH and the activated fatty acids. However, under these conditions the yields of product are variable and depend on the polarity of the fatty acid used.

For micro-scale synthesis involving highly radioactive fatty acids and analogues such as photoreactive fatty acids reproducible and high yields are clearly essential. Conditions that solubilize both CoASH and the acylating agent under anhydrous conditions avoid hydrolysis of the activated acid. The solubility of the activated fatty acid would be improved under these conditions, while a polar salt of CoASH would be insoluble. In order to render the CoASH soluble under anhydrous conditions, the free acid of CoASH was suspended in dry $CHCl_3$ and reacted with 4 equivalents of anhydrous triethylamine. Addition of dry DMF to a concentration of 20% (v/v) resulted in a clear solution of the tetra-triethylammonium salt of CoASH; this salt of CoASH is also soluble in pyridine, DMF or mixtures of these solvents in $CHCl_3$. As determined by HPLC analysis, this solubilization procedure did not promote oxidation of the coenzyme A and resulted in solution of the CoASH under anhydrous conditions.

A variety of fatty acid acylating agents can be used to acylate the tetra-triethylammonium salt of CoASH under these anhydrous conditions. Since the thiol is a good nucleophile, it is possible to avoid highly reactive acylating fatty

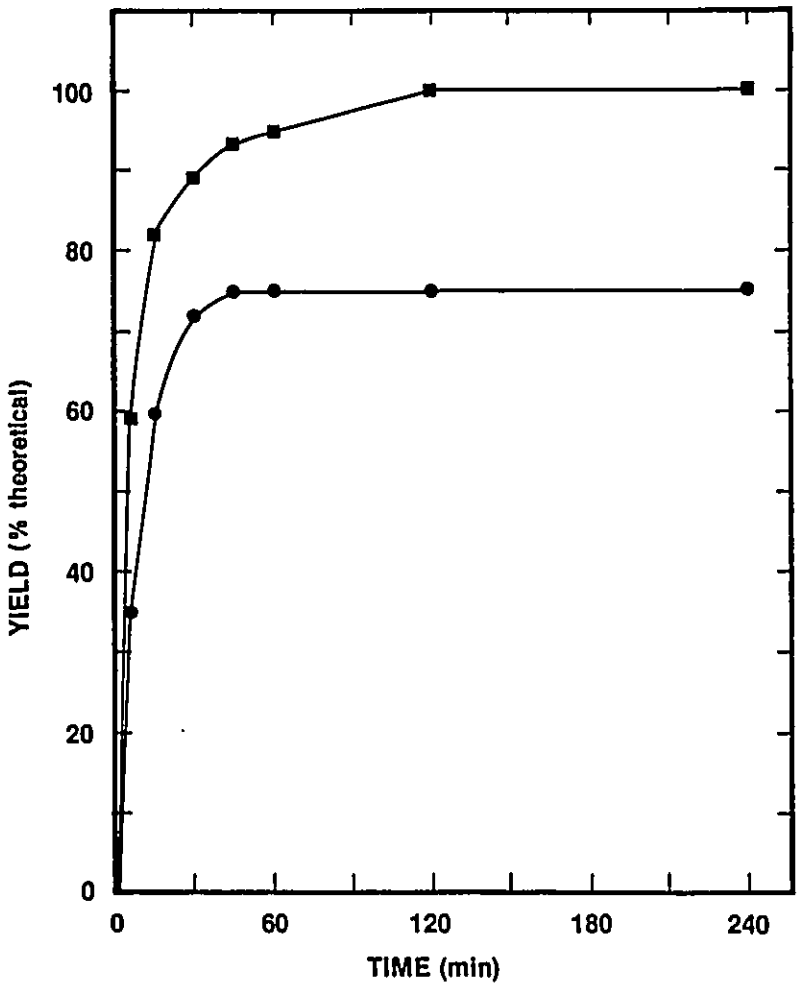

Figure 1: Time course of activation of palmitic acid with varying amounts of CDI. Palmitic acid (1.2 μmoles, 13.3 Ci/mole) was reacted with 1 (●) or 2 (■) equivalents of CDI in 20% benzene in $CHCl_3$ as described under small scale synthesis of Materials and Methods. The extent of activation was assessed by diluting an aliquot (2 μl) of the activation reaction at the specified times into 18 μl of 0.5 M ethanolamine in dry pyridine. The reaction was allowed to proceed for 1 h at room temperature and 10 μl was spotted on a TLC plate. The plate was developed with $CHCl_3$/MeOH (9:1, v/v) containing 1% acetic acid. The radioactive products were visualized by fluorography, scraped from the plate and quantitated by liquid scintillation counting.

acid derivatives which are likely to result in degradation of sensitive fatty acids or acylation of the hydroxyl groups on the CoA. We have previously shown that the fatty acyl imidazolide is less reactive than the anhydride or the acid chloride (Mangroo and Gerber, 1988). Its use avoids acylation of hydroxyl groups present on the CoASH; these can be easily acylated by the more reactive reagents under anhydrous conditions, while this would require strong base catlysis in the case of imidazolides (Mangroo and Gerber, 1988). The fatty acid imidazolide was chosen for this study since it avoids these side reactions and affords quantitative recovery of the fatty acid in the desired product.

The reactivity of the fatty acyl imidazolide was determined in the anhydrous solvents pyridine, DMF and $CHCl_3$ as well as in mixtures of these (data not shown); it was found that the reactivity of the imidazolide increased as the polarity of the solvent decreased, thus being highest in chloroform; although the addition of 20% of one of DMF or pyridine to $CHCl_3$ resulted in substantial loss of activity, the solvent chosen for these studies was 20% DMF in $CHCl_3$ since the tetra-triethylammonium salt of coenzyme A was found to be readily soluble in this mixture while it was insoluble in chloroform.

Small scale synthesis of fatty acyl coenzyme A involving scarce fatty acids must be accomplished using only a small amount of the acid and thus requires the activation of the fatty acid with CDI to be performed under dilute conditions. The rate of activation of the fatty acid with CDI under these conditions is expected to be slow and the extent of formation of the fatty acid imidazolide was therefore

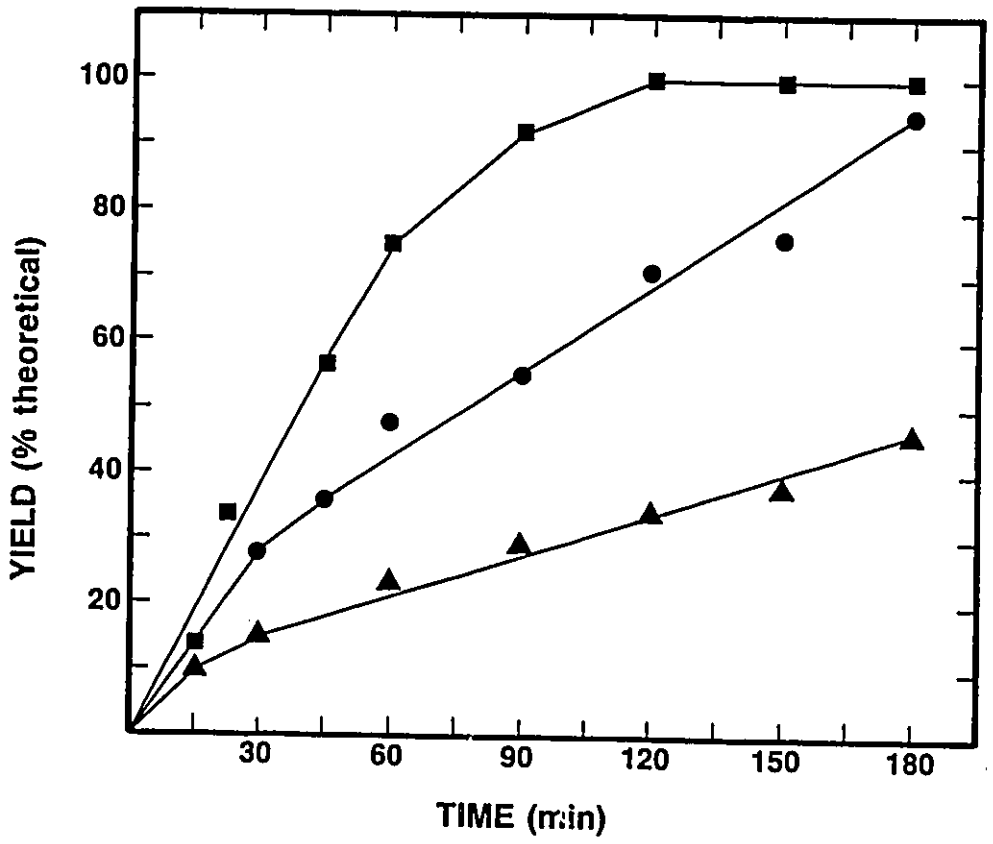

Figure 2: Time course of fatty acid acylation of varying amounts of coenzyme A in the presence of CDI. Palmitoyl imidazolide (3 μmoles) prepared as described under small scale synthesis in Materials and Methods, was reacted with 3 μmoles (▲), 4.5 μmoles (●) or 6 μmoles (■) of the tetra-triethylammonium salt of coenzyme A in a total volume of 300 μl $CHCl_3$/DMF (4:1). At the times indicated, aliquots of the reaction were diluted into methanol/100 mM sodium acetate, pH 4.4 (1:1, v/v) and analyzed by HPLC.

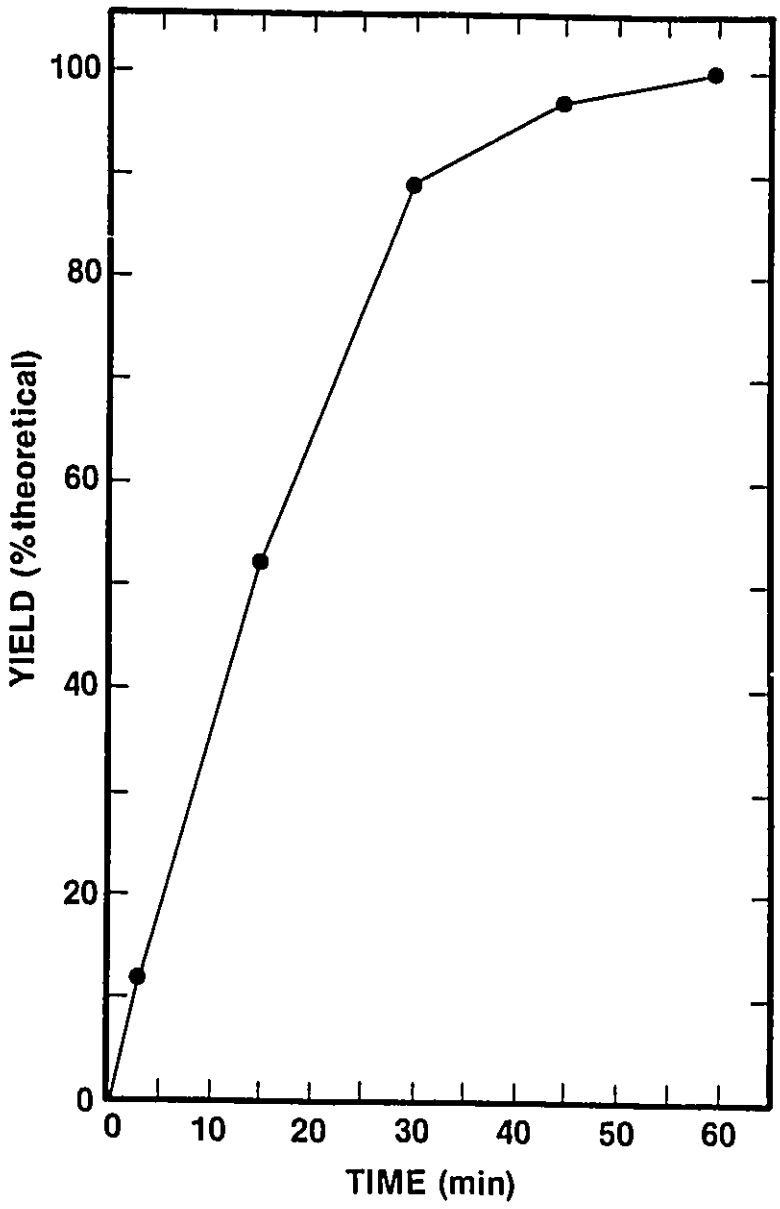

Figure 3: Time course of fatty acid acylation of coenzyme A in the absence of CDI. Palmitoyl imidazolide (1.8 μmoles), prepared as described under preparative synthesis of Materials and Methods, was reacted with the tetra-triethylammonium salt of coenzyme A (1.2 μmoles) in 25 μl of $CHCl_3$/DMF (4:1). At the times indicated, an aliquot of the reaction was diluted into methanol/100 mM sodium acetate, pH 4.4 (1:1, v/v) and analyzed by HPLC.

monitored indirectly by its quantitative conversion to the fatty acid ethanolamine derivative. The latter was purified by TLC and the radioactivity determined. As shown in Fig. 1, activation of palmitic acid with 1 equivalent of CDI was slow and incomplete; however, with 2 equivalents of CDI, activation of the fatty acid was faster and proceeded to completion within two hours.

The time course of acylation of the tetra-triethylammonium salt of coenzyme A with palmitoyl imidazolide prepared as described above is shown in Fig. 2. This activation procedure used an excess of CDI and the direct acylation of the CoASH without removal of this excess CDI resulted in only 38% derivatization of the CoASH within 3 h when 1 equivalent of CoASH was added. Furthermore, the reaction did not proceed to completion even when longer reaction times were used (data not shown). This was due to the excess CDI reacting with the thiol group of coenzyme A, thus preventing the desired acylation reaction. However, as shown in Fig. 2, addition of an excess of CoASH resulted in complete conversion of the fatty acyl imidazolide to the coenzyme A thioester.

The addition of an excess CoASH is the simplest means to obtain complete conversion of the fatty acyl imidazolide and this is the preferred route for synthesis where availability of the fatty acid is limiting. In large scale syntheses where the addition of an excess of CoASH may be too expensive, an alternate means of ensuring complete acylation involves the removal of residual CDI prior to the acylation. It has been shown that this can be readily done (Morton et al. 1988) by the use of anhydrous Sephadex LH-20. This procedure results in the complete

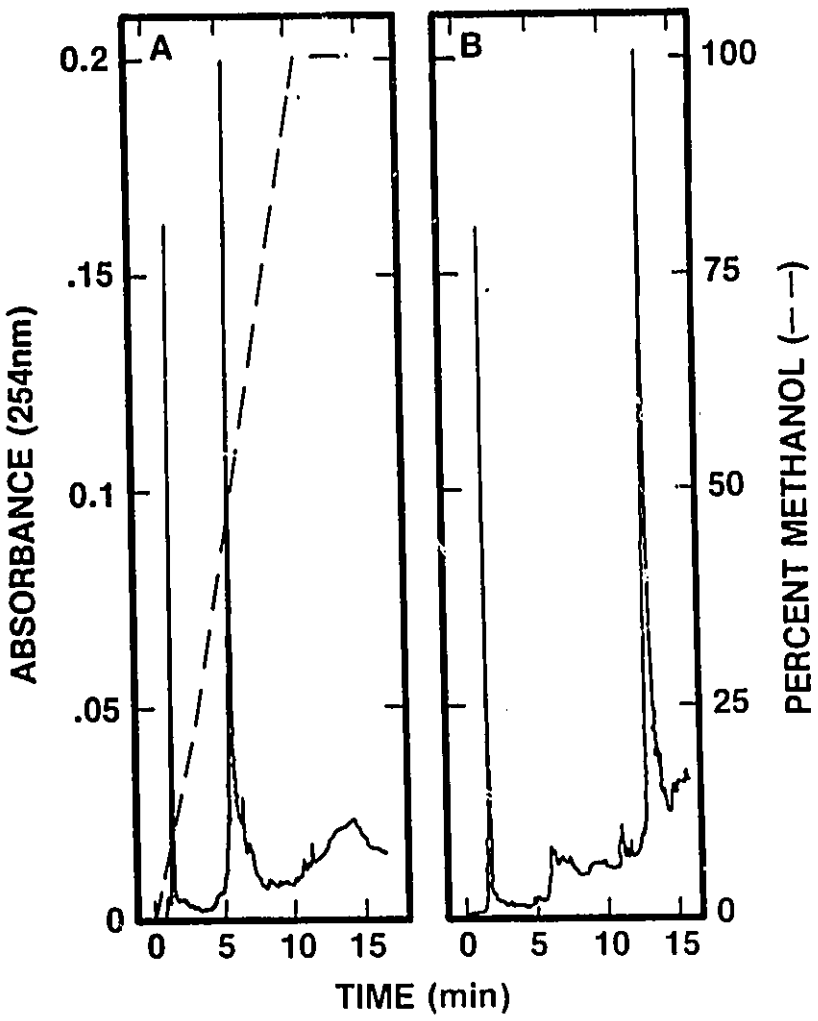

Figure 4: HPLC analysis of fatty acid acylation of coenzyme A. Coenzyme A as the tetra-triethylammonium salt (1.2 μmoles) was incubated without (A) or with (B) palmitoyl imidazolide (1.8 μmoles) prepared as described under large scale synthesis of Materials and Methods, in 25 μl $CHCl_3$/DMF (4:1). After 1 h 3 μl of each incubation was diluted into 97 μl methanol/100 mM sodium acetate, pH 4.4 (1:1, v/v) and 50 μl of the quenched reactions were subjected to HPLC analysis.

removal of any excess CDI and leaves the fatty acid as the imidazolide. The time course of the acylation by the imidazolide which had the excess CDI removed by prior incubation with anhydrous Sephadex LH-20 is shown in Fig. 3; the acylation now proceeded to completion even when the imidazolide and CoASH were present in equimmolar amounts.

The purification of fatty acyl coenzyme A derivatives using reverse phase HPLC is shown in Fig. 4. The separation shown represents a substantial improvement over earlier methods (Seubert 1960; Pullman 1973; Kawaguchi et al. 1981) this method was used for monitoring the acylation reaction as well as for preparative isolation of the fatty acyl coenzyme A. An alternate preparative isolation also used was chromatography on Sephadex LH-20 in $CHCl_3$/MeOH/H_20 (1:11:0.2, v/v/v). In cases where the procedure is to be used for very large scale syntheses, chromatography of the reaction on a Dowex 50 column in the H^+ form would afford the free acid of the fatty acyl coenzyme A and this could then readily be converted to the desired counterion form.

The characterization of the fatty acyl coenzyme A was done by both chemical and biochemical means. Reaction of the coenzyme A derivative with ethanolamine, as described in Materials and Methods, resulted in total recovery of the fatty acid as the fatty acyl-ethanolammide (data not shown). Hence, the fatty acid must be present in the form of an active thioester in the CoA derivative. It was also determined, as described in Materials and Methods, that rat liver microsomes were able to utilize the synthetic coenzyme A derivative for the

synthesis of phosphatidylcholine from lysophosphatidylcholine; all the fatty acid of the coenzyme A derivative was recovered in the phosphatidylcholine formed (data not shown). The synthetic product was therefore concluded to be the pure fatty acyl thioester of coenzyme A. The procedure described thus results in essentially quantitative conversion of a fatty acid to the fatty acyl CoA derivative.

REFERENCES

1. Bishop, J.E., and Hajra, A.K. 1980. A method for the chemical synthesis of ^{14}C-labelled fatty acyl coenzyme A's of high specific activity. Anal. Biochem., **106**: 344-350.

2. Chauban, M.S. and Dakshinamurti, K. 1980. Synthesis of S-erucyl coenzyme A. Prep. Biochem., **10**: 37-41.

3. Goldman, P., and Vagelos, P.R. 1961. The specificity of triglyceride synthesis from diacylglycerides in chicken adipose tissue. J. Biol. Chem., **236**: 2620-2623.

4. Hajra, A.K., and Bishop, J.E. 1986. Preparation of radioactive acyl coenzyme A. Methods in Enzymology, **122**: 50-53.

5. Kawaguchi, A., Yoshimura, T., and Okuda, S. 1981. A new method for the preparation of acyl-CoA thioesters. J. Biochem., **89**: 337-339.

6. Lapidot, Y., Rapport, S., and Wolman, Y. 1967. Use of esters of N-hydroxysuccinimide int he synthesis of N-acyl amino acids. J. Lipid Res., **8**: 142-145.

7. LeBlanc, P., and Gerber, G.E. 1984. Biosynthetic utlization of photoreactive fatty acids by rat liver microsomes. Can. J. Biochem. Cell Biol., **62**: 375-378.

8. Lowry, O.H., Rosebrough, N.J., Farry, A.L., and Randall, R.J. 1951. Protein measurement with the folin phenol reagent. J. Biol. Chem., **193**: 265-275.

9. Mangroo, D., and Gerber, G.E. 1988. Phospholipid synthesis: effects of solvent and catalysts on acylation. Chem. Phys. Lipids, 48: 99-108.

10. Morton, R.C., Mangroo, D., and Gerber, G.E. 1988. A novel method of complete activation by carbonyldiimidazole: Application to ester synthesis. Can. J. Chem., 66: 1701-1705.

11. Morton, R.C. and Gerber, G.E. 1988. Water solubilization of membrane proteins: Extensive derivatization with a novel polar derivatization reagent. J. Biol. Chem. 263: 4989-4995.

12. Pullman, M.E. 1973. A convenient and versatile method for the purification of CoA thiol esters. Anal. Biochem., 54: 188-198.

13. Seubert, W. 1960. S-palmityl coenzyme A. Biochem. Prep., 7: 89-83.

14. Simon, E.S., and Shemin, D. 1953. Preparation of S-succinyl coenzyme A. J. Am. Chem. Soc., 75: 2520.

15. Stadtman, E.R. 1957. Preparation and assay of acyl coenzyme A and other thiol esters: Use of hydroxylamine. Methods of Enzymology, 3: 931-941.

16. Suzue, G., and Marcel, Y.L. 1972. Specificity of long-chain acyl coenzyme A synthetase from rat liver microsomes. Influence of the position of double bonds in octadecadienoic acid. Biochemistry 11: 1704-1708.